Le rôle du complexe de remodelage de la chromatine NURF dans les mélanocytes et les mélanomes

Dana Koludrovic

UNIVERSITÉ DE STRASBOURG

ÉCOLE DOCTORALE DES SCIENCES DE LA VIE ET LA SANTE

Institut de Génétique et de Biologie Moléculaire et Cellulaire

THÈSE présentée par :

Dana KOLUDROVIC

soutenue le : **30 Septembre 2014**

pour obtenir le grade de : **Docteur de l'université de Strasbourg**

Discipline/ Spécialité : Aspects moléculaires et cellulaires de la biologie

Le rôle du complexe de remodelage de la chromatine NURF dans les mélanocytes et les mélanomes

THÈSE dirigée par :

M DAVIDSON Irwin Docteur, université de Strasbourg

RAPPORTEURS :

Mme BERTOLOTTO Corine Docteur, Centre Méditerranéen de Médicine Moléculaire, Nice

Mme GALIBERT Marie-Dominique Professeur, Institut de Génétique et Développement, Département de Biochimie et Génétique Moléculaire, Rennes

---

AUTRES MEMBRES DU JURY :

M HAMICHE Ali Docteur, université de Strasbourg

Dedicated to my mother, Ljiljana

Acknowledgements

I would like to thank my thesis committee, dr. Corine Bertolotto, dr. Ali Hamiche and prof. Marie-Dominique Galibert for kindly of accepting to be members of my thesis jury and for their critical evaluation of my manuscript.

I would like acknowledge my funding agencies, CERBM GIE for funding the first three years and the Association de recherche contre le cancer (ARC) for funding the fourth year of my thesis.

I would like to thank my supervisor dr. Irwin Davidson, for giving me the opportunity to join his group. Irwin, I thank you for his endless support, patience and trust in me and my project.
I would like to thank all members of the lab, past and present.
Patrick, thank you for numerous discussions (yeah I have to leave in 15 min, ….and 1 hour later, oh my god, look at the time…) and your ideas how to make things better. I believe I'm really lucky to be your lab mate.
Thomas, for his cool and patience in the beginning of my project helped me a lot in the project setup and general organization.
Shilpy, thank you for your moral support, your friendship and insight.
Daniel, thank you for very honest helpful discussions on many parts of my project.
Gabrielle, thank you for your help and support, Marie for your everlasting smile and support , Diana, thank you for looking after me and being helpful in every step of the way. Thank you to Igor, Sylvia, Frederica, Amin, Isabelle for your help and company.
Tao, thank you for your time and your patience with me and my billion questions, Celine for your help and diligence.
I would like to thank the members of the common facilities, cell culture facility, especially Betty Heller, the sequencing facility, Bernard and Muriel.
I would like to thank my family for supporting me through all the parts of my thesis, for their love and support.

Table of content

LIST OF ABBREVIATIONS

ACF	ATP-utilizing chromatin assembly and remodeling factor
ACTH	adrenocorticotropic
AD1	activating domain 1
ALM	Acral lentiginous melanoma
APC	adenomatosis polyposis coli
ARF	alternative reading frame
ATAC	Ada2a-containing
ATP	adenosine triphosphate
BAC	bacterial artificial chromosome
BAD	Bcl2 Antagonist of death
BCC	basal cell carcinoma
Bcl2	B-cell lymphoma 2
bHLH-LZ	basic helix loop helic leucine zipper
BMP	Bone morphogenetic proteins
BPTF	bromodomain phd finger transcription factor
BRCA1	Breast Cancer Susceptibility Gene 1
BrdU	bromo deouxyuridine
BRG1	Brahma-related gene 1
CAF-1	Chromatin assembly factor 1
cAMP	cyclic adenosine monophosphate
CCND1	cycline D1
CHD	chromodomain
ChIP	Chromatin immuno-precipitation
CHRAC	chromatin accessibility complex
CRE	cAMP response element
CREB	cAMP response element-binding protein
CTLA-4	cytotoxic T-lymphocyte-associated antigen-4

DCT	dopachrome tautomerase
DNA	Deoxyribonucleic acid
DOPA	L-3,4-dihydro xyphenylalanine
DSB	double strand break
DSH	Dishevelled
DVE	distal visceral endoderm
E2F	Transcription factor E2
ECM	extracellular matrix
EDN3	endothelin 3
EDNRB	enrothelin receptor B
EGF	Epidermal Growth Factor
EMT	epithelial-mesenchymal transition
ERK	Extracellular-signal Regulated Kinase
ES	embryonic stem
ESC	Epidermal stem cell
FGF	fibroblast growth factor
FOXD3	Forkhead box D3
FOXO	Forkhead box O
FRET	Fluorescence resonance energy transfer
FZ	frizzeld
GEF	guanine exchange
GSK3	Glycogen Synthetase Kinase 3
GTP	guanine triphosphate
HAT	histone acetyltransferases
HDAC	histone deacetylase
HES	Hairy/Enhancer of Split
HGF	Hepatocyte growth factor
HKMT	histone lysine methyltranferase

HMGA	high mobility group A
IGF	insulin growth factor
INK4A	inhibitor of cyclin-dependent kinase 4
INO80	inositol requiring 80
ISWI	imitation switch
KITL	KIT ligand
LM	Lentigo maligna
LPP	lower permanent portion
LRP	low-density-lipoprotein-related protein
MAPK	Mitogen-Activated Protein Kinase
MC1R	Melanocortin-1-receptor
MITF	Microphthalmia-associated transcription factor
MSC	melanocyte stem cell
MYC	Avian MYelocytomatosis virus Oncogene Cellular homolog
NC	neural crest
NCC	neural crest cell
NIC	Notch intracellular domain
NM	Nodular melanoma
NMSC	non-melanoma skin cancer
NURF	nucleosome remodeling factor
PAX	Paired box
PCAF	p300/CREB-binding protein associated factor
PCP	planar cell polarity
PD-1	programed cell death protein 1
PDGF	plarelet-derivied growth factor
PDGFR	plarelet-derivied growth factor receptor
PHD	plant homology domain

PI3K Phosphatidyl Inositol-3-kianse
PIP3 phosphatidylinositol triphosphate
PKA protein kinase A
PKB/AKT protein kinase B
P-number postnatal day-number
POMC pro-opiomelanocortin
PTEN Phosphatase and tensin homologue
PTM post-translational modification

RB retino blastoma
RBP-J recombination signal binding protein-J
RGF Radial growth phase
RNA Pol RNA polimeraze
ROS reactive oxygen species
RPE retinal pigment epithelium
RSF Remodeling and Spacing Factor

SAGA Spt–Ada–Gcn5–acetyltransferase
SARA Smad anchor for receptor activation
SAXS small-angle X-ray scattering
SCC squamous cell carcinoma
SCF stem cell factor
SCP Schwann cell precursors
sHG secondary hair germ
siRNA Small interfering RNA
SMARCA1,5 SWI/SNF related, matrix associated, actin dependent regulator of chromatin, subfamily a, member 1
SOX Sry-related HMG box
SSM Superficial spreading melanoma
SUMO Small Ubiquitin-like MOdifier
SWI/SNF SWItch/Sucrose NonFermentable

TFE3, B, C Transcription Factor E 3, B, C

TGFβ	Transforming growth factor
TRP1, 2	tyrosinase related protein 1, 2
TYR	tyrosinase
UPP	upper permanent portion
USF1	Upstream Stimulating Factor 1
UV	ultra violet
VEGF	Vascular Endothelium Growth Factor
VGF	Vertical growth phase
WHO	World Health Organization
WICH	William syndrome transcription factor
WNT	Wingless integration
WS	Waardenburg syndrome
ZEB	Zinc finger E-box-binding homeobox
α-MSH	α-melanocyte-stimulating hormone

LIST OF FIGURES

LIST OF TABLES

ABSTRACTS

1. En Français/ In French

Le rôle du complexe de remodelage de la chromatine NURF dans les mélanocytes et les mélanomes

La mélanome malin est le plus agressif de tous les cancers de la peau et a un très mauvais pronostic en raison de sa résistance intrinsèque à la chimiothérapie et à la radiothérapie. Une des causes principales de cette résistance se trouve dans la plasticité des cellules de mélanome. Les mélanomes sont constitués d'au moins deux sous-populations cellulaires mutuellement exclusives ; des cellules prolifératives et des cellules invasives. Ces populations sont capables de commuter entre les deux phénotypes sous l'influence de signaux du microenvironnement.

Le facteur de transcription MITF (Microphthalmia-associated transcription factor) est le facteur clé du réseau de régulation des gènes de la lignée mélanocytaire et du mélanome. MITF contrôle la différenciation, la survie des melanocytes ainsi que la prolifération et les propriétés migratoires et invasives des cellules mélanome. Des niveaux élevés de MITF sont caractéristiques des cellules prolifératives, alors que la faible expression MITF est associée à des cellules peu prolifératives possédant des capacités migratoires et invasives augmentées.

Pour déterminer le répertoire complet de gènes cibles de MITF, nous avons réalisé le séquençage des ARN messagers présents dans les cellules de mélanome après la perte de MITF induite par un siARN, couplé avec la ChIP-séq de cellules exprimant MITF marqué avec 3HA. Les deux ensembles de données ont été comparés afin d'identifier des gènes directement régulés par MITF. Les résultats ont permis de montrer que MITF agit comme un activateur direct de gènes impliqués dans la réplication de l'ADN, la réparation et la mitose, mais qu'il réprime des gènes impliqués dans la motilité et l'invasion. Le fait que MITF agit comme un activateur ou un répresseur de façon promoteur spécifique permet d'expliquer son rôle central dans la biologie du mélanome à l'échelle moléculaire.

Afin de mieux comprendre comment MITF active ou réprime la transcription, nous avons cherché à identifier ses partenaires d'interaction. A cette fin, des cellules de mélanome exprimant MITF avec une double étiquette ont été utilisées pour effectuer une immuno – précipitation en tandem sur les fractions nucléaires solubles et insolubles (associée à la

chromatine) couplés à une analyse par spectrométrie de masse. Parmi les protéines interagissant avec MITF dans la fraction associée à la chromatine, nous avons identifié toutes les principales sous-unités du complexe de remodelage de chromatine NURF (Nucleosome Remodeling Factor), y compris BPTF, SMARCA1, SMARCA5 et RBBP4.

Les facteurs de remodelage de chromatine de la famille ISWI optimisent l'espacement des nucléosomes et jouent donc un rôle important dans la transcription, la réplication de l'hétérochromatine et l'assemblage de la chromatine. La composition du complexe NURF, membre fondateur de cette famille, a récemment été déterminée avec haute précision, grâce à la spectrométrie de masse quantitative, montrant que NURF est composé de six sous-unités: BPTF, SMARCA1, SMARCA5, HMG2L1, RBBP4 et BAP18. La plus grande sous-unité de NURF, BPTF (Bromodomain PHD- finger transcription factor) , d'abord identifiée chez Drosophila melanogaster, est une protéine contenant un domaine PHD (plant-homology domain) et un bromodomain. Ces domaines interagissent avec les modifications des histones: le domaine PHD interagit avec de la lysine triméthylée 4 de l'histone H3, tandis que le bromodomain reconnaît la lysine acétylée 16 de l'histone H4, deux marques bien connues pour leur association avec la transcription active.

L'implication de NURF dans la régulation transcriptionnelle au niveau biochimique est connue depuis longtemps, mais il existe peu de données concernant ses fonctions biologiques. Les données publiées récemment décrivent des fonctions extrêmement variées de ce complexe. Il est impliqué dans la coordination de mécanismes de régulation épigénétique qui empêche la différenciation précoce des cellules souches épidermiques. Par ailleurs, la sous- unité SMARCA1 supprime la prolifération et la migration cellulaire et atténue la signalisation Wnt. L'amplification du locus codant BPTF a été impliquée dans le développement de divers cancers humains, touchant le cerveau, le sein, le poumon, le foie et la prostate. En se servant de souris génétiquement modifiées, le rôle du BPTF a été montré dans le développement embryonnaire, et le rôle dans la différentiation des thymocytes. Malgré l'accumulation de preuves indiquant un rôle crucial du complexe de remodelage de la chromatine NURF dans différents aspects de la biologie cellulaire et du cancer, son rôle potentiel dans la physiopathologie des mélanocytes et dans le mélanome malin reste inconnu.

J'ai d'abord étudié l'interaction entre MITF et NURF par immunoprécipitation et immunoblot. J'ai pu confirmer la co-précipitation dans la fraction associée à la chromatine entre MITF et les sous-unités BPTF, SMARCA1 et SMARCA5 de NURF. Pour évaluer le rôle de NURF dans le mélanome, je me suis concentrée sur le rôle de BPTF, la plus grande sous-unité de NURF et la seule qui est spécifique à ce complexe, les autres sous-unités étant présentes dans d'autres complexes de remodelage. J'ai infecté plusieurs lignées cellulaires de

mélanome avec des vecteurs lentiviraux exprimant des shRNA dirigés contre BPTF. Le silencing de BPTF conduit à l'arrêt de la prolifération, à des modifications de la morphologie, à une mitose défectueuse, avec apparition de cellules multi-nucléés et à la sénescence, alors que l'infection avec des shRNA de contrôle n'avait aucun effet significatif. Les cellules BPTF knock-down présentent de nombreuses caractéristiques observées dans les cellules infectées en parallèle avec des vecteurs exprimant des shRNA contre MITF. Par immunoblot, j'ai montré qu'une perte de BPTF n'affecte pas l'expression de MITF de façon significative et vice-versa. Par conséquent, le phénotype de perte de BPTF ne peut être attribué à la perte de MITF. Les similitudes dans le phénotype suggèrent plutôt que NURF joue éventuellement le rôle de cofacteur pour MITF d'un sous-ensemble de ses gènes cibles. Afin de tester cette idée, j'ai effectué des expériences d'ARN-Seq sur les cellules shBPTF et shMITF à l'aide de deux shRNAs distincts pour chaque facteur afin d'exclure les effets hors - cible. Le séquençage a montré un chevauchement significatif entre les gènes régulés par MITF et BPTF. 42 % des gènes dont l'expression est augmentée et 30 % des gènes dont l'expression est diminuée suite au shBPTF sont régulés de la même façon suite au shMITF. J'ai analysé de manière plus approfondie les gènes régulés en commun et j'ai pu démontrer que 32% des gènes augmentés et 49% des gènes diminués sont associés à des sites de liaison de MITF, suggérant que leur régulation par MITF est directe. J'ai également remarqué que MITF et BPTF co-régulent de nombreux gènes impliqués dans la migration et de l'invasion. ZEB1 est l'un des facteurs de transcription connus pour réguler la transition épithélio- mésenchymateuse (TEM), en agissant comme un répresseur de la E-cadhérine. L'TEM est l'un des événements majeurs dans le développement de tumeurs métastatiques, par lequel les cellules cancéreuses acquièrent des propriétés invasives. Or, l'expression de ZEB1 est fortement augmentée lors de la perte d'expression de MITF out de BPTF. Ces deux facteurs coopèrent donc pour réprimer son expression.

Pour déterminer si BPTF a un rôle indépendant de MITF dans le mélanome, j'ai réalisé le silencing de BPTF dans les cellules 1205Lu, une lignée invasive n'exprimant pas MITF. La suppression de BPTF conduit à l'arrêt de leur prolifération et au changement de morphologie, tandis que l'élimination de MITF n'a eu aucun effet, comme prévu .En revanche, le silencing de BPTF dans plusieurs lignées non-mélanome n'affecte pas leur prolifération de façon significative. L'ensemble de ces résultats montrent que BPTF/NURF est essentiel pour la prolifération des cellules issues de la lignée mélanocytaire, mais pas essentiel dans d'autres types cellulaires.

Ayant démontré le rôle essentiel de BPTF/NURF dans les cellules mélanocytaires, j'ai mis en place des lignées de souris recombinantes où BPTF peut être inactivé de façon sélective dans les mélanocytes en croisant des souris $Bptf^{lox/lox}$ avec des souris avec des souris Tyr-

Cre. De plus, ces souris ont été croisées avec la lignée DCT-LacZ permettant une coloration spécifique de mélanocytes.

Les souris Tyr-Cre ::Bptf$^{lox/lox}$ où BPTF est inactivé lors du développement embryonnaire sont nées avec un phénotype faible caractérisé par un pelage du ventre gris mais un pelage noire au dos presque normal.

De plus, un nombre de mélanocytes embryonnaires avec le DCT-lacZ a révélé une différence dans le nombre de mélanocytes à E15.5. Le phénotype était plus évident à E16.6. A ce stade, les mélanoblastes embryonnaires présentent moins de prolifération et/ou de migration, et les groupes typiques de mélanoblastes s'accumulent dans les follicules pileux sont grandement diminués. De façon intéressante, les animaux nouveau-nés présentent une dépigmentation aux extrémités, un phénotype qui rappelle celui observé dans l'embryon. Ainsi, BPTF est impliquée dans la prolifération normale, la migration et la localisation des mélanoblastes embryonnaires.

Dès l'âge de 4 semaines ces souris deviennent progressivement blanches. Dès le renouvellement du premier pelage, les souris mutantes perdent leur pigmentation. Cet effet peut être clairement mis en évidence par des expériences de dépilation, qui montrent une absence de pigmentation lors du premier cycle de renouvellement des poils. Un immuno-marquage avec un anticorps anti-DCT des follicules pileux montre une perte progressive des mélanocytes entre 2-7 semaines. BPTF est donc essentiel dans les mélanocytes au stade post-natal.

L'analyse plus poussée du phénotype des étapes post-natales P10, six semaines et un an, en utilisant la DCT-LacZ, qui colore la peau, a montré une persistance remarquable des cellules souches des mélanocytes. Les mélanocytes différenciés, quant à eux, sont complètement absents. Ceci démontre le rôle essentiel de BPTF dans la biologie de la cellule souche des mélanocytes et dans le développement de la lignée mélanocytaire.

Cette étude révèle pour la première fois une interaction fonctionnelle de NURF-MITF in vitro, participant ainsi à une meilleure compréhension de la biologie du mélanome. Les résultats in vivo montrent un phénotype unique montrant ainsi un rôle crucial de BPTF dans plusieurs étapes du développement de la lignée mélanocytaire.

Mots-clés : MITF, NURF, mélanome, remodelage de la chromatine, cellules souches mélanocytaire

2. En Anglais/ In English

The role of the complex of chromatin remodeling NURF in melanocytes and melanoma

Malignant melanoma is the most aggressive of all cancers of the skin and has a very poor prognosis due to its intrinsic resistance to chemotherapy and radiotherapy. A major cause of this resistance is in the plasticity of melanoma cells. Melanomas are constituted by at least two mutually exclusive cell subpopulations; proliferative and invasive cells. These populations are capable of switching between the two phenotypes under the influence of signals from the microenvironment.

The transcription factor MITF (Microphthalmia-associated transcription factor) is the key factor in the regulatory network of genes melanocytic lineage and melanoma. MITF controls the differentiation, survival, melanocyte proliferation and migration as well as the invasive properties of melanoma cells. High levels of MITF are characteristic of proliferative cells, while low expression of MITF is associated with slow cycling cells with increased migratory and invasive capacity.

To determine the target genes of MITF, we performed sequencing of messenger RNA present in melanoma cells after the loss of MITF induced by siRNA, coupled with ChIP-seq cells expressing MITF tagged with 3HA. Both sets of data were compared to identify genes directly regulated by MITF. The results showed that MITF acts as a direct activator of genes involved in DNA replication, repair and mitosis, but it represses genes involved in motility and invasion. That MITF acts as an activator or repressor in a promoter-specific manner can explain its central role in the biology of melanoma at the molecular level.

To better understand how MITF activates or represses transcription, we sought to identify its interaction partners. To this end, the MITF expressing melanoma cells with a double tag were used to perform a tandem immuno-precipitation on soluble and insoluble nuclear fractions (chromatin-associated) coupled to a mass spectrometry analysis. Among MITF interacting proteins in fraction associated with chromatin, we identified all major subunits of chromatin remodeling complex NURF (nucleosome Remodeling Factor) including BPTF, SMARCA1, RBBP4 and SMARCA5.

Chromatin remodeling factors of the ISWI family of provide optimum spacing of nucleosomes and thus play an important role in transcription, replication of the heterochromatin and chromatin assembly. The composition of the NURF complex, a founding member of this family, has recently been determined with high precision, thanks to the quantitative mass spectrometry, showing that NURF is composed of six subunits: BPTF, SMARCA1, SMARCA5, HMG2L1, RBBP4 and BAP18. The largest subunit of NURF, BPTF (Bromodomain PHD- finger transcription factor), first identified in Drosophila melanogaster, is

a protein containing a PHD domain (plant-homology domain) and a bromodomain. These domains interact with histone modifications: the PHD domain interacts with lysine 4 trimethylated histone H3, while the bromodomain recognizes acetylated lysine 16 of histone H4, two marks well known for their association with active transcription.

The involvement of NURF in transcriptional regulation at the biochemical level has long been known, but there are few data on its biological functions. The recently published data describe extremely versatile roles of this this complex. It is involved in the coordination of epigenetic regulation mechanisms which prevents the early differentiation of epidermal stem cells. Furthermore, the subunit SMARCA1 suppresses proliferation and cell migration and attenuates Wnt signaling. Amplification of the locus encoding BPTF was involved in the development of various human cancers, affecting the brain, breast, lung, liver and prostate. Using genetically engineered mice, BPTF was shown to have a role in embryonic development, and the differentiation of thymocytes. Despite the mounting evidence indicating a critical role of complex chromatin remodeling NURF in different aspects of cell biology and cancer, its potential role in the pathophysiology of melanocytes and malignant melanoma is unknown.

I first studied the interaction between MITF and NURF by immunoprecipitation and immunoblotting. I confirmed the co-precipitation in the fraction associated with chromatin between MITF and subunits BPTF, SMARCA1 and SMARCA5 of NURF. To evaluate the role of NURF in melanoma, I focused on the role of BPTF, the largest subunit of NURF and the only one that is specific to this complex; other subunits are present in other remodeling complexes. I infected cell lines and melanoma 501Mel SK28Mel with lentiviral vectors expressing shRNA directed against BPTF. The silencing of BPTF leads to proliferation arrest, changes in morphology, a defective mitosis, with the appearance of multinucleated cells and senescence, while infection with control shRNA had no effect significant. BPTF knockdown cells have many features observed in cells infected in parallel with vectors expressing shRNA against MITF. Using immunoblot, I showed a loss of BPTF does not affect the expression of MITF significantly and vice versa. Therefore, the loss BPTF phenotype can be attributed to loss of MITF. The similarities in the phenotype rather suggest NURF possibly acts as a cofactor for MITF subset of its target genes.

To test this idea, I performed RNA-Seq experiments on shBPTF and shMITF cells using two separate shRNAs for each factor to exclude the off - target effects. Sequencing showed a significant overlap between regulated by MITF and BPTF genes. 42% of the genes whose expression is increased and 30% of the genes whose expression is decreased due to shBPTF are regulated in the same way due to shMITF. I analyzed in more detail whether the regulated public and I was able to demonstrate that 32% of genes increased and 49% of

genes are associated with decreased binding sites MITF suggesting that their regulation by MITF gene is direct. I also noticed that MITF and BPTF co-regulate many genes involved in migration and invasion. ZEB1 is a transcription factor known to regulate epithelio-mesenchymal transition (EMT), acting as a repressor of E-cadherin. The EMT is one of the major events in the development of metastatic tumors, through which cancer cells acquire invasive properties. However, the expression of ZEB1 is greatly increased when the loss of expression of MITF out of BPTF. So these two factors cooperate to repress its expression.

To determine whether BPTF has an independent role of MITF in melanoma, I realized the silencing of BPTF in 1205Lu cells, invasive line does not express MITF. Deleting BPTF led to stopping their proliferation and change in morphology, while the elimination of MITF had no effect, as expected .In contrast, the silencing of several lines BPTF non-melanoma affect not their proliferation significantly. Together these results show that BPTF / NURF is essential for the proliferation of cells derived from melanocyte lineage, but not essential in other cell types.

Having demonstrated the essential role of BPTF / NURF in melanocytic cells, I've set up lines of recombinant mouse BPTF which can be inactivated selectively in melanocytes by crossing mice Bptflox / lox mice with mice with Tyr -Cre and Tyr-Cre-ERT2. Moreover, these mice were crossed with the DCT-LacZ lineage specific staining for melanocytes.

Tyr-Cre mice :: $Bptf^{lox/lox}$ where BPTF is inactivated during embryonic development are born with a low phenotype characterized by a coat of gray belly but a black coat to almost normal back. In addition, a count of embryonic melanocytes with the DCT-lacZ reporter revealed a difference in the melanocyte count at E15.5, and the phenotype was more obvious at E16.6. At this stage, the embryonic melanoblasts shown less proliferation and/or migration, and the typical clusters of melanoblasts accumulating at the hair follicles are greatly diminished. Interestingly, the newborn animals display depigmentation of the extremities, a phenotype reminiscent of the one seen in the embryo. Thus, BPTF is involved in normal proliferation, migration and localization of the embryonic melanoblasts.

At the age of four weeks these mice become progressively whiter. Upon renewal of the first coat, the mutant mice lose their pigmentation. This effect can be clearly demonstrated by experiments which show a complete loss of pigmentation after depilation in the first cycle of renewal of the hairs. An immunolabeling with anti-Dct antibody of the hair follicles shows a progressive loss of melanocytes between 2-7 weeks in the hair bulb. BPTF is essential in melanocytes in postnatally. These observations suggest that BPTF is required to set up and/or survival of adult melanocyte stem cells, which generate melanocytes responsible for pigmentation in the first cycle of postnatal renewal of the coat pigmentation.

The further analysis of the phenotype of the postnatal stages of P10, six weeks and one year using the Dct-LacZ staining of the skin showed a remarkable persistence of the melanocyte

stem cells, while the differentiated melanocytes were completely absent. This demonstrates the vital role of BPTF in normal biology of the melanocyte stem cell and the development of the melanocyte lineage. This is the first report of NURF-MITF functional interaction *in vitro*, adding to the general understanding of the melanoma biology. The *in vivo* results show a unique phenotype, demonstrating a crucial role of BPTF in multiple stages of the development of the melanocyte lineage.

Key words: MITF, NURF, melanoma, chromatin remodeling, melanocyte stem cells

INTRODUCTION

Chapter 1. Melanocyte – from the neural crest to malignant melanoma

1. Melanocyte localization

A. Composition of the human skin

Skin is a complex organ serving as a barrier between the organism and its environment, maintaining its integrity and homeostasis. The multiple functions of skin include protection of the organism, thermoregulation, sensation, control of transpiration, absorption, and water resistance. Skin is composed of three primary layers: The epidermis (provides waterproofness and serves as a barrier to infection), dermis (serves as a location for all skin appendages), hypodermis (subcutaneous adipose layer) (Figure 1).

Epidermis is the outermost layer of the skin. It is a waterproof surface and is consisted of stratified squamous epithelium, and basal lamina, that is underneath. The epidermis does not harbor any blood vessels, and cells in the deepest layers are nourished mainly by diffusion of oxygen from the surrounding air (Stucker et al. 2002) and by blood capillaries extending from the upper layers of the dermis. The cell lineages that contribute to the skin composition are keratinocytes, melanocytes, Merkel cells, and Langerhans cells. The epidermis is separated in several layers as follows: (beginning with the top layer): corneum, lucidum (on hand palms and bottoms of the feet), granulosum, spinosum, basale.

Dermis is the layer of connective tissue underneath the epidermis. The dermis structure is divided into two regions: the papillary region, closer to the epidermis, and the reticular region, an area 2 to 4 mm-thick in the deeper layer of the dermis. It is a layer connective tissue consisted of extracellular matrix (ECM) produced by fibroblasts (Breitkreutz, Mirancea and Nischt 2009). The dermis contains the nerves, blood and lymphatic vessels, and all the epidermal structures including excretory and secretory glands (sebaceous, eccrine and apocrine glands), hair follicles, and nails. Neural sensory organs include Merkel and Meissner's corpuscles (for touch), Pacinian corpuscles (for pressure), and Ruffini corpuscles (mechano-receptors). The receptors of heat, cold, and pain are very rarely a specialized structure. Sensory neurons have a role in this, since their plasma membrane harbors ion channels responding to specific stimuli. One neuron may contain

several ion channels and respond to different sorts of stimuli (Schmelz 2011).

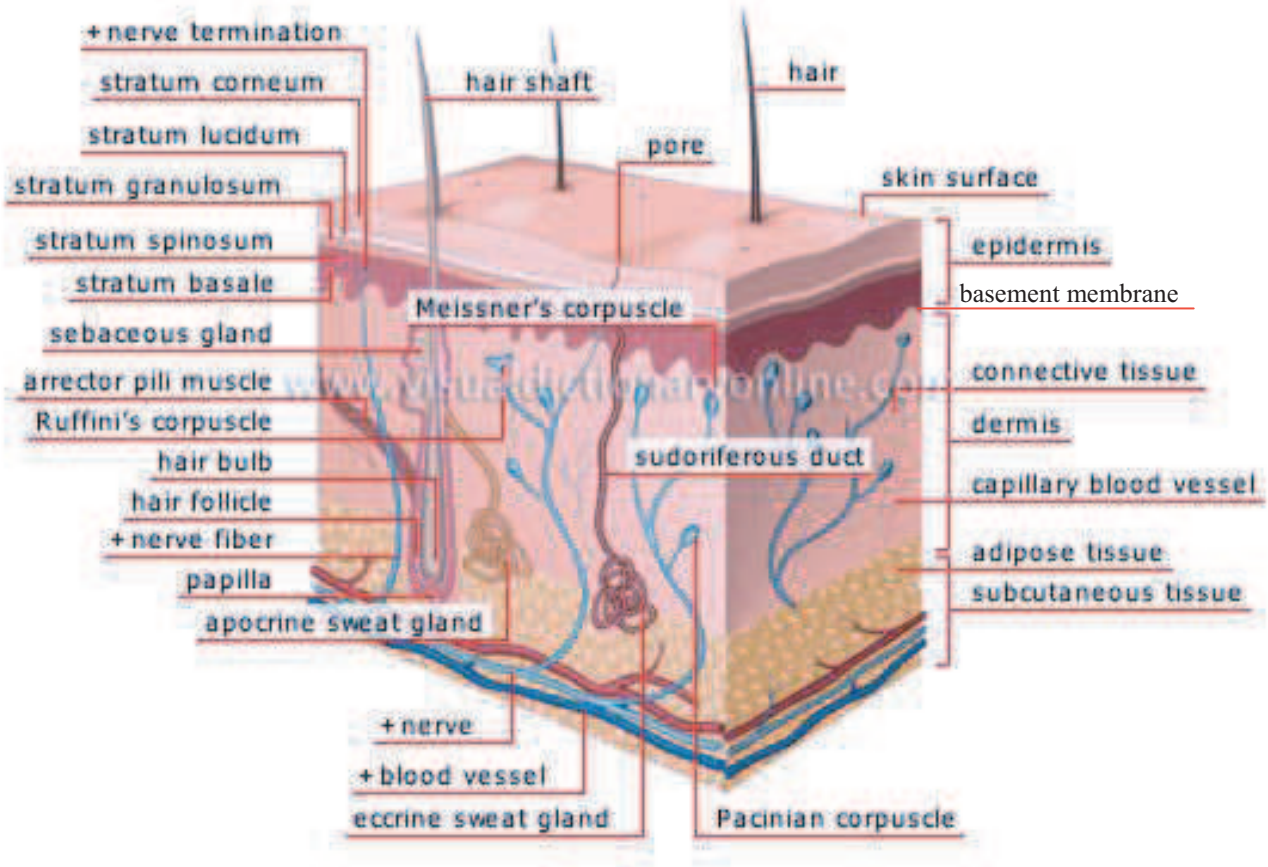

Figure 1 : Cross section of skin in three dimensions

The skin composed of the three main layers; epidermis, dermis and the hypodermis. The layers of the epidermis are equally represented. The structures present in the dermis include the hair follicle, nerve fibers associated to different sensory corpuscles, sebaceous gland, apocrine sweat gland, a layer of connective tissue and capillary blood vessels. The hypodermis contains the layer of adipose tissue, nerves and blood vessels.

Dermal-epidermal junction (basement membrane) is the section of the skin between the dermis and the epidermis. The dermal-epidermal junction serves multiple functions; it tightly interconnects of the epidermis and the dermis, determines the organization of the basal keratinocytes, their polarity and the epidermal architecture. Basal membrane is also important for generation of epidermal strata, providing the attachment point for the proliferating keratinocytes, while the daughter cells migrate towards the higher layers. It also has a role in establishing the selective barrier controlling the exchange enter the epidermis and the dermis. It has crucial role in wound healing.

Hypodermis is not a part of the skin, but it resides below the dermis. The purpose of this layer is to attach the rest of the skin to the bone and muscle tissues lying underneath. The principal cell types residing within hypodermis include fibroblasts, adipocytes, accounting for 50% of the body fat, and macrophages.

C. Epidermal cell lineages

Keratinocyte is the most abundant cell type found in the epidermis, constituting 90% of the cells. Keratinocytes in the stratum basale proliferate and the move up the strata and undergo multiple stages of cell differentiation to eventually become anucleated. This process results in formation of cellular junctions (desmosomes) between keratinocytes that start to secrete keratin, proteins and lipids taking part in formation of the extracellular matrix and provide structural integrity of the skin (Breitkreutz et al. 2009). Keratinocytes are connected to other epidermal cell types such as melanocytes and Langerhans cells, and are also in contact with nerves through tight junctions.

Langerhans cells are dendritic cells (antigen-presenting immune cells) of the skin, derived from the bone marrow. These cells reside in all epidermal layers, and are most abundant in the stratum spinosum. They are also present in the papillary dermis, around blood vessels. The role of Langerhans cells is to maintain immune homeostasis in the skin by regulating activation of resident T-cells, both having a role as antigen presenting cells during skin infections and in maintaining tolerance in normal skin (Seneschal et al. 2012).

Merkel cells are located in the basal layer of the epidermis, and are particularly concentrated in the vicinity of the hair follicles. They are attached to neighboring keratinocytes by desmosomes and have also been shown to connect to melanocytes. these cells react to stimulus and are situated close to the endings of sensory nerves, and are considered to have role as mechanoreceptors detecting touch. They are particularly abundant in the lips, fingertips, palms, back and soles of the feet (Moll et al. 2005).

Melanocytes are cells specialized for melanin production, pigment primarily responsible for skin color, and the color of hair and eyes. They are situated in the stratum

basale of the epidermis, close to the basement membrane (Figure 2). Melanocytes interact with up to 35-40 neighboring keratinocytes. In the humans, melanocytes reside mainly in the epidermis, but can also be found in the eye, inner ear, meninges, bones and the heart. In the mouse, the melanocytes are confined to the hair follicle.

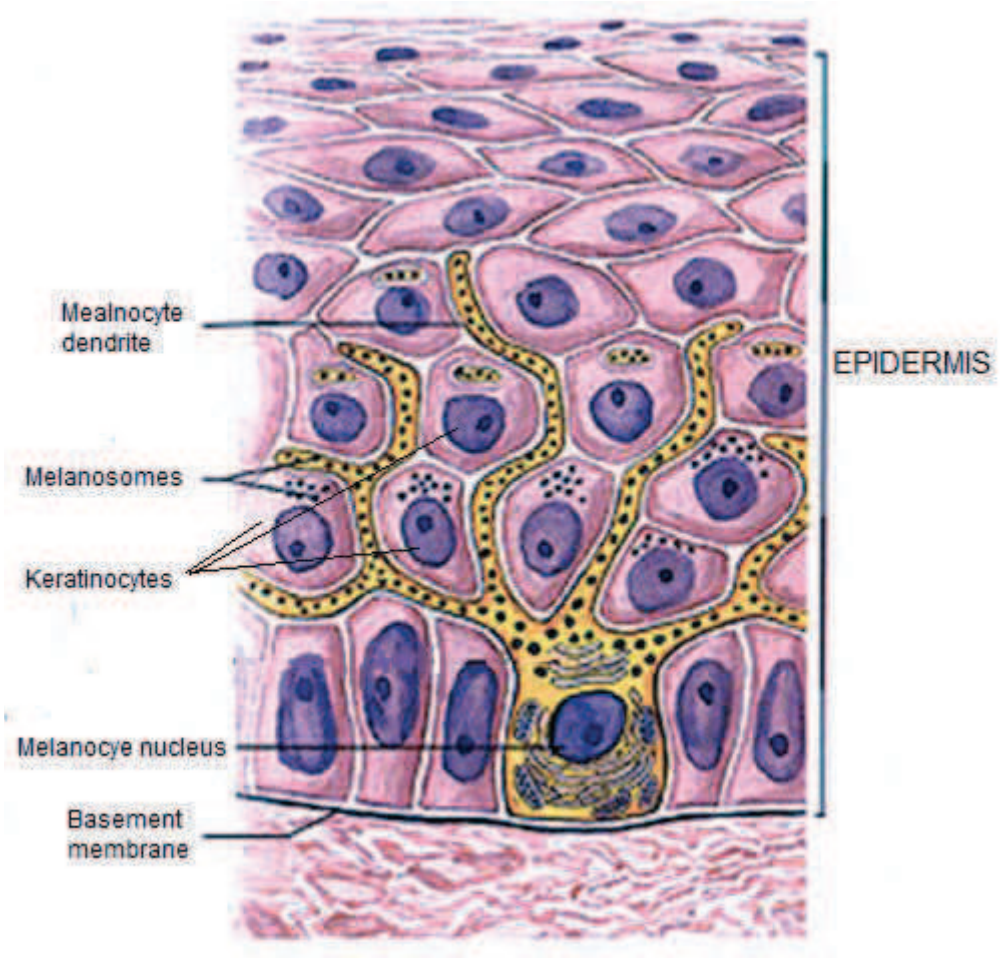

Figure 2 : Melanocyte localization in the epidermis

Melanocytes are localizes in the stratum basale of the epidermis, laying on the basement membrane. They are connected with numerous surrounding keratinocytes via melanocytic dendrites and are utilized for transport of the melanosomes containing pigment.

C. The hair follicles

I. Hair follicle structure

Hair follicle main structures are the papilla, matrix, hair shaft, root sheath, hair fiber, and the bulge. The hair follicle is contains a permanent portion, subdivided into upper (UPP) and lower permanent portion (LPP), and a transient portion (Figure 3). The transient portion of the hair follicle makes up to two thirds of the mature hair follicle is constructed and disintegrated in every hair cycle, while the permanent portion remains constant (Stenn and Paus 2001).

The papilla is an oval structure connected to the connective tissue serving as a capillary access point.

The hair matrix, enveloping the papilla, is consisted of epithelial cells and melanocytes. Cell division in the matrix enables the production cells included in the formation of the all the main structures of the hair fiber and the inner root sheath.

The root sheath is made of an external and internal root sheath. The external sheath is consisted of empty rectangular cells, originating from keratinocytes that terminally differentiate, extrude their organelles and become tightly packed with bundles of 10-nm filaments assembled from cysteine-rich hair keratins, which become physically cross-linked to give the hair shaft high tensile strength and flexibility.

The hair bulge is located in the lower permanent portion of the hair follicle. It is situated close to the sebaceous gland and the erector pili muscle. The hair bulge harbors the multipotent stem cells required for the maintenance of the epidermis and the sebaceous gland, as well as several types of stem cells that give rise to all cell types involved in the hair follicle production (Oshima et al. 2001, Taylor et al. 2000). Follicle stem cells are activated at the beginning of every anagen, during telogen-to-anagen transition (see below).

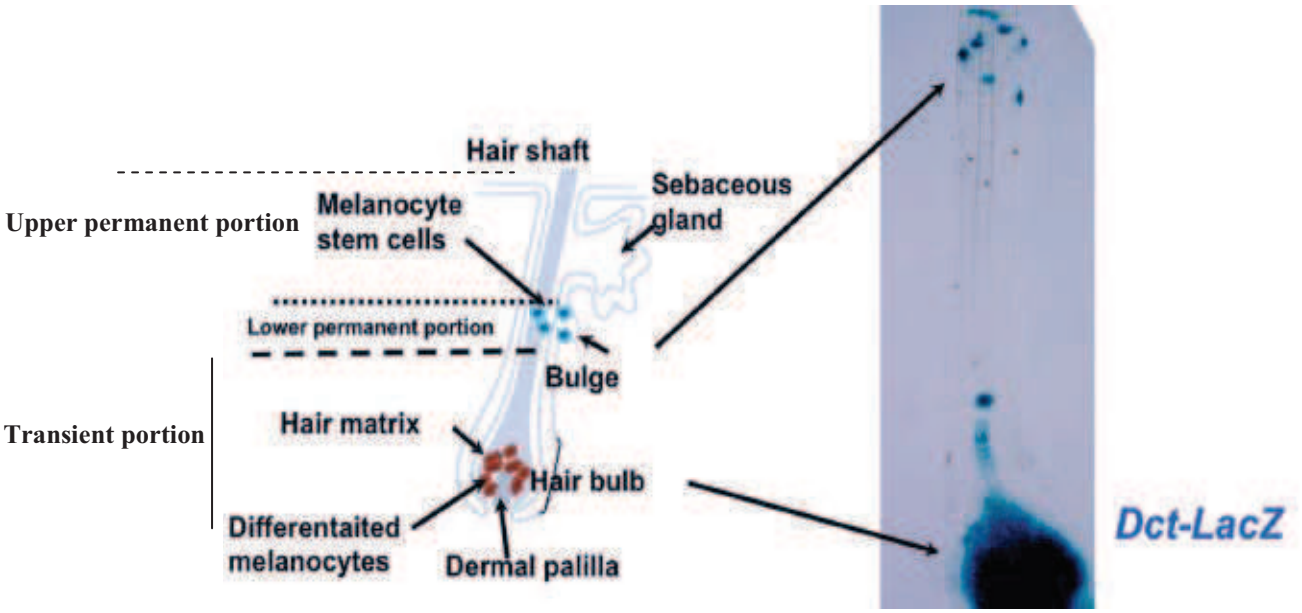

Figure 3 : Schematic representation of the hair follicle

The hair follicle is divided into three sections, upper and lower permanent portions and a transient portion. The melanocyte stem cells reside in the bulge in the lower permanent portion, and get differentiated into melanocytes that migrate into the hair matrix to differentiate and produce pigment (Osawa 2008)

II. Hair follicle cycle

Life-long cycles of hair regeneration include growth (anagen), regression (catagen), relative quiescence (telogen), and hair shedding (exogen) (Figure 4).

Anagen is the growth phase of the hair cycle. During this phase, the hair root is going through rapid cellular divisions, adding to the hair shaft. The duration of this phase is different for different hair types and is genetically determined. At the end of anagen phase, an unknown signal causes the transition into catagen phase. The proliferating matrix cells have cell-cycle length of approximately 18 hours.

Anagen-to-catagen transition. The matrix cells are referred to as transit amplifying cells (TAC) since they go through a limited number of cell divisions before differentiation. As the supply of the matrix cells is being exhausted, hair shaft and the inner root shaft differentiation slow down and the follicle enters the phase of hair follicle disintegration, the catagen. In mice, the first catagen begins in a wave, spreading from the top of the head towards the tail and laterally to the sides of the animal. The onset of first catagen is different for different body parts, and it ranges from P14 for the upper back region to P18 at the lower back. Catagen lasts 3-4 days. (Alonso and Fuchs 2006).

Catagen is the hair involution phase. It lasts for a short time and it signals the end of

active hair growth. It is a dynamic transition between anagen and telogen (Muller-Rover et al. 2001). The process starts with the lower portion connection to the hair shaft, stopping the contact with the blood supply and the proliferating cell population. During this phase, the follicle retracts from a fully grown hair bulb to a structure called the club through the disintegration process of the transient portion of the follicle. The epithelial cells in the bulb and the outer root sheath are eliminated through apoptosis. The bottom of the hair shaft sealed in a club structure moves upward and reaches the non-cycling upper follicle and stays anchored at this position throughout telogen.

Telogen is a dormant phase of the hair follicle cycle. In mice, the telogen length is variable and it depends both of the region of the body and the age of the animal. The first telogen lasts 1 or 2 days. The second telogen lasts longer, 2 weeks or more, beginning at P42 (Alonso and Fuchs 2006).

Telogen-to-anagen transition. The transition back into the growth phase occurs when quiescent stem cells are activated to produce a new hair shaft (Blanpain et al. 2004, Tumbar et al. 2004). These cells begin to proliferate rapidly, produce the transit amplifying cells that have a crucial role in the production of the new hair follicle. The growing hair follicle forms next to the old socket where the old club hair resides which will eventually be shed. The new hair sprouts out from the same pore on the skin as the old one.

Exogen or the hair shedding phase is independent of the telogen and the anagen phases. In the mouse, the exogen phase is overlapping with the mid to late anagen phase. This mechanism ensures the preservation of the integrity of the coat. Since the exogen phase is not synchronized with the hair growth in the mouse, the hair follicle can contain 2-3 hair shafts simultaneously (Milner et al. 2002). In the human, the hair follicle rarely contains more than one hair shaft.

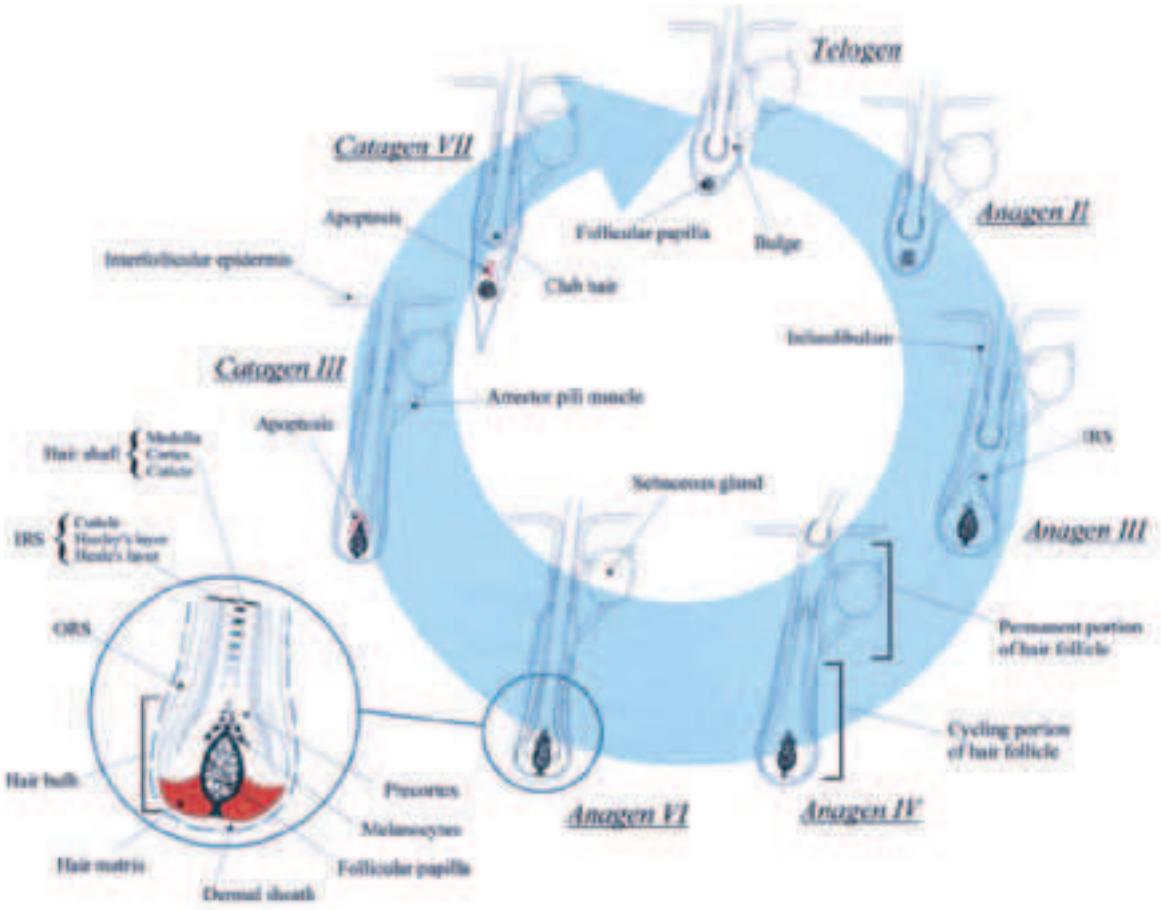

Figure 4 : Hair follicle cycle

The hair follicle cycle includes several stages, starting with anagen, when the cells located in the bulge start proliferation and produce a new hair follicle. The follicles grow through different stages of anagen, reaching the size of the mature follicle, and produce pigmented hair shaft. At the end of anagen, the follicle goes through the catagen, regression phase including the apoptosis of the cells in the hair matrix. The final stage is telogen, the follicle stays quiescent. The close-up on the hair bulb depicts the spatial organization of the matrix cells that are rapidly proliferations, adding to the hair shaft, and the differentiated melanocytes, situated above the dermal papilla (Panteleyev, Jahoda and Christiano 2001).

D. Mouse models utilized in melanocyte and melanoma studies

One of the most commonly used animal models *in vivo* genetic studies is the mouse model. For more than two decades a conditional knock-out models have been used to study the role of multiple genes in various tissues. The Cre/loxP system is used to generate specific spatial or spatio/temporal conditional transgenic mouse lines (Feil 2007).

The Cre recombinase from the phage P1 is a site specific recombinase that recognizes specific sites, termed *loxP* sites and is catalyzing efficient DNA recombination between pairs of *loxP* sites. Cre-mediated recombination between two directly repeated *loxP* sites results in excision of the DNA between them as a covalently closed circle. If the two sites are in inverted orientation, the result will be inversion of the intervening DNA, rather than excision. Breaking and joining of DNA is confined to specific positions in the core region of the recognition site, ensuring a specific recombination down to a nucleotide (Sauer 1998).

The crossing between a transgenic mouse line carrying the locus of a desired gene with inserted loxP sites on either side of the gene, or a part of the gene (floxed gene) with a transgenic mouse with Cre recombinase under the control of a tissue specific promoter will enable a tissue specific ablation of the gene expression. Additional specificity has been accomplished by using the fusion construct of the Cre recombinase with the estrogen receptor (Cre-ER) yielding a mouse transgenic Cre recombinase line in which the expression of the Cre is controlled both spatially, since it is controlled by tissue specific promoter, but also temporally, since the expression of Cre is inducible with tamoxifen (estrogen antagonist) treatment (Metzger et al. 1995).

In the case of the melanocyte lineage the usage of the conditional knock-out has been particularly convenient since the genetic defects can very soon be observed by monitoring the coat color of the animal. Tyrosinase is an enzyme taking part in melanin synthesis and it has melanocyte-specific expression. The mouse transgenic line expressing Cre under regulation of the Tyrosinase (Tyr) promoter was the first model used to study melanocyte biology (Delmas et al. 2003). Subsequently created transgenic mouse lines created also utilized the Tyr promoter, but under the Cre-ER^{T2} regulation (Bosenberg et al. 2006, Yajima et al. 2006).

Another transgenic mouse model widely used is the knock-in line carrying a lacZ construct coding for β-galactosidase under the control of the *Dct* promoter. *Dct* (*TRP2*) is a gene involved in the pigment production, but additionally, it is expressed as early as primary and secondary melanoblasts, enabling more detailed study of melanoblast migration and proliferation during embryonic development. Furthermore, *Dct* is one of the rare genes that are marking the melanocyte stem cells in the hair bulge of the mouse hairs, enabling the study of the stem cell niche in the adult (Mackenzie et al. 1997).

2. Melanocyte cell lineage establishment and maintenance

During embryonic development, melanoblast survival, migration and their subsequent differentiation into melanocytes depends on multiple signaling pathways and transcription factors. These include Wnt signaling, Endothelin3/Endothelin B receptor, KIT/KITL, Notch, TGFβ. Additionally, important transcription factors such as PAX3, SOX10 and MITF are also crucial for the lineage.

The Microphthalmia-associated transcription factor (MITF) is a member of the basic helix-loop-helix-leucine zipper (bHLH-LZ or hHLHZip) transcription factor protein family. MITF has been shown to be a master regulator of the melanocyte cell lineage. It has a pivotal role in many different aspects of the melanocyte biology, including melanocyte survival, proliferation and differentiation. Because to the crucial importance of MITF in this work, a more elaborate description of the MITF locus organization, and associated functions will be discussed later.

The above mentioned signaling pathways and transcription factors have been shown to regulate melanocyte cell lineage specification from the neural crest, the survival and migration during embryonic development, establishment and maintenance of the lineage in the epidermis and the hair follicle, and melanocyte function in pigment production. Many of the transcription regulators and signaling pathways regulate each other and form a very intricate network of regulation in all stages of melanocyte biology. This will be discussed in detail in the upcoming sections.

A. Melanocytes originate in the neural crest

All melanocytes are derived from a group of migratory embryonic cells referred to as the neural crest (NC) (Dupin, Creuzet and Le Douarin 2006, Le Douarin and Kalcheim 1999). Neural crest cells (NCC) initially arise in the central nervous system, at the interface between the neural plate and the adjacent non-neural ectoderm. The neural crest formation is induced by BMP, Wnt, Fgf and Notch signaling coming from the surrounding structures of the mesoderm and prospective epidermis (Figure 5). These signals induce the expression of the transcription factors that will drive the further specification of the neural plate border and the formation of the neural crest (Meulemans and Bronner-Fraser 2004). Multiple studies striving to elucidate the interactions and relationships between the neural crest specifiers have shown Msx1 induces the expression of Pax3 and Zic1, that is in turn inducing Snail2 (Slug) in a Wnt-dependent manner by combined action of Pax3 and Zic1 (Monsoro-Burq, Wang

and Harland 2005). Once the neural crest is formed, the individual neural crest cells are specified under the control of the neural crest specifiers, including Snail, AP2, FoxD3, Twist, Id, Sox9 and Sox10, and c-Myc (Meulemans and Bronner-Fraser 2004).

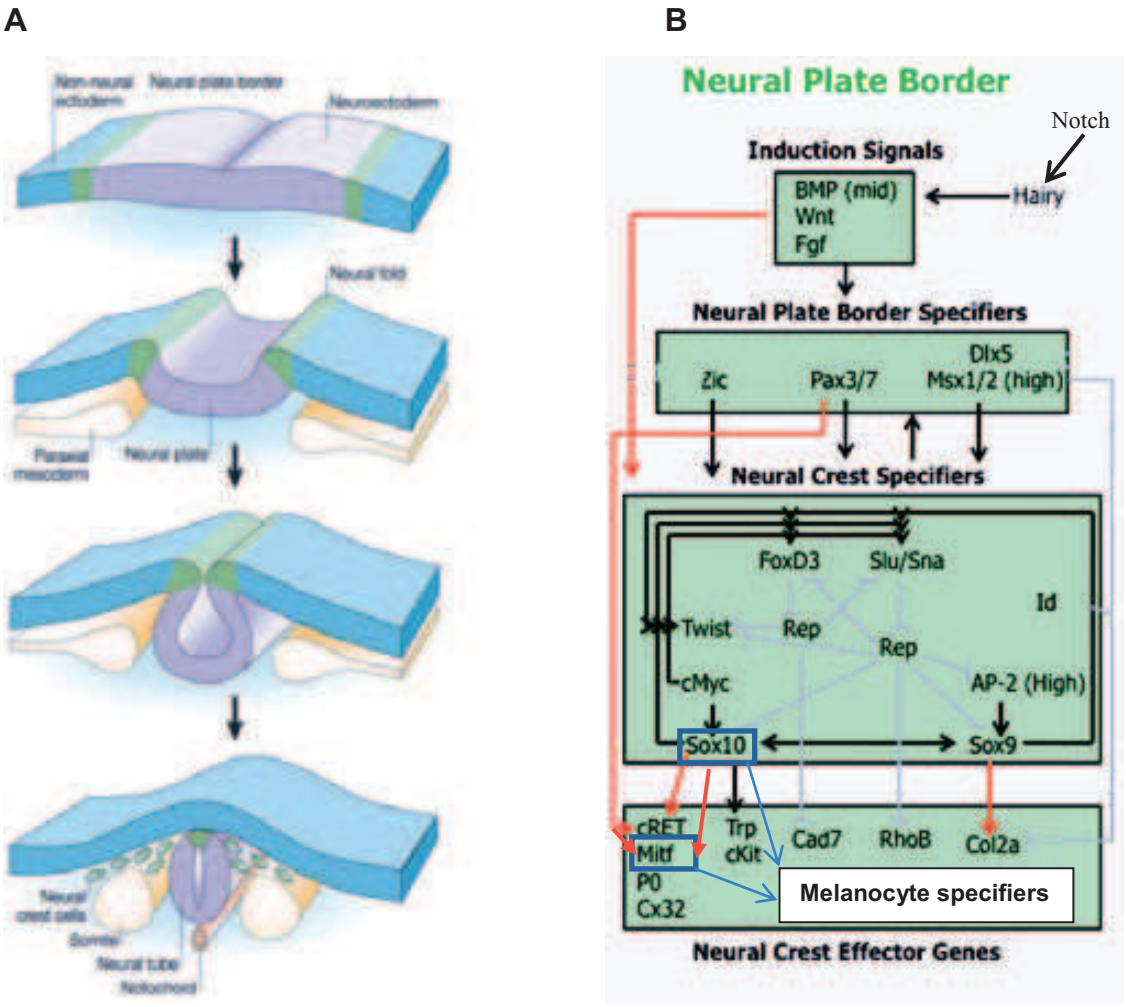

Figure 5 : Transcriptional network regulating neural crest differentiation

A) Stepwise development of the neural crest (green) from the surrounding tissues, epidermis (blue) and the neural plate/neural tube (purple) **B)** The signaling pathways in differentiation of the neural crest include BMP, Wnt and Fgf signaling during the specification of the neural plate border, Pax3, Zic Msx1, Sox10 during the neural crest specification. Further cell type specifiers are listed in the bottom panel. The specifiers of melanocyte lineage include Pax3, Sox10 and Mitf (Gammill and Bronner-Fraser 2003, Meulemans and Bronner-Fraser 2004).

Neural crest cells detach from the neuroepithelium after fusion of the neural folds, migrate extensively throughout the developing embryo and give rise to a wide range of cell and tissue types. These include neurons and glial cells of the peripheral nervous system, the secretory cells of the adrenal medulla, certain cardiac structures, enteric ganglia, and connective tissues of the craniofacial skeleton. The cells originating from the neural crest adopt two migration paths, dorsolateral or dorsoventral. Early cells migrate dorsoventrally providing peripheral glia, sympathetic and sensory neurons, whereas dorsolateral cells differentiate exclusively as melanocytes (Marmigere and Ernfors 2007) (Figure 6).

The basis of the cell fate specification lies both in the temporal emergence of the cells form the NC and multiple signaling pathways regulating the lineage specification. A study by Krispin et al. (Krispin et al. 2010) proposed the NC derivatives follow ventral to dorsal migration pathway within the NC prior their delamination, and their temporal emergence is dictating the cell fate. Furthermore, the differences in the expression level of the NC specifiers FoxD3, Sox9 and Snail2 throughout the process of NCC delamination, namely their gradual down-regulation, is also suggested to play an important role in the NCC fate determination. Previous reports have shown that down-regulation of FoxD3 is required for MITF up-regulation and melanogenesis (Thomas and Erickson 2009). The differential expression of FoxD3, Sox9 and Snail2 in prospective neural lineages, but not melanoblasts points to the early molecular differences between the individual fates and suggests that all the cell lineages originating from the NC are lineally segregated prior their emergence (Krispin et al. 2010).

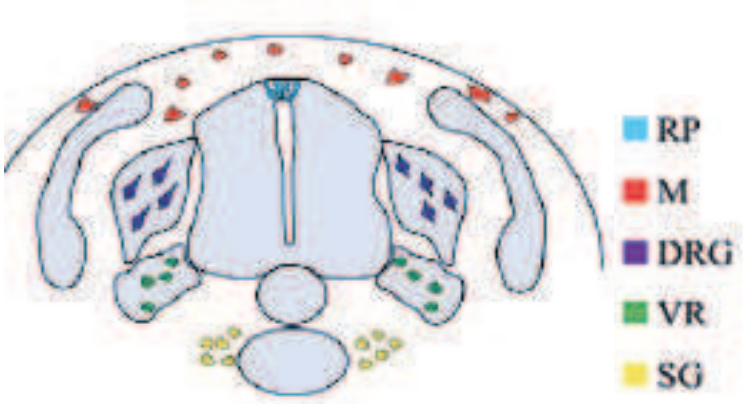

Figure 6 : Spatial delamination of the NC derivatives

The representation of the migration routes of the NC derivatives. Color code presents their final homing sites. The different lineages include RP (roof plate, light blue), M (melanocytes, red), DRG (dorsal root ganglia, purple), VR (ventral root, green), SG (sympathetic ganglia, yellow) (Krispin et al. 2010).

Human conditions related to the genes involved in NC-melanocyte regulatory network

I. *Waardenburg syndrome (WS).* This syndrome is a hereditary disorder that causes hypopigmentation of the hair and eyes, patchy depigmentation of the skin and hearing impairment. Based on the additional symptoms, WS is classified into WS1, WS2, WS3 and WS4. WS1 and 3 is caused by Pax3 mutations, and additional symptoms include ocular deformation for WS1, and severe defects in the limb muscles for WS3. WS2 displays the typical WS symptoms listed above. It is caused by mutations in *MITF*, *SOX10, EDN3/EDNRB* and very rarely *SNAIL2.* The *SOX10* mutation also causes a syndrome called Yemenite deaf-blind hypopigmentation syndrome (YDBS), considered to be as a WS2. WS4, also known as Waardenburg–Shah or Hirschsprung Waardenburg syndromes, displays a range of phenotypes reminiscent of both WS (pigment deficiencies and deafness) and Hirschsprung disease (HSCR) (aganglionic megacolon), and it is caused by *SOX10* and *EDN3/EDNRB* mutations (Pingault et al. 2010).

II. *Teitz syndrome.* It is a syndrome closely related to the WS2, and it is caused by *MITF* mutations. However, it is characterized by a uniform dilution of pigmentation and not the patchy depigmentation seen in WS (Pingault et al. 2010).

III. *Piebaldism*. It is a depigmentation disorder, characterized by patches of white skin. The hearing and eye pigmentation are normal. It is caused by *KIT* and *SNAIL2* mutations (Sanchez-Martin et al. 2003).

B. Signaling pathways involved in melanocyte development

I. The Wnt signaling pathway in melanocyte development

The Wnt signaling pathway has been shown to have a crucial role in melanoblast and melanocyte cell lineage. WNT are secreted glycoproteins that have multiple roles in neural crest induction, specification and melanocyte differentiation. Wnt signaling comprises several modes of activation, including canonical Wnt/β-catenin pathway, and non-canonical Wnt/Ca^{2+} and planar cell polarity (PCP) pathways.

In the best understood canonical WNT/β-catenin signaling pathway, WNT ligands bind to the receptor Frizzled (Fz), and activate the signaling pathway resulting in β-catenin accumulation and translocation into the nucleus. β-catenin is a structural protein associated to adherens junctions. In the absence of the Wnt signal, cytoplasmic β-catenin is degraded by a β-catenin destruction complex, composed of Axin, adenomatosis polyposis coli (APC), protein phosphatase 2A (PP2A), glycogen synthase kinase 3 (GSK3) and casein kinase 1α (CK1α) Phosphorylation of β-catenin within this complex by CK1α and GSK3 targets it for ubiquitination and subsequent proteolytic destruction by the proteosomal machinery. Binding of Wnt to its receptor complex composed of the Fz and the low-density-lipoprotein-related protein5/6 (LRP5/6) triggers a series of events that disrupts the APC/Axin/GSK3 complex that is required for the targeted destruction of β-catenin. The binding of Wnt to the Fz/LRP5/6 complex induces a conformational change of the receptor enables the interaction of the Fz with the Dishevelled (Dsh) protein that facilitates the binding of Axin to a conserved sequence in the cytoplasmic tail of LRP5/6, thus disrupting the destruction complex (Clevers and Nusse 2012). As a result, β-catenin accumulates in the cytoplasm and translocates into the nucleus, where it interacts with members of the lymphoid enhancer binding factor 1/T-cell specific factor (Lef1/Tcf) family of transcription factors (Nelson and Nusse 2004). Wnt/β-catenin and LEF1 interact functionally in the nucleus, resulting in β-catenin mediated transcriptional regulation (Behrens et al. 1996).

In vitro studies of cultured both mouse and avian neural crest cell cultures activation of the Wnt signaling, either by treatment with Wnt or activation of β-catenin promoted pigment cell development (Dunn et al. 2000, Jin et al. 2001). In vivo, in zebrafish a constitutive activation of β-catenin in the NC promotes the formation of melanocytes while the neural cell lineages are suppressed. On the contrary, upon the Wnt signaling inhibition, the NCCs assume the neural rather than melanocyte fate (Dorsky, Moon and Raible 1998). Two Wnt factors, Wnt1 and 3a, are necessary for melanoblast development in the embryo (Dorsky et al. 1998, Ikeya et al. 1997). In the mouse, the β-catenin expression in the

migratory NCC population is regulating cell specification. Ectopic expression of β-catenin in the premigratory NC results in development of the neural lineages and abolishes melanocyte development. (Lee et al. 2004). On the other hand, constitutive β-catenin in the early migratory NCC population results in strong reduction of the neural lineages, but leads to the ectopic melanoblast formation (Hari et al. 2012). The ectopic expression of β-catenin in the later developmental stages, using the Tyr-Cre model, enabling the constitutive expression of β-catenin in the already established melanoblasts did not alter their proliferation rate (Delmas et al. 2007, Hari et al. 2012).

Mitf is a target Wnt pathway in various species (Widlund et al. 2002). In zebrafish, the reduced TCF signaling or mutations in the promoter binding site resulted in loss of Mitf expression, indicating β-catenin is required for Mitf transcription activation Wnt/β-catenin activates Mitf by binding to the TCF/LEF1 binding site in the *Mitf* promoter (Dorsky, Raible and Moon 2000). In cultured melanocytes, Wnt-3a induces the expression of endogenous *Mitf* by transactivating the MITF promoter via the LEF-1-binding site. (Takeda et al. 2000b). Furthermore, MITF physically interacts with LEF-1, activating of the *Dct* promoter. The bHLH-LZ region of MITF-M is responsible for the unique interaction with LEF-1, as it is not interacting with TCF1 (Yasumoto et al. 2002). In addition, MITF is cooperating with LEF1 to regulate its own expression. The two factors act synergistically and the interaction with the β-catenin is important for their cooperation. Moreover, MITF recruited on the M promoter functions as a non-DNA-binding cofactor for LEF-1 (Saito et al. 2002). It has also been shown Mitf interacts directly with β-catenin, and via this interaction, Mitf acts to sequester β-catenin form the Wnt/ β-catenin signaling target-genes in order to activate transcription of the Mitf-specific target promoters (Schepsky et al. 2006).

The non-canonical Wnt planar cell polarity (PCP) pathway is activating the small GTP hydrolases belonging to the Rho superfamily (most studied are Rac1 and RhoA), via guanine exchange factor (GEF). One of the functions of the Rho GTPases is activating Rho-associated kinase (ROCK), one of the major cytoskeleton regulators (Gordon and Nusse 2006, Komiya and Habas 2008). Deletion of Rac1 in embryonic mouse melanoblasts results in aberrant migration, and also defects in cell cycle progression and cytokinesis (Li et al. 2011a). Furthermore, Rac1 has an important role downstream of mutant $NRas^{Q61K}$ in the survival of the melanocytes (Li et al. 2012a). Another factor in this pathway, P-Rex1, a Rac-specific Rho GTPase guanine nucleotide exchange factor (GEF), is crucial for embryonic melanoblast migration, since its deletion results in a white belly phenotype (Lindsay et al. 2011).

II. The KIT (c-Kit)/KITL (SCF) signaling pathway

Kit (also known as *c-Kit*) is a receptor tyrosine kinase that has been shown to be encoded by the locus *W (Chabot et al. 1988)*. The ligand activating the kinase, KITL (Kit ligand, also known as stem cell factor (SCF), Steel factor or mast cell growth factor-MGF) is encoded by *Sl(Steel)* locus (Copeland et al. 1990). Activation of KIT receptor by KITL ligand results in receptor dimerization and its subsequent autophosphorylation. KIT signaling is required for the melanoblast survival and migration (Cable, Jackson and Steel 1995, Mackenzie et al. 1997, Wehrle-Haller and Weston 1995). A mouse line with point mutations in c-Kit displays multiple defects related to the neural crest-derived pigment cells, hematopoietic cells, and primordial germ cells. Indeed, homozygote mice are black-eyed, white, deaf, sterile and anemic (Ruan, Zhang and Gao 2005).

Kitl produces two KITL proteins, a transmembrane and a soluble form. The transmembrane form is required for melanocyte precursor survival in the dermis, while the soluble form is needed during early melanoblast dispersal on the lateral migration pathway form the neural crest, and also for their initial survival within the neural crest premigration area (Wehrle-Haller and Weston 1995). Experiments using a monoclonal anti-KIT antibody (ACK2) also revealed an important role of SCF/KIT signaling in the postnatal melanocytes (Nishikawa et al. 1991, Okura et al. 1995). Melanocyte stem cells (MSC) survive independently of c-kit signaling in a transgenic mouse model. However, MSCs migration out of the hair follicles is KIT-signaling dependent (Kunisada et al. 1998). Botchkareva et al. demonstrated the anti-c-KIT antibody completely abolished the transient melanocyte population, evidenced by the white coat of the animals, but the melanocyte stem cells were intact, showing c-KIT is not required for their function (Botchkareva et al. 2001). Recently, a study performed in zebrafish aimed to decipher what part of the melanocyte regeneration is c-Kit regulating, establishment of the MSC niche, production of daughter cells or proliferation and differentiation of the daughter cells. The Kit mutants were not able to regenerate the MSCs, and the undelaying cause of this phenotype was shown to be the aberrant establishment of the MSCs (O'Reilly-Pol and Johnson 2013).

III. Endothelin 3 (Edn3) / Endothelin receptor B (EdnrB) signaling

The endothelin signaling system consists of the G protein coupled-receptors, endothelin receptors A (EndrA) and B (EndrB), and three ligands binding the receptors, endothelin- 1, 2 and 3. Ednrb binds all three isopeptides with equal affinity (Saldana-Caboverde and Kos 2010). Edn1 or Edn3 binding to Ednrb results in the activation of multiple

signaling pathways, such as protein kinase C (PKC), MAPK and CREB/A-CREB (Bohm et al. 1995, Sato-Jin et al. 2008).

The interaction of EDN3 with EDNRB is essential for development of neural crest-derived cell lineages, including melanocytes and enteric neurons, evidenced by studies on mice carrying *Ednrb* mutations (Baynash et al. 1994, Hosoda et al. 1994, Lee, Levorse and Shin 2003, Reid et al. 1996). Ednrb is required for the melanoblast proliferation, migration and survival E10 and E12.5, which corresponds to the period the NCCs are about to leave the premigration area. Since the Ednrb mutant phenotype could be rescued by activating the Ednrb gene as late as E10, it appears that Ednrb is not required prior to the melanoblast migration. Furthermore, the rescue of the phenotype was not efficient after E12.5, suggesting End3/EdnrB is not required after melanoblasts leave the NC (Shin et al. 1999). Antother study also showed a severe phenotype at E12.5 using combined transgenic model harboring mutation in *Ednrb* and Ednrb-LacZ reporter line (Lee et al. 2003).

End3/EdnrB signaling has been shown to cooperate with Sox10 during enteric nervous system and melanocyte development. Animals that were heterozygous for both mutations exhibited an increase in white spotting and loss of melanocytes in the inner ear (Stanchina et al. 2006).

IV. TGFβ signaling pathway

The transforming growth factor beta (TGFβ) pathway is involved in multiple acpects of cell biology, including proliferation, differentiation and apoptosis, and is important both in the embryonic development and in the adult.

The TGFβ signaling pathway involved two kinds of receptors, type I and type II. Ligand binding induces heterodimerization involving two type II and two type I receptors, resulting in phosphorylation of a glycine-serine (GS)-rich region in the type I receptor by the type II receptor. The downstream target of this signaling is the Smad pathway, for the phospho-GS region serves as a binding site for the Smad proteins (R-Smads). R-Smad proteins are divided in two distinct branches: the TGFb-Smad pathway (R-Smad2/3) or the BMP-Smad pathway (RSmad1/ 5/8). TGFb signaling-mediated Smad pathway is further activated by Smad anchor for receptor activation (SARA). Binding of R-Smads phosphorylates two serines in the C-terminus of the protein by the type I, resulting in R-Smad dissociation from the receptor complex and binding to the common Smad (coSmad), Smad4. The R-SMAD/coSMAD complexes translocate in the nucleus, where they take part regulation their target genes (Wrana 2013).

In melanocytes, TGFβ1 cooperates with the KIT/KITL signaling to promote

melanoblast proliferation and differentiation. The anti-TGFβ1 antibody inhibits the cell growth, and results in repression of the expression of the KIT protein and mRNA (Kawakami et al. 2002). TGFβ has also been shown to have a crucial role in melanocyte differentiation and sun tanning response, since in the absence of UV radiation, keratinocytes secrete TGFβ which blocks melanocyte differentiation via PAX3 inhibition (Yang et al. 2008). In the melanocyte stem cells, TGFβ signaling is activated at the point when stem cells re-enter the quiescent state (Nishimura et al. 2010), discussed further in the section on melanocyte stem cells below.

C. Transcription factors regulating the melanocyte lineage

Melanocyte cell lineage is regulated by a wide collection of transcription factors involved in neural crest development, and are mediators of the connection between multiple signaling pathways controlling melanocyte development, differentiation, survival and melanocyte stem cell maintenance.

I. SOX transcription factors

The Sry-related HMG box (Sox) family consists of transcription factors that contain a conserved HMG box DNA-binding domain. Sox genes have multiple roles in cell specification and differentiation, many of them functioning together with cell type-specific transcription factors (Bowles, Schepers and Koopman 2000).

SOX10

Sox10 is expressed early during neural crest development; it starts to be expressed in the NCC as they start migrating from the premigration area in the NC (Hari et al. 2012).

SOX10 mutations have been associated to multiple human conditions, including WS4, HSCR and YDBS. Using the mutant Sox10 mouse model several studies have shown crucial roles of Sox10 in peripheral nervous system and melanocyte development. (Britsch et al. 2001). Moreover, the mutant embryos completely lack melanoblast population and the NCC primary cultures generated from these embryos are unable to produce melanocytes (Potterf et al. 2001).

Sox10 cooperates with other crucial transcription factors expressed during melanocyte, such as Mitf and Pax3. Mitf promoter contains several SOX binding sites, flanking a PAX3 binding site. Both Sox10 and Pax3 activate *Mitf* promoter, whereas Sox10 activation (100x) is notably higher than the one with Pax3 (5x). However, these two factors

activate the promoter synergistically (200x) when co-transfected. These results suggest that MITF is downstream of SOX10 and PAX3, and that the hypopigmentation and deafness observed in WS individuals with mutations in these three genes are all ultimately caused by a disruption in MITF function (Potterf et al. 2000).

Sox10 and Pax3 also bind melanocyte-specific *Mitf* enhancer, resulting in synergistic activation of *Mitf*. Due to a specific enhancer organization, Pax3 and Sox10 need to bind individually in order to achieve synergism. The mutation in the transactivation domain of Sox10 abrogates Pax3-Sox10 interaction, and leads to loss of Mitf expression. (Lang and Epstein 2003, Potterf et al. 2000).

Apart from the role of SOX10 in melanocyte differentiation, it serves as a co-activator of a set of Mitf target genes critical for pigmentation, including Dct, Tyr, and Trp1. Sox10 and Mitf directly activate *Dct* transcription on their own, identifying *Dct* as the direct Sox10 target in melanocytes. Moreover, Sox10-dependent activation of *Dct* is synergistically enhanced by Mitf (Ludwig, Rehberg and Wegner 2004).

Sox10 and Mitf are co-expressed in migrating melanoblasts in the mouse embryos but their expression differs in cells of the newborn inner ear (Watanabe et al. 2002). Moreover, Sox10 is not expressed in the hair follicle MSCs, but it is expressed in the differentiated cells in the hair bulb (Osawa et al. 2005). Recently, SOX10 has also been shown to be important in the MSC pool renewal. A mouse model constitutively expressing Sox10 was used to assess the role of ectopic expression of Sox10 on the melanocyte lineage. Sustained Sox10 expression causes premature differentiation of the MSCs. This leads to exhaustion of the MSC pool and results in a premature hair graying, confirming the importance of precise regulation of Sox10 expression in all aspects of melanocyte cell lineage biology (Harris et al. 2013).

SOX2.

Expression of Sox2 is associated to development of the melanocytes arising from Schwann stem cell precursors. Expression of Sox2 is gradually diminished during development of development of both neural crest- and SCPs. The expression of Sox2 has also been shown to be inversely correlated with Mitf expression, and it has been suggested Sox2 and Mitf co-repress one another. SCP-derived melanocytes arise from a small population of nerve associated melanoblasts and their migration is regulated by receptor B (Ednrb) and Wnt5a signaling. (Adameyko et al. 2012).

Recently, a possible alternative origin and migratory pathway of in the trunk proposes melanocytes differentiate from Schwann cell precursors (SCPs) situated in nerves. (Adameyko et al. 2009, Budi, Patterson and Parichy 2011). The cranial melanocytes are derived both from neural crest- and SCP-derived progenitors regulated by interactions of

SOX2 and MITF. Nerve-arising melanocytes are further regulated by endothelin receptor B (Ednrb) and Wnt5a signaling (Adameyko et al. 2012).

II. PAX transcription factors

Vertebrate Pax genes are related to the *Drosophila* paired-rule gene, *paired*, which encodes a protein with two DNA binding domains, a paired domain (PD) and a paired-like homeodomain (HD).

PAX3

Pax3 is expressed very early in the development of the neural crest and it has a role in neural crest specification (Meulemans and Bronner-Fraser 2004). NCCs migrating in the dorsolateral pathway differentiate into the melanoblast lineage, and maintain Pax3 expression. Pax3 is one of the factors in a transcriptional network (along with Sox10 and Mitf) crucial for melanocyte lineage survival and differentiation, MSCs and melanin synthesis (Boissy and Nordlund 1997, Sommer 2005). The role of Pax3 in melanocytes in exerted through its direct binding to the promoters of multiple melanocyte specific genes, such as the *Mitf* (Watanabe et al. 1998) and *Trp1* (Galibert et al. 1999) and *Dct* (Lang et al. 2005).

Pax3 can act both as an activator or a repressor, and Sox10 has been shown to enhance Pax3 activity. Pax3 and Sox10 bind *c-RET* and *Mitf* enhancers and synergistically activate the expression of these target genes, but the mechanisms to modulate their expression differ. In the case of *c-RET* enhancer, only Pax3 DNA-binding is sufficient for synergistic action of Sox10 and Pax3, while on the *Mitf* enhancer, binding of both factors is required for synergistic activation (Lang and Epstein 2003). Furthermore, Sox10 and Pax3 synergistically activate *Mitf* when bound to the consensus sites within its promoter (Potterf et al. 2000). Pax3 binding to a cis regulatory enhancer located upstream of *Mitf* involves its paired and homeodomain (Corry and Underhill 2005, Watanabe et al. 1998).

Pax3 also been shown to have a crucial role in MSC maintenance. Pax3 cooperates with Sox10 to activate Mitf. At the same time it acts as a repressor of the Dct enhancer, competing with Mitf for the binding. Pax3 is further exerting repression of the Dct enhancer by recruiting repressor Grg4. The repression mediated by Pax3 has been shown to be relieved through activation of the Wnt signaling in the embryonic melanoblasts (Lang et al. 2005). In contrast, Pax3 has been shown to be expressed in the MSCs together with Dct. Besides Dct, Pax3 is the only other protein shown to be expressed in the MSC in the LPP (Osawa et al. 2005).

Recently, a novel strategy of pigmentation induction has been reported. FGF2/STAT3 pathway has been shown to modulate Pax3 expression in response to UVB radiation. Fgf2 has been shown to be secreted by the keratinocytes in response to UVB, the signal which stimulated STAT3 phosphorilation (P-STAT3). Furthermore, P-STAT3 directly targets Pax3

and activates its expression. Pax3::Tyr-Cre mouse model showed increased pigmentation compared to the wild type, evidenced by increase in both melanocyte count and melanin production (Dong et al. 2012)

PAX6

Pax6 has been shown to be important for development of the retina (Marquardt et al. 2001). A transgenic mouse line with abolished Pax6 expression in retinal pigment epithelium (RPE) showed Pax6 has multiple roles in pigment production in the retina. Pax6 is regulating the RPE-specific isoform of Mitf and is also anting synergistically with Mitf to activate genes involved in pigmentation (Raviv et al. 2014).

D. Melanocyte colonization of the epidermis and the hair follicles

In the mouse, in all hair covered regions the melanocytes are confined to the hair follicles, but it the regions of non-hairy skin (tail, snout, ears) the melanocytes are in the epidermis and are pigmented (Mayer 1973). Melanocytes migrating thorough the skin enter the hair follicles at very early stage of their morphogenesis. Once they colonize the epidermis, melanoblasts proliferate extensively in the first 24 hours. Since given area of skin can support limited number of melanocytes, the numbers of melanocytes remain constant while they redistribute between epidermis and the dermis. They colonize the hair follicles in regular spacing, resulting in increased number of melanoblasts residing in the hair follicles. At E19 interfollicular melanoblasts undergo a second round of proliferation. By P4, over 90% of the melanocytes are confined to the hair follicles. Localization of melanoblasts to hair follicles is an active process and it requires KIT/KIT ligand signaling to enhance migration of the melanoblasts into the hair follicles (Jordan and Jackson 2000).

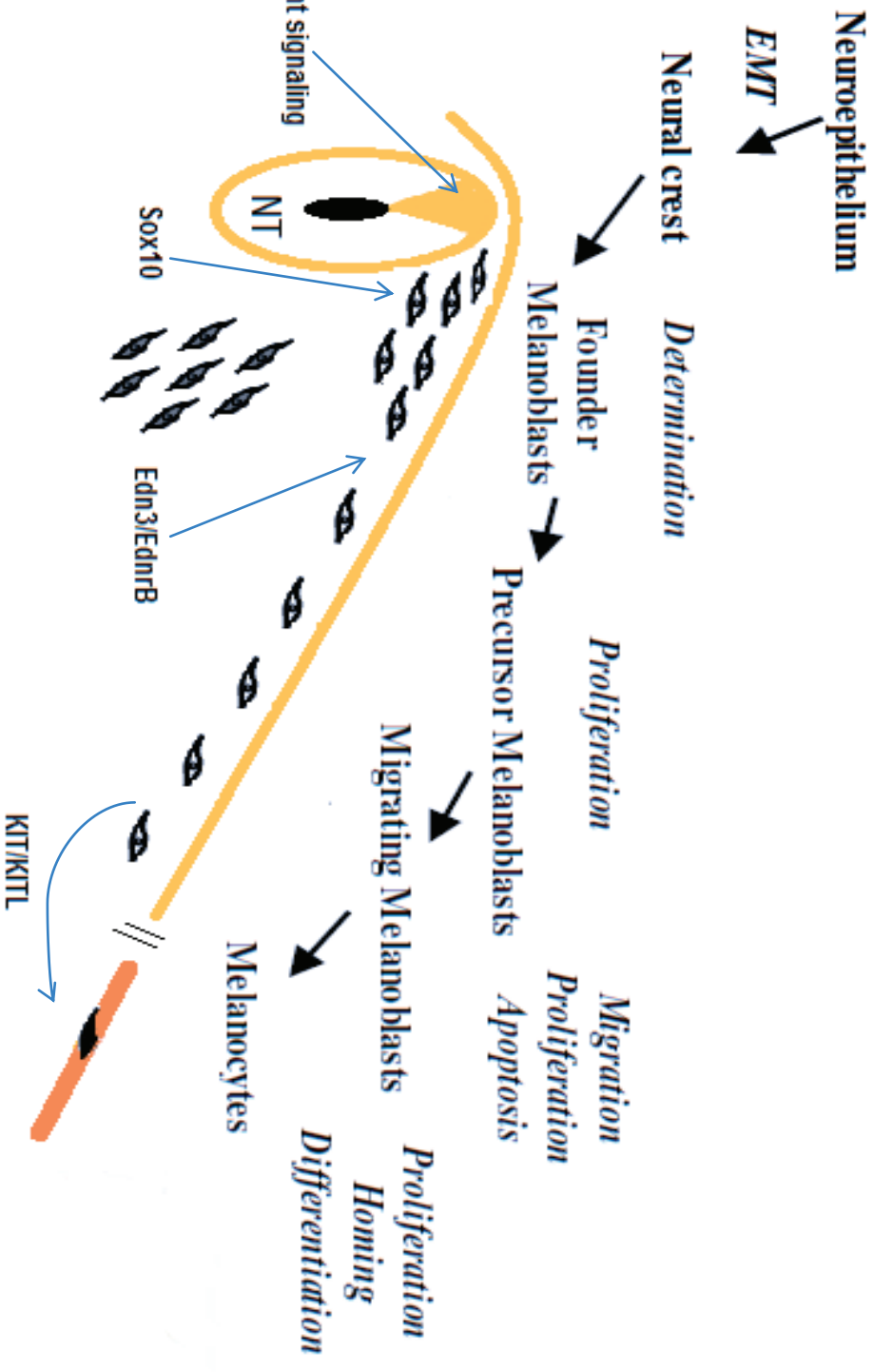

Figure 7 : Development, migration and homing of the melanocyte lineage

The melanocyte lineage is delaminated from the neural crest and specified under control of Wnt signaling and Sox10 expressed in the neural crest and immediately after the NCCs leave the NC. Further migration and survival of the melanoblasts is regulated by endothelin 3 signaling. Final homing step is regulated by KIT/KITL signaling (Adapted from (Larue, Kumasaka and Goding 2003)).

E. Melanocyte stem cells

Generally, cells need to fulfill two conditions to be considered stem cells. First is the stem cell self-renewal; as they divide, they maintain the stem cell population. Second, they provide the specialized and differentiated daughter cells of their specific tissue type.

Melanocyte stem cells (MSC) are a source of transient amplifying cells and differentiated melanocytes, and have been studied most extensively in the mouse. An advantage to studying the murine melanocyte is that growth and apoptosis are paired to the growth cycle of the hair follicle. The stem cells were first identified using the BrdU incorporation staining, since these cells are slow cycling and were described as label-retaining cells (Cotsarelis, Sun and Lavker 1990). The Dct-LacZ transgenic mouse model has been used to study MSCs in vivo, taking advantage of the fact Dct is one of the rare MSC markers identified to date (Mackenzie et al. 1997).

I. Melanocyte stem cell discovery and establishment of the niche

A remarkable study by Nishimura et al. has been the first to demonstrate the cells in the LPP as the MSCs together with the role the niche in the stem cell determination. By using the anti-Kit antibody, the authors have depleted the dividing and pigment-producing cells, without affecting quiescent unpigmented MSCs. After the first hair cycle, there was a partial recovery of pigmentation, from the hair follicles that retained Dct-LacZ expression in the bulge, namely in the dorsal over hairs and in ventral sensory hairs, which develop earlier than other hairs. Furthermore, the LacZ+ cells colonized the bulge area as early as P0.5 and survived in Kit-independent manner, with low or undetectable Kit expression. The BrdU-label retaining capacity of the Dct-LacZ+ cells situated in the LPP was also shown, confirming these cells as the quiescent, slow cycling cells.

In order to confirm the Dct-LacZ+ cells in the LPP are indeed stem cells, the authors implanted different portions of the hair (UPP, LPP and bulb) into albino neonatal mice, to reconstitute the hair follicles. Only the LPP implants produced pigmented hair, demonstrating the LPP region to be the stem cell niche, and the Dct-LacZ+ cells to be MSCs (Nishimura et al. 2002).

II. Proliferation and differentiation of the MSCs

Apart from the MSC, the hair follicle is also a niche for epithelial stem cells (ESC). The ESCs are multipotent and can give rise to multiple cell types, including keratinocytes and

follicular cells. Because these two stem cell populations reside at the same location, it is possible there would be interactions between them. The hair follicle The HF undergoes cylices driven by the proliferation and differentiation of epithelial stem cells (EpSCs) residing in the bulge area as well as the secondary hair germ (sHG) (Ito et al. 2004).

In a study conducted by Rabbani et al, the authors demonstrate interactivation between the two stem cell populations within the niche. Furthermore the study demonstrates the role of the Wnt signaling pathway in the biology of the both of the stem cell types.

During telogen, β-catenin could be detected only in the cytoplasm of Trp2+ MSCs in the bulge-sHG area. At the anagen onset, both ESCs and MSCs that co-localize in the sHG display nuclear β-catenin, indicating active canonical Wnt signaling. The authors utilized two different strategies to investigate the role of Wnt/β-catenin signaling. First was the constitutive activation of β-catenin using Tyr-CreER^{T2}:: β-catenin$^{fl(ex3)/+}$ mouse line. The mutant MSCs displayed ectopic accumulation of β-catenin in the nucleus, which resulted in the premature differentiation of the MSCs, and ectopic pigmentation in the bulge area. After several hair cycles, the mutant mice started to display premature hair graying, suggesting that constitutive Wnt signaling drives MSC premature differentiation, their loss of self-renewal capacity, and ultimately leads to exhaustion of the MSC pool.

β-catenin depletion in the MSCs in the transgenic mouse model also resulted in premature hair graying. This resulted in aberrant differentiation of the bulb melanocytes. However, the bulge MSCs were still present and unpigmented. Furthermore, the Wnt ligands expressed by ESCs activate Wnt signaling the MSCs during early anagen. β-catenin stabilization in ESCs promotes melanocyte proliferation, which is mediated by Edn3/EdnrB signaling (Rabbani et al. 2011).

III. MSC quiescence, maintenance in undifferentiated state and self-renewal

While Wnt signaling pathway is important in MSC proliferation and differentiation, several other signaling proteins and pathways have a role in MSC quiescence, maintenance in undifferentiated state and their self-renewal such as TGFβ signaling pathway, Bcl2, and the Notch pathway.

TGFβ signaling proteins are expressed during catagen and promote apoptosis that results in complete regression of the hair shaft. In the cells of the bulge, expression of the nuclear phospho-Smad2 can be detected, indicating activated TGFβ signaling. The exposure to TGFβ signaling pathway promotes cell-cycle arrest, both in vitro and in vivo. In vitro, TGFβ induces cell cycle arrest, and it also abrogates pigment production by down-regulating MITF and its downstream target genes required for melanogenesis. In the mouse, TGFβ signaling is required to maintain the MSC pool by regulating the re-entry of the cells in the quiescent

state. Conditional ablation of TGFβ signaling by one of the TGFβ signaling, TGF-b type II receptor (TGFbRII) in the melanocyte lineage in the mouse causes incomplete maintenance of MSCs and results in mild hair graying (Nishimura et al. 2010). The process of establishment of the quiescent state is dependent of Bcl2. The mutant mouse harboring melanocyte-specific expression of mutant Bcl2 also results in progressive hair graying and complete loss of the MSCs in the bulge region due to apoptosis as they re-enter the quiescent state. However, the Bcl2 ablation has more pronounced phenotype, since the hair graying is faster and more complete (Nishimura, Granter and Fisher 2005).

The Notch signaling pathway components comprise the surface receptors Notch1-4, and ligands Jagged-1, 2 and Delta-like (Dll)1-3. Ligand binding to the receptor stimulates proteolytic cleavage, resulting in the release of the intracellular domain of Notch (NIC), which is translocating to the nucleus and binding to CSL transcription factors, in mouse known as recombination signal binding protein-J (RBP-J), activating various target genes, including transcription of repressors belonging to the HES (Hairy/Enhancer of Split) family (Radtke, Schweisguth and Pear 2005).

In melanocytes, the conditional knockout of the Notch1 and Notch2 receptors using the Tyr-Cre mouse line does not show any defects in melanoblast proliferation and/or migration during the embryonic development (Schouwey et al. 2007).

The result of conditional ablation of RBP-J was a striking loss of coat color from birth, and the phenotype was further accelerated by depilation. Histological analysis of the mutant animals showed a dramatic reduction of the melanocytes in the hair follicles at P4 and virtually complete absence if the melanocytes at P34. In addition, Notch signaling has a vital role in the maintenance of the MSCs in the mutant animals, evidenced by complete absence of Dct-expressing cells in the bulge. Ectopic expression of Hes1 under the control of Dct promoter was able to rescue the mutant phenotype, indicating Hes1 is the predominant Hes transcription factor governing the Notch signaling-activated transcription regulation in melanocytes. (Moriyama et al. 2006).

Additional studies using RBP-Jk, Notch1 and Notch2 conditional ablation using the Tyr-Cre mice have shown both of the receptors are essential for regeneration of the pigment cell population during the hair cycle. Both homozygous Notch1 and Notch2 mutants are very similar to the RBP-J mutant, while the double knockout of the receptors exhibits even more accelerated process of coat color loss (Schouwey et al. 2007). Further characterization of the RBP-J mutant in combination with Dct-lacZ expression showed several additional roles of the Notch signaling in melanocytes. The absence of the Notch signal causes MSC premature differentiation in the bulge. Furthermore, Notch-deficient matrix melanocytes cannot produce pigment. Finally, MSCs and melanocytes exhibited ectopic localization in the mutant animals,

such as the area within the dermal papillae, or the dermis in vicinity of the LPP (Aubin-Houzelstein et al. 2008).

A

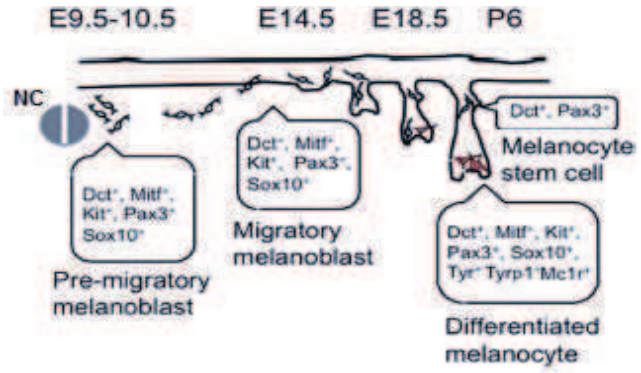

B

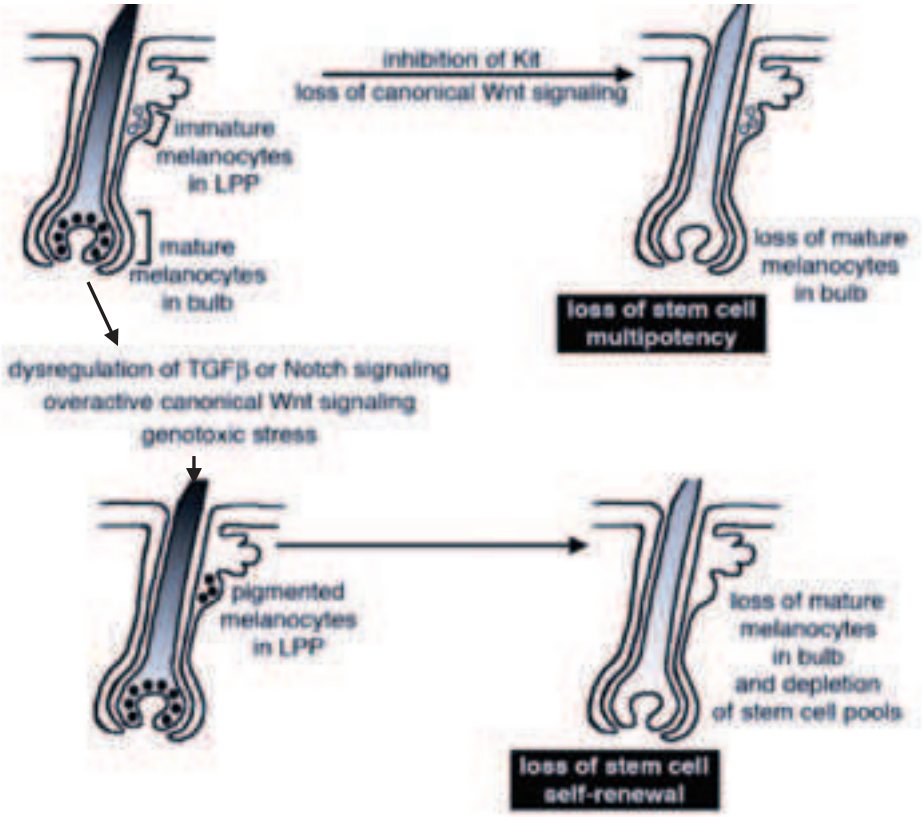

Figure 8 : Melanocyte stem cell establishment and maintenance

A) The regulatory network controlling the melanocyte lineage includes expression of Dct and Pax3 from very early stages of melanocyte development and is maintained in the melanocyte stem cells (adapted from (Osawa 2008)).
B) Different mechanism regulating melanocyte stem cell maintenance and self-renewal. Inhibition of the KIT signaling and loss of canonical Wnt signaling results is loss of multipotency of the MSCs. The MSCs remain in the bulge, but are unable to generate progeny. TGFβ and Notch signaling loss, overactive Wnt signaling and genotowic stress results in premature differentiation of the and exhaustion of the MSC pool (adapted from (Lang, Mascarenhas and Shea 2013)).

F. The role of melanocytes in pigmentation

Pigmentation of the skin is a multi-step process, occurring both in the epidermis and the hair follicles. It starts with the synthesis of melanin in melanosomes, the specialized melanocytes, followed by their transfer to keratinocytes by the use of melanocyte dendrites.

I. The melanin unit – epidermal and follicular melanocyte interactions

The functional organization of the keratinocytes and the melanocytes in the epidermis in termed “the epidermal melanin unit” (Haass et al. 2005). Keratinocytes stimulate melanocyte growth dendricity and pigment production by secreting multiple factors such as growth factors (FGF, SCF, HGF), hormones like α-MSH, and cytokines such as TGFβ (Figure 9).

In the hair follicles, the melanocytes to keratinocytes ratio is 1:5 (Slominski et al. 2005). Pigmentation of the hair follicle is more complex and it involved coordinated action of the follicular melanocytes, keratinocytes in the matrix and fibroblasts residing in the dermal papilla. The pigmentation system in the follicle is called “hair melanin unit” or “follicular melanin unit”. Hair melanocytes are larger and have more dendritic projections than their epidermal counterparts (Slominski et al. 2005, Tobin 2011). Epidermal melanocytes are long-living cells, while hair follicle melanocytes die through apoptosis at the end of every the hair cycle. The pigment production is initiated and ongoing only during the anagen phase; it is significantly reduced in the catagen, and completely absent during telogen (Tobin 2011, Nishimura 2011).

II. Molecular basis of the suntan response

External signals of melanogenesis in the epidermis, also known as suntan response, primarily include UV radiation-mediated production of α-melanocyte-stimulating hormone (α-MSH). The gene encoding α-MSH is pro-opiomelanocortin (POMC), a multicomponent precursor for α -MSH (melanotropic), ACTH (adrenocorticotropic), and the opioid peptide -endorphin (Kippenberger et al. 1996). α-MSH is produced and secreted following UV by both keratinocytes and melanocytes in the skin (Schauer et al. 1994). The levels of POMC/ α-MSH are greatly elevated as a response to the UV radiation, and the main sensor and effector of this response is p53 (Cui et al. 2007). Melanocortin-1-receptor (MC1R) is expressed in melanocytes and is activated upon stimulation with the α-MSH. MC1R has been shown to be important in tanning and pigmentation in humans (Valverde et al. 1995). TGFβ signaling has been shown to be crucial for regulation of the tanning response. In the

absence of the UV radiation, TGFβ is secreted by the keratinocytes and is repressing PAX3, resulting in low expression of MITF and pigmentation related genes. Upon UV radiation, TGFβ repression of PAX3 is released through p53 activation of AP-1, acting as a repressor of TGFβ (Yang et al. 2008). Additionally, the signaling cascade αMSH/MC1R is also regulated by MITF, since MC1R is a direct MITF target (Aoki and Moro 2002).

The α-MSH/MC1R signaling, through G-protein coupled receptor, activates the adenylate cyclase (AC) and results in production of cAMP. Signaling via cAMP has multiple downstream targets. These include protein kinase A (PKA), MAPK/ERK (mitogen activated protein kinase/extracellular signal-regulated kinase) signaling pathway. Phosphatidyl Inositol-3-kianse (PI3K) pathway is in turn inhibited by the cAMP signaling. The activated PKA further phosphorylated the cAMP response element-binding protein (CREB). CREB is a transcription factor that is principally responsive to the α-MSH/AMPc that is going through the surface receptor MC1R, which can be antagonized by Agouti protein (Goding 2000). The isolation of the MITF promoter revealed a cyclic AMP (cAMP) responsive element (CRE) at position -140 to -147 to the transcription start site (Bertolotto et al. 1998a, Fuse et al. 1999). Elevated cAMP levels are inducing the CREB binding to the promoters of MITF, which is activating the enzymes involved in pigment production, tyrosinase, Trp1 and Dct, through highly conserved M-box in their promoters (Bertolotto et al. 1998a, Bertolotto et al. 1996, Bertolotto et al. 1998b). Sox10 is also required for Mitf activation by cAMP signaling through Creb1. Direct Creb1 activation of Mitf requires Sox10 to bind a second DNA element upstream of CRE. The MITF promoter responsiveness to cAMP has been shown to be SOX10-dependent, and vice versa, SOX10 transactivation required the presence of CRE. (Huber et al. 2003).

The MAPK/ERK signaling pathway is also induced by cAMP signaling and is further phosphorylating MITF. The phosphorylation of MITF regulates the protein level by inducing its degradation by the proteosomal machinery, and thus inhibiting melanogenesis. This negative regulation of MITF levels protects the cell of toxic effects of melanin overproduction (Busca and Ballotti 2000).

The PI3K pathway is inhibited by the cAMP activation, resulting in the further inhibition of the Rho-GTPases which are regulating the actin cytoskeleton. The cAMP-mediated inhibition of the Rho-GTPases results is morphological changes increasing the melanocyte dendricity. Furthermore, targeted inhibition of the p70S6-kinase, a downstream target of PI3K singaling, results in augmentation of tyrosinase expression (Busca and Ballotti 2000).

The stress-mediated p38 activaton in response to UV radiation activates CREB, resulting in activation of MITF mediated transcription (Saha et al. 2006). Furthermore, activated p38 phosphorylates Upstream stimulatory factor 1 (USF1), another bHLH-LZ

transcription factor. Activated USF1 binds tyrosinase promoter and promotes its expression (Galibert, Carreira and Goding 2001). A mouse model harboring mutant USF1 lacks the UV radiation-mediated tanning response. Namely, the activation of POMC, MC1R and the melanogenesis enzymes is abolished in the absence of USF1 (Corre et al. 2004).

III. Melanin synthesis and melanosome production

Two main types of melanin are synthesized within melanosomes, pheomelanin and eumelanin. Melanin production has multiple beneficial traits including absorption of UV radiation, protecting the DNA from UV-induced damage, scavenging of the free radicals, ion storage and coupling of the redox (oxidation-reduction) reactions (Bush and Simon 2007, Costin and Hearing 2007, Riley 1997).

Pigment production starts with hydroxylation of tyrosine catalyzed by tyrosinase (Tyr), resulting in production of L-3,4-dihydro xyphenylalanine (DOPA). DOPA is then oxidized, giving DOPAquinone, which is the common precursor of the two types of melanin. Pheomelanin is produced in a reaction of DOPAquinone with cysteine, producing 3- or 5-cysteinylDOPA, that gives rise to the red pigment. DOPAquinone undergoes spontaneous cyclization producing DOPAchrome. DOPAchrome subsequently diverges into two pathways of eumelanin production, one involving the loss of the carboxylic acid and generation of 5,6-dihydroxyindole (DHI), which undergoes oxidation and polymerization giving rise to the brown-black melanin. The second eumelanin pathway involves several additional enzymatic reactions; DCT (DOPAchrome tautomerase) catalyzes production of the DHI-2-carboxylic acid (DHICA). Tyrosinase and TRP1 catalyze further conversions obtaining finally a lighter brown color DHICA-melanin (Simon et al. 2009, Slominski et al. 2005).

MITF is also regulating the melanosome biosynthesis and transport by regulation genes important for this process. These genes include the membrane transporter Aim1, shown to have a role in albinism (Du and Fisher 2002), MLANA/MART1 and SILV/PMEL17/GP100 involved in melanin biosynthesis, melanosome maturation and structure, (Du et al. 2003, Kobayashi et al. 1994) and RAB27a involved in melanosome transport (Chiaverini et al. 2008).

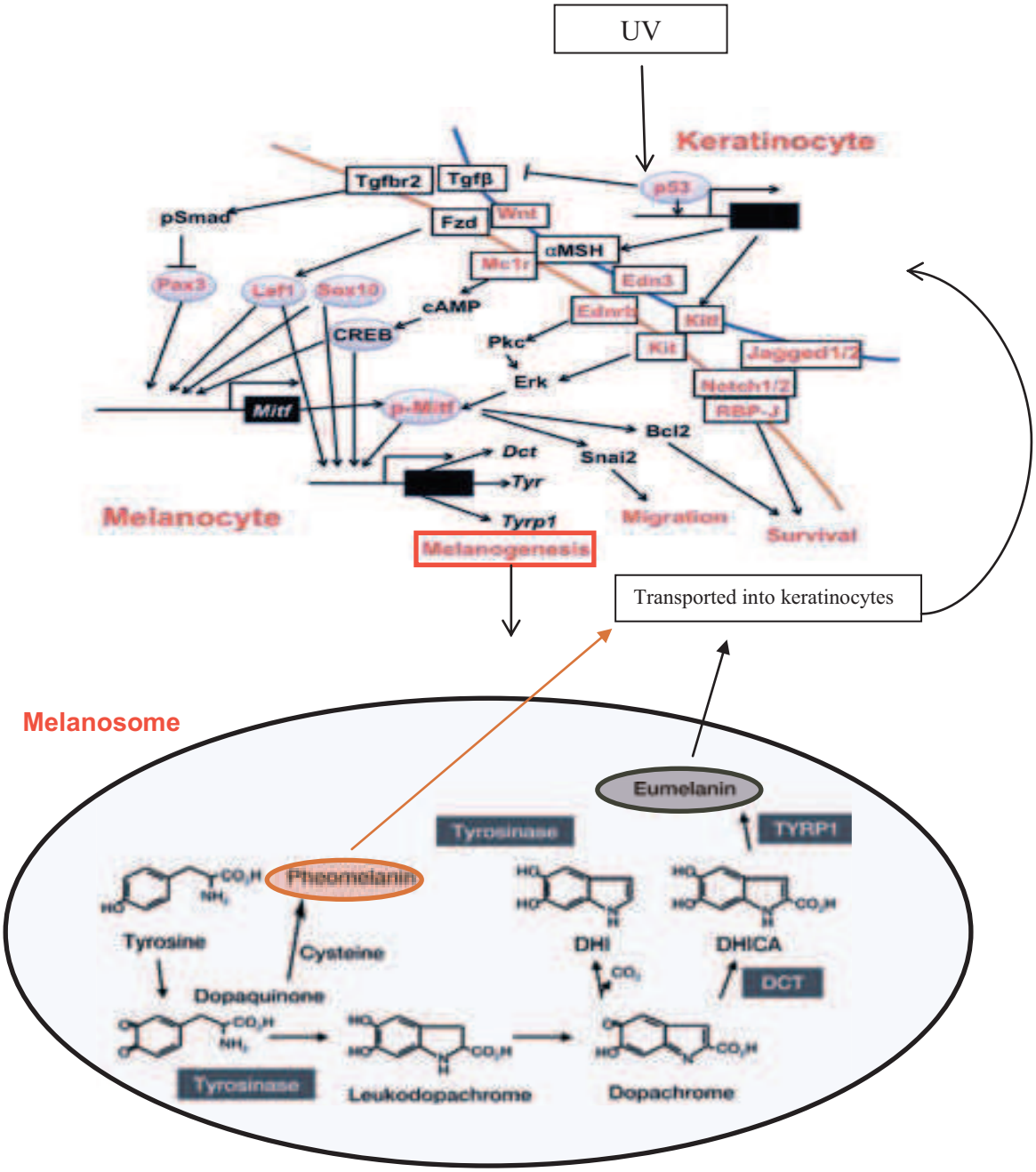

Figure 9 : Tanning response – keratinocyte-melanocyte interaction leading to pigment production

Keratinocytes and melanocytes interact in the epidermis, where upon UV radiation keratinocytes secrete multiple signaling molecules, including KITL, αMSH, TGFβ and others resulting in onset of pigment production. The details of the pigment production reactions are described in the text. (adapted from (Osawa 2008)).

IV. Role of melanocytes in diversity of human pigmentation

Human skin harbors all types of melanin, and the ratio between them determines pigmentation (Yamaguchi, Brenner and Hearing 2007). For different ethnic groups, pigmentation is preserved and is dependent on the ratio of eumelanin versus the other pigments (Slominski et al. 2004). Eumelanin possesses better photoprotective properties when compared to the pheomelanin, including its increased stability and its ability to eliminate reactive oxygen species (ROS) (Abdel-Malek, Kadekaro and Swope 2010).

The human skin type classification was first proposed by Fitzpatrick et al in 1975, and was later modified to include non-white skin types (Fitzpatrick 1988). The scale proposes six different skin types on the basis of respective content of pigmentation in each case and the ability of every type of skin to develop appropriate tanning response. The different skin types range from very fair to dark brown or black (Table 1).

Skin Type	Skin color	Hair Color	Reaction to the UV radiation
I	White or very pale	Red	Always burns, never tans
II	Pale white with beige tint	Blond	Always burns, sometimes tans
III	Beige to light brown (olive)	Chesnutt	Sometime burns, always tans
IV	Light to moderate brown	Dark brown	Rarely burns, always tans
V	Medium to dark brown	Black	Rarely burns, tans more than average
VI	Dark brown to black	Black	Never burns

Table 1 : Fitzpatrick (1988) scale for skin-type classification

G. MITF – the master regulator of the melanocyte cell lineage

One of the prototypical pigmentation loci is the *microphthalmia* locus, becoming more important for many divergent fields of research. The first mutation at this locus was discovered by researcher Paula Hertwig in Berlin in 1942 (Hertwig, 1942, also in (Steingrimsson 2010)) among the progeny of the mice irradiated with X rays. The author describes the mice with the mutation in the locus as white with very small eyes (microphthalmic) and had named the locus *mi*. The gene corresponding to this locus, *Mitf,* was cloned in 1992 and first published in 1993 (Hodgkinson et al. 1993).

I. The MITF locus organization

The *mi* locus coding the *Mitf* gene is a complex locus mapped to human chromosome 3p14. 1-p12.3.(Tachibana et al. 1994, Tassabehji, Newton and Read 1994), and in the mouse it is mapped to chromosome 6 (Hodgkinson et al. 1993). In mice and humans, the gene contains nine distinct promoters, six of which are linked to different coding exons and three to non-coding exons (Hallsson et al. 2000, Hallsson et al. 2007, Hershey and Fisher 2005, Steingrimsson, Copeland and Jenkins 2004), Figure 10. These alternative promoters code for nine different isoforms that have been identified to date expressed from the *mi* locus: MITF – A, B, C, D, E, H, J, M and Mc. The first 5' exon differs for all the isoforms, and it is spliced to common exons 2 through 9, resulting in proteins differing in their sequence. All isoforms however share a common set of C-terminal exons encoding the transactivation and bHLH-Zip DNA binding and dimerization domains (Steingrimsson et al. 2004). The MITF-M isoform originates from an intronic promoter that is active only in the melanocyte lineage (Hodgkinson et al. 1993). Isoforms A, B and H are principally expressed in the RPE and the heart, respectively, but are ubiquitously expressed at lower levels in various tissues (Oboki et al. 2002, Udono et al. 2000) Isoforms C and J are expressed in many cell types, including RPE (isoform C), but absent from melanocytes (Fuse et al. 1999, Hershey and Fisher 2005). MITF-D is preferentially expressed in RPE, macrophages and osteoclasts, but it is not expressed in melanocytes (Takeda et al. 2002). MITF-E and MITF-Mc are preferentially expressed in mast cells (Takemoto, Yoon and Fisher 2002).

The additional complexity of the locus is evident in the splicing not only the first exon, generation the different isoforms, but also the exons 2 and 6, generation variants of the different isoforms. The differential splicing of the exon 6 of the gene is giving rise to two distinct mRNA populations, named (+) and (-). The sequence that differs in the two proteins is located upstream from the basic region required for DNA binding. As a consequence, the two variants have different DNA binding affinity (Hemesath et al. 1994, Steingrimsson et al. 2002). The importance of the different splicing isoforms has been demonstrated by the

analysis of the *mi-sp* mutation in the 6a, that is a Mitf (-) specific mutation, showing the Mitf (+) is able to compensate for additional mutations, while Mitf (-) is not (Bismuth, Maric and Arnheiter 2005, Moore 1995). In addition, the Mitf (+) and not Mitf (-) isoform has been shown to inhibit cell proliferation *in vitro*, by interfering with the S-phase of the cell cycle (Bismuth et al. 2005). A study performed on a number of melanoma samples demonstrated the differential expression of the two isoforms, namely a substantial increase in the expression of the Mitf (-) isoform in a subset of metastatic tumors (Primot et al. 2010), demonstrating an additional mechanism of regulation of the function of MITF and a possible role in melanoma development.

To date, at least 25 different mouse lines harboring different *Mitf* mutations have been characterized, (Hou and Pavan 2008). Homozygous Mitf mice mutants, like $Mitf^{Mi}$ (microphthalmia), $Mitf^{mi\text{-}ew}$ (mi-eyeless-white), $Mitf^{Mi\text{-}wh}$ (Mi-white), $Mitf^{mi\text{-}vga\text{-}9}$ (a transgenic insertion allele) survive but have very small eyes (microphthalmic), are devoid of coat pigmentation and are profoundly deaf due to the loss of the melanocyte lineage. $Mitf^{mi\text{-}vga\text{-}9}$ harbors an insertion in the sequence of the Mitf-M promoter, attesting the Mitf-M to be the indispensable in the melanocytes, since none of the other isoforms compensate for this loss (Hou and Pavan 2008), Figure 10.

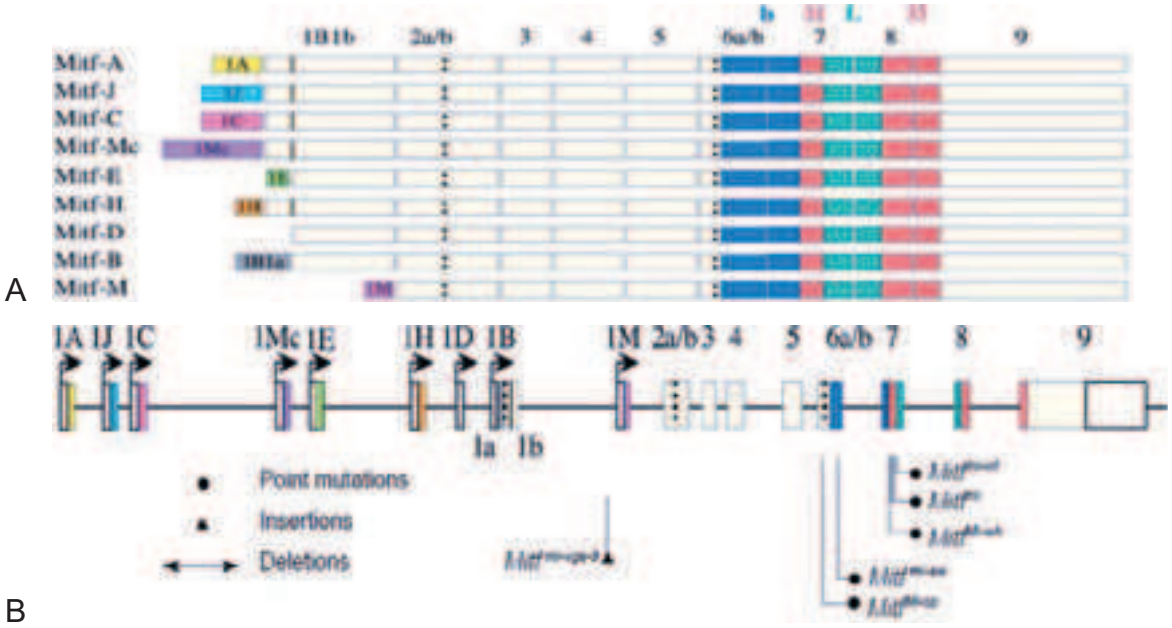

Figure 10 : MITF locus organization

A) All the isoforms encoded by the MITF locus have alternative first exon and share the exons from 2-9. The colored boxes represent exons belonging to their respective isoforms. Melanocyte specific isoform M is depicted in the bottom of the panel (magenta 1M exon). The bHLH domain is depicted by basic region in blue, both helix domains are in red and loop is in green. B) Schematic representation of MITF locus gene and the mutations found in different mouse lines (adapted from (Hou and Pavan 2008)).

II. The MITF protein structure

The Microphthalmia-associated transcription factor (MITF) is a member of the basic helix-loop-helix-leucine zipper (bHLH-LZ or hHLHZip) transcription factor protein family. The gene was first isolated at the *mi* locus (Hodgkinson et al. 1993, Hughes et al. 1993). The modular configuration of MITF includes, starting from the amino-terminus; MITF-M specific region, transactivation AD1 domain, basic and helix-loop-helix domains (encoded by exons 6 to 8) followed by a leucine zipper domain (encoded by exons 8 and 9). The final domain of the protein is the transactivation AD4 domain. (Figure 11).

MITF belongs to the family of closely related transcription factors, sharing a very similar structure, MiT transcription factor family, including also TFE3, TFEB and TFEC transcription factors. MITF was shown to bind DNA either as a homodimer or to heterodimerize with the proteins of the MiT family. The bHLH LZ domain is the critical to form homodimers and heterodimers and to bind specific DNA elements, Ephrussi (E)-boxes, 5'CANNTG3', in target gene promoters. All the members of the MiT family can heterodymerize with each other but not with other bHLH-LZ or bHLH proteins, such as MYC, MAX, or USF (Beckmann and Kadesch 1991, Hemesath et al. 1994), even though all these factors have the common ability to bind to the E-box sequences. Unlike other factors, MITF can also bind an asymmetric 10bp sequence termed the M-box (GTCATGTGCT) with the core E-box sequences 5'-CACGTG-3' and 5'-CACATG-3' (Aksan and Goding 1998). Recently, the MITF protein structure has been solved giving an insight into the molecular structure basis of this specificity. The characterization of the DNA-binding and dimerization specificities of MITF show that, unlike other known bHLHZip transcription factors (MAX, MYC, MAD), leucine zipper contains additional three residues that generate a kink in the structure (Figure 11). This insert limits the ability of MITF to dimerize only with those related bHLHZip transcription factors that contain the same type of insertion (TFEB, TFEC and TFE3). More interestingly, when the three residues are deleted, MITF can heterodimerize with MAX and it loses its ability to bind asymmetric M-box motifs. The specificity of binding to the M-box comes from specific features of the MITF dimer DNA-binding interface. Residues His209 and Ile212 form specific interactions to the M-boxes, stabilizing the MITF binding to these motifs (Pogenberg et al. 2012).

The transactivating domain of MITF, AD1 has been shown to have a role in transcriptional activation and 18 amino acids are sufficient. The minimal activation region of MITF is highly conserved in the related transcription factor TFE3. This region of MITF is also essential for binding the CBP/p300 transcription cofactor (Sato et al. 1997).

Roles of the other MiT family proteins are versatile, including the role of TFEB in the

lysosome biogenesis and autophagy (Settembre et al. 2011). TFE3, TFEC, TFEB have been shown to heterodimerize with MITF (Hemesath et al. 1994). The elimination of these factors did not show an effect on melanocyte pigmentation (Steingrimsson et al. 2002).

A

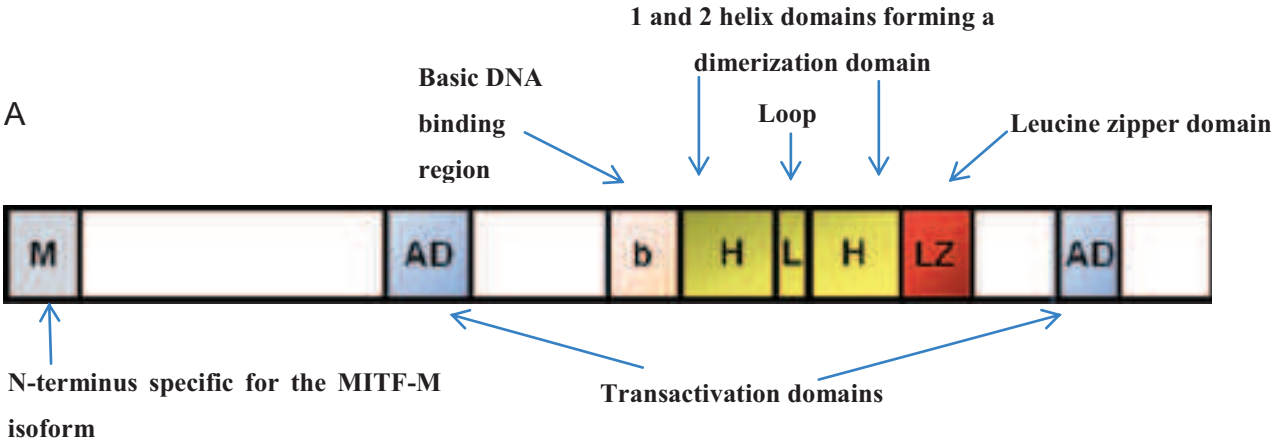

B

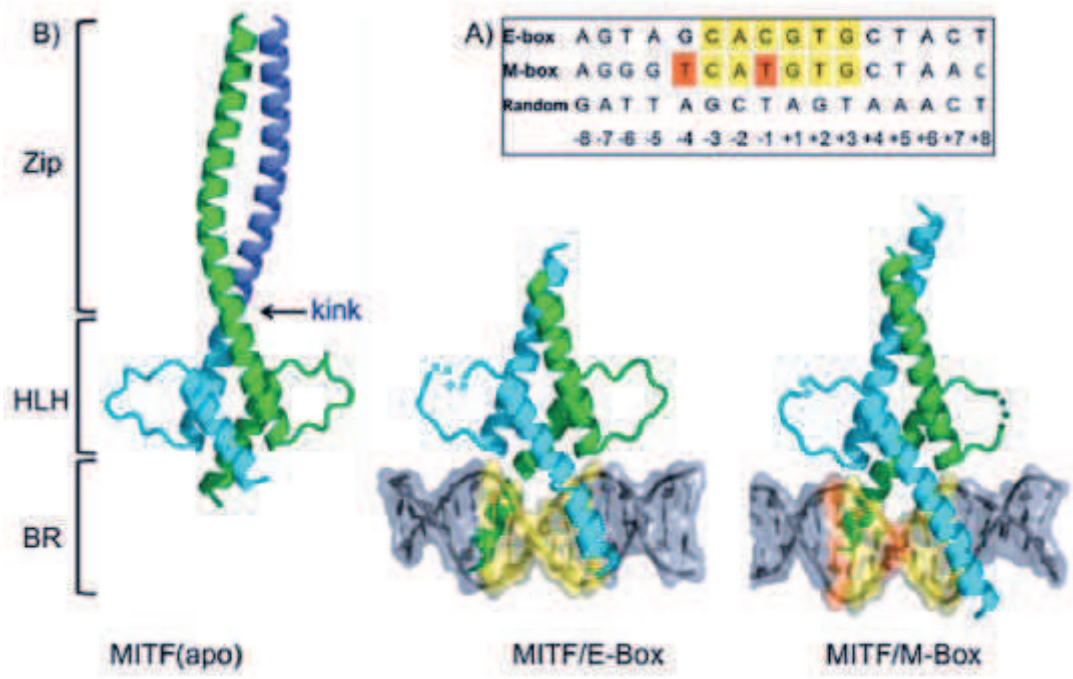

Figure 11 : Organization of MITF protein, 3D structure of the bHLH domain

A) Modular organization of the MITF protein including all the important parts of the protein. **B)** Three dimensional structure of the bHLH domain depicting the structural kink allowing specific dimerization with only members of the Mit family (left, MITF(apo)). Structure of the bHLH domain bound to DNA, both to the E- and M- boxes. The two residues within M-box specifically interacting with MITF are depicted in red.

III. Post-transcriptional modifications of MITF

Post-translational modifications (PTMs) of MITF represent an additional level of regulation of MITF function, affecting the protein activity and stability.

Phosphorilation

In the melanocytes, MITF is a downstream target of two important signaling cascades αMHS/cAMP and KITL/KIT. In the melanoma cell line 501Mel, the KIT-tyrosine kinase receptor activation results in the phosphorylation of the Ser73 and Ser409 amino acids of MITF (Hemesath et al. 1998, Wu et al. 2000b). Several other phospho-receptor sites are known in the MITF protein. These include Ser307, which has been phosphorylated by p38 upon RANKL/RANK signaling in osteoclasts, (Mansky et al. 2002), and Ser298, shown to be phosphorylated by GSK3β (Takeda et al. 2000a). Phosphorilation of Ser73 enables specific recruitment of CBP/p300, resulting in enhancing the transactivation properties of MITF (Price et al. 1998). The in vivo relevance these findings were put under question by a set of experiments rescue performed using the bacterial artificial chromosome (BAC) transgene rescue strategy. The full length MITF that was introduced in the mutant MITFmi-vga-9 mouse line contained either single serine-to-alanine point mutation of the two phosphorilation sites, or both of them. The BAC rescue fully restored the coat pigmentation and the eye development (Bauer et al. 2009). Recent results demonstrated c-KIT stimulation leads to the activation of Mitf specifically through the c-KIT phosphorylation sites Y721 (PI3 kinase binding site), Y568 and Y570 (Src binding site). Using specific inhibitors showed c-KIT induced activation of Mitf is dependent on PI3-, Akt-, Src-, p38- or Mek kinases (Phung et al. 2011).

SUMOylation

Sumoylation is the post-translational modification of proteins by the addition of the small ubiquitin-like-modifier (SUMO). SUMO-1 is added to substrates at lysine residues in a ψKXE consensus sequence (Rodriguez, Dargemont and Hay 2001). The conjugation system of sumoylation is analogous to ubiquitination, with Uba2/Aos1 acting as E1, UBC9 as E2 and RanBP2 or PIAS proteins as E3. There are several functional consequences of SUMO modification; it may compete with ubiquitination and affect protein stability, alter subcellular localization, affect localization to pro-myelocytic leukemia (PML) nuclear bodies, or affect transcriptional activity (Long et al. 2004, Schmidt and Muller 2003).

MITF interacts with UBC9 and PIAS3, and MITF amino sequence harbors two conserved SUMOylation consensus sites at lysines 182 and 316 in the human sequence. Mutation of the both sites abrogate the SUMO modification, but notably, the mutation on the Lys-316 has a stronger effect, indicating this as a site that is more frequently modified by

SUMO (Miller et al. 2005). Furthermore, MITF with lysine-to-arginine substitutions of both SUMOylation sites showed a large increase of the MITF binding to the promoters with multiple binding sites. Also, double mutated MITF had an increased cooperation with Sox10 on the Dct promoter. (Murakami and Arnheiter 2005). Recently, the importance of the K316 SUMOylation site has been shown in vivo context of melanoma. A newly discovered MITF mutation in the SUMOylation consensus sequence on the E318 position has been shown to have a profound effect on the MITF SUMOylation status. The mutation MITF E318K affects the acidic residue that is critical for SUMOylation. This mutation profoundly affects the MITF binding genome wide and as a consequence it is predisposing to melanoma and renal cell carcinoma in the rate of 5-fold higher over the control subjects. Additionally, MITF harboring E318K enhances migration and invasiveness of melanoma cells in vitro and is enhancing the colony formation for immortalized melanocytes (Bertolotto et al. 2011). Another study has been published approximately at the same time, confirming the incidence of the E318K mutation correlated with higher risk for melanoma development both in Australian and UK patient cohorts (Yokoyama et al. 2011). Following the same line of research, the MITF E318K variant was later found in a group of melanoma patients in Italy (Ghiorzo et al. 2013) and another one in Australia (Sturm et al. 2014), showing similar allele frequency. The E318K mutation is the first recorded MITF mutation that is correlated with increased melanoma risk.

3. Cutaneous melanoma

Skin cancer is commonly categorized as malignant melanoma and non-melanoma skin cancer (NMSC), the latter including basal cell carcinoma (BCC) and squamous cell carcinoma (SCC) as the major subtypes.

Although melanoma accounts for only 4 percent of all dermatologic cancers, it is responsible for 80 percent of deaths from skin cancer. In addition, only 14 percent of patients with metastatic melanoma survive for five years (Miller and Mihm 2006).

A. Melanoma epidemiology

Melanoma is an increasingly important public health problem worldwide. Overall, melanoma incidence rise 3.1% yearly during the last 20 years (Rigel 2010). Judging from the figures for 2010, In the USA the incidence of melanoma is $19.4/10^5$ and $14.4/10^5$ yearly for males and females in Caucasians. The highest melanoma incidence recorded worldwide is in Queensland, Australia, $55.8/10^5$ per year for males and $41.1/10^5$ for females. Incidence is also high for New Zealand at $34.8/10^5$ for males and $31.4/10^5$ for females per year. The incidence rates for Europe vary depending on the country and are highest in Switzerland and the Scandinavian countries of Norway, Sweden and Denmark. All European countries report a higher incidence in females than males, in contrast to Australasia and North America (MacKie, Hauschild and Eggermont 2009).

The country factsheets provided by EUCAN, supported by World Health Organization (WHO) reports the incidence, mortality and prevalence data for the European Union and each of the 40 individual European countries. The latest data available for the melanoma incidence and mortality across Europe is for 2012 (Figure 12A). However, it has also shown that western European countries such as UK and France have high incidence but do not have high mortality rates, while eastern European countries such as Croatia or Poland have lower incidence, but higher mortality rates (Figure 12B) (Bray et al. 2013, Ferlay et al. 2013).

A

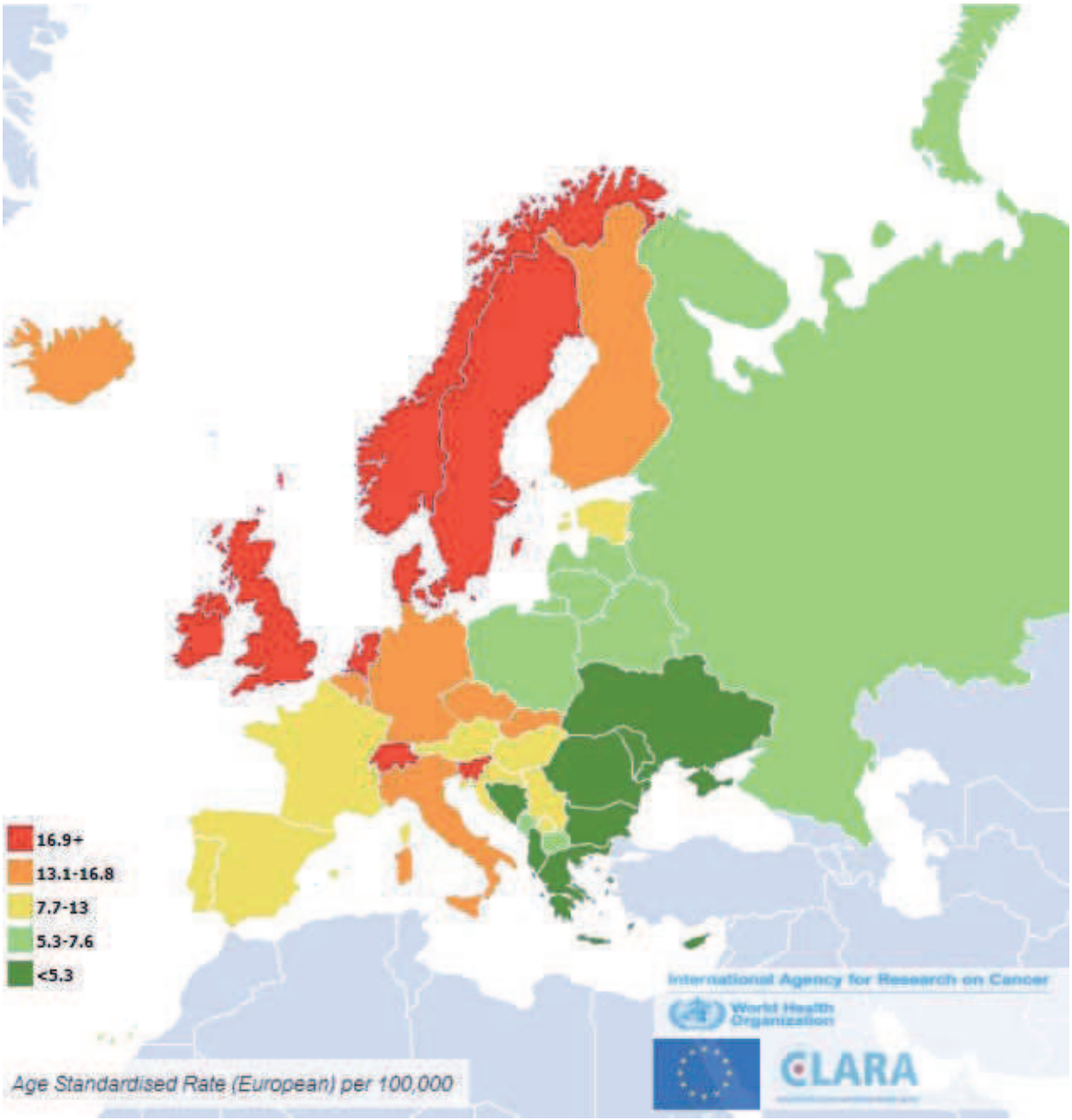
16.9+
13.1-16.8
7.7-13
5.3-7.6
<5.3
International Agency for Research on Cancer
World Health Organization
CLARA
Age Standardised Rate (European) per 100,000

B

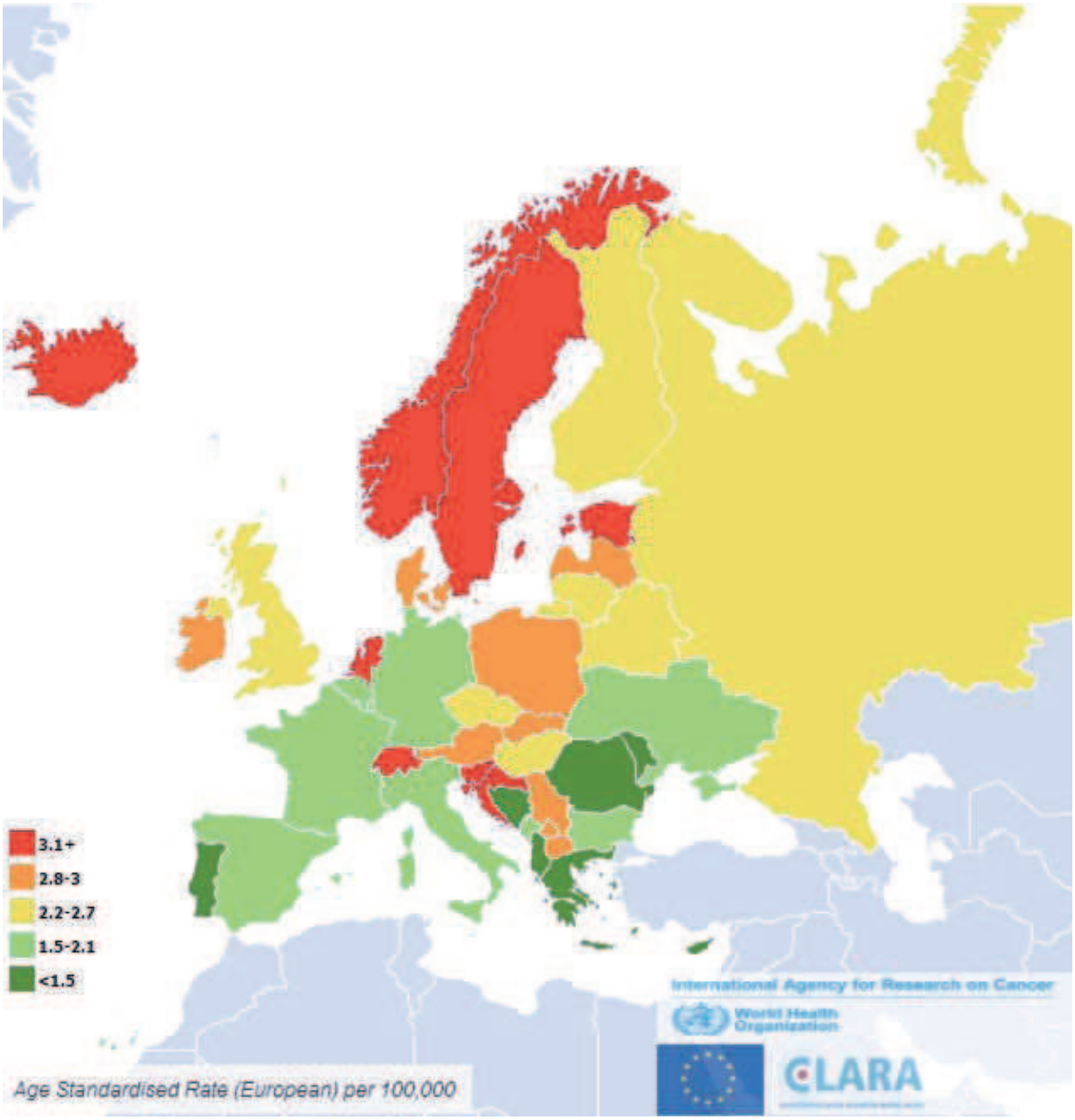

Figure 12 : Incidence and mortality of melanoma in Europe
A) Map of Europe with color coded estimated incidence of malignant melanoma, with age standardized number per 10^5 for both sexes in 2012.
B) Map of Europe with color coded estimated mortality from malignant melanoma, with age standardized number per 10^5 for both sexes in 2012.

B. Risk factors for melanoma development

Ultraviolet (UV) light exposure

Ultraviolet (UV) light exposure is one of the main risk factors for majority of the melanoma cases. Multiple studies have found a link between the melanoma development on the torso area (chest and back) and legs to repeated sunburns (particularly in childhood).

Fair skin, freckling, and light hair

Phototype presents one of the risk factors for melanoma, and it is 10 times higher for Caucasian people than for dark-skinned people. Caucasians with red or blond hair, blue or green eyes, or fair skin that freckles or burns easily are at higher risk (Hearing 2011).

Moles (Nevi)

Dysplastic nevi, also known as atypical nevi, are often larger in size and have an abnormal shape or color. In individuals with the dysplastic nevus syndrome, a lifetime risk of melanoma development is around 10%.

Family history of melanoma

Around 10% of all subjects with melanoma have a family history of the disease. Susceptibility genes in familial melanoma include cell cycle regulators CDKN2A, coding for both p16 (INK4A) and p14(ARF), and cyclin dependent-kinase 4 (CDK4), and Melanocortin 1 receptor (MC1R), and the mutations in these genes have been associated with cutaneous malignant melanoma risk.

C. Different types of melanoma

Clark et al (Clark et al. 1969) was the first report distinguishing different melanomas subtypes based on their clinical and histologic properties, that were later used by other researchers (Smoller 2006). The majority of all melanomas fall into the following four subtypes (the World Health Organization (WHO) classification of melanoma):

Superficial spreading melanoma (SSM) is by far the most common type, accounting for about 70 percent of all cases. This melanoma may grow along the top layer of the skin for a relatively long time before penetrating more deeply. This type of melanoma can rise from a previous benign nevus, and is more often seen in younger people.

Lentigo maligna (LM) is similar to the SSM since it also spreads on the surface of the skin. It usually remains on the surface for a long time before penetrating into the deeper layers of the skin. This type is reported more often in the elderly people, appearing on regions of the body that are chronically exposed to the sun, such as the face, ears, arms and upper trunk.

Acral lentiginous melanoma (ALM) is also spreading on the surface of the skin in the beginning of its development. The characteristic feature of this type is it appears under the nails or on the soles of the feet or palms, as black or brown regions. This type of melanoma is the most common in African-Americans and Asians, and the least common among Caucasians. It can also often progress more quickly than SSM and LM.

Nodular melanoma (NM) is often invasive at the time of the diagnosis. It is most common in the elderly. The typical locations include the trunk, arms, legs, and the scalp region in men. This type is the most aggressive of all the types of melanomas, and is reported in 10% to 15% of cases.

Melanoma type/Activating mutation	**BRAF**	**NRAS**	**KIT**
Superficial spreading melanoma	60%	20%	<1%
Lentigo maligna	10%	15%	28%
Acral lentiginous melanoma	20%	10%	36%
Nodular melanoma	70%	12%	<2%

Table 2 : The percentage of accurance of different activating mutations (BRAF,NRAS, KIT) in the main melanoma types

Adapted from (Kabbarah and Chin 2005)

D. A molecular model of melanoma progression

The Clark model, a detailed study of precursor lesions leading to the development and the progression of metastatic melanoma emphasizes the stepwise transformation of melanocytes to melanoma; it describes all the histologic changes accompanying different phases of progression (Clark et al. 1984) (Figure 13).

The model recapitulates six different steps of disease progression:

Benign nevus, characterized by melanocyte proliferation and benign lesions. These nevi contain melanocytes that will in most cases undergo terminal differentiation.

Hyperplastic nevus, characterized as melanocytic hyperplasia, has as its main feature the aberrant differentiation of the melanocytes. These nevi contain increased number of melanocytes, are located along the basal layer, and their growth is limited.

Dysplastic nevus, consisted of dysplastic cells that have acquired the properties of aberrant growth. Such structures are identified as asymmetric, with irregular borders, increasing in diameter and have multiple colors within the nevus.

Radial-growth phase is characterized by an intra-epidermal cell growth. These lesions show cytomorphological features of cancer. They start to penetrate the papillary dermis, but fail to form colonies in soft agar.

Vertical-growth phase, considered to be the tipping point of metastatic melanoma development, is characterized by dermal invasion. These lesions contain the cells that have acquired the ability to invade the dermis, expand through the papillary and reticular dermis and fat. They are capable of growing in soft agar and form tumor modules when injected into nude mice.

Metastasis, the final step in the model, encapsulates the successful spread of cells in other areas of the skin, their intravasation into blood and lymphatic vessels and ability to form metastatic foci in other organs.

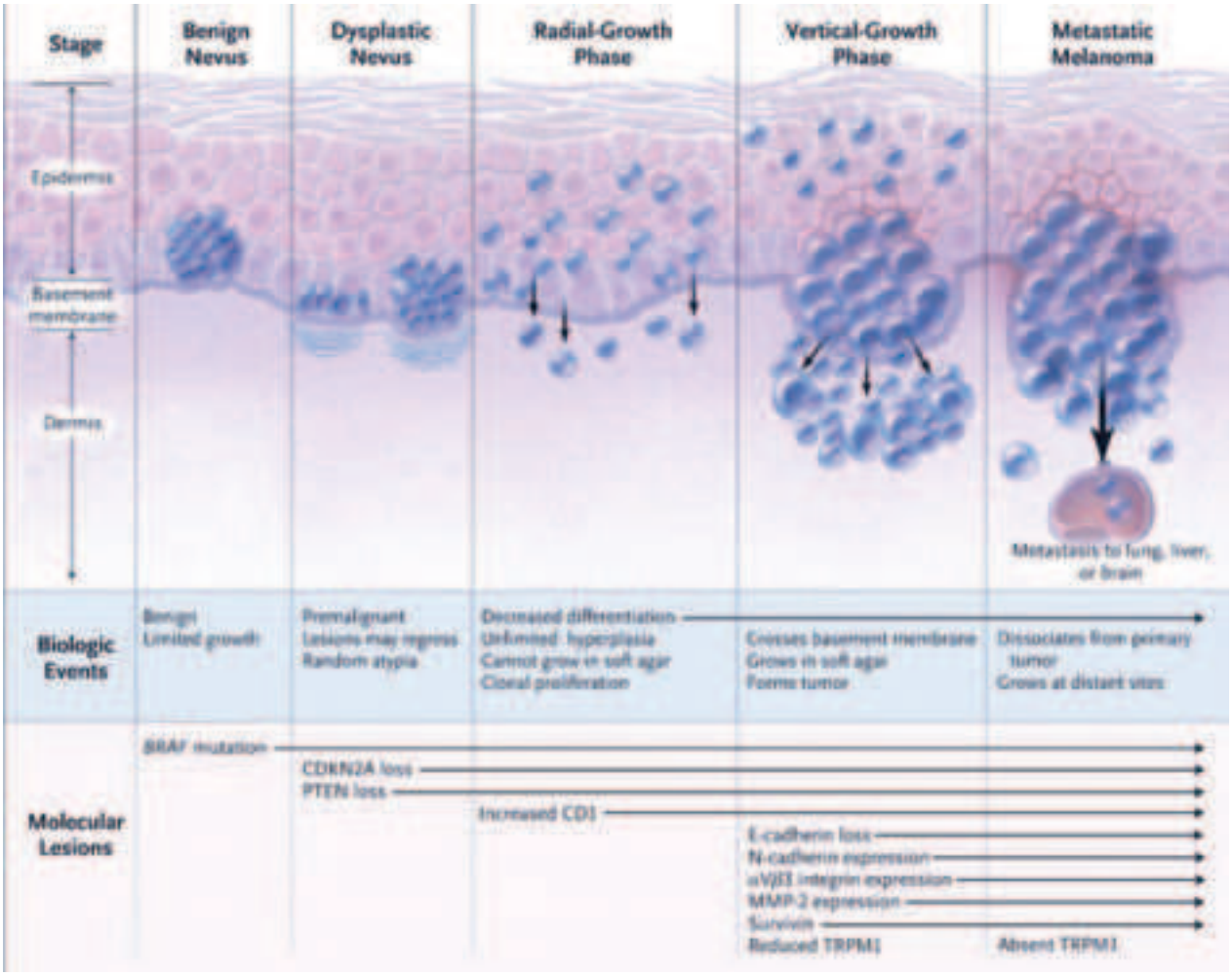

Figure 13 : Model of melanoma progression

In the model of melanoma progression, melanocytes are represented in blue, and passing through different phases of melanoma development. In the lower panel are all the mutations recorded to contribute to melanoma progression. However, not every case of melanoma progression goes through all the depicted steps (Miller and Mihm 2006).

I. Benign nevus formation – BRAF and NRAS as driver mutations

In the Clark model, the initial stage of melanocyte transformation is a benign nevus (Figure 13). The main cause of the nevus formation is an abnormal activation of the MAPK/ERK signaling pathway. The most common mechanism of this pathway is a somatic gain-of-function mutations of Ras proteins (most common NRAF), or Raf proteins (most common BRAF), which are present in 90% of melanoma cases (Zhuang et al. 2005).

Initial findings suggested that ERK hyperactivation is a result of NRAS mutation, since it has been reported in between 15-30% of melanomas (van Elsas et al. 1995). NRAS is a part of RAS family of small GTPases (along with HRAS and KRAS). The most common mutation of NRAS is a substitution of glutamine to lysine or arginine at position 61 (Q61K, Q61R) (Davies et al. 2002, Ellerhorst et al. 2011).

It was later discovered that most commonly mutated component of this pathway is BRAF, one of the three Raf proteins (along with ARAF and CRAF). It is mutated in 50-70% of the cases with the phospho-mimic substitution of valine-to-glutamic acid at the position 600 (V600E) representing the vast majority of the activating mutations (Davies et al. 2002). In melanomas, NRAS and BRAF mutations are in general mutually exclusive, indicating either of the two mutations is sufficient to constitutively activate the MAPK signaling pathway (Goel et al. 2006).

Even though BRAF activation is the most prevalent primary mutation driving melanoma development, BRAF mutations occur at a similar frequency in benign nevi and in primary and metastatic melanomas (Pollock et al. 2003). The explanation for this came from a study demonstrating that oncogenic BRAF triggers a program of oncogene-induced senescence, causing cells to enter irreversible growth arrest, and remain static (Dhomen et al. 2009, Michaloglou et al. 2005). This suggests that nevi acquire additional mutations in order to bypass the senescence block and develop a malignant lesion.

II. Dysplastic nevus formation – CDKN2A and PTEN inactivation

Main characteristic of dysplastic nevi are mutations in the *CDKN2A* and *PTEN,* causing the inactivation of the protein these loci encode. A germline mutation deactivates CDKN2A in 25-40 % of familial melanoma (Thompson, Scolyer and Kefford 2005), while PTEN is mutated in 25-50% of non-familial melanoma (Wu, Goel and Haluska 2003).

CDKN2A is a tumor suppressor gene situated at the 9p21 locus. It is complex and it encodes two distinct proteins, INK4A and ARF through alternative promoters and first exons encodes two tumor suppressor proteins (Chin, Pomerantz and DePinho 1998) (Figure 14).

The second exon that is shared is translated in different reading frame for the two proteins, rendering two proteins with no amino acid homology, but nevertheless having a crucial role in antitumoral responses.

INK4A ($p16^{INK4A}$), the founding member of INK4 (inhibitor of cyclin-dependent kinase 4) family of proteins, inhibits the cell cycle in the G1 phase by inhibiting cyclin-dependent kinases (CDKs) 4/6. These CDKs phosphorylate and inactivate retinoblastoma (Rb) protein, thereby allowing the S phase entry (Serrano, Hannon and Beach 1993). Loss of INK4A promotes Rb inactivation through its hyperphosphorylation and activation of transcription factor E2F1, resulting in an unrestrained cell cycle progression. INK4A has an important role in control of cellular senescence since through INK4A-RB pathway (Sviderskaya et al. 2003).

ARF (alternative reading frame) protein ($p14^{ARF}$ in humans and $p19^{ARF}$ in mice) has a role in the inhibition of MDM2-mediated ubiquitination and proteasome degradation of p53. Inactivation of ARF, through inactivation of p53, affects cell cycle control, DNA damage response and the regulation of cell death (Chin, Pomerantz and DePinho 1998, Kamijo et al. 1998, Zhang, Xiong and Yarbrough 1998). In context of melanoma, ARF inactivation abolishes oncogene induced senescence and renders the melanoma cells capable of malignant transformation. Although p53 has a low frequency of mutations, it is downstream of the ARF, which functionally replaces p53 loss (Sharpless and Chin 2003).

Phosphatase and tensin homologue (PTEN) is a lipid protein phosphatase that is situated on chromosome 10q, a region known to be subjected to loss of heterozygosity (LOH) in many human cancers including melanoma (Bastian 2003, Wu et al. 2003). It regulates extracellular growth signals by negative regulation of phosphoinositol 3-kinase (PI3K)-AKT pathway. PI3K catalyzes phosphatidylinositol triphosphate (PIP3) production, which serves as an intracellular second messenger, leading to phosphorylation of AKT, which is known to promote cell cycle progression and inhibit apoptosis. AKT regulates numerous factors, such as BAD (Bcl2 Antagonist of death), CCND1 (cyclin D1), FOXO and NF-κB (Dillon and Muller 2010, Soengas and Lowe 2003).

The PI3 kinase–AKT pathway is often hyperactive in melanoma. AKT is present in the cells in three isoforms, AKT1, 2 and 3. In melanoma, AKT3 is a predominant isoform, and is present in 40-60% of the cases. AKT3 inhibition in melanoma context is resulting in increased apoptosis and inhibition of tumor development. Indeed, AKT3 silencing by siRNA leads to decreased survival of melanoma cells. (Stahl et al. 2004). Elevated phospho-AKT levels inversely correlate with patient survival (Dai, Martinka and Li 2005), while allelic loss or altered expression of PTEN comprises 20% - 40% of melanoma tumors, respectively (Goel et al. 2006, Pollock et al. 2002).

Multiple studies show that $BRAF^{V600E}$ mutation and loss of PTEN, or $NRAS^{Q61K}$

mutation and loss of INK4A cooperate to promote the development of more malignant stages of melanoma (Goel et al. 2006, Tsao et al. 2004b, You et al. 2002). This is further supported by murine melanoma models, where $NRAS^{Q61K}$ in combination with INK4a loss (Ackermann et al. 2005), or $BRAF^{V600E}$ in combination with PTEN loss (Dankort et al. 2009) results in development of malignant melanoma.

III. Radial growth phase (RGF) – expansion within the epidermis

The characteristic feature of the radial growth phase is the bypass of senescence, immortalization and proliferation of the cells along the line of the basement membrane, horizontally in the epidermis. Besides the MAPK activation mentioned above as the primary pathway to stimulate cell proliferation, cells in the radial growth phase proliferate either due to CCND1 (cyclin D1) or CDK4 amplification. During the radial growth phase cells grow predominantly close to the basal membrane, since their growth is still dependent on the exocrine factors produced by the keratinocytes.

CCND1, coding for a cyclin D1, is a proto-oncogene with an important role in numerous cancers, including melanoma. Amplification of the *CCND1* locus as well as CCND1 protein overexpression is detected in 20% of melanoma cases, and it is most common in acral melanoma, with (44%). Furthermore, ablation of CCND1 in melanoma cells by siRNA induces apoptosis and reduces tumor growth in mouse xerographs. (Sauter et al. 2002).

CDK4 mutations are rare, but CDK4R24C mutation renders the protein insensitive to INK4A regulation, while preserving the interaction with cyclin D1, causing a constitutive activation of the kinase. Also, a small percentage of familial melanoma contains germline mutations of CDK4 (Ceha et al. 1998, Zuo et al. 1996).

Ras/Raf/MEK/ERK pathway also regulates the cell signals downstream from receptors activated by SCF, FGF or HGF factors, or by KIT. Individually, these factors evoke a weak or transient ERK activation (Bohm et al. 1995, Wellbrock et al. 2002). The combined activity of these factors or the mutations of the receptors might result in melanoma development, but this mechanism of activation is rare in melanomas (Willmore-Payne et al. 2005). KIT mutations are present in only 2% of melanomas, also genetic amplification of KIT has been shown in the case of acral, mucosal and melanoma on the face. A subgroup of melanomas overexpressing KIT and CDK4 offer and explanation of a mechanism of malignant transformation in melanomas that don’t carry BRAF or NRAS mutations (Smalley et al. 2008)

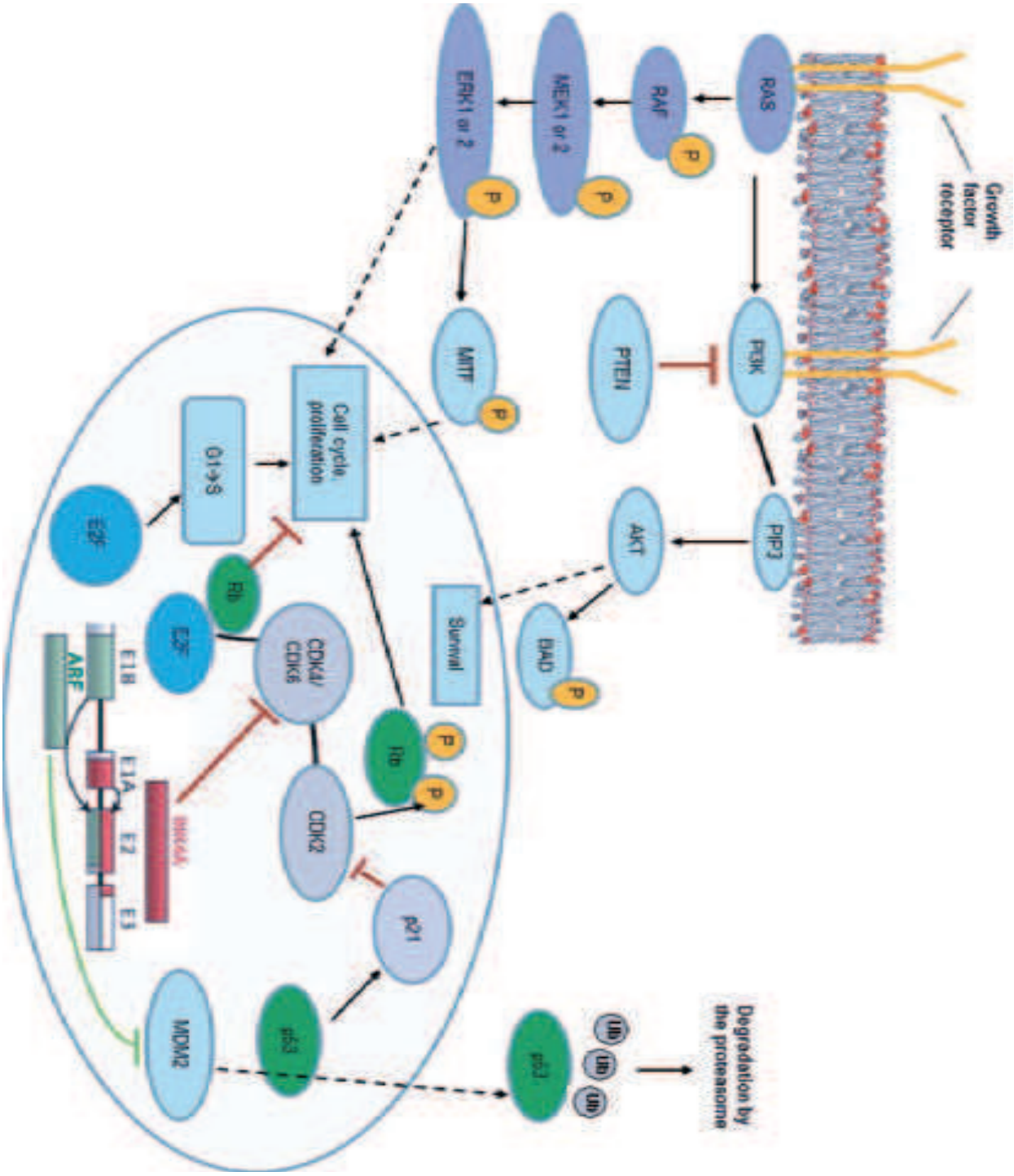

Figure 14 : Main signaling pathways and proteins mutated in melanoma
The main pathways deregulated in melanoma, MAPK and PI3K (repressed by PTEN). The gene regulation network in the nucleus involves E2F, CDK4/6 and CDK2 promoting the cell cycle by inactivating RB. CDK4/6 get repressed by INK4A. ARF is repressing MDM2, which is negatively regulating p53 stability. The CDKN2A locus, coding both INK4A and ARF is depicted with the alternatively spliced exons (adapted from (Miller and Mihm 2006, Nelson and Tsao 2009)).

IV. Vertical growth phase (VGF)

Vertical growth phase is considered to be a crucial tipping point in malignant melanoma development. At this stage melanomas acquire invasive potential. Using injections into nude mice, Herlyn et al has been able to show the VGF injected melanomas form tumors, while RGF injected melanomas do not (Herlyn et al. 1985).

While melanoma cells are in the earlier phases of development, they are still dependent on keratinocytes for grown factors (Bogenrieder and Herlyn 2002). To bypass this requirement, more advanced melanomas develop autocrine activation by secreting various growth factors. These include PDGF (pellet-derived grown factor), bFGF, IGF-1 (insulin grown factor 1), TGFβ (transforming growth factor β), chemokines, VEGF, HGF, EGF (Li et al. 2003).

In order to be able to invade the surrounding tissues, the cells undergo the process of epithelial-to-mesenchymal transition (EMT). EMT-like (pseudo-EMT) properties in the context of melanoma refers to loss of contact with keratinocytes and development of migration and invasiveness (Bennett 2008). Several pathways have been shown to induce EMT, all of which function through three transcription factor families including the Snail (SNAIL, SLUG), Zeb (ZEB1, ZEB2) and basic helix-loop-helix (E47, TWIST1). The altered gene expression network in the cells undergoing EMT increases expression of these transcription factors, and this in turn down regulating expression of E-cadherin (Peinado, Olmeda and Cano 2007, Olmeda et al. 2007). Down-regulation of E-cadherin and expression of N-cadherin is one of hallmarks of EMT (Hsu et al. 1996, Thiery et al. 2009).

Recently, pivotal importance of the ZEB1 and ZEB2 transcription factors in melanocyte lineage and melanoma has been shown. Zeb2 transgenic knockout mouse line was used to ablate Zeb2 specifically in melanocytes. Zeb2 loss affected melanoblast migration and melanocyte differentiation, resulting in an ablation of the melanocyte cell lineage and a loss of coat color. Loss of Zeb2 in the melanocyte lineage results in a downregulation of Mitf and melanocyte differentiation markers, which explained the loss of coat color phenotype. Additionally, the loss of Mitf led to significant upregulation of Zeb1 (over 10x) in melanoma cell lines. Furthermore, several Mitf binding sites could be detected in the vicinity of the Zeb1 locus, indicating Zeb1 is a direct Mitf target. Moreover, the loss of Zeb2 expression is implicated human melanoma development, evidenced by the positive correlation between loss of Zeb2 expression and patient survival (Denecker et al. 2014a). Another study also reported additional factors involved in EMT to be important for melanoma development. SNAIL2 and ZEB2 have been shown to be expressed in melanocytes and to have anti-tumoral properties, since these two proteins activate MITF and as a result

melanocytes undergo terminal differentiation. In response to NRAS/BRAF activation, EMT transcription factor network reorganizes and as a result, TWIST1 and ZEB1 are upregulated. This switch cooperated with BRAF and results in E-cadherin loss, enhanced invasion and progression to a more malignant phenotype (Caramel et al. 2013).

Besides the onset of EMT, the ability to suppress apoptosis is one of the hallmarks of the cells in the VGF, since they are no longer dependent on survival signals form the surrounding cells. The primary changes that suppress apoptosis are highly selected in advanced melanoma. Apoptosis can occur via mitochondria dependent intrinsic, and "death receptor" dependent extrinsic pathways. In the case of melanoma, defective regulation of the intrinsic pathway is the cause of melanoma resistance.

The pathways the lead to reduced apoptosis once deregulated include the intrinsic apoptotic pathway via loss of Apaf1 and reduced activity of p53 (Soengas and Lowe 2003). Additionally, surviving signaling pathways that are often mutated in melanoma include loss of PTEN, resulting in activation of PI3K/AKT signaling, and also NF-κB activation that can potentiate survival and oncogenesis. NRAS signaling overexpression can also affect cell survival since it has been shown it can act through PI3K (Bennett 2008, Soengas and Lowe 2003). Additionally, Factors TBX2 and TBX3 repress $p21^{CIP1}$ and ARF, impinging of their roles as tumor suppressors. TBX3 also has a role in E-cadherin repression and melanoma invasiveness (Rodriguez et al. 2008). Serine Threonine kinase 11 (STK11) is involved in p^{21} activation through p53 in multiple cell types, is found mutated in 10% of melanoma cases (Bennett 2008).

Wnt/ β-catenin pathway has also been shown to be important in the development of more aggressive melanoma phenotype. Constitutive activation of β-catenin is frequently found in more than 30 % of malignant melanoma, and the activation is caused by deletion of β-catenin exon 3 (Rimm et al. 1999).

To better understand how β-catenin acts in melanoma, Delmas et al. created transgenic mice expressing a stabilized mutant β-catenin (bcat*), lacking the exon3, that, as mentioned before, renders it resistant to GSK3 phosphorylation and subsequent degradation. By using this model, the authors have shown β-catenin cooperates with NRAS to promote melanoma. Also, β-catenin does not affect melanocyte proliferation in culture, but bypasses the requirement for CDKN2A mutations by repressing the CDKN2A promoter (Delmas et al. 2007).

Wnt/β-catenin signaling has also been shown to regulate expression of POU domain transcription factor BRN2 in melanoma. BRN2 is highly upregulated in melanoma and is involved in proliferation and survival. Regulation BRN2 expression by β-catenin has been shown in melanoma cell lines and in transgenic mice. Moreover, silencing of Brn2 in

melanoma cell lines overexpressing β-catenin significantly reduces the proliferation rate of these cells (Goodall et al. 2004).

Paradoxically, although β-catenin expression is seen in the context of cancers such as colon or liver cancer to have a poor prognosis (Boye et al. 2010, Liu et al. 2010), in melanoma high nuclear β-catenin is associated with good prognosis (Chien et al. 2009). Increased expression of β-catenin suppresses melanoma cell invasion (Arozarena et al. 2011), a process that may be explained by the up-regulation of MITF favoring a proliferative phenotype. Nevertheless, it has also been reported that β-catenin can favor lung metastasis in the NRAS-bcat* mouse model, while repressing migration (Gallagher et al. 2012). Thus, β-catenin signaling affects many aspects of melanoma cell physiology and *in vitro* cell based models do not always recapitulate the more complex effects seen *in vivo.*

V. Melanoma metastasis

Metastatic melanomas are fully transformed, immortal, have gained the ability to suppress apoptosis and have increased migratory and invasive properties. In order to successfully disseminate throughout the body, these cells need to enter blood and lymphatic vessels through a process of intravasation, travel to distant organs within the blood flow, attach to the vessel wall and exit through the process of extravasation and establish a secondary tumor.

Factors involved in EMT in the VGF of melanoma development continue to have crucial roles in the establishment of melanoma metastasis. Genes such as SNAIL and SLUG, regulated by the PI3K/AKT pathway are involved in intravasation and extravasation process. SNAIL and SLUG downregulate epithelial marker E-cadherin, and upregulate mesenchymal markers such as Vimentin, implicated in migration and invasion (Gupta et al. 2005, Poser et al. 2001). Furthermore, activated form of AKT promotes overexpression of VEGF, a key regulator of angiogenesis, resulting in proliferation and reorganization of blood vessel epithelium (Murukesh, Dive and Jayson 2010).

One of the PI3K targets, phosphoinositide-dependent kinase-1 (PDK1) has recently been reported to promote melanoma development and to be crucial for metastasis development. PDK1 is a serine/threonine protein kinase that phosphorylates protein kinases A (PKA), B (PKB, including PKB/AKT) and C (PKC) families. PDK1 inactivation using a mouse model, or pharmacological inhibition delays melanoma development and inhibits metastasis when crossed to $Braf^{V600E}$::$Pten^{-/-}$ melanoma model. Indeed, PDK1 mutant mice develop significantly less metastasis in lymph node, lungs and spleen (Scortegagna et al. 2014).

A mode of Wnt signaling shown to be involved in development of melanoma metastasis is Wnt planar cell polarity (PCP) pathway. This mode of Wnt signaling involves Rho family of GTP hydrolases that play many major roles in cytoskeleton regulation. The two members of the family that have been the most extensively studied are RAC1 and RHOA (Burridge and Wennerberg 2004).

The role of RAC1 in malignant melanoma has recently been reported. A study using exome sequencing identified recurrent somatic mutations in RAC1 in malignant melanoma (Krauthammer et al. 2012). Additionally, a mutation of RAC1, substitution of proline 29 to serine ($RAC1^{P29S}$) induces spontaneous activation of the GTP-ase, leading to increased binding of its downstream effectors. Consequently, melanocyte proliferation and migration increases and accounts for RAC1 cancer-inducing properties (Davis et al. 2013).

Upstream regulator of the GTPases, GEF PREX1 has important role in melanoblast migration. In the mouse melanoma model, PREX1 ablation has been shown to have remarkable effect on melanoma metastasis development. Indeed, using the PREX1 model crossed to the mouse melanoma model displayed no lung metastasis, even though primary tumors developed at the same rate as in the control (Lindsay et al. 2011). Additionally, another GEF, PREX2 has been shown to be frequently mutated in melanoma (Berger et al. 2012).

The role of non-canonical Wnt/Ca^{2+} signaling though WNT5A has also been shown to have a role in metastatic melanoma. WTN5A was shown to directly affect metastatic melanoma since its overexpression enhances their motility and invasive properties (Weeraratna et al. 2002). WNT5A/PKC signaling mediates melanoma motility and metastasis by inhibiting metastasis repressors and promoting EMT (Dissanayake et al. 2007).

TGF-β and Sonic hedgehog pathways regulate melanoma tumorigenesis and metastasis. Proliferative melanoma cells are sensitive to TGF-β induced inhibition of proliferation as activation of this pathway represses MITF expression (Hoek et al. 2006). In melanoma cells, TGF-β regulates expression of GLI2, a transcription factor downstream of the sonic hedgehog pathway (Dennler et al. 2009). Increased GLI2 expression in melanoma tumors is associated with loss of E-cadherin expression, an increased capacity *in vitro* and formation of bone metastases *in vivo* (Alexaki et al. 2010). Furthermore, GLI2 also cooperates with ZEB1 in repression of CDH1 in melanoma cells, leading to more aggressive tumor phenotype (Perrot et al. 2013). GLI2 and MITF show reciprocal expression patterns in a wide range of melanoma cells *in vitro* (Javelaud et al. 2011). GLI2 binds to and represses the MITF promoter. In addition however, activation of the TGF-β pathway also down-regulates cAMP/PKA activity leading to a reduction in CREB transcriptional activity and hence down-regulation of MITF expression (Pierrat et al. 2012).

E. Versatile roles of MITF in melanoma

I. Phenotype switching

To gain an overview of the global gene expression profile in melanomas, Hoek et al. analyzed a substantial number of melanoma cell lines and short-term human tumor cultures. This analysis gave rise to the phenotype-switching hypothesis, since the authors revealed the existence of two distinct cell populations within melanomas. The phenotypic differences of these two populations, one proliferative and the other invasive, were correlated to global changes in gene expression patterns identifying gene expression signatures for the different states (Hoek et al. 2008). Recently, analysis of about 500 melanoma short-term tumor cultures proposed 130 genes to have a predictive correlation with the two different phenotypes (Widmer et al. 2012). MITF has been shown to be one of the most prominent markers of different phenotypic states, being present and highly expressed in 90% of proliferative melanomas, and expressed at low level or undetectable in the invasive cultures.

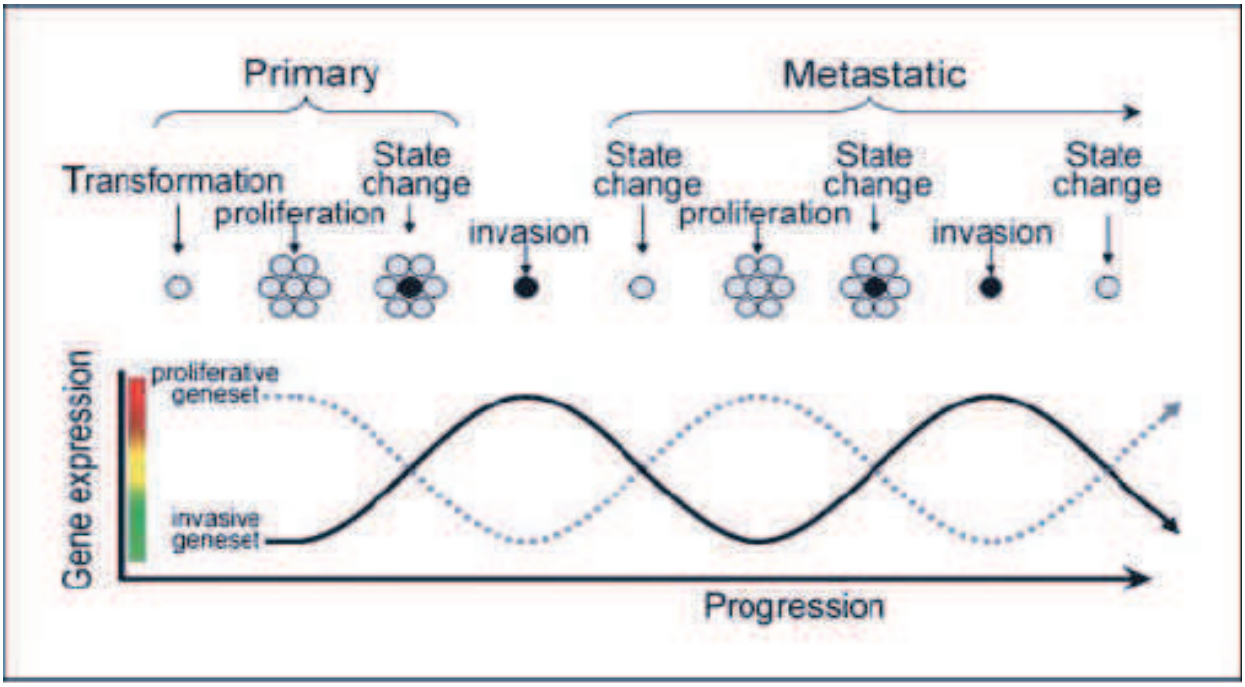

Figure 15 : Phenotype switching model

The phenotype switching model demonstrates the two interchanging phenotypes, proliferative and invasive. The cell that is in proliferative population (grey) switches to the invasive phenotype (black), invades and upon reaching the new location reverts into proliferative phenotype. The switch between the phenotypes is accompanied by expression of a specific geneset supporting a given phenotype (lower pannel) (Hoek et al. 2008).

II. Genome wide MITF occupancy and target genes

The complex role of MITF in melanoma has been studied with high throughput genomics in order to elucidate a more complete repertoire of its target genes. (Strub et al. 2011). In order to identify MITF direct targets, chromatin immuno-precipitation (ChIP)-sequencing was utilized. This analysis revealed about 12000 MITF binding sites containing mainly 5'-CACGTG-3' or 5'-CATGTG-3 E-box sequences. Out of these, 5000 potential novel direct targets were identified, due to MITF binding site close to the TSS of the gene. To determine which of these were regulated by MITF, the ChIP-seq data was integrated with RNA-seq data from siMITF knockdown cells identifying genes that were either activated or repressed by MITF amongst which are direct targets with MITF binding sites. Up-regulated transcripts were associated with ontology terms such as cytoskeleton, cell adhesion and cancer signaling pathways suggesting they may contribute to changes in cell morphology and increased motility and invasiveness. Down-regulated transcripts are rather associated with cell cycle, mitosis, DNA replication and repair. MITF acts therefore both as an activator and a repressor in a promoter-specific manner.

MITF activates many genes with a role in DNA replication and repair. LIG1 (DNA ligase 1), re-ligating of DNA nicks formed during DNA replication, has a role in DNA repair and genome stability (Bentley et al. 2002, Tomkinson and Mackey 1998), or BRCA1 and FANCA well-known for their role in replication/repair with and genomic stability (Wang 2007) are some of the genes regulated by MITF. MITF also regulates TERT (telomerase reverse transcriptase) that is required for the replication of telomeres and is often re-expressed in human tumors. (Artandi and DePinho 2000, Artandi and DePinho 2010, Kim et al. 1994, Rudolph et al. 1999). MITF silencing results in mitotic defects, and in agreement with is the detections of CCNB1 and PLK1 as direct MITF targets. In addition, MITF regulates a large class of mitosis genes (Strub et al. 2011).

On the other hand, the MCAM (Ouhtit et al. 2009) and SHC4 (also known as RaLP; (Fagiani et al. 2007)) genes have MITF binding sites in their regulatory regions and are up-regulated upon MITF silencing and thus appear to be directly repressed. Both of these genes play a critical role in melanoma invasion and metastasis. These results further extended the ‘rheostat’ model for MITF function in melanoma (Carreira et al. 2006) and provided a molecular basis of the MITF expression regulation and its role in various effects in melanoma cells. It has also been found that around 30% of MITF occupied sites are associated with YY1 occupancy and that MITF and YY1 interact physically and functionally to regulate target gene expression (Li et al. 2012b).

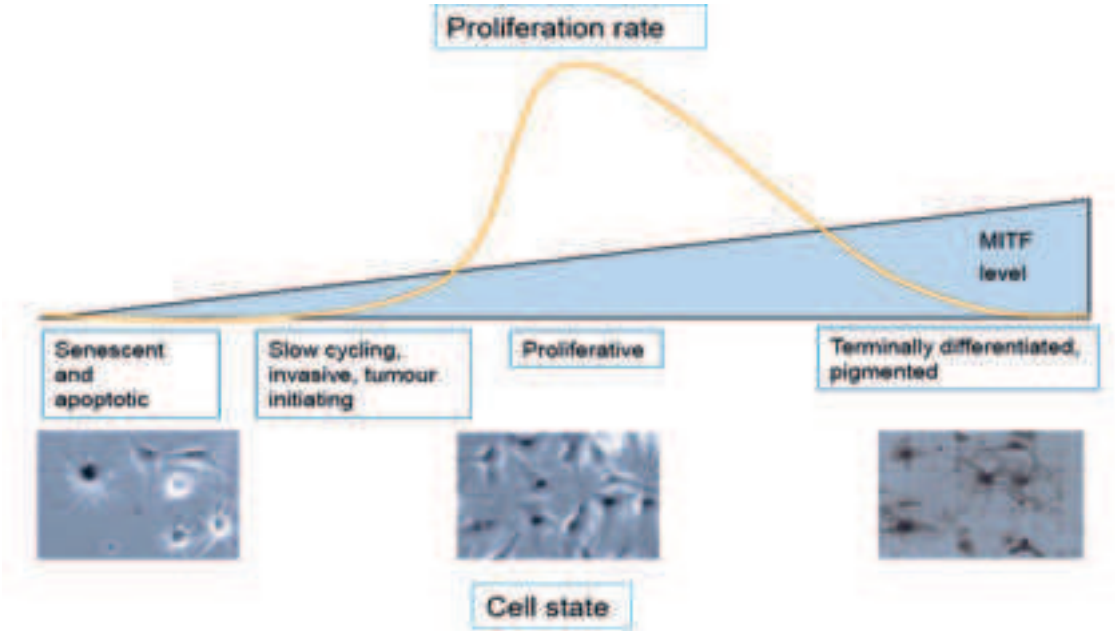

A

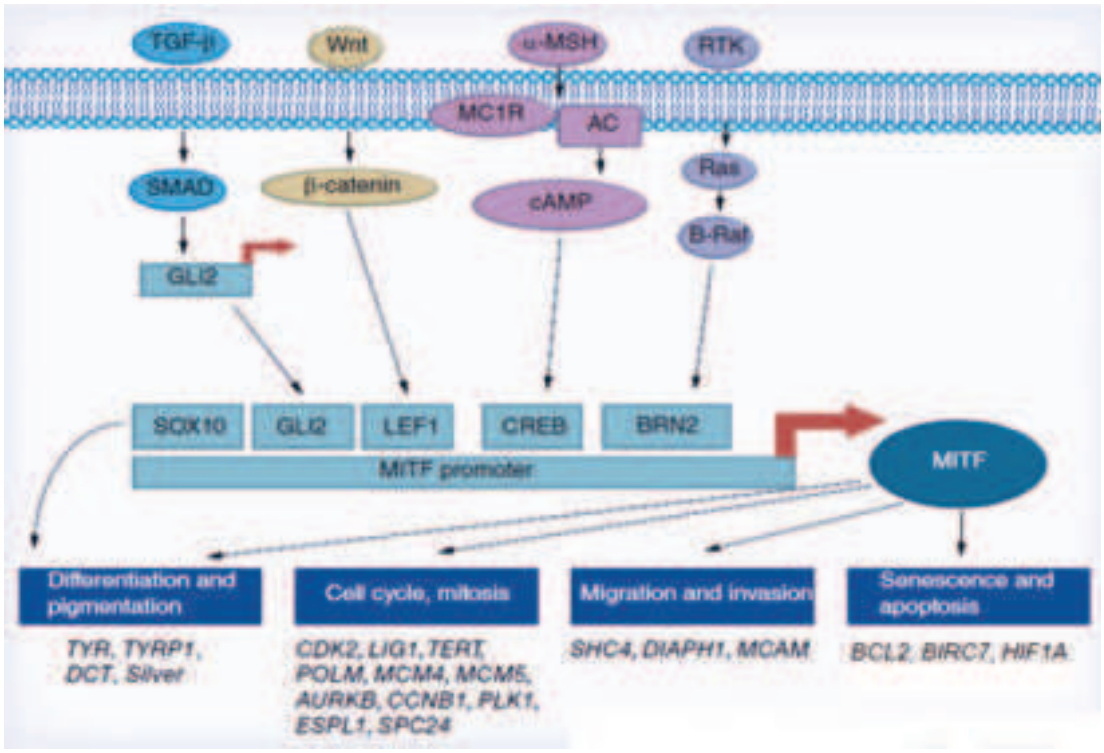

B

Figure 16 : MITF rheostat model supported by MITF regulatory network in melanoma

A) MITF rheostat model depicting different proliferation and phenotypic traits of melanoma cells with corresponding MITF expression B) Examples of MITF-regulated genes involved in various cellular processes such as DNA replication and repair, cell cycle, mitosis that are being activated by MITF, and genes involved in invasion and motility, repressed by MITF (Koludrovic and Davidson 2013)

F. Treatment of melanoma

Metastatic melanoma has very poor prognosis, since none of the treatments developed to date for this stage of melanoma development have been shown to be successful in the long run. The main reason for such a high mortality rate is the resistance of metastatic melanoma to any of the available single or combination drug treatments (Eggermont and Robert 2011). However, since 2011, several treatments have been approved by the Food and Drug administration (FDA) and European Medicines Agency (EMA) that have had a high response rates in patients with metastatic melanoma.

I. Conventional chemotherapy

Conventional chemotherapy is based on alkylating agents that result in cytotoxic effects by blocking cell replication. These include dacarbazine, carmustine, fotemustine, temozolomide or cysplatine analogues. However, these therapies result in only 10% objective response and offer no improvement in overall survival (Tarhini and Agarwala 2006, Tsao, Atkins and Sober 2004a).

II. KIT inhibitors

Somatic KIT mutations occur infrequently in melanoma patients, and are most often in acral and mucosal melanoma (15%-20%). KIT harbors various mutations and only certain of the mutations are oncogenic and can serve as effective therapeutic targets. Imatinib mesylate is a kinase inhibitor that is effective in targeting bcr-Abl, c-kit, plarelet-derivied growth factor receptor (PDGFR)-alpha and PDGFR-beta. This inhibitor displayed clinical responses in various cancer types and phase 2 clinical trials, where 28 patients with *KIT* mutations or amplifications were treated, and 16% of the patients responded. The same study also suggested patients carrying mutations in exon 11 and 13 or have *c-KIT* amplifications may benefit more from this treatment (Carvajal et al. 2011).

III. RAS/RAF/MEK/ERK pathway targeted therapy

BRAF is the most frequently mutated kinase in human melanomas and its mutation rate is around 70%. A specific potent BRAF inhibitor vemurafenib (Figure 17, a) was developed in order to target oncogenic BRAF. In the course of the phase 3 clinical trial most of the patients had a detectable reduction of the tumor size, and 48% had a response of 6 months (Chapman et al. 2011). However, all patients, including the ones with initial strong and full response eventually developed resistance (Sullivan and Flaherty 2013). Additionally, a combined therapy with MEK inhibitors showed to have a better outcome than either of the inhibitors alone. Another agent against BRAF is dabrafenib (Figure 17, a), had similar response rates to treatment as vemurafenib, but it showed less severe adverse effects. Additionally, dabrafenib was shown to be effective in treatment of melanoma brain metastasis (Shah and Dronca 2014).

BRAF mutations were associated with enhanced sensitivity to MEK inhibition in the preclinical models. Trametinib is a potent and highly sensitive MEK1/2 inhibitor and was shown to have better effect on the overall survival that chemotherapy (Flaherty et al. 2012b). Additionally, the combined therapy of dabrafenib and trametinib showed response rate of 76% for 10 months (Flaherty et al. 2012a).

IV. Immunotherapy – CTLA-4 and PD-1 blockage

The tumors adaptation to the local microenvironment includes acquired resistance to the immune responses. Recently, various molecular mechanisms regarding cancer cell evasion of the immune detection have been characterized. This led to development of the cancer immunotherapy targeting tumor microenvironment modulators favoring the anti-tumor immune response. The initial immunotherapy for melanoma consisted of high dose interferon (IFN) or interleukin IL-2 treatment, which unfortunately had badly tolerated adverse effects and did not improve the overall response rates (Eggermont and Robert 2011). However, most of tumors escape the immune control either due to the fact the mutated protein is recognized as “self” or the immune suppressive tumor milieu (Schreiber, Old and Smyth 2011). Signaling via co-inhibitory receptors, or “checkpoint molecules” such as cytotoxic T-lymphocyte-associated antigen-4 (CTLA-4) and programed cell death protein 1 (PD-1), contribute to the down-modulation of the $CD8^+$ and $CD4^+$ effector T-cell function. Their function is arresting the proliferation, survival and effector functions of the activated T-cells, resulting in limited duration of the immune response.

CTLA-4 inhibitor ipilimumab is a monoclonal antibody blocking its function, allowing a sustained immune response to tumor. Ipilimumab has been FDA approved in 2011 based on a phase 3 trial on 676 patients with the response rate of 10.9%. Furthermore, a long-term follow-up of the responders who were treated in earlier trial has shown a prolonged tumor regression in a small group of patients (Hodi et al. 2010).

PD1 and PD1L inhibitors, monoclonal antibodies targeting PD-1 can enrich the exhausted T cell population, enhance their expansion, cytokine production and cytolytic functions. Nivolumab is a fully human IgG4 anti-PD-1 antibody (Taneja 2012). In a phase 1 trial of nivolumab alone, 31% of the patients responded with median duration of the response of 2 years. Additionally, it has been shown that CTLA-4 and PD-1 could have complementary roles. A combined drug phase 1 trial on 86 patients with metastatic melanoma had 40% response rate, with 82% of the responding patients having 1 year tumor free survival (Wolchok et al. 2013). Additional PD-1 inhibitors include Lambromizumab, MPDL32801A and BMS-936559, also showing very good response rates in phase 1 trials of 51%, 26% and 29%, respectively (Shah and Dronca 2014).

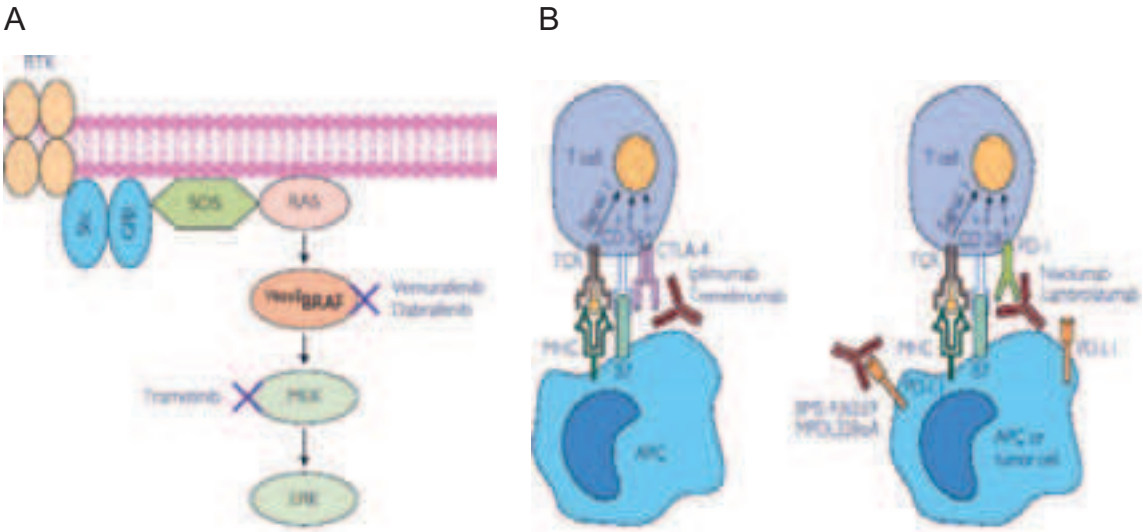

Figure 17 : Melanoma treatment

A) Personalized therapy for melanoma is based on specific inhibitors of $BRAF^{V600E}$ (vemurafenib and dabrafenib) and MEK (Trametinib) **B)** Treatment of melanoma based on immunotherapy consists of inhibitors of CTLA-4 (left panel, Ipilimumab and Tremelimumab) and PD-1 (right panel, Nivolumab, Lambrolizumab) (adapted from (Shah and Dronca 2014))

Chapter 2. Chromatin structure and regulation

1. Nucleosome as the core unit of genomic organization

A. Nucleosome structure

The publication Oudet et al. provided the electron microscope image of the eukaryotic genome, vividly demonstrating the existence of uniformly organized particles that were forming a “beads on a string” structure (Oudet, Gross-Bellard and Chambon 1975). Chromatin compaction is based on a histone octamer core, with the DNA wrapped twice around it.

The core histones. Histones present in the nucleosome core are H2A, H2B, H3 and H4. Each histone form a structure consisting of a three-helix domain termed the histone fold. These domains form “handshake” connections form the histone heterodimers H2A-H2B and H3-H4 (Arents et al. 1991). These components subsequently associate to form the histone octamer in the presence of DNA. H3 has a unique role in the nucleosome, since a 2-fold symmetry in the nucleosome is set directly along the dimer interface of the two H3 histones. H3 forms heterodimers with H4, but it also forms direct contacts with H2A. The H2A-H2Bd dimers are positioned so the two H2A proteins interact with each other. In addition to structured histone fold core, each histone forms extensions protruding out from the nucleosome consisted of disordered N-terminal and/or C-terminal histone tails. The tails show no secondary structures, and are subjected to multiple post-translational modifications. The fifth histone protein, H1 (or H5), also called the linker histone, is not contributing to the nucleosome core particle, but it is associated with linker DNA between the two nucleosomes. It forms interactions with the DNA at either entry or exit strand but not with the core histones (Zhou et al. 1998).

Within the nucleosome core particle, the DNA is wrapped forming 1.7 turns of a left-handed superhelix (Figure 18,c). DNA entry and exit points of the nucleosome are in contact with N-terminal H3 tail, and it is binding to the histones within the octamer core through the minor grooves. An extensive digestion with DNA-ases (Micrococcal nuclease) resulted in homogenous core particle containing 146 ± 2 base pairs of DNA (Noll and Kornberg 1977). Limited DNA digestion of chromatin gave rise to a so-called chromatosome units, comprising

160 base pairs of wrapped DNA and one H1 molecule (Simpson 1978). The solved crystal structure of nucleosome was revealed both histone/histone and histone/DNA interactions depend on the histone fold domains and other structure elements (Luger et al. 1997).

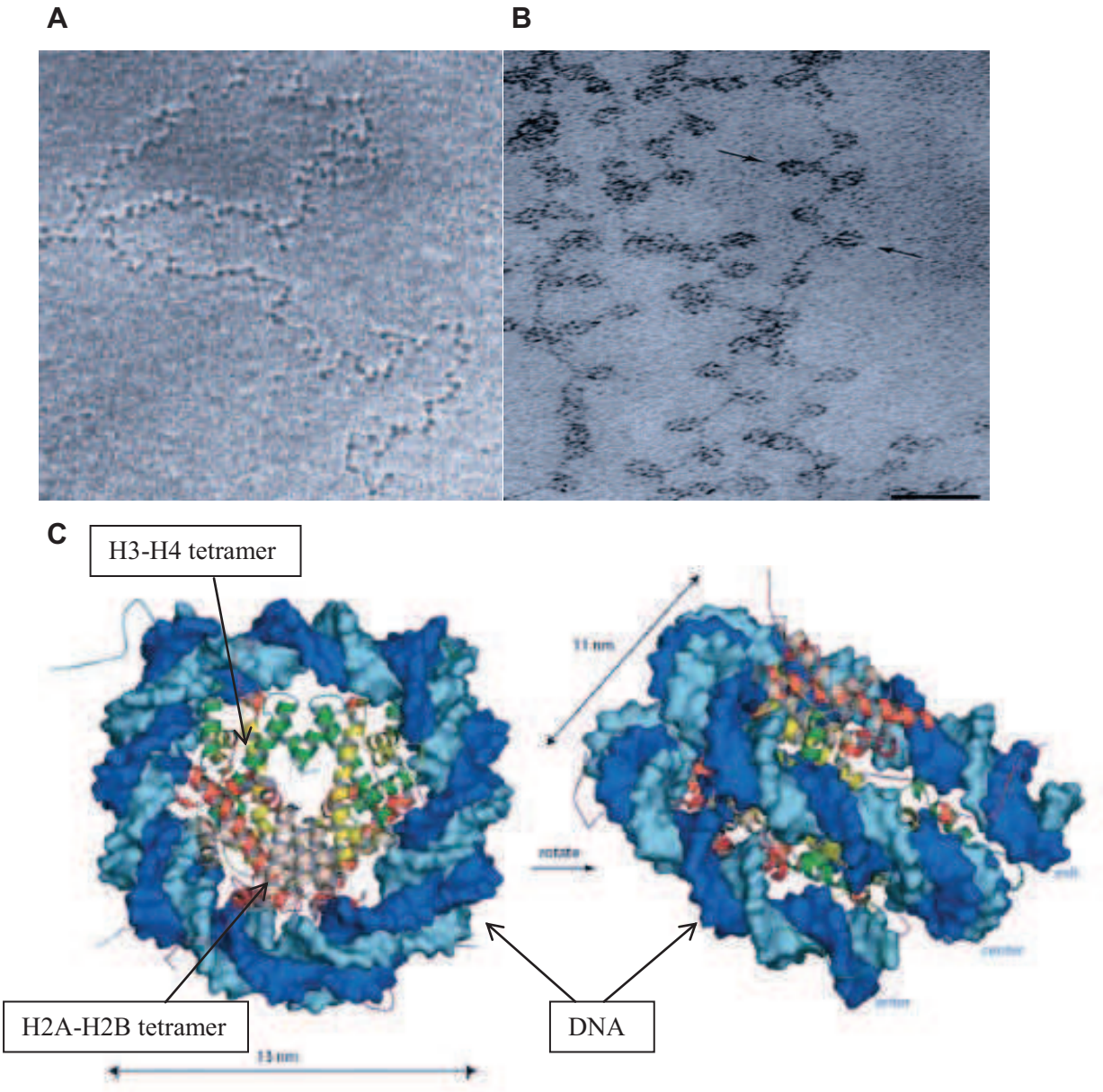

Figure 18 : Basic chromatin organization unit, the nucleosome
A) The first published electron microscopy image of the chromatin structure, appearing as “beads-on-string” (Oudet et al. 1975). B) A higher magnification of the chromatin structure, arrows are pointing to the individual nucleosomes (Olins and Olins 2003). C) A solved crystal structure of the nucleosome, depicting the positions of the histone octamer core containing H3-H4 and H2A-H2B tetramers, in a complex with DNA double wrapped around the octamer (Khorasanizadeh 2004).

B. Chromatin higher-order organization

In eukaryotic genomes, the nucleosome represents the simplest form of chromatin compaction. Nucleosomes are assembled into long, linear arrays in which each nucleosome is connected by 10-70 base pairs of linker DNA, with the length varying between species and cell types (Woodcock and Ghosh 2010). A landmark discovery using X-ray diffraction has shown chromatin was organized in highly compacted 30 nm wide solenoidal coils (Figure 18, a), and histones were proposed to function primarily as genome packaging material (Finch and Klug 1976). However, the existence of the 30 nm fiber has seriously been put under question in the light of recent theoretical and experimental analyses; computational modeling of the chromatin fiber suggested the nucleoprotein polymer is theoretically far less efficient as a mode of packaging than previously assumed (Rosa and Everaers 2008, Tokuda, Terada and Sasai 2012). Furthermore, cryo-electron microscopy (EM) coupled with a set of precise measurements, 30 nm fibers could not be detected in the interphase nuclei or metaphase chromosomes (Eltsov et al. 2008, Fussner et al. 2012). Using small-angle X-ray scattering (SAXS), another group reported it was unable to detect 30 nm fibers *in vivo*, but rather suggested the possibility the data first reported 30 nm fibers might instead have been periodic reiterations of ribosomes, which are 30 nm in diameter and were found to coat the chromatin under certain preparative procedures (Joti et al. 2012).

The debate on this startling matter is still ongoing, but it appears much of the chromatin exists as a 10 nm fiber (“beads on a string”, figure 18 a and b), with locally folded areas holding 5-10 nucleosomes and 3D “fractal globule” arrangements of chromatin fibers stabilized in a cross-array, where the density of these areas might be coordinated by histone H1 and networks of non-histone proteins (Lieberman-Aiden et al. 2009).

C. The role of the nucleosome in transcription regulation

I. Histone and DNA modifications and modifiers

A major mechanism by which chromatin structure is regulated is through the histone post-translational modifications (PTMs). Histone PTMs can regulate the specific composition and structure of nucleosomes at individual genes. These modifications include lysine acetylation, lysine and arginine methylation, lysine ubiquitination, serine/threonine/tyrosine phosphorylation, lysine sumoylation (Bannister and Kouzarides 2011, Greer and Shi 2012, Klose and Bird 2006, Kohli and Zhang 2013, Kouzarides 2007) . While the major part of the modifications are found in the flexible N- and C-terminal histone 'tail' domains that protrude from the nucleosome core particle, a number of the modifications are also reported in the histone fold or globular domains and have a function in regulating histone–histone and histone–DNA interactions (Cosgrove, Boeke and Wolberger 2004, Cosgrove and Wolberger 2005). The function of histone PTM has been elucidated through the identification of the protein machineries that incorporate (writers), remove (erasers), and bind (readers) histone PTMs. Two hallmark discoveries were the identifications of p55/Gcn5 and HDAC1/Rpd3 as transcription associated histone acetyltransferases (Brownell et al. 1996) and deacetylases (Taunton, Hassig and Schreiber 1996), linking dynamic histone modification activity directly to the transcription process. The concept of a 'histone code' was proposed, offering an explanation of histone PTMs function (Strahl and Allis 2000, Turner 2000). This concept stated that histone modifications are read by specific proteins capable of reading the different marks, enabling distinct downstream events, such as transcription activation or repression. The intricate network of the histone modifications has been shown to be ever-more complex, since both the nature and the location of the modification within the nucleosome are crucial for the transmission of a particular signal.

Histone acetylation

Acetylation as a modification has so far been exclusively associated to activation of transcription. It takes place on lysines of histones and it is a highly dynamic, regulated by opposing actions of two classes of enzymes, histone acetyl-transferases (HATs) and histone deacetylases (HDACs).

The HATs use acetyl CoA as cofactor and catalyze the transfer of an acetyl group to the ε-amino group of lysine side chains. As a result, the lysine positive charge in neutralized which ultimately causes the potential weakening of DNA-histone interactions (Bannister and

Kouzarides 2011). Two main types of HATs include type-A and type-B. Type-B HATs are predominantly cytoplasmic and are acetylating free histones, and not those already incorporated into chromatin. This class of HATs share sequence homology with the yeast scHat1, which is the founding member of this class. Cytoplasmic HATs acetylate histone H4 at lysines K5 and K12, and also sites on H3, and this modification pattern is later required for histone deposition within chromatin, which is followed by removal of the marks (Parthun 2007). The type-A HATs are more diverse and can be classified into three groups based on sequence homology and structure, including GNAT, MYST and CBP/p300 families (Hodawadekar and Marmorstein 2007). Each of the above mentioned enzymes modify multiple sites within the histone N-terminal tails resulting in the neutralization of the positive charges. The disruption of the stabilizing electrostatic interactions between histones and DNA correlates with the function of this class of enzymes as transcriptional co-activators, such as SAGA, SLIK, STAGA, ADA, and A2 complexes, Gcn5L, p300/CREB-binding protein associated factor (PCAF), Elp3, HPA2 and HAT1 (Yang and Seto 2007). Additionally, apart from the regulation of transcription via histone tail modifications, the globular histone core has also been shown to me modified, namely at the H3K56 residue by hGCN5 in humans. This residue is facing the DNA major groove, pointing to the role of this acetylation site in histone-DNA interactions (Tjeertes, Miller and Jackson 2009). As multiple other histone modifiers, type-A HATs are often associated with multi-protein complexes (Yang and Seto 2007). The composition of the given complex has an important role in the recruitment, activity and specificity of the enzyme. For instance, the purified yeast scGCN5 acetylates the free histones but not the nucleosomal histones. Once it takes part of the SAGA complex, scGCN5 is capable of efficient acetylation of the nucleosomal histones (Grant et al. 1997).

HDAC enzymes oppose the effects of the HATs and deacetylase the histones, restoring the positive charge of the lysine. This stabilizes chromatin architecture and strengthens the histone-DNA interactions and this action accounts for HDACs serving predominantly as transcriptional repressors (Yang and Seto 2007). HDACs are separated in four classes. The first two, classes I and II are enzymes related to yeast scRpd3 and scHda1. Furthermore, class III, also referred to as sirtuins, contains the enzymes that are homologous to yeast scSir2 and require a specific cofactor for its activity, NAD^+. Finally, class IV that has only one member, HDAC11. Overall view of HDAC activity shows low substrate specificity, with a single enzyme deacetylating multiple sites (Yang and Seto 2008).

Histone methylation

Methylation mainly takes place on the lysines and arginines. Unlike acetylation, this modification does not alter the charge of the protein. Methylation adds

additional level of complexity to the histone regulation since it can be mono-, di-, or tri-methylated in the case of lysines, and mono-, symmetrically or asymmetrically di-methylated on arginines (Bedford and Clarke 2009, Lan and Shi 2009, Ng et al. 2009, Wood and Shilatifard 2004).

Lysine methylation is performed by histone lysine methyltranferase enzyme (HKMT). The first identified was SUV39H1 and it targets H3K9 (Rea et al. 2000). Since this report, many more HKMT enzymes have been discovered. The structures involved in the activity of the methyltransferases are the SET domain, and also the pre-SET and lastly the post-SET domains. Formation of β-sheets between β-strands of both pre-SET domain and the SET domain bring about small changes in the structure of the SET domain. This changes cause alteration of the specificity for the target residue site and enable the SET domain methyltransferases to target a wide range of the substrate residues. The non-SET methyltransferasease, Dot1 targets H3K79 within the histone globular domain, and is so far the only enzyme recorded to have this ability (Wood and Shilatifard 2004). Regardless of the catalytic core utilized, the catalyzing reaction of all the HKMT enzymes involves the transfer of a methyl group from S-adenosylmethionine (SAM) to a lysine ε-amino group (Trievel et al. 2002). Lysine methyltransferases modification reaction output can be either activation or repression of transcription.

Arginine methylation is being performed by two classes of methyltransferases, type-I and type-II enzymes. Type-I can modify arginines as Rme1 (mono-methyl) and Rme2as (di-methyl asymmetric), whereas type-II generate Rme1 and Rme2s (di-methyl symmetric). The two types of enzymes form a protein family of PRTMs. Their mechanism of action involves enzymatic transfer of a methyl group from SAM to the ω-guanidino group of arginine. The most relevant enzymes for histone arginine methylation are PRMT1, 4, 5 and 6 (Bedford and Clarke 2009, Wolf 2009).

Histone demethylases are the enzymes that are removing the methyl mark from histones. The first identified lysine demethylase, LSD1 uses FAD as a co-factor (Shi et al. 2004). In vitro, LSD1 cannot demetylate the histones already incorporated in the nucleosome, but when it is a part of the Co-REST complex, it functions as a demethylase in the nucleosomal context. The precise association determines which lysine is to be modified; LSD1 in the context of Co-REST demethylates H3K4me1/2, but when it is in complex with the androgen receptor, it demethylases H3K9. As a result of this switch, LSD1 changes its activity from a repressor to a co-activator (Klose and Zhang 2007). Another class of histone demethylases was also recorded, the first enzyme being JMJD2 that demethylases H3K9me3 and H3K36me3, using Fe(II) and α-ketoglutarate as co-factors (Tsukada et al. 2006, Whetstine et al. 2006). The JMJD2 enzymatic activity lies in the JmjC jumonji domain.

Many histone lysine demethylases have been identified and they all, apart from LSD1, contain a catalytic jumonji domain (Mosammaparast and Shi 2010).

Other histone modifications

Apart from histone acetylation and methylation that are mainly recognized by chromatin regulating proteins and protein complexes, histones harbor many additional modifications that have various roles in chromatin biology.

Histone phosphorylation is a highly dynamic modification, taking place on serines, threonines and tyrosines predominantly in the N-terminal histone tails. This modification is performed by kinases and is consisted of a transfer of phosphate group from ATP to the hydroxyl group of the target side chain. The opposite reaction is performed by phosphatases that are removing the phosphorilation mark (Oki, Aihara and Ito 2007). The phosphate is adding a significant negative charge to the histone and influences the chromatin structure. An example is Aurora kinase B that has a role in histone phosphorylation during mitosis, marking H3S10ph and H3S28ph genome-wide, and is antagonized by PP1 phosphatase (Goto et al. 2002, Sugiyama et al. 2002).

Ubiquitylation and sumoylation; these modifications results is a much larger covalent modification compared to all the previously mentioned modifications. Ubiquitin is a 76-amino acid protein attached to histone lysines in a step-wise manner that involve E1-activating, E2-conjugating and E3-ligating enzymes (Hershko and Ciechanover 1998). These enzyme complexes determine both substrate specificity as well as the degree of ubiquitylation (mono- or poly-ub). Two well-known sites are situated within H2A and H2B. H2A119ub1 is involved in gene silencing (Wang et al. 2004), whereas H2BK123ub1 has an important role in transcription initiation and elongation (Kim et al. 2009, Lee et al. 2007). Sumoylation is a modification related to ubiquitylation, and it is consisted of covalent binding of a small ubiquitin-like modifier to histone lysines via E1, E2 and E3 enzymatic system (Seeler and Dejean 2003). Sumoylation has been reported on all core histones, with the role of an antagonist for acetylation and ubiquitylation by competing for the binding site, and is therefore considered to have a repressive role in chromatin regulation (Nathan et al. 2006, Shiio and Eisenman 2003).

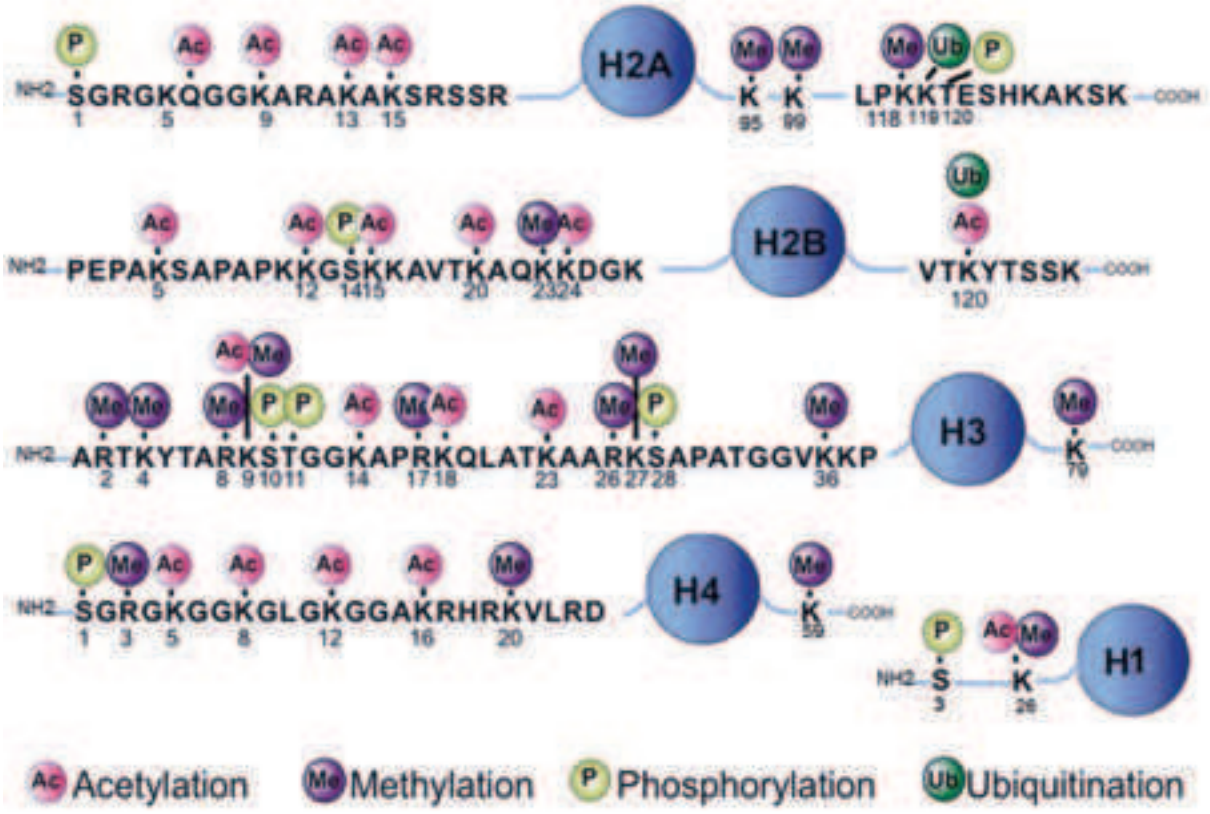

Figure 19 : Histone tail modifications

Schematic representation of histone tail modifications including acetylation (in pink), methylation (in purple), phosphorylation (in yellow) and ubiquitination (in green) (adapted from Cota, 2013, Stem cells and epigenetic reprograming, Intech).

II. Histone modification binding proteins – "readers" of the histone marks

As mentioned above, histone post-translational modifications (PTMs) can either have a direct effect of the chromatin structure, such as acetylation, that is weakening histone-DNA interactions. On the other hand PTMs function as a signal platform to recruit effectors, namely various readers of histone modifications in order to alter local chromatin. Multiple efforts have identified conserved domains within chromatin associated proteins responsible for recognition of specific histone modifications, functioning as a bridge between a given histone modification and the cellular protein machinery.

Lysine acetylation readout domains

Lysine acetylation marks are indirectly interpreted via binding of effector proteins containing either the bromodomain or tandem PHD finger. Bromodomains were

initially identified in the context of the histone acetyltransferases (HATs), such as Gcn5p, targeting H4K16ac. They have also been shown to be present in proteins playing important roles in transcriptional activation (eg. TAF1, a subunit of the general transcription factor TFIID; PCAF co-activation) and chromatin remodeling (eg. Rcs4p, subunit of the yeast RSC complex; BPTF, subunit of the NURF complex). Bromodomain can be present in the reader either as a single bromodomain (Gcn5p, BPTF), double bromodomain (TAF1) or tandem bromodomain (Rsc4p). In all cases, bromodomains adopt a characteristic structural fold of a left-handed four-helix bundle (αZ, αA, αB and αC), termed the `BRD fold'. The inter-helical αZ-αA (ZA) and αB-αC (BC) loops form a hydrophobic pocket accommodating the acetyl-lysine (Figure 20) (Sanchez and Zhou 2009). Acetyllysine can also be recognized by the tandem PHD domain. DPF3(b), a the subunit of the BAF chromatin remodeling complex, it is capable of binding the acetylated histones since the tandem PHD domains form a hydrophobic pocket, but it can bind both H3 and H4 (Zeng et al. 2010).

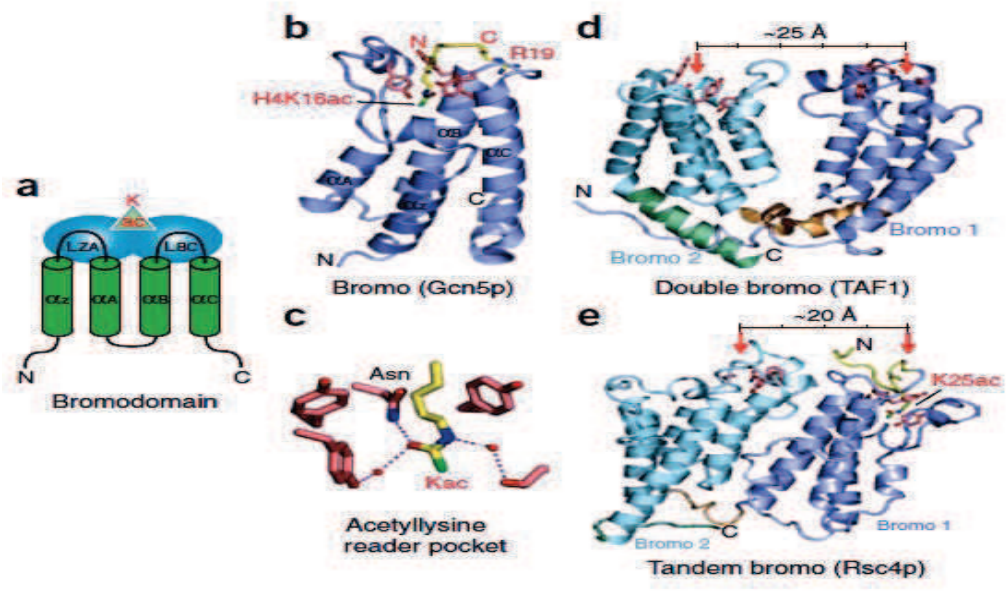

Figure 20 : Bromodomain binding on acetyllysine marks

Bromodomain binding of the acetyllysine marks in different configurations

A) Schematic representation of the bromodomain structure. C) Structure of the acteyllysine reader pocket. B, D, E) Examples of the configurations of the bromodomain in different readers. Adopted from (Taverna et al. 2007).

Methylation mark readers

Lysine methylation includes four types of signals: unmethylated (me0), mono- (me1), di- (me2) and tri- (me3) methylation. Unmodified lysine is included in the methylation signaling group since this modification is the only modification of residues that have been

shown to be recognized by unmodified lysine binders, and additionally, all me0 (non-modified lysine) binders are sensitive to addition of the methyl group. Since there is a greater heterogeneity in different types of the methyl marks, there are multiple domains that recognize histone lysine methylation. These include PHD, chromo, WD40, Tudor, double/tandem Tudor, MBT, Ankyrin Repeats, zf-CW and PWWP domains. Unlike acetylation, methylation is a highly specific mark. Many of the domains binding the methyl mark are a part of the Royal superfamily containing the SH3-like barrel, which, depending on the protein, can read both multivalent (di- and tri- methyl marks) and monomethylation (Figure 21). The Binding of an unmethylated lysine does not require an apparent pocket, like in case of BHC80 (Lan et al. 2007).

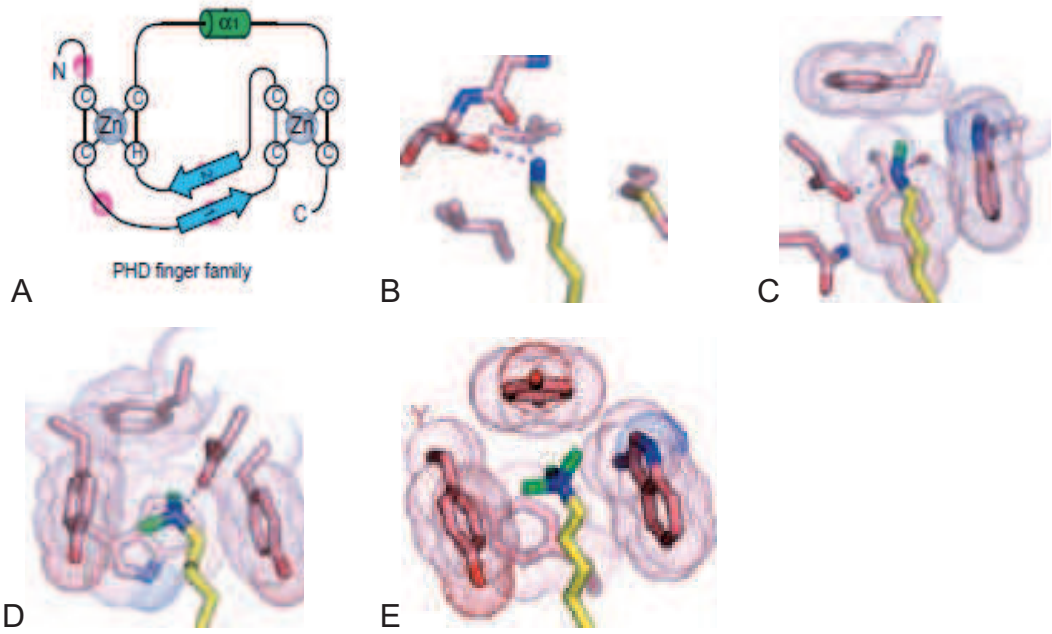

Figure 21 : PHD finger domain binding methyl marks

A) Schematic representation of the structure of the PHD finger domain. Blue arrows represent the two β strands bridging the two zinc-finger motifs (grey circles); green tube is a short α1 helix next to the C-terminal end; pink circles represent the residues forming a cage responsible for the readout of the specific methyl marks. **B)** Structure of the Kme0 bound by PHD domain of BHC80, **C)** Structure of the Kme1 bound by MBT domain of the L3MBTL1, **D**) Structure of the Kme2 bound by the tudor domain of the 53BP1 **E)** Structure of the Kme3 bound by the PHD finger domain of BPTF (Taverna et al. 2007).

III. Multiple layers of the histone code readout

Increasing complexity of the histone code readout has been suggested with the reports of histone modification being read both in asymmetric and multivalent combinations, including asymmetric and multiple histone PTM binding.

PTM combinations asymmetry

The asymmetric distribution of the post-translational modifications adds to the diversity of the histone functions. While the co-occurrence and mutual exclusivity of the different PTMs has been reported, it has been technically difficult the address the question if the two histones of the homodimer are modified in the same way. The study conducted to determine histone PTM pattern by using the specific antibodies revealed that the marks H3K27me2 and H3K27me3 as well as H4K20me1 exist on two different subpopulations of nucleosomes, both symmetric and asymmetric (Voigt et al. 2012). A potential role of asymmetric PTM distribution has been shown in context of development, in the study conducted on the genome-wide mapping of histone marks. A co-occurrence of H3K4me3 (mark of active transcription) and H3K27me3 (associated with transcription repression) has been documented at developmental gene promoters in embryonic stem cells, was termed “bivalency” (Voigt, Tee and Reinberg 2013). The bivalent binding was suggested to function as a mechanism to keep the target loci in a “poised” arrangement, ready to react to different external stimuli.

Multivalent PTM recognition

Ever increasing body of evidence is suggesting a diverse family of histone reader domains (discussed in more detail in passages below) that are capable of recognizing and binding specific histone modifications. It has also become more apparent many of the proteins or protein complexes employ multivalent binding including cis-histone, inter or intra-nucleosomal or trans DNA:histone combinations (Rothbart and Strahl 2014).

The different binding configurations include *cis*-histone involving two modifications within the same histone tail (eg. TAF1 binding H4K5/8/12/16ac, also TRIM24 binding H3K4me0 and H3K23ac). *Trans* intranucleosomal binding involves binding of two marks situated within the same nucleosome but on different histones (eg. BPTF binding H3K4me3 and H4K16ac, also JMJD2A binding H3K4me3 and H4K20me3), while *trans* internucleosomal binding includes binding of two marks on two different nucleosomes (eg. HP1 dimer binding H3K9me3). Multivalent binding can be by single protein with multiple binding domains, or by a complex, with different subunits containing the binding domains (Ruthenburg et al. 2007, Wang and Patel 2011).

IV. Histone variants

The canonical histones ensure nucleosome integrity and regulate access to DNA, but along the canonical histone molecules, a set of specialized histone variants has evolved to regulate various cellular processes. Histones H1, H2A and H3 have been shown to have multiple variants, differencing across species and their functions (Yuan and Zhu 2013).

H1 variants include H1.1, H1.2, H1.3, H1.4, H1.5, H1x, expressed ubiquitously, H1t, H1T2, HILS1, expressed in spermatids and spermatocytes, H1oo, expressed in oocytes and H1.0, expressed in differentiated cells (Happel and Doenecke 2009).

H2A variants are the most diverse, H2A.Z arising in early eukaryotic evolution is expressed ubiquitously, and is distinct from H2A (Talbert and Henikoff 2010). Even though H2A and H2A.Z share only 60% of the amino-acid sequence, the nucleosomes comprising these two variants are very similar, but have key structural differences (Suto et al. 2000). On the surface H2A.Z has an extended acidic patch, stimulating remodeling activity by ISWI class of chromatin remodelers (Goldman, Garlick and Kingston 2010). It was also reported that H2A.Z regulates nucleosome positioning around promoters, which could influence accessibility of cis-regulatory regions (Guillemette et al. 2005, Marques et al. 2010).

Other H2A transcription related variants that are not dependent on replication are present only in animals. H2A.B knockdown in HeLa cells showed a significant changes in gene expression, with a more obvious role of an activator than a repressor. H2A.B has also been shown to associate with components of the spliceosome, and, upon knockdown, RNA splicing is less efficient (Tolstorukov et al. 2012). macroH2A localization on the inactivated female X chromosome, silent SAHF, and large transcriptionally silent domains (Costanzi and Pehrson 1998, Gamble and Kraus 2010, Tolstorukov et al. 2012, Zhang et al. 2005) suggests a role in transcriptional repression, although macroH2A is not required for X-chromosome inactivation (Changolkar et al. 2007).

The number of H3 histone variants is different across different species. All eukaryotes have a centromere specific H3 (CenH3, or CENP-A in mammals), which contains an amino acid sequence that is significantly different from the other H3 histone variants. In addition to CENP-A, mammals have three ubiquitously expressed H3 variants (H3.1, H3.2, and H3.3) as well as an H3 isoform that is specifically expressed in the testis (H3t). Other higher eukaryotes have two non-centromeric H3 variants, H3.3 and H3.1 (identical to mammalian H3.2). Yeast has only one non-centromeric H3, which is similar to H3.3 in higher eukaryotes (Henikoff and Ahmad 2005). Additionally, two primate-specific H3 variants (H3.X and H3.Y) (Wiedemann et al. 2010) were identified, and so was H3.5 variant that is specific for humans (Schenk et al. 2011).

V. Histone chaperones

Histone chaperones are proteins that function at multiple steps of nucleosome formation. Chaperones associate to the histones during their incorporation and eviction, and prevent aberrant histone-DNA aggregation during nucleosome assembly. Canonical and variant histones are deposited during replication-coupled and replication-independent nucleosome assembly with the help of histone chaperones.

Histone chaperone Asf1 has a more general role in histone biology, since its roles include histone H3-H4 import and transfer to other histone chaperones CAF-1 and HIRA. Asf1 also has a role in regulation of H3K56ac (English et al. 2006, Li et al. 2008, Tyler et al. 1999). CAF-1 complex has a role in de novo deposition of replicative H3.1-H4 in a DNA synthesis-coupled pathway. CAF-1 complex is comprised of three subunits p150, p60 and p48 (RbAp48) in human cells. CAF-1 complex receives histone dimers from Asf1, but is is also involved I formation if the $(H3\text{-}H4)_2$ tetramers. CAF-1 is involved in DNA replication and repair (Stillman 1986, Tagami et al. 2004, Verreault et al. 1996, Winkler et al. 2012). HIRA is a H3.3 chaperone that deposits H3.3-H4 histones throughout interphase, independently of DNA synthesis, primarily at genic regions and regulator elements (Ray-Gallet et al. 2002). HIRA is functioning within a complex that also contains ubinuclein 1 (UBN1) and calcineurin-binding protein 1 (CABIN1) proteins in humans (Balaji, Iyer and Aravind 2009, Rai et al. 2011). Histone chaperone DAXX also serves as H3.3-H4 histone chaperone, and deposits this histone dimer to telomeres (Drane et al. 2010, Goldberg et al. 2010, Lewis et al. 2010). ChIP-seq experiments demonstrated DAXX-dependent H3.3 enrichment profile that was shown to differ from the one from HIRA (Drane et al. 2010, Goldberg et al. 2010). DAXX can associate with the α-thalassemia/mental retardation X-linked (ATRX) protein, which is also found in the soluble H3.3 complex (Tagami et al. 2004). ATRX is a SNF2-related ATPase with a PHD and it forms a chromatin-remodeling complex with Daxx (Xue et al. 2003). The association between ATRX with Daxx, might increase the accessibility to nucleosomal DNA at Daxx target promoters and recruit Daxx activity to specific genomic loci (Drane et al. 2010, Goldberg et al. 2010).

Holliday junction recognition protein (HJURP) regulates the incorporation of the histone H3 variant CENP-A in centromere regions in a cell-cycle-dependent manner. HJURP and its functional homologs are essential for CENP-A incorporation and therefore are crucial for centromere establishment and maintenance (Dunleavy et al. 2009, Foltz et al. 2009). Some of the multiple other histone chaperones include NASP (involved in histone supply and turnover), DEK (regulates H3.3-4 incorporation and maintenance in heterochromatin), FACT (deposits and exchanges H3–H4, H2A–H2B, H2A.X–H2B) and Nap1 (involved in H2A–H2B nuclear import and deposition) (Burgess and Zhang 2013)

2. ATP-dependent chromatin remodeling

There are currently four different families of chromatin remodeling complexes. All four utilize ATP hydrolysis to alter histone-DNA contacts and share a similar ATPase domain. However, all four are also specialized for particular purposes and biological contexts, imparted by unique domains residing in their catalytic ATPases and also by their unique associated subunits. The four families of the ATP-dependent chromatin remodelers include the SWI/SNF, ISWI, CHD and INO80 families. The remodeling reaction can result in multiple outcomes, depending on the chromosome remodeler. The possible remodeling reactions include site exposure by repositioning the nucleosome (done by all the remodelers), nucleosome ejection and sire unwrapping (done by SWI/SNF). Furthermore, altered composition of chromatin is also performed by the chromatin remodelers, and it includes histone dimer exchange, or histone dimer ejection (SWI/SNF, INO80) (Figure 22, (Clapier and Cairns 2009)).

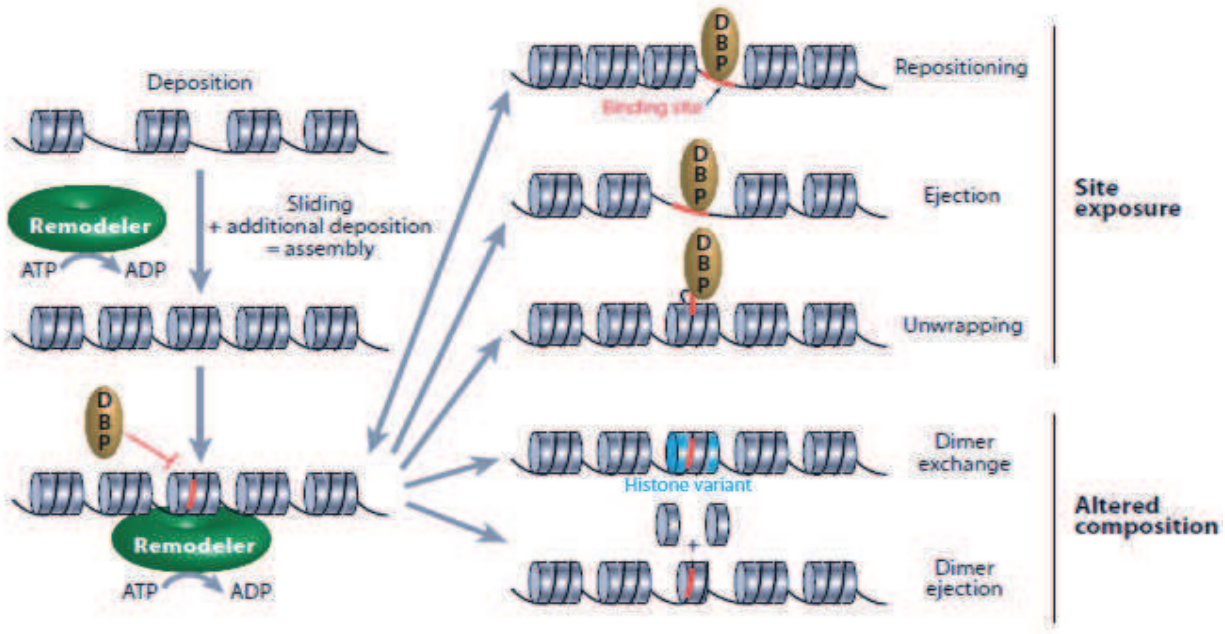

Figure 22 : Chromatin remodeling reactions result in different outcomes

The outcomes of the chromatin remodeling reactions can are divided into two groups. The first is the site exposure for the DNA binding proteins (DBP, depicted as a yellow circle). If the binding site (depicted in red) for the DBP is wrapped around the nucleosome, it is inaccessible (left lower panel). In order to expose the site for binding, the chromatin remodeling complexes reposition the nucleosome, eject the octamer core, or unwrap the fragment of DNA (right upper panel). The second outcome of chromatin remodeling can be alteration of the chromatin structure by exchanging or ejecting the histone dimer (Clapier and Cairns 2009).

A. ATP-ase domains in different remodeling families

All remodeler complexes contain an ATPase subunit, characterized by an ATPase domain that is split in two parts: DExx domain and HELICc domain. ATP-ase remodelers of the SWI/SNF, ISWI, and CHD contain a short ATPase domain insertion, INO80 family remodelers harbor a longer insertion between the two parts of the ATP-ase domain. Each family has additional domains that are involved in complex composition and ATP-ase functions. Bromodomain and HSA (helicase-SANT) are present in the SWI/SNF family ATP-ase, HAND-SANT-SLIDE tripartite domain are characteristic for the ISWI family, double chromodomains are present in the CHD family, and HSA domain for the INO80 family (Figure 23).

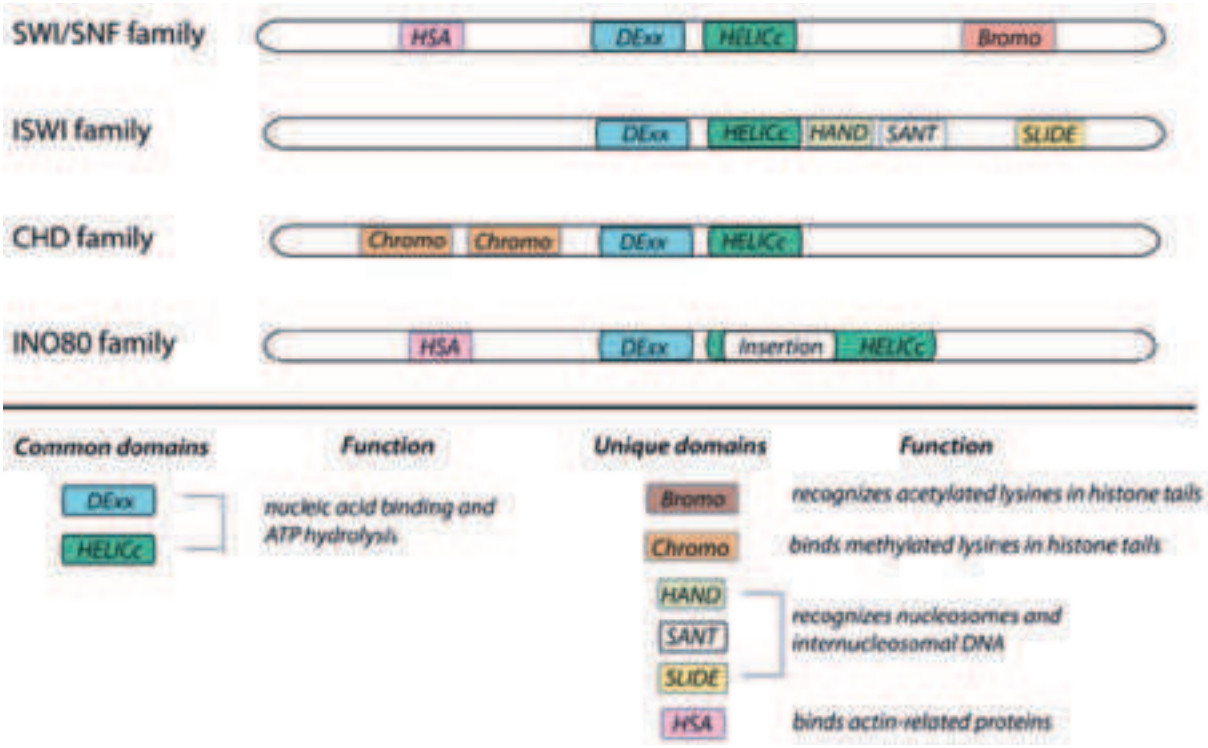

Figure 23 : Catalytic ATP-ase subunit in different chromatin remodeling families

All the ATP-ase subunits contain the ATP-ase domain, consisted of Dexx (in light blue) and HELICc (in green) domains, involved in DNA binding and ATP hydrolysis. Every family of ATP-ases contains additional unique domains, depending on their functions and additional subunits of the complex. (adapted from Manelyte et al. 2013, Chromatin Remodelers and Their Way of Action, Intech)

B. INO80 family of chromatin remodelers

The INO80 (inositol requiring 80) family remodelers are comprised of 10 subunits, include the SWR1-related complexes (Table 3), and were initially purified from S. cerevisiae. The characteristic feature of this family is the ATPase domain that harbors an extended insertion within the ATPase domain. Both yINO80 and ySWR1 complexes also contain actin and Arp4. In D. melanogaster, the complexes present are Pho-dINO80 and Tip60, and in human, INO80 family includes INO80, SRCAP (SNF2-related CREB-activator protein), and TRRAP/Tip60, with p400 as an ATP-ase, which also contains HAT activity (Bao and Shen 2007, Clapier and Cairns 2009).

The characteristic of the INO80 family is their ability to deposit and exchange histones. Yeast INO80 has been shown to exchange the histone variant H2A.Z with a H2A (Kobor et al. 2004, Papamichos-Chronakis et al. 2011). Ino80 complex has also been involved in embryonic stem cell self-renewal, somatic cell reprogramming, and blastocyst development. Ino80 co-occupies pluripotency gene promoters and its occupancy is dependent on OCT4 and WDR5. At the pluripotency genes, Ino80 has a role of keeping the open chromatin structure in order to allow the recruitment of the Mediator complex and the RNA Pol II (Wang et al. 2014).

C. CHD family of chromatin remodelers

Chromodomain (CHD) family of chromatin remodelers is further subdivided into three subfamilies with distinct structures and domain composition. Subfamily I has a standard composition with an addition of a DNA binding domain on the C-terminus consisting of a SANT-SLIDE domain. This subfamily includes Chd1 in yeast and *D. melanogaster* and CHD1 and CHD2 in mammals. CHD1 in vivo functions both as a transcriptional activator and repressor, as well as transcription elongation, and pre-mRNA splicing events. Subfamily II has a double PHD finger in the N-terminus in addition to the common family domains. This subfamily includes Chd3 and Chd4 in *D. melanogaster* and in mammals. Both CHD3 and 4 are components of the NURD complex in humans, and CH4 also interacts with HDAC1. NURD is the sole remodeling complex performing as a transcriptional repressor. NURD interacts with specific transcription factors in order to be recruited target genes promoters. When it is recruited, NURD remodels the neighboring nucleosomes, making the histone tails more accessible for deacetylation. The reaction results in more compacted nucleosome arrays and transcriptional repression (Murawska and Brehm 2011).

Organism	Complex	Catalytic subunit	Auxiliary subunits	Function
INO80 family of chromatin remodeling complexes				
Yeast	INO80	Ino80	Rvb1, Rvb2, Arp5, Arp8, Arp4, Act1, Taf14, Ies1, Ies2, Ies3, Ies4, Ies5, Ies6, Nhp10	Transcription regulation DNA repair regulation DNA replication regulation
	SWR1	Swr1	Rvb1, Rvb2, Arp6, Arp4, Act1, Yaf9, Swc4/Eaf2, Swc2, Swc3, Swc4, Swc5, Swc6, Yaf9, Bdf1, Swc7, H2AZ, H2B	H2A.Z deposition at the boundary of hetero- , eu- chromatin, loading H2A.Z around DSB
CHD family of chromatin remodeling complexes				
Fly	Chd1	Chd1		Nucleosome spacing, chromatin assembly
	Chd2	Chd2		
	NuRD	Mi-2	MBD2/3, MTA, RPD3, p55, p66/68	
Mammals	Chd1	Chd1		Maintenance of stem cells
	Chd2	Chd2		Development, DNA damage, tumor suppression
	NuRD	Chd3/Chd4	MBD3, MTA1/2/3, HDAC1/2, RbAp46/48, p66α/β, DOC-1	Transcriptional repression

Table 3 : INO80 and CHD chromatin remodeling complexes
Adapted from (Bao and Shen 2011, Sims and Wade 2011)

D. SWI/SNF family of chromatin remodelers

SWI/SNF complexes in drosophila include BAP (Brahma Associated Protein) and PBAP (Polybromo-associated BAP) complexes. In human, these two complexes are called BAF (Brg1 Associated Factors) and PBAF (Polybromo-associated BAF) (Table 4).

I. Mechanism of action of SWI/SNF remodelers

The mechanism of SWI/SNF remodeling action has been proposed based on single molecule experiments. The translocation domain, consisted of tracking and torsion subdomains is initially bound to the DNA within the nucleosome at a specific location. In the

presence of ATP hydrolysis (Havas et al. 2000), the torsion domain creates a DNA loop on the side of the nucleosome by translocating the DNA along the nucleosome core. The remodeling mechanism involves continuous movement of the loop around the nucleosome until it reaches the exit site. The tracking domain has a role in DNA loop regulation, in order to avoid the loop backtracking (Zhang et al. 2006). The creation of the loop weakens the histone-DNA interactions, and this mechanism is the same one proposed to function during histone dimer exchange or ejection mediated by histone chaperones (Boeger et al. 2003, Lorch, Maier-Davis and Kornberg 2006).

III. Functions of SWI/SNF remodelers in cancer and melanoma

SWI/SNF have been implicated in many cellular processes including transcription regulation, nuclear organization, centromere, and chromosomal stability, and mutations in SWI/SNF components have been linked to several types of cancer.

Components of human SWI/SNF complexes are mutated at a very high frequency, 19% across various human cancers (Kadoch et al. 2013). The association of SWI-SNF mutations with cancer is further explained by a study reporting a high frequency of anaphase bridges upon BRG1 silencing (Dykhuizen et al. 2013)

In melanoma BRG1 has been shown to have a pro-survival role after UV irradiation or chemotherapy and also to promote melanocyte differentiation (Keenen et al. 2010). One of the BRG1-mediated anti-apoptotic mechanisms in UV irradiated melanoma relies on up-regulation of MITF target gene, ML-IAP (BIRC7, livin) (Lazar et al. 2012). Additionally, BRG1-mediated ML-IAP activation has been shown to involve cooperation with MITF (Saladi et al. 2013). Furthermore, SWI/SNF chromatin remodeling has been shown to have a vital role in MITF expression in human melanoma (Vachtenheim, Ondrusova and Borovansky 2010). BRG1 chromatin remodeling has a role in facilitating MITF binding. BRG1 function in melanoma progression also encapsulates MITF-independent functions, such as regulation of the expression of IGF1, TGFß2 and survivin, genes involved in tumor progression and anti-apoptotic properties (Ondrusova et al. 2013). Several studies have reported on BRG1 status in melanoma. One of the studies reported BRG1 expression was reported lost in significant number of metastatic melanoma. (Becker et al. 2009). A larger study analyzing primary and metastatic melanoma alongside dysplastic nevi, BRG1 expression was found upregulated in metastatic melanoma (Lin et al. 2010). And yet another study reported higher expression of BRG1 in stage IV melanoma compared to stage III samples (Saladi et al. 2010). Finally, recently performed exome sequencing reported a low frequency of BRG1 mutations in patient-derived melanoma samples (Hodis et al. 2012).

Organism	Complex	Catalytic subunit	Auxiliary subunits	Function
Yeast	SWI/SNF	Swi2/Snf2	Swi1/Adr6, Swi3, Swp73, Snf5, Arp7, Arp9, Swp82, Snf11, Taf14, Snf6, Rtt102	Pol II activation Elongation DNA replication, repair
	RSC	Sth1	Sth1, Rsc8/Swh3, Rsc6, Sfhl, Arp7, Arp9, Rsc1,2 or 4, Rsc7, Rsc30, Rsc3, Rsc5, Rtt102, Rsc14/Ldb7, Rsc10, Rsc9	Pol II and III activation DSB repair Cell signaling Cell-cycle progression
Fly	BAP	Brahma	BAF155/MOR, BAP45/SNR1, BAP111/dalao, BAP55, BAP60 Actin, Osa/Eyelid	Pol II regulation Elongation Cell-cycle/proliferation Immune system functions
	PBAP	Brahma	BAF155/MOR, BAP45/SNR1, BAP111/dalao, BAP55, BAP60 Actin, Polybromo, BAF170	
Mammals	BAF	BRM or BRG1	BAF250, BAF155, BAF170,BAF60 (A,B or C), SNF5, BAF57, BAF53(A or B), β-actin, BAF45 (A,B,C or D)	Elongation DSB repair, nucleotide excision repair DNA replication Signaling Proliferation and differentiation Stem cell self-renewal/pluripotency Tumor suppressor
	PBAF	BRG1	BAF180, BAF200, BRD7,BAF155, BAF45(A,B,C or D), BAF170,BAF60 (A, B or C), SNF5, BAF57, BAF53(A or B), β-actin	

Table 4 SWI/SNF family of chromatin remodeling complexes (Adapted from (Kasten, Clapier and Cairns 2011))

E. ISWI family of chromatin remodelers

The ISWI (imitation switch) family remodelers include dNURF, dCHRAC, and dACF complexes were initially purified from *Drosophila melanogaster* and with RSF, WICH and NoRC in vertebrates. Multiple ISWI family complexes consist of one or two different catalytic subunits, and contain additional specialized proteins (Table 5).

Organism	Complex	Catalytic subunit	Auxiliary subunits	Function
Yeast	Isw1a	Isw1	Ioc3	Transcription regulation
	Isw1b		Ioc2, Ioc4	
	Isw2	Isw2	Itc1	Replication, transcription, Ty1 regulation
	Isw2		Itc1, Dls1, Dls4	
Fly	ACF	ISWI	Acf1	Nucleosome assembly, transcription, replication
	CHRAC		Acf1, Chrac15, Chrac16	
	NURF		NURF301, NURF38, NURF55/p55/RbAp46/48	Chromatin structure and transcription regulation
	RSF		Rsf1	
Mammals	NURF	SNF2L/SMARCA1, SNF2L/SMARCA5	BPTF, RbAp48/RBBP4, BAP18, HMG2L1	Transcription regulation, cell differentiation
	CERF	SNF2L/SMARCA1	CECR2	Transcription regulation and development
	ACF1	SNF2H/SMARCA5	Acf1	Replication and transcription regulation
	CHRAC		Acf1, Chrac15, Chrac17	
	RSF		RSF1	Chromatin structure and centromere maintenance
	NoRC		TIP5	Transcription regulation
	WICH		WSTF	DNA replication and repair
	WCRF		WCRF180	

Table 5 : ISWI family of chromatin remodeling complexes (Adapted from (Yadon and Tsukiyama 2011))

I. Functions of the ISWI remodelers

ISWI family remodelers are involved in multiple cellular processes, which include DNA replication and repair, and transcription by RNA polymerase I, II, and III. All the complexes are involved in transcription regulation, namely NURF, CERF, CHRAC and RSF in RNA polymerase II transcription, while NoRC and WICH have a role in transcription by RNApol I and III. The detailed description of the NURF role in transcription is described in the last section of this chapter.

ACF and WICH have distinct roles in DNA replication process. ACF complex has a function in replication of DNA within condensed chromatin regions. Silencing of Acf1 leads to lag toward the end of S phase, due to disturbed replication of pericentric chromatin, and this can be rescued by artificial chromatin decondensation (Collins et al. 2002). The WICH has a function in incorporating of the newly synthesized DNA into chromatin. (Poot et al. 2004).

Complexes Acf1/CHRAC/ACF or Snf2H have been shown to be recruited to DNA damage sites, since their knockdown leads to increased sensitivity to DNA damage (Lan et al. 2010). Also, WSTF protein has been shown to phosphorylate the H2A.X histone variant at the DNA damage sites (Xiao et al. 2009).

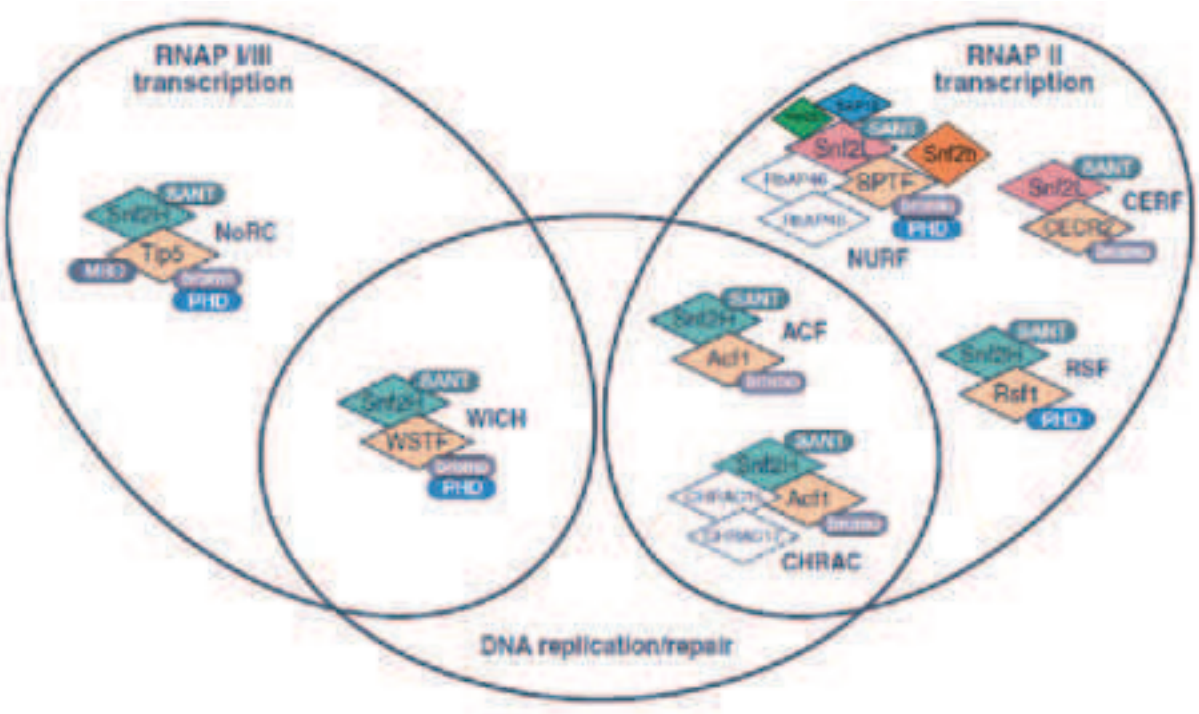

Figure 24 : Functions of ISWI chromatin remodelers

All the remodelers of the ISWI family are involved in transcription regulation, and some of them are also involved in DNA replication and repair. The figure is depicting the division of the complexes by their functions (adapted from (Erdel and Rippe 2011)).

II. Mechanism of action of ISWI remodelers

The mechanism of action of the ISWI ATP-ase has been shown to be nucleosome dependent, since the ISWI-dependent ATP hydrolysis does not occur if the template of remodeling in naked DNA (Corona et al. 1999). Furthermore, the ISWI subfamily of chromatin remodelers requires a linker DNA for mobilizing nucleosomes (Kagalwala et al. 2004).

Detailed mechanism of the ISWI remodeling enzyme was recently elucidated utilizing single-molecule FRET experiments. The authors used the specially constructed nucleosomes that contained the acceptor and donor FRET molecules one on the H2A of the nucleosome and the other at the end of the DNA wrapped around that nucleosome. In order to measure the individual movements of the DNA during the translocation reaction, the authors either decreased the ATP concentration or used an ATP analog ATP-gama-S that significantly reduces the hydrolyzation time. From the measurements of the FRET emission, it was reported the first translocation step is consisted of 7 base pair (bp), followed by 3 bp translocation, and these steps were comprised of 1bp sub steps, noting the 1bp step as a single translocation event utilizing 1 ATP molecule. Indeed, if the ATP concentration was increased, the translocation speed also increases. In order to define the coordination of the DNA translocation at the entry and at the exit site, the authors compared the FRET lag times for both events. To their surprise, the authors noted the lag time notably longer at the entry site than it is at the exit site, suggesting that the DNA first exits the nucleosome, in the step of 7 bp, and only then can the entry of the DNA into the nucleosome be detected. The presumed role of this step is creation of torsion tension that will catalyze the entry of the DNA into the nucleosome. Lastly, it was also reported that once DNA enters the nucleosome, it does so in 3 bp steps at a time (Deindl et al. 2013).

Translocation of the DNA into the nucleosome results in shortening of the linker length. This progressive shortening of the linker on one side of the nucleosome is triggering a negative feedback loop slowing down the further movement of the nucleosome. The remodeling enzyme is activated by the linker DNA, therefore shortening of the linker will result in translocation in the opposite direction. This remodeling process ultimately results in the uniformly repositioned nucleosome arrays, with the nucleosome placed in the central position of the array (Kagalwala et al. 2004, Yang et al. 2006). Further confirmation of this mechanism was provided in a study performed by Blosser et al. who performed three color experiments of single nucleosomes under the action of a remodeling enzyme. The setup of the experiment enabled observation of bidirectional motion. At steady state, ACF complex

binding to the nucleosomes was continuous and the remodeling caused the movement of nucleosomes back and forth in one binding event (Blosser et al. 2009).

III. Regulation of the ISWI remodeling complexes

HAND-SANT-SLIDE domain is a combination of three domains at the C terminus of ATPases belonging to the ISWI family. (Boyer et al. 2002, Boyer, Latek and Peterson 2004, Grune et al. 2003). Upon binding of the ISWI to the nucleosome, HAND and SLIDE domain bind to the linker DNA leaving the nucleosome (Dang and Bartholomew 2007). In the context of the isolated ISWI protein, deleting the HAND-SANT-SLIDE domain slightly reduces the rates of chromatin remodeling demonstrating the ATP-ase domain is capable to function autonomously in nucleosome remodeling (Mueller-Planitz et al., 2013). Another study reports that deletion of the SLIDE domain does not affect DNA binding, but it causes notable defects in the rate of ATP hydrolysis, nucleosome remodeling and it also impairs the remodeler to bind longer linker DNA (Hota et al., 2013).

Additionally, a unique feature of the ISWI ATP-ases is their stimulation by a region on the H4 tail (Clapier et al. 2001, Clapier, Nightingale and Becker 2002, Hamiche et al. 2001), with attenuated stimulation by the acetylated (H4K16ac) tail. For yISW2 and yChd1, H4 acetylation affects the ATP-ase function, without having an effect on their binding of the nucleosome. H4 acetylation in turn increases yRSC remodeling (Ferreira, Flaus and Owen-Hughes 2007). Additionally, the chromatin-remodeling enzyme ACF has been shown to be a sensor of the length of the linker DNA, and thereby regulator of the nucleosome spacing (Yang et al. 2006).

In human cells, ATP-ase SNF2L is ubiquitously expressed in different human tissues. Silencing of SNF2L in HeLa cells led to increase in proliferation and migration. Transcriptome profiling showed SNF2L was involved in modulation of the Wnt signaling pathway regulatory network. SNF2L is expressed at high levels in normal melanocytes, while its expression level is very low or undetectable in melanoma (Eckey et al. 2012).

3. NURF chromatin remodeling complex

Nucleosome remodeling factor (NURF) was first discovered in *Drosophila melanogaster* as an ATP-dependent nucleosome disrupting element, enhancing the nucleosome accessibility mediated by the GAGA factor (GAGAG binging factor) an the heat-shock protein *hsp70* promoter (Tsukiyama, Becker and Wu 1994). The complex was later identified in the *Caenorhabditis elegans*, mouse and human. Complex has variable number of subunits across species. NURF complex is generally associated with transcription activation.

A. Identification of the NURF complex across species

I. Identification of NURF composition in D. melanogaster

Following the initial experiments identifying the activation of the GAGA-mediated activation of *hsp70* promoter is ATP-dependent, biochemical purification of the ATP-dependent element identified a four-subunit complex named NURF. In *D. melanogaster*, it is composed of four members, NURF301, ISWI (NURF140), NURF55 and NURF38 (Tsukiyama and Wu 1995). The complex was shown to work in concert with GAGA on the *hsp70* promoter and functioned as an ATP-ase. Furthermore, activity of the NURF was assayed in mononucleosomes, reconstituted by salt gradient. In combination with naked DNA, NURF had no effect on the pattern of DNAase I digestion of the sample. However, once NURF was in the combination with reconstituted nucleosomes, DNase I it had shown a preferential digestion of the hsp70 promoter, demonstrating that NURF is actively remodeling the nucleosomes, making the *hsp70* promoter more accessible. Additionally, GAGA alone had a weak affinity for its binding sites in nucleosome context (Tsukiyama and Wu 1995).

II. Identification of the NURF complex in mammals

Purification of the complex from the human cells identified a complex highly homologous to *D. melanogaster* NURF, suggesting it has been evolutionally conserved (Barak et al. 2003). The homologous subunits identified in the human NURF complex included NURF301, known as BPTF in the human, NURF55 also known as RBBP4, and NURF140 also known as SNF2L. The fourth subunit, NURF38 was not identified in the human NURF.

Mass spectrometry (MS)-based proteomics is used in functional biological studies to determine interactions between proteins. In order to detect protein-protein interaction with high-accuracy, SILAC ("stable isotope labeling by amino acids in cell culture") method has been coupled with mass spectroscopy. Using this method, several novel subunits of the NURF complex have been identified, including SNF2H, HMG2L1, and a newly discovered protein named BAP18 (BPTF associated protein 18 kDa) (Vermeulen et al. 2010). The interaction between BPTF and SMARCA5 within the NURF complex was later confirmed by co-immunoprecipitation of the endogenous proteins (Mulder et al. 2012).

B. NURF subunits and their function

After NURF complex composition was determined, a considerable effort was made to further identify the composition and mechanism of its action. Initially, the subunits were studied in more detail in *D. melanogaster*, but once the complex was identified in humans, structure and function of the NURF subunits was also determined in human cells, particularly BPTF, which will be discussed later.

I. NURF140 / SNF2L (SMARCA1) and SNFLH (SMARCA5)

In an effort to elucidate the role of the NURF140 subunit, Tsukiyama et al have micro-sequenced the purified protein, and the peptides obtained specifically matched the *D. melanogaster* ISWI protein (Tsukiyama et al. 1995). The sequence comparison of the ISWI subunit of the NURF complex revealed a high level of conservation among eukaryotes, namely the human *SNF2-like* (*SNF2L*) (Okabe et al. 1992). SNF2H and SNF2L are ATPase catalytic core subunit of a variety of complexes and thus have a general role as ATP-ases in chromatin remodeling, and are involved in multiple different biological conditions (Table 5).

II. NURF55 / RBBP4 (RbAp48)

NURF55 has been isolated in *D. melanogaster*, and from the sequence homology, it was determined this protein is identical to the p55 from the CAF-1 complex, and to be homologous to the human RbAp46 and 48 (Martinez-Balbas et al., 1998). The protein harbors WD-40 repeats, a protein domain that has been shown to have a role in protein-protein interactions. NURF55 associates with the histone acetyltransferase in *D. melanogaster* (Martinez-Balbas et al., 1998). RbAp46 and RbAp48 (pRB-associated proteins p46 and p48, also known as RBBP7 and RBBP4, respectively) are highly homologous histone chaperones. Both *D. melanogaster* NURF55 and mammal RbAp46 interact with the

histone H4. P55/RBBP4 is present within multiple protein complexes that function to establish and maintain chromatin structure (Stirnimann et al. 2010).

III. NURF38

NURF38 encodes an inorganic pyrophosphatase, with important roles in catalyzing the nucleotide incorporation of into DNA during transcription, replication, and DNA repair (Gdula et al., 1998). This protein has been found only within *D. melanogaster* NURF complex, and is absent in mammalian NURF (Barak et al. 2003, Vermeulen et al. 2010). It is also shown to take part in other complexes such as TRF2 (Hochheimer et al. 2002).

C. NURF remodeling activity

Already mentioned studies showed NURF remodeling is ATP-dependent process (Tsukiyama et al. 1994, Tsukiyama et al. 1995). A study conducted by Mizuguchi et al. reported that the NURF has a role in transcription activation and was required for chromatin remodeling. The authors utilized GAL4 derivate carrying constitutive activation region from the heat shock transcription factor HSF (GAL4-HSF) to assess transcription activation on a chromatin template. NURF nucleosome remodeling was required for transcription activation on preassembled chromatin. Once the remodeling reaction is complete, adding surplus of NURF did not enhance the reaction, indicating NURF is not required to maintain the remodeled state. NURF directly facilitates GAL4-mediated transcription and is required early in the process of transcription initiation (Mizuguchi et al. 1997).

The mechanism of NURF chromatin remodeling was determined by using a histone octamer in complex with DNA. NURF activity was shown to be greater on an array of nucleosomes as opposed to a single mononucleosome with 161 bp of DNA (Tsukiyama et al. 1995). To resolve the mechanism of chromatin remodeling, Hamiche et al. used a mononucleosome in a complex with a longer 359 bp DNA, reconstituted by salt gradient. Using this reconstitution assay yields a mixture of 4 different types of arrays, with the mononucleosome positioned in different sites on the DNA, and the different positions depend on the underlying DNA sequence. In the remodeling assay, a 359 bp fragment of *D. melanogaster hsp70* promoter was used, and the positions of the nucleosomes generated in this system produce four different mononucleosome species.

The different types of the reconstituted arrays can be separated by native PAGE on the basis of nucleosome position on the linker DNA, with the mobility increasing from N1 as the minimal and N4 with the highest (N4 and N4’ are considered as N4). When NURF

complex and ATP were added to the mixture of N1-N4 arrays, a clear increase of the N3 array could be observed. Additionally, in the case of the remodeling purified species, N1 nucleosomes were remodeled to the N3 position, but a small amount was also present at N2 position, indicating the remodeling is bidirectional. The remodeling process does not involve a dissociation of the histone octamer from the DNA. By combining the reconstitution assay with the restriction enzyme digest for varying periods of time, a migrating intermediates differing in few base pairs could be detected, suggesting the remodeling process proceeds in small advancing steps, rather than big leaps on DNA (Hamiche et al. 1999).

Histone N-terminal tails have also been shown to modulate nucleosome positioning. Upon removal of the histone tails, the reconstitution assay shows a different pattern when compared to the WT. The NURF chromatin remodeling reaction was altered upon histone tail removal. Firstly, the modified mononucleosomes lacking either H2A, H2B or H3 were shown to stimulate the ATP-ase activity of NURF the same as the WT, while in the case of H4 tail removal, ATP-ase activity, measured by the degree of ATP hydrolysis, was completely abrogated. Secondly, the ability of NURF to remodel the nucleosomes was assayed using the different histone tail mutants, H2A and H3 tail removal does not appear to have an effect on the remodeling. H2B removal disturbs the WT remodeling equilibrium, while H4 removal causes complete lack of the remodeling reaction (Hamiche et al. 2001).

To further identify the mechanism by which NURF performs nucleosome sliding, Schwanbeck et al. used hydroxyl radical foot-printing. The authors determined the position where NURF is initially contacting the nucleosome. Furthermore, NURF has been shown to get in contact with two distinct locations within the nucleosome; the first is the continuous linker DNA on nucleosome entry site, and the other the region asymmetrically surrounding the nucleosome dyad within the minor grooves, close to the H4 tail, that is also implicated in ISWI activity. Furthermore, the cleavage by hydroxyl radicals determined nucleosome mobilization by NURF occurs in 10 bp steps. In order to determine the exact kinetics of the remodeling reaction, a fluorescently end-labeled DNA was used for the nucleosome reconstitution. The kinetic experiments demonstrated NURF moves positioned nucleosomes within seconds (Schwanbeck, Xiao and Wu 2004).

D. NURF301 / BPTF – the defining subunit of the NURF complex

I. NURF301 - Drosophila melanogaster

NURF301 is the founding subunit of the NURF complex, it is the only unique subunit and it serves multiple roles both is complex structure and function.

NURF301 is consisted of multiple domains found in proteins associated with chromatin. The N-terminal region of the protein harbors a HMGA (high mobility group A) followed by a DDT domain (involved in DNA binding), three PHD fingers, one in the N-terminal part, and two in the C- terminal part of the protein, WAC and WAKZ motif, A glutamine-rich region and finally a bromodomain (Xiao et al. 2001). To determine the precise role of the NURF301 in chromatin remodeling, Xiao et al performed experiments in which they reconstituted either the full NURF complex, or the complex containing only part of the NURF subunits. Full NURF had the ability to remodel chromatin in an ATP dependent manner. Partial complexes enabled ATP-dependent nucleosome sliding only if the NURF301 and the ATP-ase subunit ISWI were reconstituted together. This indicates both of these two subunits are required for catalyzing specific nucleosome remodeling.

NURF301 also serves as a structural core protein for the assembly of the NURF complex. NURF301 forms direct interactions to all the other NURF subunits, while none of the subunits form interactions with one another.

The interactions of the NURF301 and the nucleosomes was also detected, furthermore, three regions of the NURF301 are nucleosome binding; N-terminal HMGA, DDT, WAKZ, and the C-terminals PHD fingers, bromodomain. Furthermore, HMGA deletion impairs nucleosome remodeling. Additionally, NURF301 can also bind transcription factors such as GAGA factor, HSF and VP16 (Xiao et al. 2001). NURF301 has also been shown to have three isoforms in *D. melanogaster*. NURF301-A corresponds to the full-length isoform. NURF301-B harbors an extra intron that results in deletion of 60 base pairs exon 6. NURF301-C is a truncated isoform and it is transcribed as far as the exon 7. This truncation removes the C-terminal PHD fingers and bromodomain that are present in NURF301-A and NURF301-B. The different isoforms are forming distinct complexes, and are active in different processes in D. melanogaster development. The full-length NURF301 is not required during larval development, but it is required for spermatogenesis (Kwon et al. 2009).

II. BPTF – Mammals

The bromodomain PHD finger transcription factor (BPTF) was first identified by Jones et all. in a study aiming to characterize bromodomain proteins genome wide. Full-length *BPTF* encodes an extensive open reading frame (ORF) of 9700 nt, for a protein of 2781 amino acids. The molecular mass of the protein in the SDS-PAGE was 311 kDa. (Jones, Hamana and Shimane 2000).

BPTF protein, despite the high sequence similarity, displays several significant differences when compared to NURF301. Starting from the N-terminal region, BPTF contains the DDT domain, but it lacks the AT hooks present in the NURF301. Next, it contains two PHD fingers, one at the N-terminal part of the protein juxtaposed to the DDT domain, and the other on the C-terminal end of the protein, followed by a bromodomain. A BAZ domain present in many ISWI binding partners is situated next to the first PHD finger. Additionally, the protein contains and a glutamine-rich region in the central part of the protein. Three LXXLL putative nuclear receptor-binding motifs can be found throughout the sequence (Barak et al. 2003, Jones et al. 2000).

Figure 25 : BPTF protein modular composition

Schematic representation of the BPTF protein containing the High mobility group – A (HMGA) and the putative DDT domain on the N-terminus. The C-terminus contains the histone recognition module including the second PHD finger (PHD2) and bromodomain.

Human NURF (hNURF) has been shown to remodel chromatin in mammalian HEK293T cell nuclear extracts. The chromatin remodeling affinity has been assessed using the restriction enzyme accessibility assay, and in accordance to the previously demonstrated results, hNURF displayed ATP-dependent nucleosome remodeling activity exclusively in nucleosome context, and not on naked DNA (Barak et al. 2003).

Co-localization of SNF2L and BPTF was detected in adult mouse brain, in the hippocampus and cerebellum, indicating hNURF might a functional role in these tissues. Indeed, hNURF localizes to the human engrailed genes *EN1* and *EN2,* genes involved in cerebellar development and it regulates their endogenous expression (Barak et al. 2003).

Isoforms expressed form the BPTF locus

In mammals, *BPTF* locus codes for the two isoforms. A truncated isoform of BPTF, also known as fetal Alzheimer's clone 1 (FAC1), contains the first third of the BPTF sequence and was initially found in the Alzheimer's disease senile plaques protein screen (Bowser, Giambrone and Davies 1995). Furthermore, FAC1 was shown to be upregulated in motor neurons during development and in the neurodegenerative disease amyotrophic lateral sclerosis (Mu, Springer and Bowser 1997). FAC1 was also shown to exhibit sequence-specific DNA binding activity and functions in transcriptional regulation by interacting with Myc-associated zinc finger protein (ZF87/MAZ) (Jordan-Sciutto, Dragich and Bowser 1999, Jordan-Sciutto et al. 2000).

Histone binding module of BPTF

The histone binding module of BPTF in situated on the C-terminal end of the protein and it comprises the PHD finger and a bromodomain. The histone binding properties of BPTF have been studied in great detail, since it presents a noteworthy example of the multivalent histone PTM recognition within one protein.

The first report of BPTF ability to bind histone modifications came from study by Wysocka et al, demonstrating for the first time PHD finger of BPTF is binding an H3K4me3 histone modification, representing the link between chromatin remodeling and this histone mark associated to active transcription (Wysocka et al. 2006).

Genomic-scale experiments have associated the H3K4me3 mark to actively transcribed genes (Santos-Rosa et al. 2002). BPTF was identified as a H3K4me3 mark binder in series of experiments aiming to gain more knowledge on the proteins that specifically bind this mark. More specifically, BPTF is bound to the H3K4me3, but not H3K4me2 or other lysines within histone H3 that can be trimethylated, such as H3K9me3 or H3K27me3. To determine more precisely what domain is responsible for binding, NURF301 both C-terminal PHD domains and bromodomain were assayed for binding of unmodified, 1, 2 and 3 methylated H3, and so were the C-terminal PHD and bromodomain of BPTF. In both cases of NURF301 and BPTF, the PHD domain juxtaposed to the bromodomain was required for the binding to the H3K4me3, and did not bind any of the other H3 peptides. Also, none of the other PHD domains was bound to the H3K4me3 mark.

Finally it was also demonstrated the loss of BPTF does not affect the H3K4me3 deposition, but loss of the H3K4me3 resulted in decrease of binding of both BPTF and SNF2L to the locus of one of the target genes. This indicates BPTF binging to chromatin stabilized in part by its biding to the H3K4me3 mark (Wysocka et al. 2006).

The molecular basis of interaction of the BPTF to the H3K4me3 –specific binding was subsequently identified through the analysis of the crystal structure of the PHD finger-linker-bromodomain fragment of BPTF free and in combinations with both H3K4me3 and H3k4me2. This peptide segment is positioned of the surface of BPTF. Li et al. have determined the PHD finger binds to the H3K4me3 mark with the highest affinity, which is notably reduced in the case of dimethylated residue, and completely absent for monomethylated H3 (Li et al. 2006).

The specificity of the BPTF PHD finger-H3 interaction is depicted on the detailed molecular structure including 6 first residues of H3 and the PHD finger domain of BPTF. The histone H3-R2 residue and K3me3 fit into neighboring surface grooves within the PHD finger of BPTF, and this alignment is further supported by the T3 and Q5 residues of the histone H3 tail that are interacting with the peptide backbone of the PHD finger (Figure 25, a). These interactions explain the specificity for the H3K4 (as opposed to K9 or K27).

Aromatic cage formed within the PHD finger structure accommodating the K4me3 consists of four crucial amino acid residues, Y23, that takes the place at the base of the trimethylated K4me3, while Y10, Y17 and W32 stabilize the interactions by forming the three surrounding surfaces around the K4me3 group, thus completing the cage (Figure 25, b). Point mutations of any of these important residues results in a significant loss of the binding of the PHD finger to the H3K4me3.

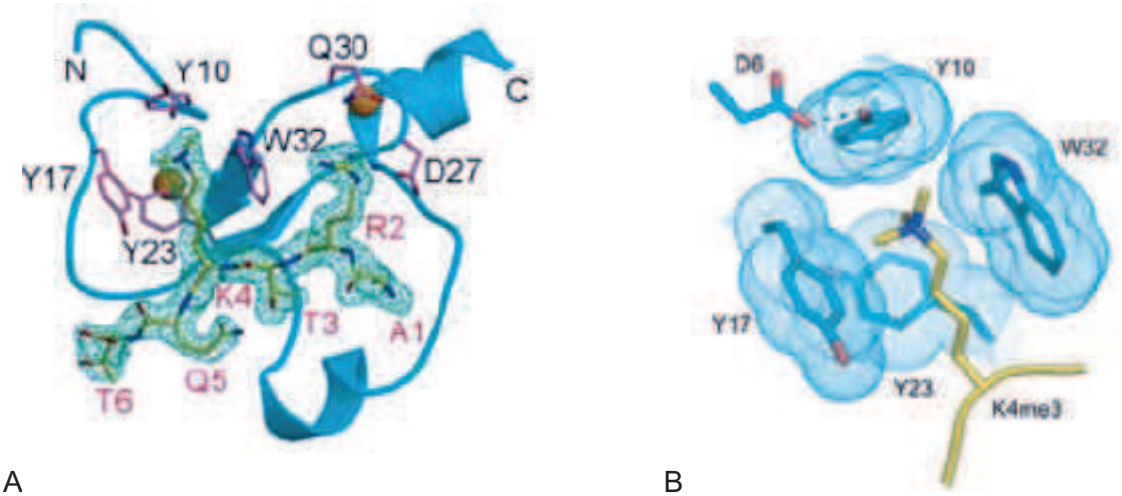

A B

Figure 26 : Molecular structure of BPTF PHD finger binding to H3K4me3

A) The structure of the BPTF PHF finger binding the histone H3K4me3 mark. **B)** The structural details of H3K4me3 stabilization by the BPTF PHD finger aromatic cage (Li et al. 2006).

Another hallmark study demonstrated the role of the bromodomain in binding acetylated residues in the histone H4, and also more remarkably, synergistic effect of PHD finger and bromodomain binding within the same mononucleosome.

The role of the bromodomain BPTF was assayed both using the SPOT blotting and peptide pull-down. The bromodomain alone showed no discrimination in binding H4K12, H4K16 and H4K20 acetylated residues. The binding was not evident in the case of acetylated residues in the histones H2B and H3.

In order to study whether BPTF binds multiple marks on the nucleosome, reconstituted nucleosomes were utilized displaying different combinations of histone marks. For the binding assay, a tagged version of the histone binding module consisting of a PHD finger-bromodomain was used to test the different nucleosomal binding combinations. The results showed that only mononucleosomes harboring both H3K4me3 and H4K16Ac mark displayed synergistic binding by the PHD finger-bromodomain construct. The multivalent binding occurs within the single mononucleosome, since the combination of the marks on two different nucleosomes in a binucleosomal reconstitution assay did not enhance the binding. Furthermore, these finding were corroborated with genome-wide ChIP sequencing of the BPTF PHD finger-linker-bromodomain. The PHD-bromodomain binding co-localizes with the doubly modified nucleosomes (Ruthenburg et al. 2011). Based on the multivalent binding data, depicts a model of the BPTF-NURF binding to the nucleosome.

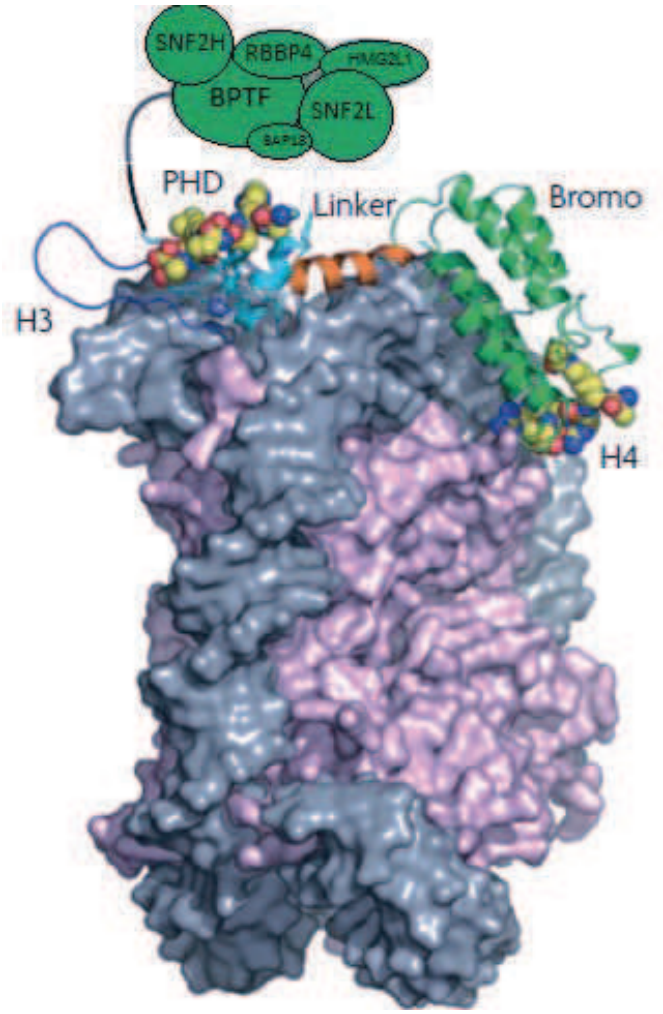

Figure 27 : Model of BPTF binding to the nucleosome

Model of BPTF binding to the nucleosome depicts multivalent binding of BPTF PHD finger (in light blue) to the histone H3 and BPTF bromodomain (in green) to the histone H4. Multivalent binding spans the nucleosome and the two histone binding domains are connected with a linker region (in orange) (adapted from (Ruthenburg et al. 2007)).

E. Biological roles of the NURF complex

I. Biological functions of NURF in D.melanogaster

In order to determine the role of NURF in D. melanogaster, several studies have been conducted characterizing in more detail the phenotypes of NURF301 mutant animals. The role of NURF in regulating in vivo transcription was demonstrated since the expression of heat shock proteins hsp70 and hsp26, as well as engrailed was lost. The analysis of the mutant *Enhancer–of–bithorax* gene, a positive regulator of the bithorax complex has revealed the *Enhancer-of-bithorax* and *NURF301* in fact are mapped to the same site in the

genome, and are in fact the same gene. The mechanism of the transformation and the tumor development has been shown to regulate JAK/STAT signaling, since this pathway was upregulated in NURF301 mutants (Badenhorst et al. 2002). The genome-wide analysis of the NURF301 mutants revealed that NURF has acts both as an activator and a repressor, since the analysis of the mutants revealed numerous genes both up- and down- regulated. Furthermore, NURF physically interacts with the ecdysone receptor (EcR), nuclear receptor controlling development and reproduction in arthropods, and NURF mutations result in metamorphosis defects (Badenhorst et al. 2005). Additionally, NURF mutants exhibit the same responses of the innate immune system as the JAK/STAT gain-of-function mutants. Microarray analysis of the two mutants revealed a common set of genes that are activated in both cases. Furthermore, NURF interacts physically and functionally with Ken, the repressor of the JAK/STAT signaling. ChIP analysis co-localized NURF to Ken binding sites in hemocytes, suggesting Ken recruits NURF to repress a set of STAT genes (Kwon et al. 2008).

Another study reported NURF is involved in stem cell maintenance in the *D. melanogaster* testis. Namely, in local JAK/STAT signaling maintains germline and somatic stem cells (GSCs and cyst progenitor cells, CPCs) in a single niche. NURF is regulating GSC and CPC maintenance by positively regulating JAK/STAT signaling and therefore preventing premature differentiation (Cherry and Matunis 2010). These findings, alongside previous studies indicate NURF functions as both an activator and a repressor of the JAK/STAT pathway in *D. melanogaster*. The role of the NURF is also involved in female germline cells. The steroid hormone ecdysone directly regulates adult GSC proliferation and self-renewal. Ecdysone regulates the GSCs through functional interaction with the ISWI and NURF301, acting as intrinsic epigenetic factors required for GSC development (Ables and Drummond-Barbosa 2010).

NURF301 mutants display aberrant morphology of the male X chromosome, appearing decondensed, reminiscent of the ISWI mutant phenotype (Badenhorst et al. 2002, Deuring et al. 2000). This aberrant morphology is dependent on the male-specific-lethal (MSL) complex that has been shown to contain five proteins and two non-coding *roX* (RNA on X). The mutant *roX* is able to rescue the NURF mutant phenotype of the X chromosome in particular regions, demonstrating the NURF and MSL have opposing effects of male X organization. Additionally, NURF and MSL complexes have opposing effects on *roX* transcription (Bai et al. 2007).

Another aspect of NURF function in transcription regulation is through its interaction with the ATAC complex. *D. melanogaster* SAGA subunit Gcn5 and ATAC subunit Ada2a mutants result in X chromosome decondensation, a phenotype similar to that induced by

ISWI and NURF301. Functional studies along with the transcriptome profiling suggest ATAC and NURF partly account for this overlap in the phenotype regulate overlapping set of target genes during development (Carre et al. 2008).

D. melanogaster gene *putzig (pzg)* is a member of the TRF2-DREF complex, which is involved in selection of the core promoter. Furthermore, putzig has a role in Notch signaling regulation independently of DREF. A study by Kugler et al. demonstrated Putzig (Pzg) associates with the NURF complex and the loss of NURF301 impairs binding of the Putzig to the Notch target genes, suggesting NURF is recruiting Putzig to these sites. Additionally, Putzig co-purifies with all the NURF members. Furthermore, the analysis of the NURF301 mutants revealed a reduction in the Notch target gene activity. Also, NURF301 mutants enhance the *Notch* mutant phenotype (Kugler and Nagel 2010). Interestingly, it has also been reported that Pzg is mediating NURF binding to the EcR and functions as a JAK/STAT regulator. Indeed, Pzg associates with the EcR in vivo and is required for the transcriptional induction of the EcR genes. Moreover, Pzg interferes with JAK/STAT signaling by acting as a co-repressor of Ken (a repressor of the JAK/STAT signaling) (Kugler et al. 2011).

II. Biological functions of BPTF/NURF in mammals

a) Roles of BPTF/NURF in development

The pivotal importance of Bptf and NURF in the mammals was demonstrated in the studies performed using the transgenic mouse line targeting *Bptf* locus. The mouse line created generated a mutant with loxP sites flanking the exon 3 of Bptf, resulting in expression of out-of-frame mRNA and functions as a loss of function allele. In the case on non-conditional *Bptf* knock-out, a homozygous animals display an embryonic-lethal phenotype between E7.5 and E8.5 with 100% penetrance. In order to investigate what is the exact time point of the onset of defects in embryonic development, the authors performed analysis of the whole mount embryos. The results indicate the embryos were not affected as early as E3.5 or E4.5. However, at the embryonic day E.5.5 to E7.5 a severed developmental defect started to arise, causing the embryo to be absorbed. Subsequent histological studies determined the Bptf knockout phenotype causes lethality due to the lack of development of the embryonic tissues, such as distal visceral endoderm (DVE).

In order to assess the role of Bptf on the cells in culture, both embryonic stem (ES) cells and mouse embryonic fibroblast cell lines were generated. The Bptf knockout resulted in merely slight reduction of the proliferation rate in these cells. Furthermore, the isolated cells in culture were also utilized for genome-wide analysis using the microarray. The gene

expression analysis showed that Bptf is involved in regulation of genes involved in development, nervous system, proliferation, morphogenesis and cell death.

To further elucidate the mechanisms of the DVE development failure, the authors sought to determine which of the signaling pathways governing the development of the pre-gastrulation embryo is being disturbed due to Bptf ablation. The Nodal/Smad signaling pathway, involved in the development of the early embryo. Smad signaling-dependent genes such as p21, Cer1 and Lefty1 were shown to be regulated by Bptf (Landry et al. 2008).

The role of Bptf was also studied in T-cell development. Landry et al utilized *LCK proximal-Cre* conditional mouse model in the thymocyte development, to excise $Bptf^{lox}$ specifically in T-cells. Depletion of *Bptf* results in defective specialization and development of T-cells past the $CD4^{+}CD8^{int}$. This defect results in complete absence of mature thymocytes. Furthermore, in accordance to the experiments conducted on the ES and MEF cells, *Bptf* ablation does not affect cellular proliferation, cellular apoptosis (Landry et al. 2011a).

Bptf/NURF has also been shown to be important for erythrocyte differentiation. In the final stages of erythropoiesis, only small portion of the genes remain active, since the cells will eventually become de-nucleated. Chromatin insulators serve as a mechanism that ensures the expression of the erythroid genes against the general heretochromatization. Defects in insulator action can result in anemia. Factor USF1/2 is controlling insulator expression in erythrocytes by establishing a barrier keeping the insulators active. Proteome analysis identified hSET1 and NURF as USF1 binding partners. Knock-down of NURF results in loss of insulator barrier, and SET1 silencing reduces the barrier activity and Bptf recruitment to insulator-specific sites (Li et al. 2011b).

NURF also plays an important role in progesterone signaling. In order to transmit a signal, hormone signaling relies on the rapid chromosome rearrangements, including histone H1 eviction from its target genes in order to enable gene expression. The complex system put into action upon the activation of the progesterone receptor (PR), involves NURF and ASCOM, which are recruited by PR, to hormone target genes. ASCOM places a H3K4me3 mark, which is stabilizing NURF binding. NURF then facilitates PR-mediated recruitment of CDK2/CyclinA, required for histone H1 displacement (Vicent et al. 2011).

NURF components BPTF and SMARCA5 are involved in stem cell self-renewal and differentiation of epidermal cells. In a study aiming to identify factors regulating the involved in epidermal stem cell biology, EZH2, UHRF1 (epidermal stem cell regulators), ING5 (MORF subunit), BPTF and SMARCA5 have been shown to form a indicate system of interactions that is crucial part of the epidermal differentiation. Furthermore, NURF and MORF have a role in maintaining the undifferentiated state of the epidermal stem cells. Double knock-down of BPTF and SMARCA5 led to a more severe proliferation phenotype in primary

keratinocytes that of either of them alone, indicating a functional interaction between these factors. Primary human keratinocytes treated with shRNA silencing ING5, SMARCA5, BPTF, EZH2 or UHRF1 were utilized in human epidermis reconstitution experiments. This resulted in reduced proliferation for all the five modifiers and the clones were not anchored in the basal layer, indicating they have undergone terminal differentiation (Mulder et al. 2012).

b) Roles of the BPTF/NURF in cancer

Primary human cancers, and cancer cell lines from many tissues including brain, breast, lung, liver, and prostate, frequently duplicate the 17q distal chromosome arm containing the BPTF gene (Bown et al. 1999, Choi et al. 2006, Raidl et al. 2004, Sun et al. 2008). Many genes have been proposed to be responsible for selection of this chromosomal duplication; however, none of the reports considered BPTF as a possible candidate (Beser et al. 2007, Monni et al. 2001, Vandesompele et al. 2008, Wu et al. 2000a).

A study by Buganim et al. identified a non-reciprocal translocation in the BPTF gene when human embryonic lung cells were maintained in continuous culture. The chromosomal translocation resulted in increased BPTF mRNA levels and correlated with increased cellular proliferation. Consistent with the literature on 17q distal duplications, the authors also report frequent BPTF duplications in neuroblastomas, lung tumors, leukemia and colon cancers using both *in silico* analysis and various cancer cell lines (Buganim et al. 2010).

Recently, BPTF was shown to be frequently mutated several high-throughput sequencing reports. Whole-genome sequencing of liver cancers reported recurrent mutations of multiple chromatin regulators, including BPTF, which was mutated in 1.7% of the cases (Fujimoto et al. 2012). Exome sequencing of breast cancer families also revealed a frequent mutation in BPTF, N315T (Xiao et al. 2014). In exome sequencing of urothelial bladder cancer (UBC), BPTF was found to be frequently mutated, and a knock-down of BPTF led to decreased colony formation in three UBC cell lines (Balbas-Martinez et al. 2013).

The involvement of BPTF in bladder cancer was shown to be related to the H2A.Z histone variant. Coupling of the H2A.Z ChIP-seq with microarray data demonstrates that H2A.Z is enriched around the TSS of cell cycle regulatory genes in bladder cancer cells, and this enrichment is correlated with the elevated expression. RNAi-mediated knockdown of H2A.Z in the cancer cells causes transcriptional suppression of multiple cell cycle regulatory genes, followed by a decrease in proliferation. H2A.Z nucleosomes around the TSS have higher levels of H3K4me2/me3, which coincides with the recruitment of WDR5 and BPTF.

The recruitment was shown to be functional, since the activity of H2A.Z target genes was largely diminished by WDR5 or BPTF suppression (Kim et al. 2013).

RESULTS

Context and the aims of research

Melanoma is a highly aggressive form of skin cancer. In the last 20 years, the incidence of melanoma is on the constant rise and is considered to be a major health problem worldwide. It is notorious for its resistance to conventional chemotherapy of any other treatment, and development of resistance to the personalized targeted therapy once the cancer becomes metastatic. Microphthalmia-associated transcription factor (MITF) is the key transcription factor specific for the melanocyte cell lineage and melanoma, and is responsible for cell proliferation, survival and differentiation. The levels of expression of MITF have been shown to be closely linked to melanoma phenotype and tumor progression. Indeed, MITF expression level is dictating the cell ability to proliferate, migrate and invade the surrounding tissues. Previous work done in our laboratory identified distinct regulation network of MITF, coupled with MITF genome-wide occupancy, indicating MITF expression is activating genes responsible for cell proliferation and survival, and repressing genes involved in cell migration and invasion.

In order to determine the underlying molecular mechanism of such versatile roles of MITF, we undertook an approach identifying MITF interacting partners. By identifying MITF interactorme, it will be possible to determine what are the different promoter-specific co-factors enabling versatile MITF functions.

The first publication discussed in the result section is a report of a first identified MITF interactome, allowing determination of the proteins and complexes involved in transcription regulating that are interacting with MITF. Within the interactiome study, the targets we focused our attention on the most are the chromatin remodeling complexes SWI/SNF BRG1 and ISWI NURF.

NURF is a chromatin remodeling complex has been shown mainly to be involved in active transcription and has been implicated in development of several other cancers. Nevertheless, the function of the NURF complex in the melanoma and the melanocyte lineage has not been reported so far. The main focus of my research is elucidating the role of the NURF chromatin remodeling complex in melanocyte lineage and melanoma. The results of this study are described in the second article of the result section.

Article 1 : **Microphthalmia-associated transcription factor (MITF) interacts with a novel BRG1-containing complex to regulate gene expression in melanoma cells.**

Microphthalmia-associated transcription factor (MITF) interacts with a novel BRG1-containing complex to regulate gene expression in melanoma cells.

Patrick Laurette1, Thomas Strub1,2, Dana Koludrovic, Céline Keime, Stéphanie Le Gras, Robert Siddaway3. Gabrielle Mengus, and Irwin Davidson#

Department of Functional Genomics and Cancer, Institut de Génétique et de Biologie Moléculaire et Cellulaire, CNRS/INSERM/ULP, 1 Rue Laurent Fries, 67404 Illkirch Cédex, France.

1. These authors contributed equally to this study.

2. Department of Oncological Sciences, Icahn School of Medicine at Mount Sinai, New York, New York, US

3. The Ludwig Institute for Cancer Research, University of Oxford, Old Road Campus Research Building, Headington, Oxford, OX3 7DQ, UK.

To whom correspondence should be addressed:

E mail : irwin@igbmc.fr

Running Title : The MITF interactome.

Key words; chromatin remodelling, CHD7, SOX10, HERC2, ubiquitin cycle, TRRAP,

The authors declare no competing conflict of interest.

Abstract

Microphthalmia-associated transcription factor (MITF) is the master regulator determining the identity and properties of the melanocyte lineage. The molecular mechanisms by which MITF regulates transcription remain however poorly characterised. By tandem affinity purification and mass spectrometry, we present a comprehensive characterisation of the MITF interactome in melanoma cells comprising multiple novel cofactors involved in transcription regulation, chromatin organisation and DNA replication and repair. We show that MITF interacts with a novel form of the BRG1 chromatin remodelling complex comprising CHD7. BRG1 binds extensively over the genome on active enhancers and to nucleosomes immediately flanking the transcription start site at a subset of promoters and regulates expression of a large set of genes. BRG1 and MITF colocalize at >6000 genomic loci and we define a set of MITF-containing regulatory elements (MCREs) at active enhancers. MCREs show a novel organisation where MITF, alone or with other transcription factors, occupies the DNA

between two BRG1 bound nucleosomes. MITF is required to recruit BRG1 to co-occupied sites, whereas BRG1 silencing enhances MITF occupancy of its cognate sites. Chromatin remodelling by BRG1 therefore ensures the dynamics of MITF genome occupancy in order to limit occupancy of non-functional sites and ensure a pool of MITF for binding to functional sites. Finally, we also show that BRG1 is essential for development of mouse melanocytes in vivo.

Introduction

MIcrophthalmia-associated Transcription Factor (MITF) is a basic helix-loop-helix leucine zipper (bHLH-Zip) factor that acts as the "master regulator" of differentiation, survival, and proliferation of normal melanocytes, and is critical in controlling the proliferation, migration and invasion of melanoma cells[19, 26, 49, 57]. The level of functional MITF expression determines many biological properties of melanoma cells. High MITF levels lead to terminal differentiation and cell cycle exit, intermediate levels to proliferation, while lower levels result in slow cycling invasive cells with tumour initiating properties[25]. Very low levels of MITF or its rapid depletion such as is achieved experimentally in siRNA experiments, lead to entry into senescence[18, 50].

We have previously reported a genome wide analysis of MITF target genes in 501Mel melanoma cells[50]. Chromatin immunoprecipitation (ChIP) coupled to deep sequencing identified >12000 genomic MITF binding sites annotated to upwards of 5000 novel potential target genes. Integration of ChIP-seq data with RNA-seq following siRNA mediated MITF knockdown showed that MITF directly and positively regulates genes involved in DNA replication and repair and mitosis. In contrast, MITF represses genes involved in invasion such as MCAM[42] and SHC4 (also known as RaLP;[16]) and AMOTL2. Thus through its dual functions as an activator and repressor, MITF promotes proliferation but represses invasion.

To better understand the molecular function of MITF, we used tandem affinity purification to isolate MITF from 501Mel melanoma cells and mass-spectrometry to identify its interacting partners. We report here the first comprehensive characterisation of the MITF interactome and we investigate functional interactions of MITF with a novel form of the BRG1 chromatin-remodelling complex that are required for proliferation of melanoma cells in vitro and melanocytes in vivo in mice.

Results

MITF associates with multiple complexes involved in transcription and DNA replication and repair

We established 501Mel cell lines stably expressing an N-terminal FLAG-HA epitope tagged MITF (F-H-MITF, Fig. 1A) and performed tandem affinity purification of soluble nuclear and chromatin associated fractions from line (L)J where F-H-MITF expression is comparable to that of endogenous MITF[13, 23]. Numerous proteins were observed selectively associated with F-H-MITF in immunoprecipitations from each fraction while almost no proteins were detected in the immunoprecipitations from the untagged 501Mel cells (Fig. 1B).

Immunoprecipitations from all fractions were analysed by mass spectrometry revealing peptides for a large number of proteins in fractions from F-H-MITF, whereas many fewer peptides were present in the untagged control (Supplementary Table S1). Two independent purifications and mass-spectrometry analyses were performed and only proteins identified specifically in the F-H-MITF precipitations with no peptides in the control experiments are discussed. In addition, many ribo-nucleoprotein particle, spliceosome components and chaperone proteins were found specifically in the MITF-containing fractions, but as these are common contaminants, they have not been considered in the subsequent analysis.

Proteins previously suggested to interact with MITF were identified by our procedure. TFEB, TFE3 and TFEC were identified in both the soluble and chromatin associated fractions (Table 1 and Supplementary Table S1). These proteins belong to the same bHLH MiT subfamily and are known MITF heterodimerisation partners[48]. Similarly, we detected the MITF cofactor β-catenin (CTNNB1) in both fractions[46]. Our procedure therefore identified previously described MITF partners.The chromatin-remodelling factor BRG1 is reported to interact with MITF[9, 32], however the nature of the BRG1-containing complex has not been described. BRG1 (SMARCA4) as well as the PBRM1 (BAF180), SMARCC2 (BAF170), SMARCD2 (BAF60B), and ACTL6A (BAF53A) subunits of the BRG1 chromatin-remodelling complex were detected in both fractions (Table 1 and Supplementary data set S1) along with CHD7 reported to associate with BRG1 in human neural crest cells[3]. This suggests that MITF interacts with a BRG1-CHD7-containing complex specific to neural crest derived cells (see below).

We also identified novel potential MITF partners. The BPTF, SMARCA1 (SNF2L), SMARCA5 (SNF2H) and RBBP4 components of the NURF chromatin-remodelling complex associated with MITF specifically in the chromatin associated fraction. Components of the DNA damage response machinery associated with MITF including XRCC5 and XRCC6 (Ku80 and Ku70), DNA-dependent protein kinase (PRKDC), BRCA2 as well as MSH2 and MSH6. We identified the HECT domain-containing E3-ligase HERC2, which has been

implicated in DNA repair[4], as well as UBR5 a second HECT domain-containing E3-ligase with functions in both DNA repair and transcription[7, 20]. NEURL4 a known HERC2 interacting protein 2 was also found along with the de-ubiquitinase enzymes USP7 and USP11 that were preferentially represented in the SNE. In contrast, USP13 that has been shown to regulate MITF stability[61] was not detected in our experiments. Many of these interactions were verified by immunoblot as HERC2, BRG1, USP7, USP11, XRCC5 and XRCC6 were detected in the F-H-MITF immunoprecipitations from the soluble nuclear fraction, but not in the untagged controls (Fig. 1C), with enrichment of USP7 and USP11 in the SNE compared to the CAE and the selective presence of HERC2 in the SNE. Alternatively, we transfected 501Mel cells with a vector expressing F-MITF or a control empty vector and performed anti- Flag immunoprecipitation. In these experiments, F-MITF specifically co-precipitates with endogenous TRRAP and NEURL4 (Supplementary Fig. S1).

We identified several other complexes interacting with MITF. Four subunits of TFIIIC, a RNA polymerase III cofactor were detected suggesting that MITF may regulate Pol III transcription. Alternatively, a fraction of TFIIIC is located at genomic loci called Extra TFIIIC sites (ETCs) in absence of the Pol III machinery where it may organize higher order chromatin structure in association with subunits of the cohesin complex[6, 33, 40]. In accordance with this idea, the SMCA1, SMC3, STAG2 and PDS5 cohesin subunits were also found. Thus, MITF may associate with TFIIIC and/or cohesin at a subset of genomic sites to regulate higher order chromatin structure.

We identified the TRIM28 (TIF1β, KAP1) co-repressor protein that belongs to a sub-family of TRIM proteins comprising TRIM24 (TIF1α) and TRIM33 (TIF1γ) 22. These proteins form multi-protein complexes along with HDAC1 and HDAC2 and the HP1 proteins[23], all of which were also identified. TRRAP is a previously characterized cofactor for cMYC[38, 43]. We identified TRRAP, RUVBL1, RUVBL2, and BAF53A in the MITF interactome. These proteins form a complex with TRRAP that acts as a MYC cofactor[44], but we did not detect GCN5 or other known subunits of SAGA associated with MITF. The precise composition of this MITF-TRRAP complex therefore remains to be determined. Interestingly, mutations in TRRAP have recently been associated with human melanoma[56]. This observation and its interaction here with MITF suggest a critical role in melanomagenesis.

In addition to transcription complexes, the RFC1, RFC2, RFC4 and RFC5 subunits of DNA replication factor C associate with MITF along with the MCM3, MCM5 and MCM7 subunits of the MCM complex that forms at DNA-replication origins. AKAP8 and AKAP8L were also

identified and AKAP8 has been shown to interact with the MCM complex [14], although these protein kinase A anchoring proteins have additional functions [8]. The kinasePLK1, that has been shown to be essential for the mitosis of melanoma cells [47], was found in the chromatin-associated fraction suggesting that it may phosphorylate MITF on chromatin. Finally, we detected multiple subunits of the nuclear pore complex suggesting that MITF sub-cellular localization may be regulated by nuclear-cytoplasmic shuttling. Together, these data describe a comprehensive set of MITF interacting proteins.

We also noted that the genes coding many of the MITF interaction partners are associated with MITF-occupied sites suggesting that their expression may be regulated specifically in the melanocyte lineage by MITF. In the case of the BRG1 complex, the genes encoding BRG1, BAF180, BAF60B and CHD7 were all associated with MITF binding sites (Supplementary Fig. S2). The XRCC5, XRCC6, PRKDC, MSH2, MSH6, USP7, USP11, UBR5, NEURL4, PLK1, TFEB, and TFEC genes also are associated with MITF binding sites [([18, 50] and unpublished observations].

MITF interacts with a BRG1-CHD7 containing complex.

It has previously been reported that MITF interacts with BRG1, but the nature of the BRG1 complex interacting with MITF has not been described. Several related BRG1-containing complexes have been described[45, 53]. Based on the mass spectrometry results, the complex that interacts with MITF most closely resembles the PBAF variant with the presence of PBRM1. To investigate the nature of the BRG1 complexes in 501Mel cells, extracts were precipitated with an anti-BRG1 antibody showing co-precipitation of BRG1 with ARID2, SMARCC1 (BAF155), ACTL6A, PBRM1, and SMARCC2 (BAF170) whereas SMARCD2 (BAF60B) and ARID1B were not co-precipitated (Supplementary Fig. 3A). BRG1 therefore interacts with these subunits to form a PBAF-type complex in 501Mel cells. Nevertheless, notably absent from the tagged-MITF mass-spectrometry analysis are the ARID1A/B and ARID2 subunits. As these are proteins of large molecular mass, it is unlikely that they were overlooked in the mass-spectrometry analysis suggesting that the complex that interacts with MITF is yet another variant amongst the known BRG1 complexes. In contrast, we identified CHD7 in the MITF interactome, and CHD7 has been reported to associate with PBAF in neural crest cells [3]. In support of this idea, BRG1 and CHD7 showed reciprocal co-precipitation (Supplementary Figs. 3A and B). In addition, SMARCC2, ACT6LA and MITF co-precipitated in anti-CHD7 immunoprecipitation (Supplementary Fig. 3B). Together, these

are consistent with the idea that MITF interacts with a novel sub-form of BRG1 complex comprising CHD7, but lacking ARID1A/B and ARID2 (Supplementary Fig. 3C).

BRG1 regulates an extensive gene expression program essential for proliferation of melanoma cells in vitro.

To address the function of BRG1 in melanoma cells, we performed si/shRNA knockdown. SiRNA knockdown of BRG1 had no effect on expression of other interactome components like HERC2, USP7 and USP11 (Fig. 2A). In contrast, BRG1 levels were strongly down-regulated along with those of BAF170 suggesting that in absence of BRG1 the complex is destabilized. Importantly however, BRG1 silencing strongly reduced MITF levels[54]. A similar result was seen after infection of cells with lentivirus expressing anti-BRG1 shRNA that knocks down expression of both BRG1 and MITF at the level of protein and mRNA (Fig. 2A).

As BRG1 silencing down-regulates MITF, the effects on gene expression and cell physiology should be very similar to the loss of MITF itself. Indeed, BRG1 knockdown reduced expression of MITF target genes involved in cell cycle, pigmentation and signaling, and induced several genes of the senescence-associated secretory phenotype (SASP), whose expression is also induced upon MITF-knockdown (Fig. 2B) [41, 50]. In accordance with this, shBRG1 silencing led to a potent arrest of 501Mel proliferation and extensive cell death with the surviving cells showing a flattened enlarged morphology and multiple cytoplasmic projections, similar to what is seen in senescent cells upon MITF knockdown (Fig. 3C, [50] and see below). Up to 40% of the BRG1 knockdown cells showed senescence-associated β-galactosidase staining (Fig. 2C). Similar results were seen in shBRG1 SK-Mel-28 cells and in both cell types, bi-nucleate and multinucleate cells were also observed, another characteristic of MITF loss [50] (Fig. 2D). BRG1 is therefore essential for MITF expression and proliferation of 501Mel cells [54].

RNA-seq following shBRG1 silencing revealed that loss of BRG1 had a dramatic effect on gene expression with >4000 genes down-regulated and >5400 genes up-regulated (Fig. 2E and Supplemental Dataset 2). We then compared the effects of BRG1 silencing with that of shMITF silencing. Similar to what has previously been described by siMITF knockdown, shMITF knockdown resulted in cell cycle arrest and morphological changes associated with senescence (Fig. 2C) accompanied by the down-regulation of around 600 genes and up-regulation of 747 genes (Fig. 2E and Supplemental Dataset 2). Comparison with BRG1 silencing showed that 60% of genes repressed by shMITF were also repressed by shBRG1

consistent with the fact that MITF is strongly repressed in the shBRG1 cells. Ontology analysis of the commonly repressed genes showed strong enrichment in terms associated with cell signalling, cell cycle, and mitosis showing that MITF and BRG1 cooperate to activate these critical pathways (Fig. 2E and Supplemental Dataset 2).

Common up-regulated genes on the other hand are enriched in terms associated with angiogenesis, adhesion, and migration consistent with the fact that these cells show dramatic changes in cell morphology. It has previously been reported that MITF silencing induces a SASP comprising CCL2, CTGF and SERPINE1A. Analysis of the RNA-seq data identified a putative SASP in shMITF cells comprising around 20 secreted factors and of these 15 are also induced in the shBRG1 cells, although several key factors such as IL8 and CCL2 are not induced upon BRG1 silencing (Fig. 2E Supplemental Dataset 2). Together these data show that BRG1 and MITF cooperate to promote 501mel cell proliferation and that their loss induces proliferation arrest and senescence.

We next investigated why BRG1 is essential for MITF expression. Several factors such as SOX10, TCF/LEF/CTNNB1 and CREB have been reported to activate MITF expression [19]. We noted that SOX10 expression is strongly repressed in the BRG1 knockdown cells. SiSOX10 silencing effectively represses endogenous MITF expression 501Mel cells (Fig. 3A-B). In 501Mel-Cl8 cells that constitutively express 3HA-tagged MITF from the CMV promoter siSOX10 represses endogenous, but not ectopic MITF. In contrast, siCREB silencing had no effect on MITF expression in either of the cell lines. SOX10 is therefore a major regulator of MITF expression in 501Mel cells and the loss of its expression in siBRG1 cells likely explains the concomitant loss of MITF [54].

To determine whether, the shared phenotypes of BRG1 and MITF knockdown cells results only from the concomitant loss of MITF upon BRG1 silencing or whether BRG1 acts also as a MITF co-factor, we performed shBRG1 silencing in the 501mel-Cl8 cells. BRG1 knockdown in these cells repressed endogenous MITF expression, but not ectopic 3HA-MITF (Fig. 3C). Nevertheless BRG1 silencing in these cells elicited a phenotype similar to 501Mel cells characterised by arrested proliferation, cell death and morphological changes. Analysis of gene expression showed that many MITF target genes are similarly repressed by BRG1 silencing in both 501Mel and Cl8 cells, while SASP components are induced (Fig. 3D). Together, these data show that BRG1 is essential for MITF expression via SOX10 and that it acts as a cofactor for MITF since ectopic MITF in the Cl8 cells does not activate target genes expression in its absence.

BRG1 binds widely over the 501Mel cell genome.

To better understand how BRG1 regulates a large gene expression programme in 501Mel cells, we performed genome profiling. Initial attempts to ChIP BRG1 using formaldehyde fixed sonicated chromatin, were unsuccessful, however we observed strong enrichment at several MITF occupied sites using "organic" ChIP [31] on native Mnase digested chromatin (data not shown). Sequencing of this material identified >37000 BRG1-occupied sites located in inter and intragenic regions with relative enrichment at the promoter (Fig. 4A and B). Comparison with public encode data show that BRG1-occupied sites often colocalise with or flank H3K27ac-marked enhancer regions, although other sites do not show this mark partially reflecting the fact that the encode data does not comprise mapping of melanocyte-specific enhancers (Fig. 4A and C). We therefore integrated the BRG1 data with public H3K27ac data from primary human foreskin melanocytes. BRG1 colocalises with enhancers that are active in melanocytes and in other cell types (Fig. 4A, C and D) as well as melanocyte specific enhancers seen at the MITF and DCT loci (see below). Clustering analysis identified a set of BRG1-occuiped loci that colocalise with melanocyte H3K27ac marked enhancers (Fig. 4D). These sites are strongly enriched at 4185 promoters, the majority of which are associated with highly expressed genes, but are also present in inter and intragenic regions. BRG1 is therefore bound widely over the 501Mel genome both at active enhancer elements and promoters.

Analysis of the DNA sequence motifs at BRG1 peaks identified binding sites for a large set of transcription factors, the most abundant of which are NRF1, KLF5, SP1-family factors, CTCF, and EGR1 (Supplementary Fig. 4). E boxes are also prevalent at BRG1-bound sites identified as sites for USF1/2. Thus, BRG1 may be recruited by many different transcription factors to its sites on the 501Mel genome.

Analysis of BRG1 occupied sites indicated that they display several profiles. A set of > 5000 highly occupied sites (Clusters A and B, Fig. 4E and F) comprise two peaks with one or the other showing a preferential occupancy. This profile is consistent with the binding of BRG1 to two nucleosomes separated by an average distance of 500-600 bp. Another possibility is that this profile may represent two alternative positions of a single nucleosome within the cell population. Clusters C and D representing >15000 peaks, display a single peak flanked on either side with smaller peaks suggesting that here BRG1 may be bound strongly to the central nucleosome and to a lesser extent to the adjacent nucleosomes or that the central position is a preferential site of a nucleosome that can also be located at either side in a minority of cells. A set of >16000 sites (cluster E) comprise a single sharp peak.

We also investigated BRG1 occupancy at the TSS identifying clusters (B-E, Fig. 5A and B) where BRG1 is located distally downstream or upstream of the TSS, and more interestingly a set of TSS where BRG1 occupies two specific sites located at -200 bp and + 72 bp relative to the TSS (Cluster A). At these TSS this profile is consistent with BRG1 occupancy of the last nucleosome before the nucleosome depleted region (NDR) and the first downstream nucleosome (Fig. 5C). Integration of RNA Polymerase II (Pol II) ChIP-seq data from 501Mel cells showed that the peak of promoter paused Pol II is located immediately upstream of the BRG1-bound downstream nucleosome. Assuming that BRG1 is bound to the center of these two nucleosomes, we determined that the NDR corresponds to around 142 bp, approximately the size of a single missing nucleosome.

Annotation of the BRG1-occupied sites identified 7168 potential target genes in a window of +/-10kb around the TSS and >10,000 potential target genes in a window of+/-30 kb (Fig. 5D). Integration of this information with the RNA-seq data showed that 34% of genes down-regulated upon BRG1 silencing have a BRG1-occupied site at +/-10 kb, while this figure attains 47% using the +/-30kb window (Fig. 5E). In contrast, only 12% and 18% of up-regulated genes are associated with BRG1-occupied sites using these windows. Ontology analysis shows that down-regulated BRG1-associated genes are enriched in those involved in pigmentation, DNA replication and glucose and fatty acid metabolism. Up-regulated genes are involved in angiogenesis and transcription regulation, notably expression of a set of ZNF transcription factors appear to be co-ordinately regulated by BRG1 (Supplemental Dataset 3). Together these data show that BRG1 is recruited by many transcription factors in 501Mel cells to regulate the expression of a large set of target genes.

MITF recruits BRG1 to a subset of its genomic sites.

If BRG1 acts as a cofactor for MITF, they should colocalize at least at a subset of sites in the genome. To investigate this, we integrated BRG1 and MITF ChIP-seq data showing that of >16000 MITF occupied sites >6000 are co-occupied by BRG1. Co-occupied sites are located in both inter and intragenic regions, but are enriched (20%) at the promoter (Fig. 6A). For example, colocalisation can be observed at the MITF locus itself, where MITF occupies multiple sites, several of which colocalise with BRG1 (Fig. 6B). It is also striking that BRG1 colocalizes with multiple melanocyte-specific H3K27ac-marked enhancers found throughout the locus. A similar situation is seen at the DCT locus, where MITF and BRG1 colocalize at H3K27ac marked melanocyte specific enhancers (Fig. 6C).

Co-occupied sites show several profiles where MITF binds with either a single sharp or broad BRG1 peak or between two BRG1 peaks (Fig. 6C). This can be clearly seen, at the TYR locus where several MITF occupied sites are located between two BRG1 peaks suggesting that MITF binds the DNA between two BRG1 bound nucleosomes. Genes associated with co-occupied sites are involved in previously defined critical functions of MITF such as pigmentation, cell cycle, apoptosis and DNA damage response, as well as lysosome organisation, and intracellular protein transport, (Supplementary Fig. 5A). Analysis of the DNA sequence at co-occupied sites showed enrichment not only in the presence of E and M boxes for MITF, but also in motifs for SOX10, PAX-domain containing factors, CREB and ETS1 (Supplementary Fig. 5B). These factors may therefore cooperate with MITF and BRG1 to regulate the associated target genes. In addition, we also identified a set of 1065 TSS, where as shown above, BRG1 occupies the nucleosomes immediately flanking the TSS and MITF binds the NDR (Fig. 6D). The genes associated with these promoters are highly enriched in lysosome formation, cell cycle and RNA processing and splicing (data not shown). BRG1-MITF co-localization therefore defines a set of MITF-containing regulatory elements (MCREs), where MITF, alone or with other factors, occupies the DNA between two BRG1-bound nucleosomes (Fig. 6E).

The above data are consistent with the idea that a subset of MITF-occupied sites lie between two BRG1 bound nucleosomes suggesting that MITF may recruit BRG1 to these sites to remodel chromatin. To test this idea we performed BRG1 ChIP-qPCR at several loci after siMITF silencing. At all tested loci, MITF silencing led to diminished BRG1 occupancy (Fig.. 7A). We next investigated whether on the other hand, MITF occupancy is affected by BRG1 silencing using Cl8 cells where BRG1 loss does not affect expression of ectopic 3HA-tagged MITF (see above). Anti-HA ChIP-qPCR at MITF sites not associated with BRG1 co-occupancy showed only a mild reduction in MITF occupancy (Fig. 7B). At many co-occupied sites, BRG1 silencing resulted in marked increased in MITF occupancy. This was observed for example at the GRP110 locus where MITF binds to sites located between BRG1-bound nucleosomes. Increased occupancy is not however seen at all such sites as for example at the DCT locus, where MITF also binds between two BRG1 bound nucleosomes but occupancy is not affected.

Together, these data are consistent with the idea that MITF recruits BRG1 to several loci not to stabilise its own binding but rather that BRG1 recruitment contributes to the dynamics of MITF binding.

BRG1 and MITF coregulate gene expression in Hermes 3A melanocytes.

The above data show that BRG1 and MITF colocalize and cooperate to regulate gene expression in 501mel melanoma cells. We also investigated whether this was the case in untransformed melanocytes. In contrast to 501Mel cells, shBRG1 silencing in had little effect on MITF expression in Hermes 3A cells (Fig. 8A), but induces changes in cell morphology with up to 80% of cells showing staining for senescence-associated β-galactosidase (Fig. 8B). Within 8 days, the BRG1 silenced cells detach from the plate. ShMITF silencing in Hermes 3A cells also led to growth arrest and a marked changes in morphology, with flattening, enlargement of the cell body and reduced neurite projections (Fig. 8B). Despite these changes indicative of senescence, in shMITF silenced cells, <50% of the cells showed staining for senescence-associated β-galactosidase that was in general weaker. As with shBRG1, MITF silencing led to cells detaching from the plate within 7 days. Thus, both BRG1 and MITF and are essential for melanocyte growth, and in their absence cell undergo growth arrest and senescence.

We performed RNA-seq on MITF- and BRG1-knockdown Hermes 3A cells. BRG1 silencing in Hermes3A cells led to down-regulation of only 587 genes, and up-regulation of 971 genes, much less than in 501Mel cells (Fig. 8C and D and Supplemental Dataset 4). Down-regulated genes are involved in pigmentation, cholesterol metabolism as well as intracellular signalling cascades and general cell morphology. Up-regulated genes are involved in cell-cell signalling and adhesion as well as angiogenesis. Many of these functions are associated with changes in expression of cell surface proteins and the appearance of a SASP of secreted growth factors and cytokines.

MITF silencing led to down-regulation of 757 genes and up-regulation of 664 genes in Hermes3A cells (Fig. 8C and D and Supplemental Dataset 4). Down-regulated genes are involved in cell-adhesion, intracellular signalling cascades and general cell morphology as well as apoptosis. MITF silencing therefore promotes apoptosis resistant senescence. Up-regulated genes are involved in cell proliferation, regulation of Pol II transcription, as well as vasculature development again reflecting the appearance of a SASP of secreted growth factors and cytokines. While the number of genes regulated by BRG1 in Hermes and 501Mel cells is very different the number regulated by MITF is very similar.

Comparison of the genes regulated by MITF and BRG1 showed that 38% of genes down-regulated upon BRG1 silencing were diminished by shMITF silencing (Fig. 8C and Supplemental Dataset 4). Commonly down-regulated genes are involved in intracellular

signalling cascades and general cell morphology as well as apoptosis. 25% of the BRG1 up-regulated genes are also increased upon MITF silencing and these common up-regulated genes are involved in cell proliferation, as well as vasculature development reflecting the appearance of a similar but not identical SASP upon shRNA-mediated silencing of each factor (Fig. 8D).

Together these results show that BRG1 is critical for Hermes3A proliferation despite the fact that it regulates a much reduced genes expression programme in these cells. As with the 501Mel cells however, MITF and BRG1 cooperate to regulate a subset of genes involved in several essential cellular processes associated with resistance to apoptosis cell morphology and signalling.

BRG1 is essential for melanocyte development in vivo.

The above data show that BRG1 is essential for proliferation and survival of both melanocytes and melanoma cells in vitro. We therefore asked if BRG1 is also essential for melanocytes in vivo in mice. As BRG1 germ-line knockout mice die during early embryogenesis [5], we crossed mice with floxed alleles of the Smarca4 gene encoding BRG1 [29] with mice expressing Cre-recombinase under the control of the Tyrosinase promoter and enhancer to allow selective inactivation of BRG1 in the melanocyte lineage [11]. We first generated Try::Cre/Smarca4lox/+ mice that were crossed to generate the resulting Smarca4mel+/- or Smarca4mel-/- genotypes. The Try::Cre/ Smarca4mel-/- mice were present in the progeny at the expected ratio indicating no loss of viability. While the heterozygous Try::Cre/Smarca4mel+/- mice were black, homozygous Try::Cre/Smarca4mel-/- mice were either completely white or had occasional black spotting arising from rare melanoblasts that had escaped Cre-driven recombination during embryogenesis (Fig. 9). Examination of the hair from two genotypes showed a total loss of melanin and no evidence for empty melanosomes in Smarca4mel-/- hair. Taken together with the essential role of BRG1 in melanoma and melanocyte cells in vitro, these data indicate that BRG1 is essential for normal melanoblast development in vivo.

Discussion

A complex network of protein interactions around MITF.

We describe for the first time a comprehensive characterisation of the MITF interactome. MITF forms multiple complexes with diverse sets of proteins that include the chromatin remodelling complexes BRG1 and NURF, TFIIIC, cohesins and multiple enzymes of the ubiquitin cycle. TFE3, TFEB and TFEC also co-purify with MITF raising the questions of

which sites are bound as MITF homodimers and which are bound by MITF-TFE heterodimers and whether binding as homo- or heterodimers has functional consequences for transcription regulation. Mouse genetic studies have not revealed functions for the TFE factors in development of the melanocyte lineage [48], however their role in melanoma has not been fully evaluated. Future ChIP-seq studies should determine which sites are bound as homo or heterodimers, and functional studies will reveal whether the TFE factors have a role in melanoma.

A striking finding of our study is the interaction of MITF with XRCC5 and XRCC6 (Ku80 and Ku70), and DNA-dependent protein kinase. These proteins are recruited to sites of double stand breaks suggesting that MITF may also be recruited to these sites and influence repair or signaling. Indeed, MITF knockdown induces a DNA damage response [17, 50]. Nevertheless, we so far found no recruitment of MITF to DNA damage sites induced by laser irradiation in 501Mel cells (unpublished observations). The significance of MITF interactions with the DNA-damage machinery therefore remains to be determined. MITF also interacts with complexes involved in DNA replication. We find three subunits of the MCM complex associated with MITF. These three subunits interact to form part of the hexamer ring, yet the other three subunits are not detected perhaps due to dissociation of the complex during purification. 4 of the 5 subunits of replication factor C also co-purify with MITF [28]. Assembly of DNA replication origins can be influenced by the presence of transcription regulatory elements and MYC that also interacts with the MCM subunits has been shown to directly influence DNA replication [12, 35]. Perhaps the MITF interaction with these replication complexes facilitates replication origin assembly at MITF-occupied sites thereby coupling replication with transcription regulation.

While our results have identified many new MITF partners, we did not identify several previously identified cofactors such as P300/CBP [19] or YY1 [34]. Perhaps the interactions with these proteins are too transient to be detected in this way or do not take place in 501Mel cells. Nevertheless, the finding that MITF associates with a large collection of proteins involved in diverse functions is in accordance with the fact that it plays a central role in melanocyte and melanoma cell physiology. The findings here reinforce this idea and provide many new avenues to understand the complex and diverse nature of MITF function in melanoma.

A novel BRG1-CDH7 containing complex is a cofactor for MITF.

While MITF-BRG1 interactions have been previously described, the composition of the BRG1 complex interacting with MITF has not been fully described [9, 32]. In the TAP-

purification experiments, we found BRG1, but not the related Brahma (BRM) protein in the mass spectrometry analysis, although both proteins are expressed in 501Mel cells [32]. Several related BRG1-containing complexes have been described [45, 53] and the complex that interacts with MITF most closely resembles the PBAF variant with the presence of PBRM1. We also identified CHD7 that has been reported to associate with PBAF in neural crest cells [3], and showed that both BRG1 and MITF co-precipitate with CHD7 in 501mel cells. In contrast, the ARID1A/B and ARID2 subunits are absent from this complex as assessed by mass-spectrometry and immunoblot (data not shown) despite that fact that ARID2 was detected in the CHD7-BRG1 complex in human neural crest like cells [3]. MITF therefore appears to interact with yet another variant amongst the known BRG1 complexes. We further attempted to colocalize BRG1 and CHD7 by ChIP-seq over the genome, but we have so far not been successful due to the lack of ChIP-grade CHD7 antibodies (our unpublished data).

In melanoma cells and melanocytes, BRG1 silencing led to arrested proliferation and cell death irrespective of the expression of BRM. This requirement for BRG1 in melanoma cells nevertheless contrasts with its tumour suppressor function in human cancers [21, 36, 45]. In 501Mel cells, loss of BRG1 diminished SOX10 expression that in turn strongly down-regulated MITF expression. As a consequence, these cells undergo growth arrest and senescence characterised by a SASP similar to that seen upon MITF silencing. While BRG1 controls a much larger gene expression programme than MITF in these cells, many MITF regulated genes are also regulated by BRG1. In addition, MITF target genes are down-regulated upon BRG1 silencing in 501Mel Cl8 cells expressing ectopic MITF and consistent with the idea that BRG1 acts not only to regulate MITF expression indirectly via SOX10, but also acts as an MITF cofactor.

In contrast, MITF expression was BRG1-independent in Hermes-3A melanocytes suggesting that its expression is likely driven by other factors in these cells. Despite the maintained MITF expression, BRG1 silencing in Hermes-3A cells leads to arrested proliferation, senescence and cell death. Moreover, the gene regulatory programmes controlled by MITF and BRG1 show a considerable overlap in Hermes-3A cells suggesting that BRG1 acts as an MITF cofactor also in this cell line for the expression of a subset of genes critical for growth and survival. In parallel with this, inactivation of BRG1 in developing mouse melanocytes in vivo leads to complete loss of pigmentation. It is possible that melanoblasts develop in these mice, but do not produce melanin/melanosomes for pigmentation. Nevertheless, given the arrested cell proliferation and cell death seen in melanoma cells and melanocytes in vitro, it is more

likely that loss of pigmentation results from absence of melanocytes in these animals. Together our data identify BRG1 as an essential MITF cofactor in melanoma and melanocyte/melanoblast cells in vitro and in vivo.

BRG1-MITF co-localization defines a set of MCREs with a specific chromatin organisation.

ChIP-seq shows that BRG1 binds extensively over the genome often at active H3K27ac-marked enhancers. In 501Mel cells, BRG1 association with melanocyte-specific enhancers was also observed consistent with previous reports of BRG1 association with cell and tissue-specific enhancer elements [27]. Nevertheless, our data revealed several BRG1 binding profiles. One of these profiles comprises two BRG1 peaks separated by around 600 base pairs. A subset of such peaks is found at sites where MITF and BRG1 colocalize and the MITF binding is located between the two adjacent BRG1 peaks. These observations are consistent with the idea that MITF binds alone or in combination with other factors cis-regulatory elements present in the exposed DNA between two BRG1 occupied nucleosomes, or that the two peaks represent alternative positions of a single nucleosome flanking such elements. In many cases, MITF binds with other factors as recognition motifs for SOX10, PAX3 and several other transcription factors are enriched at these sites. The integration of this data allowed us to define a set MCREs, where MITF binds often with SOX10 or PAX3 between two BRG1-bound nucleosomes. Many of these MCREs are further associated with melanocyte H3K27ac marked enhancers, thus defining a subset of MITF sites that likely to be those that are most active in regulating gene expression the melanocyte lineage. Also, as BRG1 is recruited to the genome by factors other than MITF, it is likely that other sites with a configuration of two spaced BRG1 binding sites represent loci where one or several of these factors bind in an analogous manner, recruiting BRG1 to remodel chromatin. Although several examples of transcription factors recruiting BRG1 have been previously described [45, 53, 15], we report here for the first time this specific organisation of their binding relative to BRG1-occupied nucleosomes.

We also found a preferential BRG1 occupancy of nucleosomes flanking the NDR at a subset of TSS with the Pol II pause site located immediately 5' of the first downstream nucleosome. This exact positioning of BRG1 at the TSS was not noted in several previous ChIP-seq studies [10, 15, 27, 59, 37], however Tolstorukov et al 51 have reported that BRG1 occupies the nucleosomes flanking the TSS and they also observed BRG1 in the NDR that is not clearly seen in our study. Nevertheless, Tolstorukov et al reported that inactivation of BRG1 does not

affect the positioning of these 2 nucleosomes, but rather elicits a strong reduction in their occupancy.

Our data show that MITF recruits BRG1 to the genome since BRG1 binding is strongly diminished upon siMITF knockdown. This suggest that MIF recruits BRG1 to facilitate its binding by remodelling the chromatin to create the nucleosome free regions where we observe its binding. Indeed, in several previous instances BRG1 chromatin remodelling has been shown to facilitate transcription factor binding, for example the binding of TAL1 1, STAT3[39], or nuclear receptors[30, 52]. In contrast, we observed that MITF occupancy of many sites increased following siBRG1 silencing. This observation indicates that BRG1 functions to increase the dynamics of MITF binding. It has previously been shown that binding of transcription factors to chromatin is often extremely dynamic and that techniques such as ChIP capture a snapshot of their occupancy[55]. This seems also to be case for MITF as the increase in occupancy seen in ChIP upon BRG1 silencing suggests an increase in the time of residence at its occupied sites.

In this context it should be considered that there are more than 7X105 Ebox elements in the human genome, much more than the 16 000 that are occupied by MITF. While many sites may be inaccessible, the excess of such sequences may compete for MITF binding to its functional sites. MITF recruitment of BRG1 may therefore be required to reduce its time of residence thus assuring the mobility of MITF to promote its binding to functional sites where it may be further stabilised by binding together with other transcription factor such as SOX10 whose binding motifs are enriched at MITF-BRG1 co-occupied sites. We therefore propose a model in which BRG1 acts to increase MITF mobility reducing its binding to non-functional E boxes thus ensuring a pool of MITF for binding to functional sites.

Materials and Methods

Generation of 501Mel cells stably expressing F-H-MITF

501Mel cells cultured in RPMI 1640 medium (Sigma, St Louis, MO, USA) supplemented with 10% foetal calf serum were transfected with a CMV based vector expressing Flag-HA-tagged MITF and a vector encoding puromycin resistance. Transfected cells were selected with puromycin (3µg/ml), and the expression of MITF verified by western blot using the antibody MITF: ab-1 (C5) from Neomarkers, the 12CA5 HA antibody (Roche, Basel, Switzerland), or the M2 Flag antibody (Sigma, St-Louis, Missouri). Details of other cell culture are provided in Supplementary material. Hermes 3A cells were obtained from the University of London St Georges repository.

Tandem immunoaffinity purification and mass-spectrometry

Cell extracts were prepared essentially as previously described and subjected to tandem Flag-HA immunoprecipitation [13, 23]. Full details can be found in the Supplementary material. Complexes were resolved by SDS-PAGE and stained using the Silver Quest kit (Invitrogen). Mass-spectrometry was performed at the Taplin Biological Mass Spectrometry Facility (Harvard Medical School, Boston, MA).

Cell culture and lentiviral infections.

All lentiviral shRNA vectors were obtained from Sigma (Mission sh-RNA series) in the PLK0 vector. Full details are in Supplementary material. Cells were infected with the viral stocks and after 5 days (or as indicated in figure legend) of puromycin selection (3μg/ml), cells were photographed and collected for preparation of cell lysates or isolation of RNA. In each case between 5X105-1X106 cells were infected with the indicated shRNA lentivirus vectors and all experiments were performed at least in triplicate. The siRNA knockdown of BRG1 was performed with ON-TARGET-plus human SMARCA4 SMARpool (L-010431-00) purchased from Dharmacon Inc. (Chicago, Il., USA). Control siRNA directed against luciferase was obtained from Eurogentec (Seraing, Belgium). siRNAs were transfected using Lipofectamine RNAiMax (Invitrogen, La Jolla, CA, USA).

Senescence-Associated β-Galactosidase Assay

The senescence-associated β -galactosidase staining kit from Cell signaling technology (Beverly, MA, USA) was used according to the manufacturer's instructions to histochemically detect β-galactosidase activity at pH 6.

Mice and genotyping

The Smarca4lox/lox and Tyr::Cre strains have been described previously [29, 11]. Genotyping of F1 offspring was carried out by PCR analysis of genomic tail DNA with primers detailed in the respective publications. All animals were handled according to institutional and national guidelines and policies.

mRNA preparation, quantitative PCR and RNA-seq.

mRNA isolation was performed according to standard procedure (Qiagen kit). qRT-PCR wascarried out with SYBR® Green I (Qiagen) and Multiscribe Reverse Transcriptase (Invitrogen) and monitored by a LightCycler® 480 (Roche). Detection of Actin gene was used to normalize the results. Primer sequences for each cDNA were designed using Primer3 Software and are available upon request. RNA-seq was performed essentially as previously

described[24]. Gene ontology analyses were performed using the functional annotation clustering function of DAVID (http://david.abcc.ncifcrf.gov/).

Chromatin-immunoprecipitation and sequencing

BRG1 ChIP experiments were performed on native Mnase-digested chromatin isolated from 501Mel cells. Nuclei isolation and chromatin preparation was performed as described in the supplemental data. SOX10 and 3HA-MITF ChIP experiments were performed on 0,4% PFA-fixed chromatin isolated from 501Mel and Cl8 cells respectively according to standard protocols as previously described [50]. ChIP-seq libraries were prepared as previously described and sequenced on the Illumina Hi- seq2500 as single-end 50-base reads. Peak detection was performed using the MACS software ([60] http://liulab.dfci. harvard.edu/MACS/). Peaks were then annotated with GPAT (http://bips.u-strasbg.fr/GPAT/Gpat_ home.html) using a window of ±10kb (or as indicated in the figures) relative to the transcription start site of RefSeq transcripts. Global clustering analysis and quantitative comparisons were performed using seqMINER ([58], http://bips.u-strasbg.fr/seqminer/) and R (http://www.r- project.org/).

De novo motif discovery on FASTA sequences corresponding to windowed peaks was performed using MEME-ChIP. Motif correlation matrix was calculated with in-house algorithms using JASPAR database.

Acknowledgements

We thank, S. Gygi and R. Tomaino for mass-spectrometry analysis, C. Goding for MITF expression vectors, L. Larue for the Tyr::Cre mice, P. Chambon and D. Metzger for the floxed Smarca4 mice, E. Sviderskaya and D. Bennet for the Hermes cells, L. Tora for the anti-TRRAP antibody, B. Jost, and all the staff of the IGBMC high throughput sequencing facility, a member of "France Génomique" consortium (ANR10-INBS-09-08). This work was supported by grants from the CNRS, the INSERM, the Association pour la Recherche contre le Cancer, the Ligue Nationale et Départementale Région Alsace contre le Cancer and the Institut National du Cancer (INCa), the ANR-10-LABX-0030-INRT French state fund through the Agence Nationale de la Recherche under the frame programme Investissements d'Avenir labelled ANR-10-IDEX-0002-02. ID is an 'équipe labellisée' of the Ligue Nationale contre le Cancer.

Author contributions.

P.L. performed and analysed the shBRG1 knockdowns, performed and analysed the ChIP-seq with T.S and R.S and the RNA-seq together with C.K. P.L. and G.M generated and analysed the Tyr-Cre::Smarcc4 recombinant mice. T.S. generated the F-HA-MITF cell line, performed

the tandem affinity purifications, and together with P.L. performed the shBRG1 knockdowns. S. L-G. assissted in analysis of the ChIP-seq data and performed the motif matrix analyses. I.D. T.S. and P.L. conceived experiments, analysed data and wrote the paper.

References.

1 Abraham BJ, Cui K, Tang Q, Zhao K. Dynamic regulation of epigenomic landscapes during hematopoiesis. BMC Genomics 2013; 14: 193.

2 Al-Hakim AK, Bashkurov M, Gingras AC, Durocher D, Pelletier L. Interaction proteomics identify NEURL4 and the HECT E3 ligase HERC2 as novel modulators of centrosome architecture. Molecular & cellular proteomics : MCP 2012; 11: M111 014233.

3 Bajpai R, Chen DA, Rada-Iglesias A, Zhang J, Xiong Y, Helms J et al. CHD7 cooperates with PBAF to control multipotent neural crest formation. Nature 2010; 463: 958-962.

4 Bekker-Jensen S, Rendtlew Danielsen J, Fugger K, Gromova I, Nerstedt A, Lukas C et al. HERC2 coordinates ubiquitin-dependent assembly of DNA repair factors on damaged chromosomes. Nature cell biology 2010; 12: 80-86; sup pp 81-12.

5 Bultman S, Gebuhr T, Yee D, La Mantia C, Nicholson J, Gilliam A et al. A Brg1 null mutation in the mouse reveals functional differences among mammalian SWI/SNF complexes. Molecular Cell 2000; 6: 1287-1295.

6 Carriere L, Graziani S, Alibert O, Ghavi-Helm Y, Boussouar F, Humbertclaude H et al. Genomic binding of Pol III transcription machinery and relationship with TFIIS transcription factor distribution in mouse embryonic stem cells. Nucleic Acids Research 2012; 40: 270-283.

7 Cojocaru M, Bouchard A, Cloutier P, Cooper JJ, Varzavand K, Price DH et al. Transcription factor IIS cooperates with the E3 ligase UBR5 to ubiquitinate the CDK9 subunit of the positive transcription elongation factor B. The Journal of biological chemistry 2011; 286: 5012-5022.

8 Collas P, Le Guellec K, Tasken K. The A-kinase-anchoring protein AKAP95 is a multivalent protein with a key role in chromatin condensation at mitosis. The Journal of cell biology 1999; 147: 1167-1180.

9 de la Serna IL, Ohkawa Y, Higashi C, Dutta C, Osias J, Kommajosyula N et al. The microphthalmia-associated transcription factor requires SWI/SNF enzymes to activate melanocyte-specific genes. The Journal of biological chemistry 2006; 281: 20233-20241.

10 De S, Wurster AL, Precht P, Wood WH, 3rd, Becker KG, Pazin MJ. Dynamic BRG1 recruitment during T helper differentiation and activation reveals distal regulatory elements. Mol Cell Biol 2011; 31: 1512-1527.

11 Delmas V, Martinozzi S, Bourgeois Y, Holzenberger M, Larue L. Cre-mediated recombination in the skin melanocyte lineage. Genesis 2003; 36: 73-80.

12 Dominguez-Sola D, Ying CY, Grandori C, Ruggiero L, Chen B, Li M et al. Non-transcriptional control of DNA replication by c-Myc. Nature 2007; 448: 445-451.

13 Drane P, Ouararhni K, Depaux A, Shuaib M, Hamiche A. The death-associated protein DAXX is a novel histone chaperone involved in the replication-independent deposition of H3.3. Genes Dev 2010; 24: 1253-1265.

14 Eide T, Tasken KA, Carlson C, Williams G, Jahnsen T, Tasken K et al. Protein kinase A-anchoring protein AKAP95 interacts with MCM2, a regulator of DNA replication. The Journal of biological chemistry 2003; 278: 26750-26756.

15 Euskirchen GM, Auerbach RK, Davidov E, Gianoulis TA, Zhong G, Rozowsky J et al. Diverse roles and interactions of the SWI/SNF chromatin remodeling complex revealed using global approaches. PLoS Genet 2011; 7: e1002008.

16 Fagiani E, Giardina G, Luzi L, Cesaroni M, Quarto M, Capra M et al. RaLP, a new member of the Src homology and collagen family, regulates cell migration and tumor growth of metastatic melanomas. Cancer Res 2007; 67: 3064-3073.

17 Giuliano S, Cheli Y, Ohanna M, Bonet C, Beuret L, Bille K et al. Microphthalmia-associated transcription factor controls the DNA damage response and a lineage-specific senescence program in melanomas. Cancer Research 2010; 70: 3813-3822.

18 Giuliano S, Ohanna M, Ballotti R, Bertolotto C. Advances in melanoma senescence and potential clinical application. Pigment Cell Melanoma Res 2011; 24: 295-308.

19 Goding CR. Mitf from neural crest to melanoma: signal transduction and transcription in the melanocyte lineage. Genes Dev 2000; 14: 1712-1728.

20 Gudjonsson T, Altmeyer M, Savic V, Toledo L, Dinant C, Grofte M et al. TRIP12 and UBR5 suppress spreading of chromatin ubiquitylation at damaged chromosomes. Cell 2012; 150: 697-709.

21 Hargreaves DC, Crabtree GR. ATP-dependent chromatin remodeling: genetics, genomics and mechanisms. Cell research 2011; 21: 396-420.

22 Herquel B, Ouararhni K, Davidson I. The TIF1alpha-related TRIM cofactors couple chromatin modifications to transcriptional regulation, signaling and tumor suppression. Transcription 2011; 2: 231-236.
23 Herquel B, Ouararhni K, Khetchoumian K, Ignat M, Teletin M, Mark M et al. Transcription cofactors TRIM24, TRIM28, and TRIM33 associate to form regulatory complexes that suppress murine hepatocellular carcinoma. Proceedings of the National Academy of Sciences of the United States of America 2011; 108: 8212-8217.
24 Herquel B, Ouararhni K, Martianov I, Le Gras S, Ye T, Keime C et al. Trim24-repressed VL30 retrotransposons regulate gene expression by producing noncoding RNA. Nature structural & molecular biology 2013; 20: 339-346.
25 Hoek KS, Goding CR. Cancer stem cells versus phenotype-switching in melanoma. Pigment Cell Melanoma Res 2010; 23: 746-759.
26 Hoek KS. MITF: the power and the glory. Pigment cell & melanoma research 2011; 24: 262-263.
27 Hu G, Schones DE, Cui K, Ybarra R, Northrup D, Tang Q et al. Regulation of nucleosome landscape and transcription factor targeting at tissue-specific enhancers by BRG1. Genome Res 2011; 21: 1650-1658.
28 Indiani C, O'Donnell M. The replication clamp-loading machine at work in the three domains of life. Nature reviews Molecular cell biology 2006; 7: 751-761.
29 Indra AK, Dupe V, Bornert JM, Messaddeq N, Yaniv M, Mark M et al. Temporally controlled targeted somatic mutagenesis in embryonic surface ectoderm and fetal epidermal keratinocytes unveils two distinct developmental functions of BRG1 in limb morphogenesis and skin barrier formation. Development 2005; 132: 4533-4544.
30 Jeong KW, Lee YH, Stallcup MR. Recruitment of the SWI/SNF chromatin remodeling complex to steroid hormone-regulated promoters by nuclear receptor coactivator flightless-I. J Biol Chem 2009; 284: 29298-29309.
31 Kasinathan S, Orsi GA, Zentner GE, Ahmad K, Henikoff S. High-resolution mapping of transcription factor binding sites on native chromatin. Nat Methods 2014; 11: 203-209.
32 Keenen B, Qi H, Saladi SV, Yeung M, de la Serna IL. Heterogeneous SWI/SNF chromatin remodeling complexes promote expression of microphthalmia-associated transcription factor target genes in melanoma. Oncogene 2010; 29: 81-92.
33 Kirkland JG, Raab JR, Kamakaka RT. TFIIIC bound DNA elements in nuclear organization and insulation. Biochimica et biophysica acta 2013; 1829: 418-424.

34 Li J, Song JS, Bell RJ, Tran TN, Haq R, Liu H et al. YY1 regulates melanocyte development and function by cooperating with MITF. PLoS genetics 2012; 8: e1002688.
35 Mechali M. Eukaryotic DNA replication origins: many choices for appropriate answers. Nature reviews Molecular cell biology 2010; 11: 728-738.
36 Medina PP, Sanchez-Cespedes M. Involvement of the chromatin-remodeling factor BRG1/SMARCA4 in human cancer. Epigenetics : official journal of the DNA Methylation Society 2008; 3: 64-68.
37 Morris SA, Baek S, Sung MH, John S, Wiench M, Johnson TA et al. Overlapping chromatin-remodeling systems collaborate genome wide at dynamic chromatin transitions. Nat Struct Mol Biol 2014; 21: 73-81.
38 Murr R, Vaissiere T, Sawan C, Shukla V, Herceg Z. Orchestration of chromatin-based processes: mind the TRRAP. Oncogene 2007; 26: 5358-5372.
39 Ni Z, Bremner R. Brahma-related gene 1-dependent STAT3 recruitment at IL-6-inducible genes. J Immunol 2007; 178: 345-351.
40 Noma K, Cam HP, Maraia RJ, Grewal SI. A role for TFIIIC transcription factor complex in genome organization. Cell 2006; 125: 859-872.
41 Ohanna M, Giuliano S, Bonet C, Imbert V, Hofman V, Zangari J et al. Senescent cells develop a PARP-1 and nuclear factor-(Lee)B-associated secretome (PNAS). Genes & development 2011; 25: 1245-1261.
42 Ouhtit A, Gaur RL, Abd Elmageed ZY, Fernando A, Thouta R, Trappey AK et al. Towards understanding the mode of action of the multifaceted cell adhesion receptor CD146. Biochim Biophys Acta 2009; 1795: 130-136.
43 Park J, Kunjibettu S, McMahon SB, Cole MD. The ATM-related domain of TRRAP is required for histone acetyltransferase recruitment and Myc-dependent oncogenesis. Genes & development 2001; 15: 1619-1624.
44 Park J, Wood MA, Cole MD. BAF53 forms distinct nuclear complexes and functions as a critical c-Myc-interacting nuclear cofactor for oncogenic transformation. Molecular and Cellular Biology 2002; 22: 1307-1316.
45 Reisman D, Glaros S, Thompson EA. The SWI/SNF complex and cancer. Oncogene 2009; 28: 1653-1668.
46 Schepsky A, Bruser K, Gunnarsson GJ, Goodall J, Hallsson JH, Goding CR et al. The microphthalmia-associated transcription factor Mitf interacts with beta-catenin to determine target gene expression. Mol Cell Biol 2006; 26: 8914-8927.

47 Schmit TL, Zhong W, Setaluri V, Spiegelman VS, Ahmad N. Targeted depletion of Polo-like kinase (Plk) 1 through lentiviral shRNA or a small-molecule inhibitor causes mitotic catastrophe and induction of apoptosis in human melanoma cells. J Invest Dermatol 2009; 129: 2843-2853.

48 Steingrimsson E, Tessarollo L, Pathak B, Hou L, Arnheiter H, Copeland NG et al. Mitf and Tfe3, two members of the Mitf-Tfe family of bHLH-Zip transcription factors, have important but functionally redundant roles in osteoclast development. Proc Natl Acad Sci U S A 2002; 99: 4477-4482.

49 Steingrimsson E, Copeland NG, Jenkins NA. Melanocytes and the microphthalmia transcription factor network. Annu Rev Genet 2004; 38: 365-411.

50 Strub T, Giuliano S, Ye T, Bonet C, Keime C, Kobi D et al. Essential role of microphthalmia transcription factor for DNA replication, mitosis and genomic stability in melanoma. Oncogene 2011; 30: 2319-2332.

51 Tolstorukov MY, Sansam CG, Lu P, Koellhoffer EC, Helming KC, Alver BH et al. Swi/Snf chromatin remodeling/tumor suppressor complex establishes nucleosome occupancy at target promoters. Proc Natl Acad Sci U S A 2013; 110: 10165-10170.

52 Trotter KW, Archer TK. Nuclear receptors and chromatin remodeling machinery. Mol Cell Endocrinol 2007; 265-266: 162-167.

53 Trotter KW, Archer TK. The BRG1 transcriptional coregulator. Nuclear receptor signaling 2008; 6: e004.

54 Vachtenheim J, Ondrusova L, Borovansky J. SWI/SNF chromatin remodeling complex is critical for the expression of microphthalmia-associated transcription factor in melanoma cells. Biochemical and biophysical research communications 2010; 392: 454-459.

55 Voss TC, Hager GL. Dynamic regulation of transcriptional states by chromatin and transcription factors. Nat Rev Genet 2014; 15: 69-81.

56 Wei X, Walia V, Lin JC, Teer JK, Prickett TD, Gartner J et al. Exome sequencing identifies GRIN2A as frequently mutated in melanoma. Nature genetics 2011; 43: 442-446.

57 Widlund HR, Fisher DE. Microphthalamia-associated transcription factor: a critical regulator of pigment cell development and survival. Oncogene 2003; 22: 3035-3041.

58 Ye T, Krebs AR, Choukrallah MA, Keime C, Plewniak F, Davidson I et al. seqMINER: an integrated ChIP-seq data interpretation platform. Nucleic Acids Res 2011; 39: e35.

59 Yu Y, Chen Y, Kim B, Wang H, Zhao C, He X et al. Olig2 targets chromatin remodelers to enhancers to initiate oligodendrocyte differentiation. Cell 2013; 152: 248-261.

60 Zhang Y, Liu T, Meyer CA, Eeckhoute J, Johnson DS, Bernstein BE et al. Model-based analysis of ChIP-Seq (MACS). Genome Biol 2008; 9: R137.
61 Zhao X, Fiske B, Kawakami A, Li J, Fisher DE. Regulation of MITF stability by the USP13 deubiquitinase. Nat Commun 2011; 2: 414.

Figure legends

Figure 1. Purification of MITF-associated complexes. A. Western blot of 501Mel cell lines stably expressing Flag-HA-tagged (F-H-MITF). Immunoblot of total extracts from wild-type cells or cells expressing F-H-MITF detected with anti-MITF, anti-Flag or anti-HA antibodies as indicated, β-actin is used as loading control. B. The immunoprecipitated material from the indicated fractions (soluble nuclear extract, SNE; chromatin-associated extract, CAE) was separated by SDS PAGE and stained with silver nitrate. Several relevant proteins are indicated. Lane M corresponds to a molecular mass marker indicated in kDa. C. Immunoblot detection of HERC2, BRG1, USP7, USP11, XRCC5 and XRCC6 in the MITF-associated complexes. Immunoprecipitations from control and F-H-MITF expressing cells were run on 8% SDS PAGE and after transfer, the blot was probed with the indicated antibodies.

Figure 2. Functional analysis of BRG1 in melanoma cells. A. Immunoblots of extracts from the indicated cell types transfected with control or anti-BRG1 siRNA or cells infected with lentiviral vectors expressing control or anti-BRG1 shRNA. B. Reverse transcription real time qPCR (RT-qPCR) performed on 501Mel cells infected with lentivirus vectors expressing control (C) or anti-BRG1 shRNA. The ratio of expression of the indicated genes is shown. C. Phase contrast microscopy of 501Mel cells infected with the indicated shRNA vectors after 5 days of puromycin selection. Magnification X10. The lower panel shows cells stained for senescence-associated b-galactosidase. Arrows indicate representative stained cells. D. Phase contrast microscopy of SK-Mel-28 cells infected with the indicated shRNA vectors after 5 days of puromycin selection. E. Comparative analysis of RNA-seq data from shBRG1 and shMITF 501Mel cells. Venn diagrammes indicate the overlap between genes that are up and down-regulated in the shBRG1 and shMITF cells. The results of ontology analysis of the commonly up- and down-regulated genes are shown graphically and classed by p value and the number of genes in each category is indicated. Lists of secreted growth factors and cytokines forming the SASP in the shBRG1 and shMITF cells are indicated.

Figure 3. SOX10 regulated MITF expression in 501Mel cells. A. Western blot analysis of MITF expression in the indicated cell types after siRNA transfections. B. RT-qPCR analysis of gene expression in the indicated cell types after siRNA transfections. C. Western blot

analysis of BRG1 and MITF expression in 501Mel CL8 cells following siRNA transfections. Phase contrast microscopy of 501Mel Cl8 cells following siRNA transfections. Magnification X10. D. RT-qPCR analysis of gene expression in the indicated cell types after siRNA transfections.

Figure 4. Genome-wide BRG1 occupancy. A and C. USCS screenshots showing BRG1 occupancy over the ARRDC2 and REL1 loci highlighting colocalization with H3K27ac-marked enhancers either in the Encode data track or in Human Foreskin Melanocytes (HFM). B. Proportional distribution of BRG1-occupied loci over the genome. D. Clustering of BRG1 occupied sites with melanocyte H3K27ac-marked enhancers and their proportional distribution over the genome. E. Read density clustering of BRG1 at its occupied sites reveals several profiles of BRG1 occupancy. The right hand panels show the meta-profiles of the different clusters (A-E). The binding profile of BRG1 to nucleosomes to selected clusters is schematised.

Figure 5. Promoter occupancy by BRG1. A. Read density clustering of BRG1 human annotated TSS sites reveals a subset of promoters with BRG1 occupancy. B. Meta-profiles of BRG1 occupancy in clusters A-E. C. Meta-profile of BRG1 occupancy in cluster A superimposed on the RNA Pol II meta-profile. The binding profile of BRG1 and Pol II around the TSS is schematised below the graph. D. Integrative analysis of BRG1 ChIP-seq data with shBRG1 RNA-seq data. A table shows the number of genes with BRG1-occupied sites +/- 10kb or +/- 30kb from the TSS. Venn diagrammes indicate the number of these genes that are up- or down-regulated following shBRG1 knockdown. E. Ontology analysis of the BRG1-associated up- and down-regulated genes.

Figure 6. Sites co-occupied by BRG1 and MITF. A. Read density clustering of BRG1 and MITF at MITF-occupied loci reveals co-occupied sites with different profiles and their proportional distribution over the genome. B. USCS screenshots showing MITF and BRG1 occupancy over the MITF and DCT loci highlighting their colocalization at a subset of sites along with colocalization with melanocyte-specific H3K27ac-marked enhancers at these loci. C. Meta-profiles of BRG1 occupancy in clusters A-E of panel A. The binding profiles of BRG1 and MITF are schematised. The lower panel shows a USCS screenshot showing MITF and BRG1 occupancy over the TYR locus highlighting the binding of MITF between two BRG1 occupied nucleosomes. D. Meta-profile showing occupancy by BRG1, MITF and Pol II at the TSS. The binding profiles of each factor BRG1 and Pol II around the TSS are schematised below the graph. E. Model for MITF-containing regulatory elements (MCREs)

where MITF binds often with SOX10 or PAX3 between two BRG1-bound nucleosomes, thus defining a subset of MITF sites that likely to be those that are most active in regulating gene expression the melanocyte lineage.

Figure 7. MITF-recruits BRG1. A. ChIP-qPCR of 3HA-MITF in 501Mel CL8 cells at the indicated loci following transfection with SiLuc or siBRG1. B. ChIP-qPCR of BRG1 in 501Mel cells at the indicated loci following transfection with SiLuc or siMITF.

Figure 8. Functional analysis of BRG1 and MITF Hermes 3A melanocytes. A. Immunoblots of Hermes 3A extracts following infection with lentiviral vectors expressing control, anti-BRG1 or anti-MITF shRNAs. B. Phase contrast microscopy of Hermes 3A cells infected with the indicated shRNA vectors after 5 days of puromycin selection and stained for senescence-associated b-galactosidase. Arrows indicate representative stained cells. C-D. Comparative analysis of RNA-seq data from shBRG1 and shMITF Hermes 3A cells. Venn diagrammes indicate the overlap between genes that are up and down-regulated in the shBRG1 and shMITF cells. The results of ontology analysis of the specifically and commonly up- and down-regulated genes are shown graphically and classed by p value and the number of genes in each category is indicated.

Figure 9. Functional analysis of BRG1 in mouse melanocytes in vivo. The upper panel shows photographs of representative mice of the indicated genotypes. The lower panel shows the statistics relevant to the phenotype of the mice lacking BRG1 in the melanocyte lineage. Note that as the Tyr-Cre transgene is present on the X chromosome, we detect black mice with the Tyr-Cre::Smarca4lox/lox genotype, but in these animals the Cre-recombinase is subjected to X-inactivation such that recombination does not occur in all melanoblasts. Bright field images of hair from the backs of 8 week old animals of the two genotypes are also shown. Magnification X40.

Table 1. Summary of proteins and complexes interacting with MITF. Shown are the proteins found specifically in the immunopurifications of F-H-MITF classified according to their function and organisation into known complexes.

Supplementary data

Materials and Methods.

Tandem immunoaffinity purification and mass-spectrometry

Cells were lysed in hypotonic buffer (10 mM Tris-HCl at pH 7.65, 1.5 mM MgCl2, 10mM KCl) and disrupted by Dounce homogenizer. The cytosolic fraction was separated from the pellet by centrifugation at 4°C. The nuclear soluble fraction was obtained by incubation of the

pellet in high salt buffer (final NaCl concentration of 300mM) and then separated by centrifugation at 4°C. To obtain the nuclear insoluble fraction (chromatin fraction), the remaining pellet was digested with micrococcal nuclease and sonicated. Tagged proteins were immunoprecipitated with anti-Flag M2-agarose (Sigma), eluted with Flag peptide (0.5 mg/mL), further affinity purified with anti-HA antibody-conjugated agarose (Sigma), and eluted with HA peptide (1 mg/mL). The HA and Flag peptides were first buffered with 50mM Tris-HCl (pH 8.5), then diluted to 4 mg/mL in TGEN 150 buffer (20 mM Tris at pH 7.65, 150 mM NaCl, 3 mM MgCl2, 0.1 mM EDTA, 10% glycerol, 0.01% NP40), and stored at -20°C until use. Between each step, beads were washed in TGEN 150 buffer. Complexes were resolved by SDS-PAGE and stained using the Silver Quest kit (Invitrogen). Mass-spectrometry was performed at the Taplin Biological Mass Spectrometry Facility (Harvard Medical School, Boston, MA).

Cell culture and lentiviral infections.

Melanoma cell lines SK-Mel-28 and 501Mel were grown in RPMI 1640 medium (Sigma, St Louis, MO, USA) supplemented with 10% foetal calf serum (FCS). 293T cells were grown in Dulbecco's modified Eagle's medium supplemented with 10% FCS and penicillin/streptomycin (7.5 µg/ml). Hermes-3A cells were grown in RPMI 1640 medium (Sigma) supplemented with 10% FCS, 200nM TPA, 200pM cholera toxin, 10ng/ml human stem cell factor (Invitrogen) 10 nM endothelin-1 (Bachem) and penicillin/streptomycin (7.5 µg/mL). All lentiviral shRNA vectors were obtained from Sigma (Mission sh-RNA series) in the PLK0 vector. The following constructs were used. shBRG1 (TRCN0000015549) and shMITF (TRCN0000019119); For lentivirus infection, virus was produced in 293T cells according to the manufacturers protocol described.

Transfections, extract preparation and antibodies.

Transient and stable transfections were performed with 5 µg of expression vectors and using FuGENE 6 reagent (Roche) following the manufacturers instructions. Medium was replaced 24 hours and cell were collected 48 hours after transfection. Cells lysis was performed using LSDB 500 buffer (500mM KCl, 25mM Tris at pH 7.9, 10% glycerol, 0;05 % NP-40, 1mM DTT and protease inhibitor cocktail). Up to 3 mg of whole cell extracts were diluted in LDSB without KCl to obtain a final concentration of 100mM KCl and incubated for 12h with 5 µg of specific antibody and 50µl Slurry of protein-G sepharose (GE Healthcare). Beads were washed three times in LSDB 300, twice in LSDB 150 and boiled in Laemmli buffer before protein separation by SDS–PAGE. For flag immunoprecipitations, extracts were incubated

with 50µl Slurry of Anti-Flag M2-agarose affinity gel (Sigma) and washed similarly prior to elution with Flag peptide (0,5 mg/mL). Immunoblots were performed with the following antibodies: MITF (Interchim, MS-771-P), BRG1 (Abcam, ab110641), HERC2 (BD Transduction Laboratories, 612366), USP11 (Epitomics, 3263-1), USP7 (Cell Signaling, #4833), TRRAP (IGBMC, 2TRR-2D5), NEURL4 (scbt, sc-243603), actin (IGBMC, 2D7), XRCC6 (scbt, sc-17789), XRCC5 (scbt, sc-5280), BAF170 (Bethyl Laboratories, A301-038A), BAF155 (scbt, sc-10756), ARID1A (scbt, sc-373784), ARID1B (scbt, sc-32762), ARID2 (Abcam, ab56082), ACTL6A (Abcam, ab131272), CHD7 (Abcam, ab31824), PBRM1 (Abcam, ab137661), BAF60A (BD Transduction Laboratories, #611728), BAF60B (Abcam, ab166622), SOX10 (Abcam, ab155279), CREB (Upstate Millipore, #06-863).

Chromatin-immunoprecipitation

BRG1 ChIP experiments were performed on native Mnase-digested chromatin. 5x107 to 5x108 freshly harvested 501Mel cells were resuspended in 2mL ice-cold hypotinic buffer (0.3M Sucrose, 60mM KCl, 15mM NaCl, 5mM MgCl2, 0.1mM EDTA, 15mM Tris-HCl (pH 7.5), 0.5mM DTT, 0.1mM PMSF, protease inhibitor cocktail) and cytoplasmic fraction was released by incubation with 2mL of lysis-buffer (0.3M sucrose, 60 mM KCl, 15mM NaCl, 5mM MgCl2, 0.1mM EDTA, 15mM Tris-HCl (pH 7.5), 0.5mM DTT, 0.1mM PMSF, PIC, 0.5% (v/v) IGEPAL CA-630) for 10 minutes on ice. The suspension was layered onto a sucrose cushion (1.2M sucrose, 60 mM KCl, 15mM NaCl, 5mM MgCl2, 0.1mM EDTA, 15 mM Tris-HCl (pH 7.5), 0.5mM DTT, 0.1mM PMSF, PIC) and centrifuged for 25 minutes at 4700 rpm in a swing rotor. The nuclear pellet was resuspended in digestion buffer (0.32M sucrose, 50mM Tris-HCl (pH 7.5), 4mM MgCl2, 1mM CaCl2, 0.1mM PMSF) and subjected to Micrococcal Nuclease digestion for 5 minutes at 37°C. The reaction was stopped by addition of EDTA and suspension chilled on ice for 10 minutes. The suspension was cleared by centrifugation at 10,000 rpm (4°C) for 10 minutes and supernatant (chromatin) was used for further purposes. ChIP was performed on up to 60 □g of native chromatin essentially as previously described.

Legends to Supplementary Tables and Figures.

Supplementary Figure 1. Interaction of MITF with TRRAP and NEURL4. 501Mel cells were transfected with a vector expressing F-MITF or the control empty vector. 48 hours after transfection the cell lysates were subjected to Flag-immunoprecipitation (F-IP) and the presence of endogenous NEURL4 and TRRAP and exogenous F-MITF were detected.

Supplementary Figure 2. Genes encoding MITF interacting factors are also often potential MITF-regulated genes. UCSC screenshot of the .wig files from HA-ChIP on cells expressing 3HA-MITF as described 3 at the indicated loci encoding subunits of the BRG1 chromatin-remodelling complex. MITF occupied sites are indicated by arrows.

Supplementary Figure 3. BRG1 associates with CHD7 in 501Mel cells. A. Following immunoprecipitation of 501Mel cell extracts with anti-BRG1 antibody or empty beads as control the eluted fractions were probed with antibodies for the indicated proteins. B. Following immunoprecipitation of 501Mel cell extracts with anti-CHD7 antibody or empty beads as control the eluted fractions were probed with antibodies for the indicated proteins. C. Table summarising the known compositions of BRG1-related complexes highlight catalytic subunits with ATPase activity, common subunits and specific subunits. The composition of the complex interacting with MITF based on mass-spectrometry and immunoblots is schematised.

Supplementary Figure 4. Frequency of occurrence of transcription factor binding motifs at BRG1 occupied sites. Known motifs were identified using using FIMO. From the FIMO results, perl scripts computed the frequency of occurrence of each motif. Randomly selected regions were used to compute an expected distribution of motif occurrence or motif co-occurrence. The significance of the motif occurrence was estimated through the computation of a Z-score computed as : $z=(x-\mu)/\sigma$, where x is the observed value (number of motif occurrence), μ is the mean of the number of occurrences of motifs (computed over controls) and σ is the standard deviation of the number of occurrences or co-occurrences of motifs (computed over controls). Z-scores were subsequently turned into p-values and a multi-testing correction was applied 1, 2.

Supplementary Figure 5. Analysis of BRG1-MITF co-occupied sites. A. Ontology analysis of genes associated with BRG1-MITF-co-occuiped sites. B. Identification of transcription factor biding motifs at BRG1-MITF-occupied sites. MEME-ChIP identified several motis enriched at these sites. The most prominent are the E-box and M-box corresponding to MITF binding, followed by sites for Pax-domain factors, in this case most probably PAX3, SOX10, CREB and ETS1 as well as motifs with no known annotation.

Supplementary Dataset 1. Mass-spectrometry identification of MITF partners. Excel table showing the data from the Mass-spectrometry analysis. Page 1 shows a summary of the number of peptides and proteins identified in the two experiments in the soluble nuclear and chromatin associated fractions. Page 2 lists the proteins identified uniquely in the F-H-MITF

immunoprecipitates from the soluble nuclear fraction along with the number of peptides for each protein. Page 3 lists the proteins identified uniquely in the F-H-MITF immunoprecipitates from the chromatin-associated fraction along with the number of peptides for each protein.

Supplementary Dataset 2. Excel spreadsheet of genes specifically and commonly regulated by BRG1 and MITF knockdown in 501Mel cells along with the appropriate gene ontology. See figure 2E

Supplementary Dataset 3. Excel spreadsheet of genes with associated BRG1 occupancy and regulated in shBRG1 along with the appropriate gene ontology as described in Figure 5E.

Supplementary Dataset 4. Excel spreadsheet of genes regulated by shBRG1 and shMITF in Hermes 3A cells along with common and specific genes and their ontology as described in Fig 8C and D.

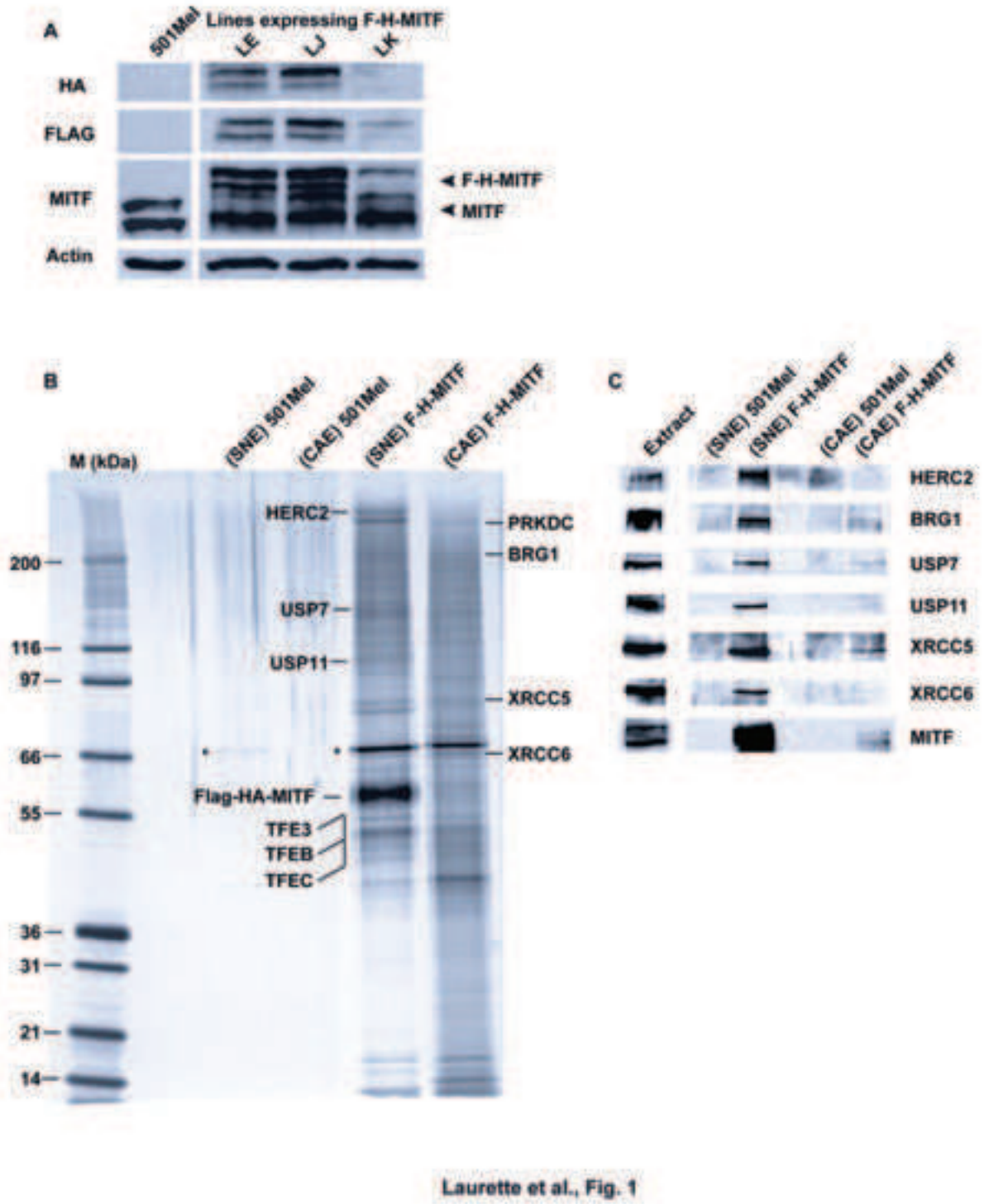

Laurette et al., Fig. 1

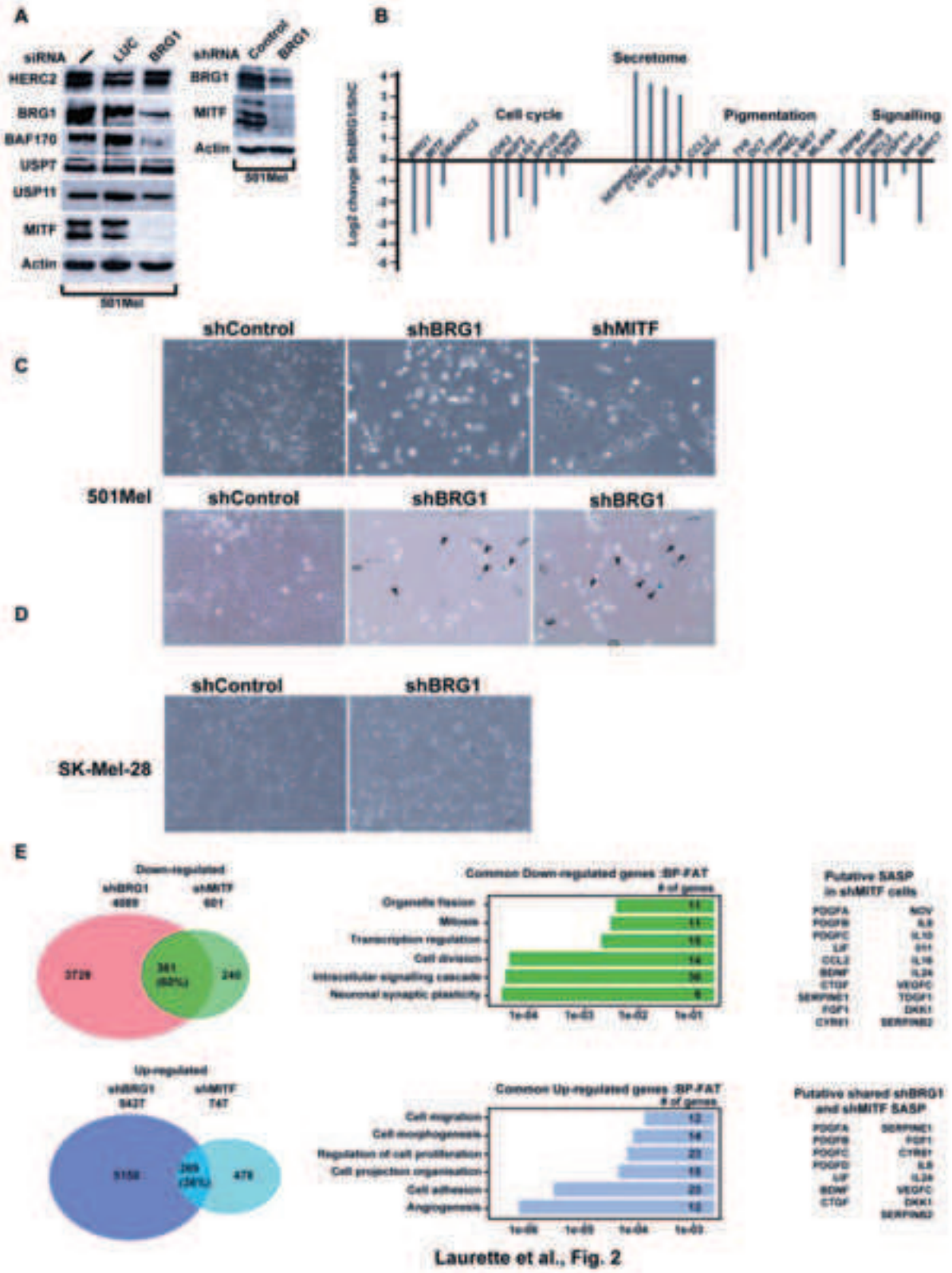

Laurette et al., Fig. 2

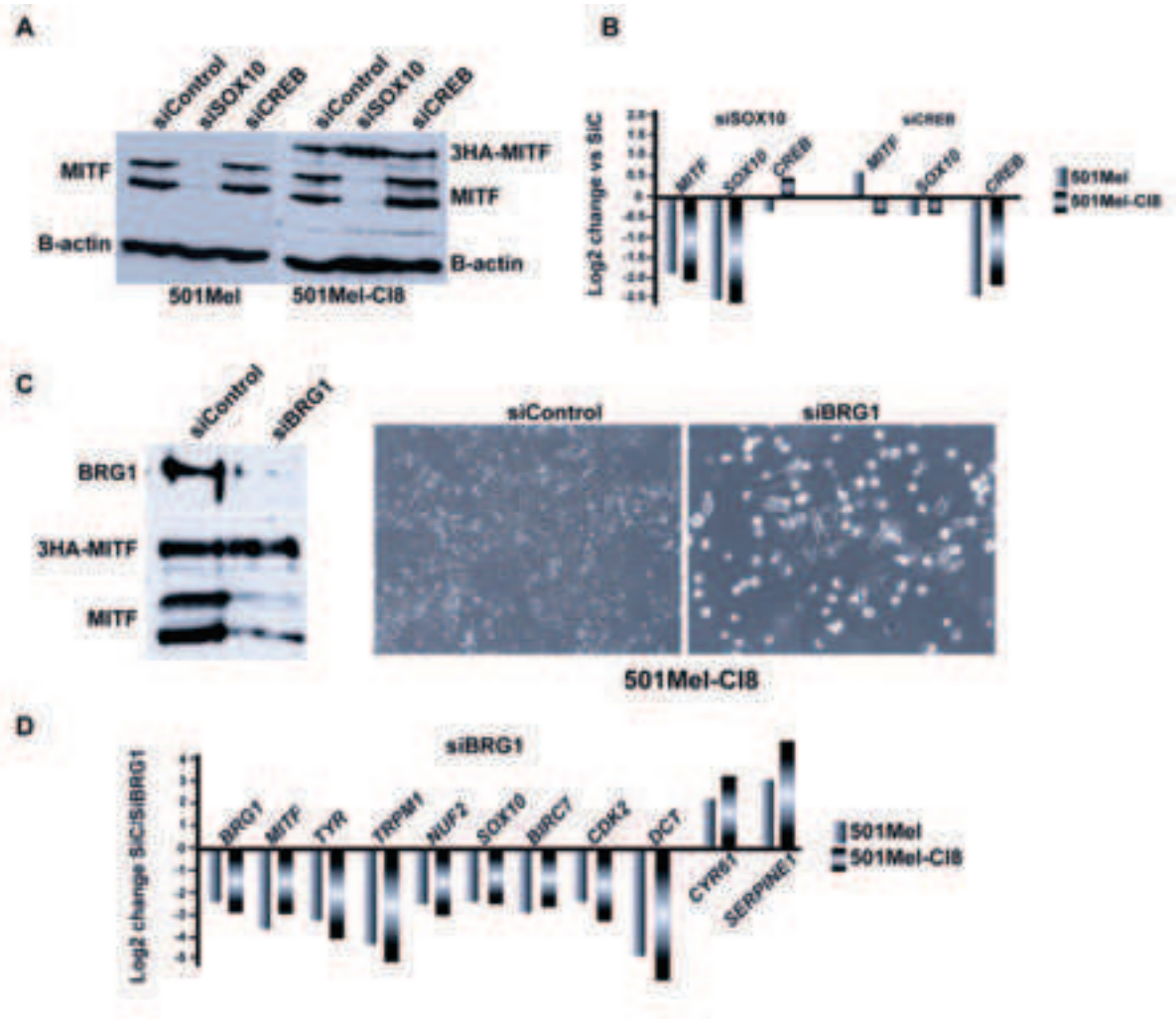

Laurette et al., Fig. 3

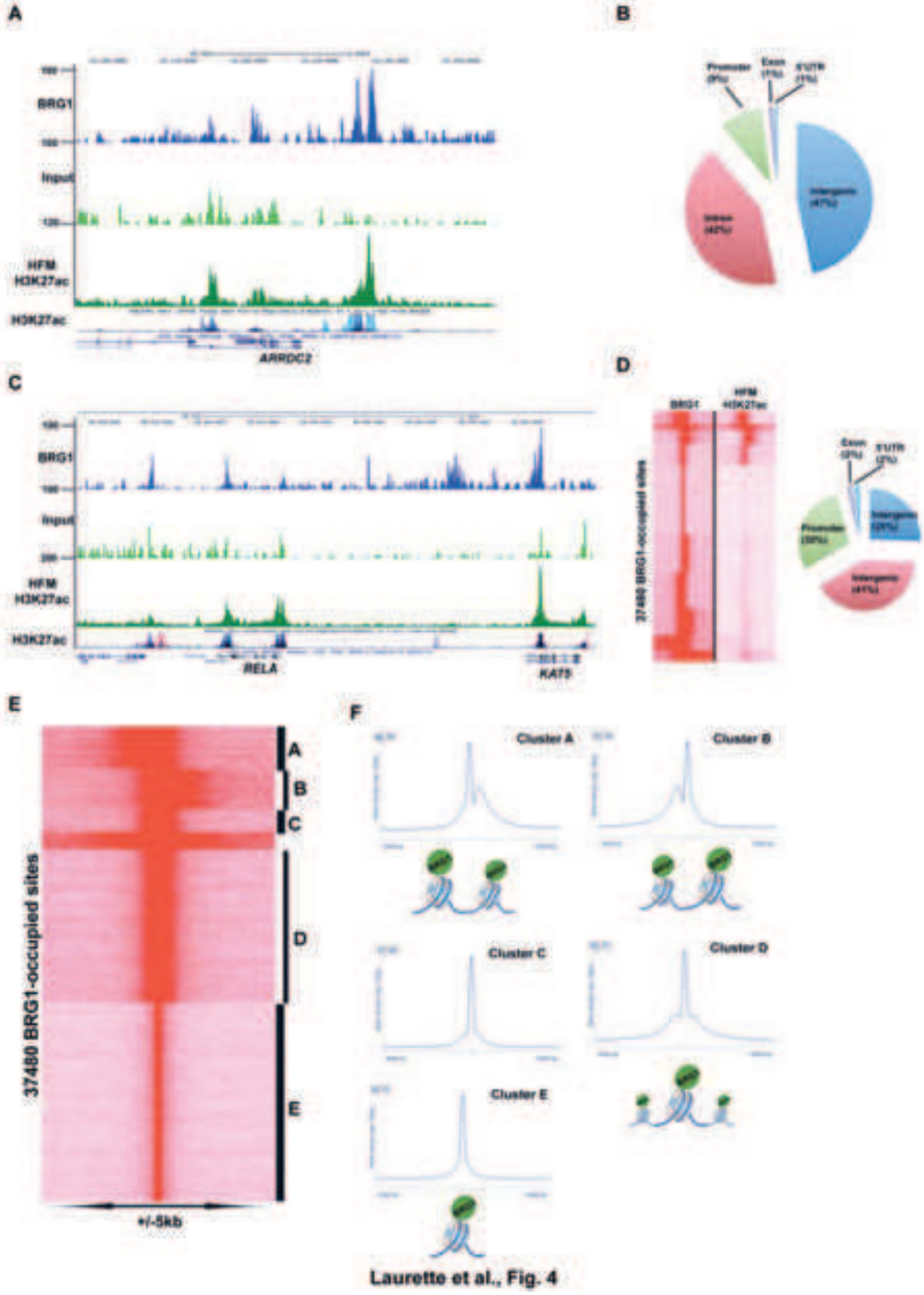

Laurette et al., Fig. 4

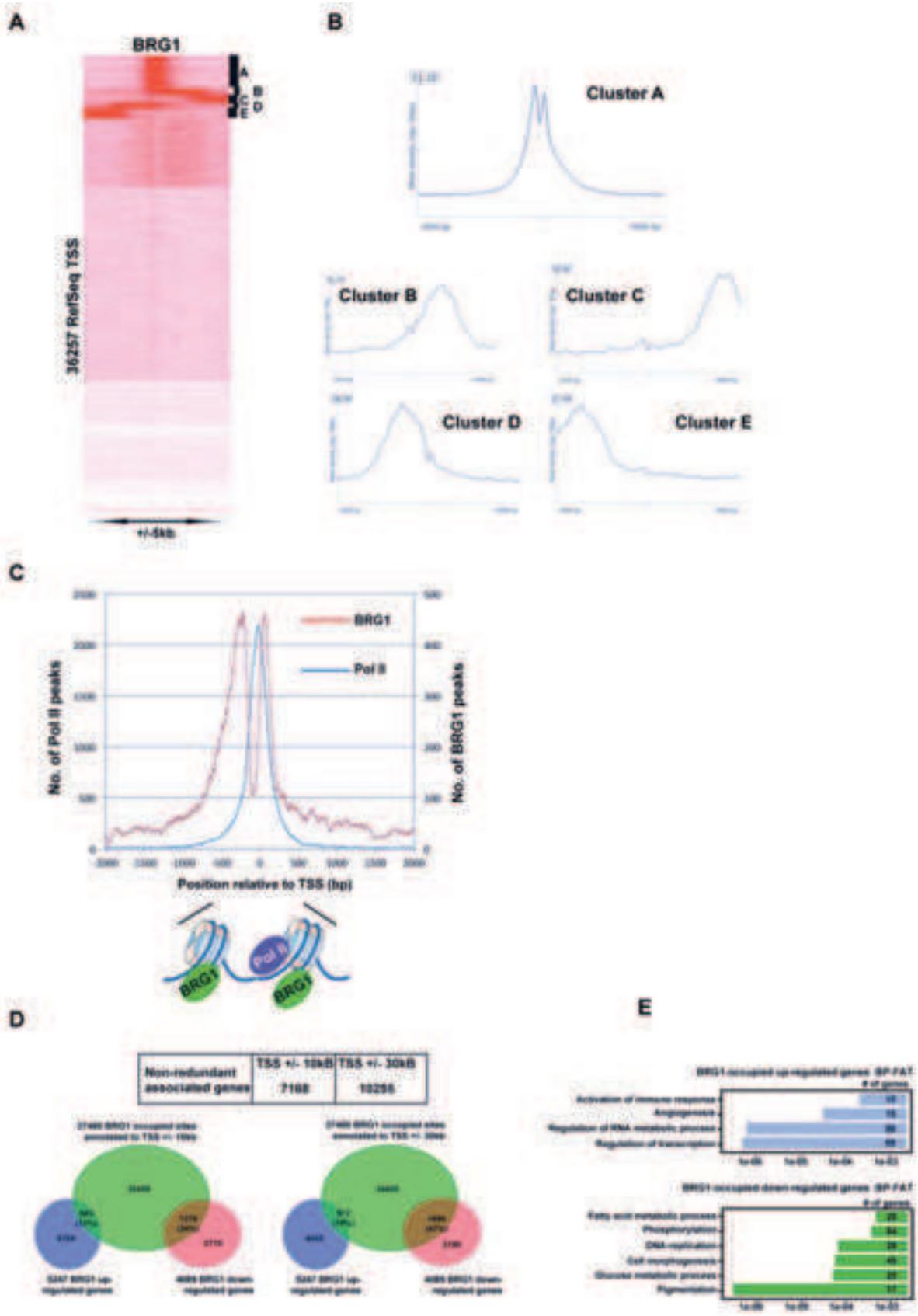

Laurette et al., Figure 5

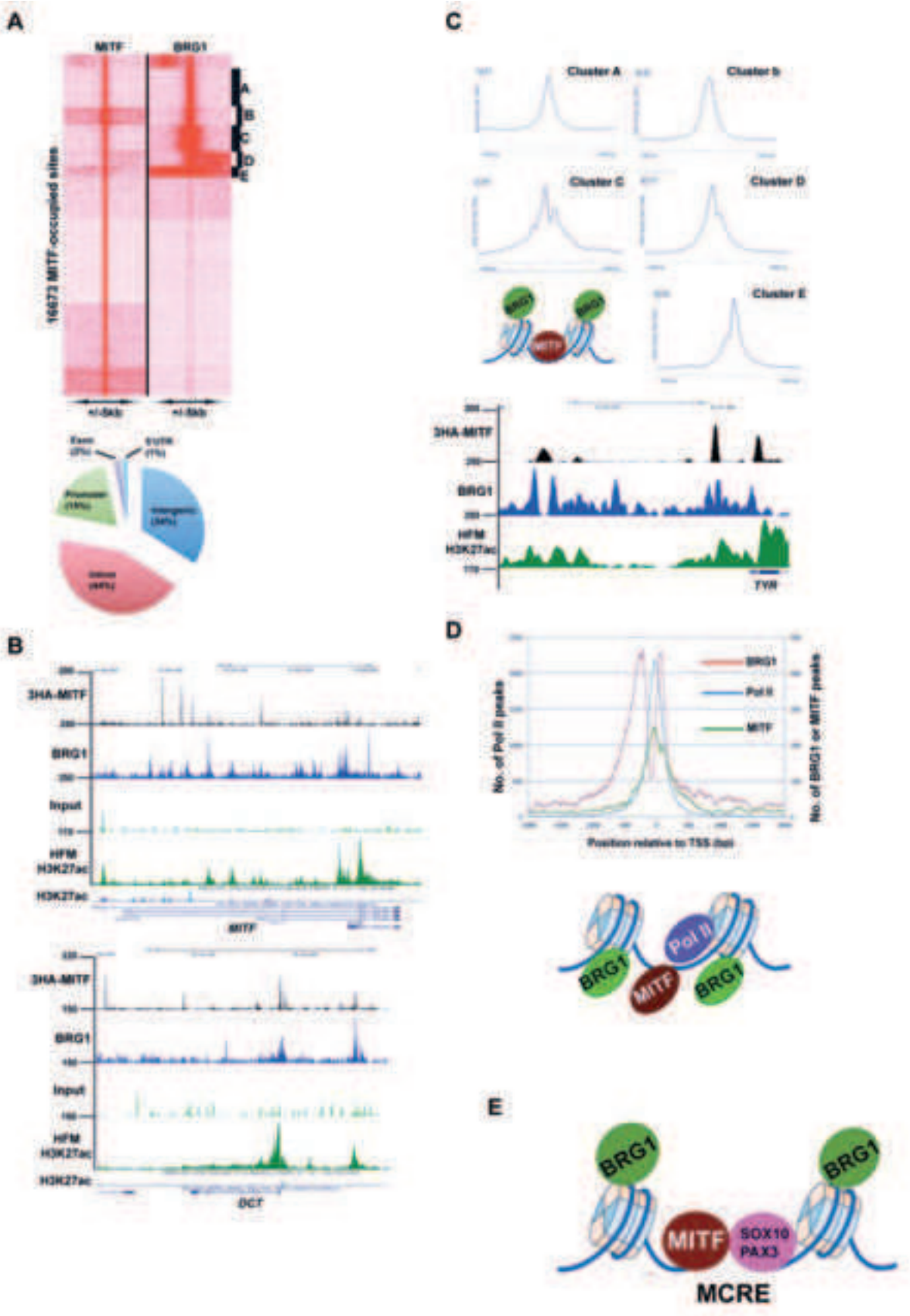

Laurette et al., Fig. 6

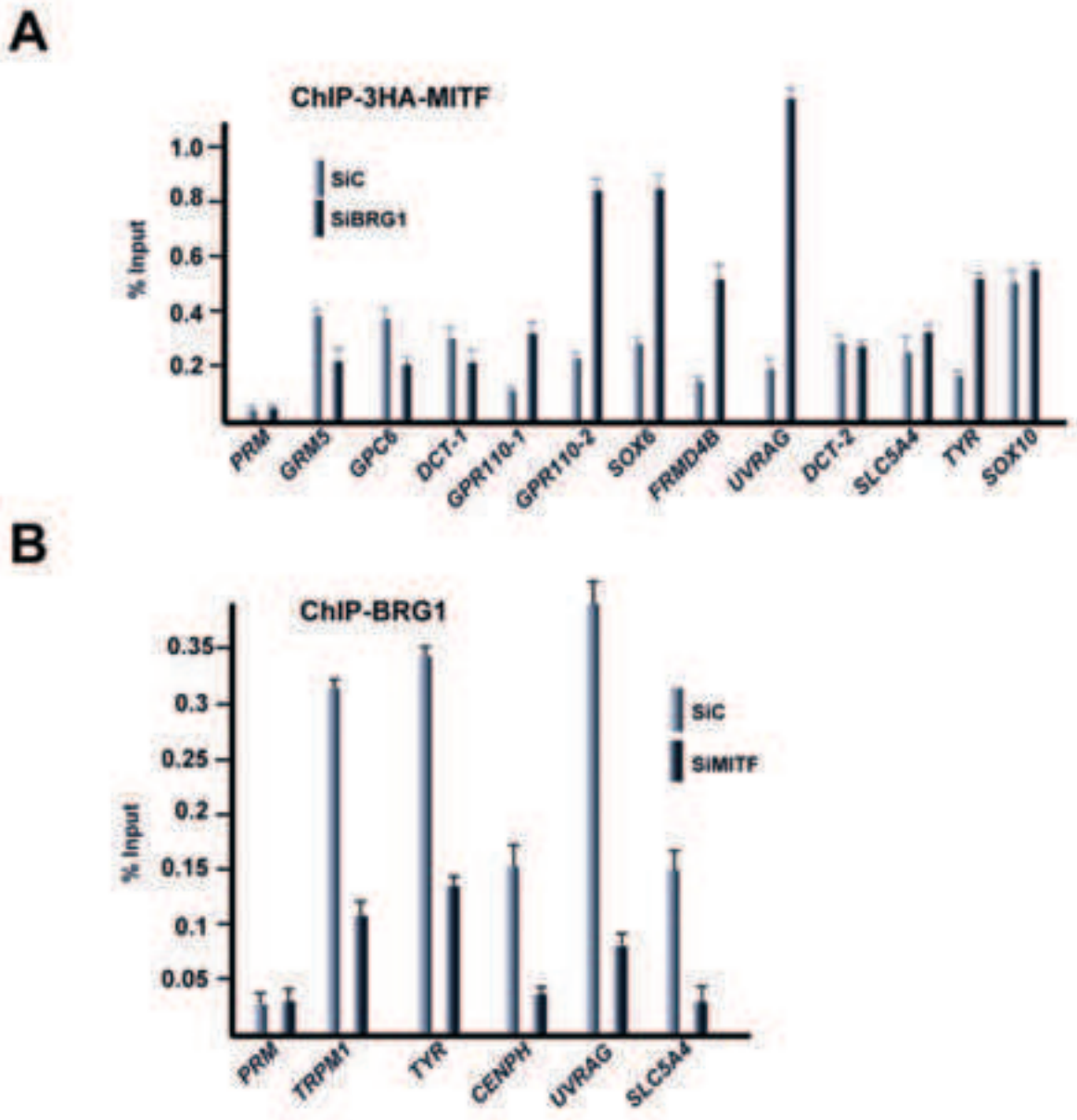

Laurette et al., Fig. 7

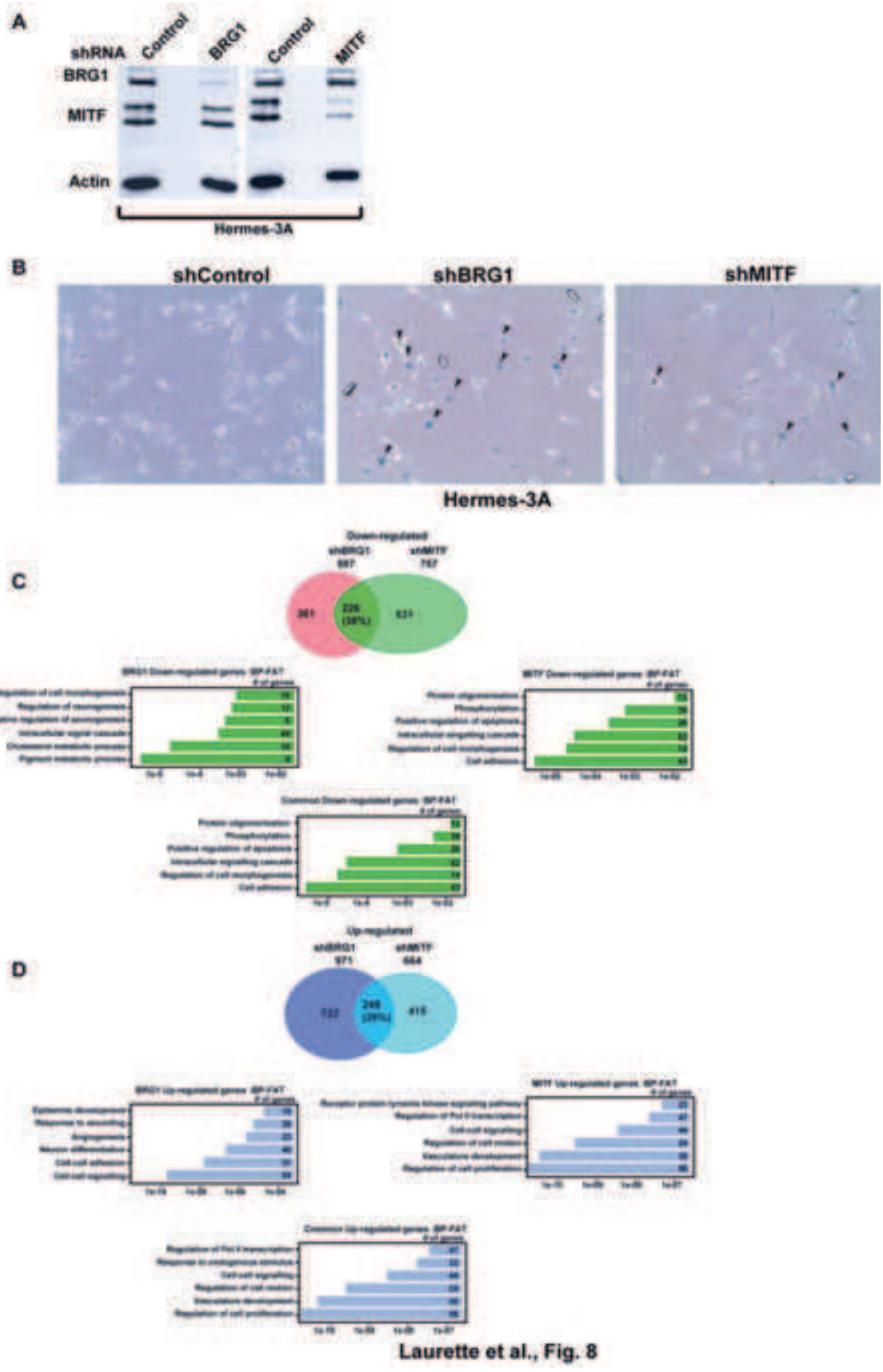

Laurette et al., Fig. 8

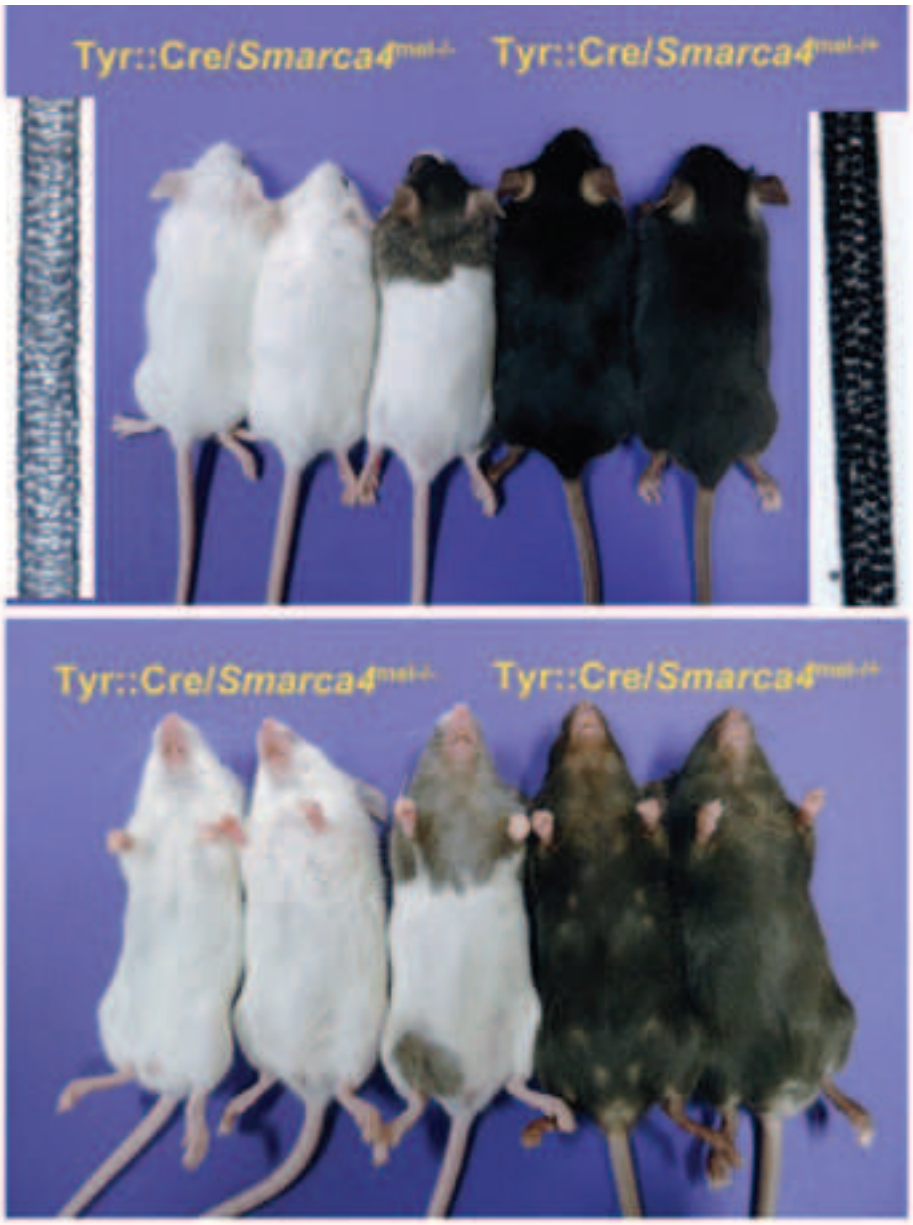

Tyr::Cre/*Smarca4*$^{Lox/+}$ X Tyr::Cre/*Smarca4*$^{Lox/+}$

		♀	♂
Tyr::Cre/*Smarca4*$^{Lox/lox}$ 27/124 (22%)	Spotted	5	4
	White	9	6
	Black	3	0
	Total	65	59

Laurette et al., Figure 9

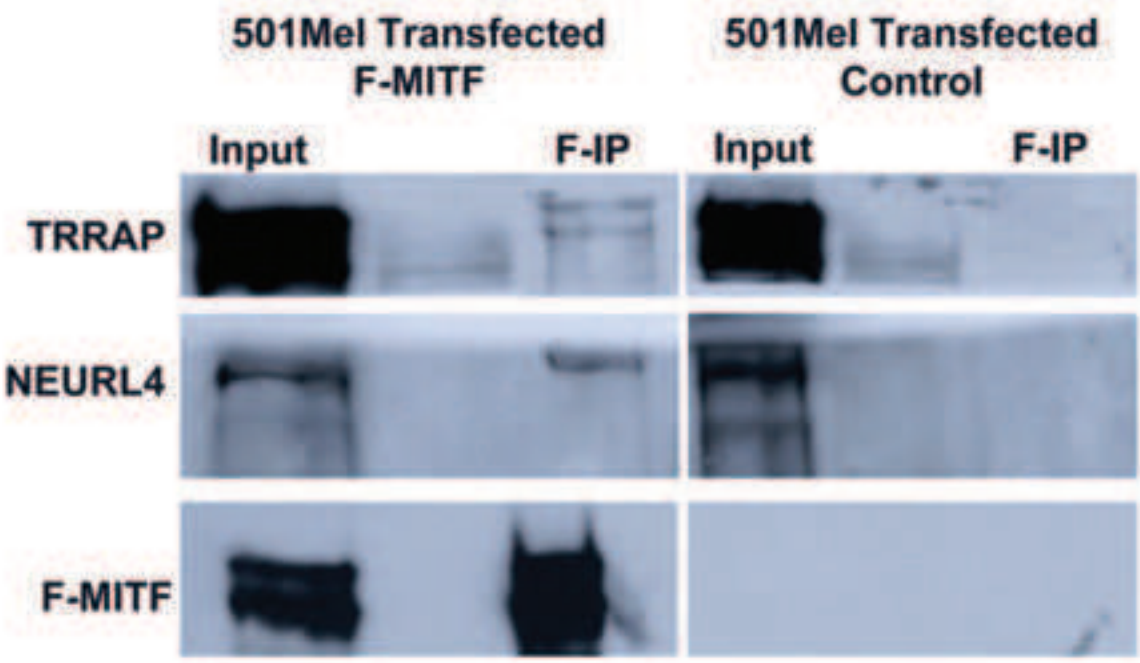

Laurette et al., Supplementary Fig. 1

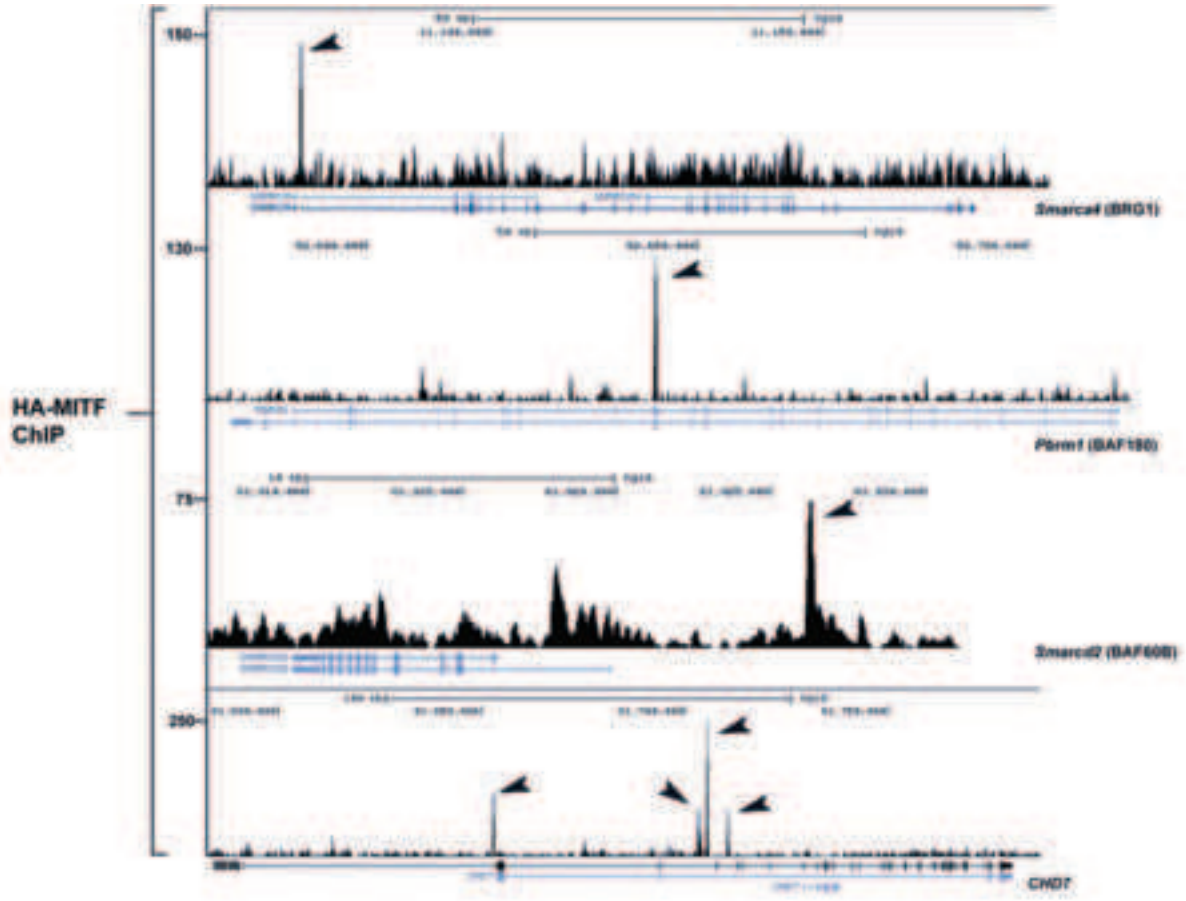

Laurette et al., Supplementary Fig. 2

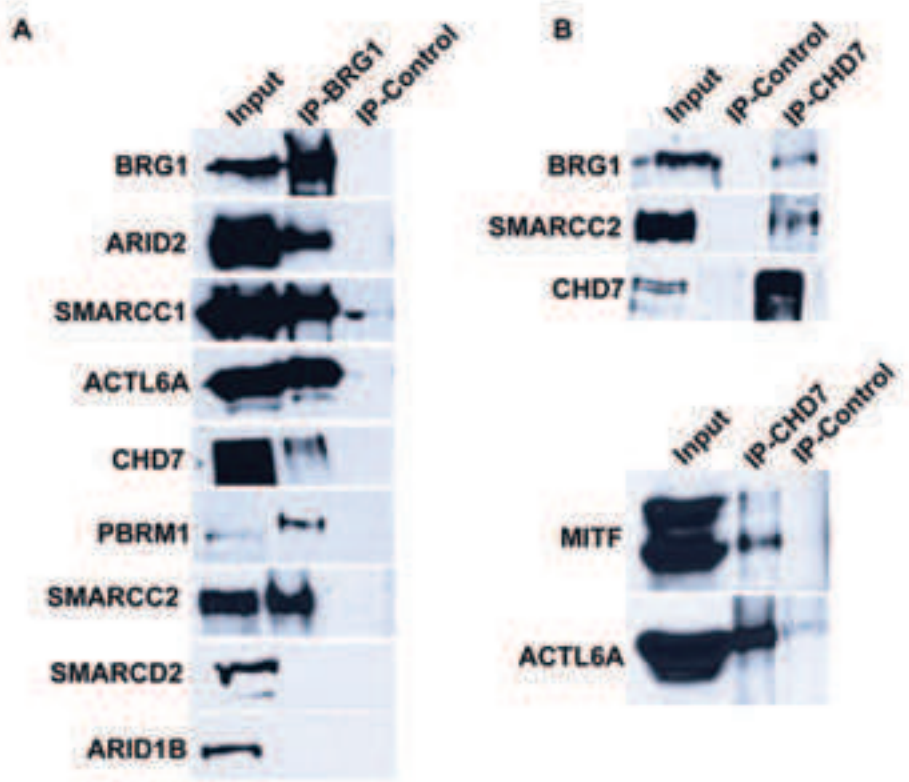

C

Catalytic subunits	Common subunits	Specific subunits	MITF-interacting complex
BRG1	BAF170	ARID1A/B	
BRM	BAF155	ARID2	
CHD7	BAF60A/B/C	BAF180/PBRM1	
	BAF57		
	ACTL6A/BAF53A		
	BAF47		

Laurette et al., Suppplemental Fig. 3

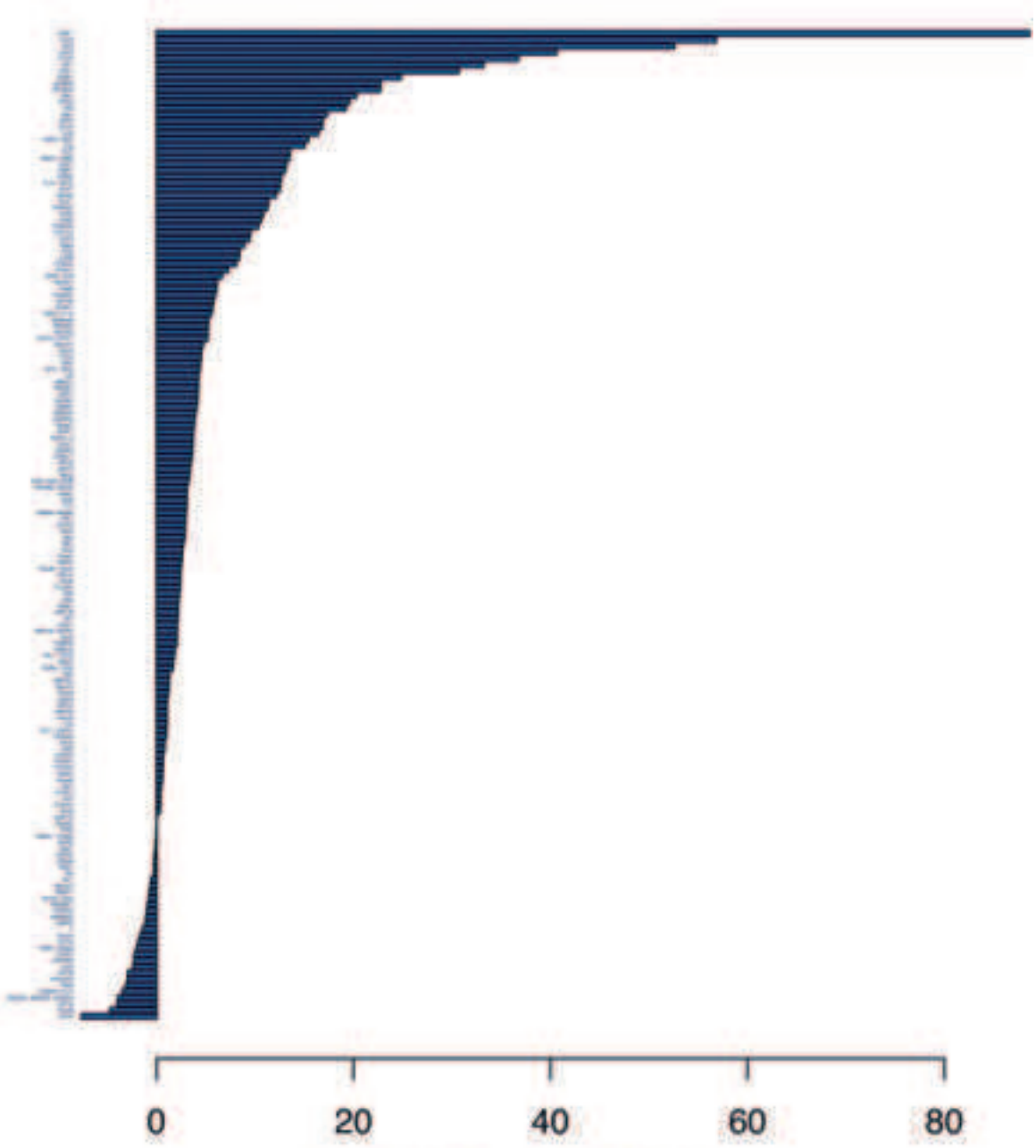

Laurette et al., Supppiemental Fig. 4

A

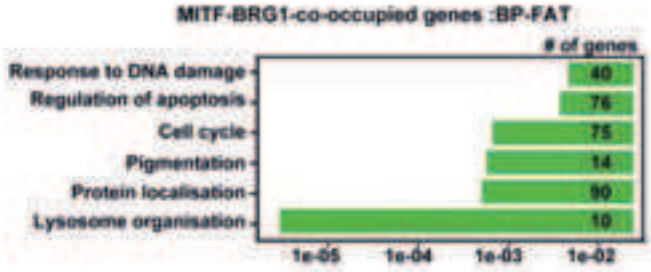

B

Motif	Number of sites (out of 4502)	E-value	Consensus	Other known binders
Ebox/Mitfa	923	5.2e-218		
	736	1.1e-022		
PAX5	12	1.5e-049		PAX3 ?
topoisomerase II binding consensus motif.. also part of ALU	Szilagyi et al. JBC 2013		GCAGGCTGG	potential transcription factor (including C/EBPalp, HNF-3, Hb.YY1, and AP-2alpha) binding sites
SOX10	1116	5.9e-10		
Unknown	68	4.2e-009		
Unknown	357	3.8e-006		
CREB/JUN/JUND	94	2.3e-004		
ETS-1	334	2.1e-003		

Laurette et al., Supplemental Fig. 5

Proteins/Complexes		Subunits
MITF/TFE family		MITF, TFE3, TFEB, TFEC
Co-activator		CTNNB1
Chromatin remodelling and modification complexes	BRG1	SMARCA4 (BRG1), PBRM1 (BAF180), SMARCC2 (BAF170), SMARCD2 (BAF60b), ACTL6A (BAF53a), CHD7
	NURF	BPTF, SMARCA1 (SNF2L) SMARCA5 (SNF2H) RBBP4
	HAT?	TRRAP, RUVBL1, RUVBL2, ACTL6A (BAF53a)
DNA damage		HERC2, UBR5, PRKDC, XRCC5, XRCC6, MSH2, MSH6, BRCA2
Ubiquitin cycle		HERC2, NEURL4, UBR5, USP7, USP11
Transcription RNA Pol III	TFIIIC	GTF3C1, GTF3C2, GTF3C3, GTF3C4
Cohesin		SMC1A, SMC3, PDS5, STAG2
Repressor		TRIM28, TRIM33, TRIM24, HDAC1, HDAC2, CBX1, CBX3, CBX4
DNA replication	MCM	MCM3, MCM5, MCM7
	RFC	RFC1, RFC2, RFC4, RFC5
Kinase signalling		AKAP8, AKAP8L, PLK1
Nuclear pore complex		KPNB1, NUP153, XPO1, NUP50, NPM1, NOP14, TNPO1, KPNA1, KPNA4, XPO5

Laurette et al., Table 1

Article 2 : **The BPTF subunit of the NURF chromatin-remodeling complex interacts with MITF and is essential for normal function of murine melanocyte stem cells.**

The BPTF subunit of the NURF chromatin-remodeling complex interacts with MITF and is essential for normal function of murine melanocyte stem cells.

Dana Koludrovic, Thomas Strub1, Patrick Laurette, Céline Keime, Gabrielle Mengus, and Irwin Davidson#

Department of Functional Genomics and Cancer, Institut de Génétique et de Biologie Moléculaire et Cellulaire, CNRS/INSERM/ULP, 1 Rue Laurent Fries, 67404 Illkirch Cédex, France.
1. Address

To whom correspondence should be addressed:
E mail : irwin@igbmc.fr
Running Title : BPTF interacts with MITF.
Key words; chromatin remodeling, DCT, BRG1, melanoma, pigmentation
The authors declare no competing conflict of interest.

Abstract

MIcrophthalmia-associated Transcription Factor (MITF) plays an essential role in transcription regulation in melanocytes and in melanoma. To understand how MITF regulates transcription, we used tandem affinity purification and mass-spectrometry to identify potential MITF cofactors. Here we show that the BPTF, SNF2H, SNF2L, and RBBP4 subunits of the chromatin-remodelling factor NURF are associated with MITF on the chromatin of 501mel melanoma cells. ShRNA-mediated BPTF silencing revealed that it plays a specific and essential role in the proliferation of several melanoma cell lines as well as Hermes-3A melanocytes in vitro. Comparative RNA-seq upon silencing of MITF and BPTF shows that these two factors regulate an overlapping gene expression programs in 501Mel and Hermes 3A cells. We further show that Bptf plays a critical role in melanocyte stem cells (MSCs) in vivo. Somatic inactivation of Bptf in the melanocyte lineage has only a mild effect during

embryogenesis, but results in an inability to pigment hair from the second post-natal anagen phase where differentiated melanocytes are derived from the MSC population. Nevertheless, the MSC population persists in Bptf-mutant adult white mice showing that Bptf is required not for the survival of the MSCs, but for their ability to proliferate and/or differentiate in response to signals in the anagen phase. Inactivation of Bptf therefore gives rise to a unique phenotype of premature hair greying.

Introduction

MIcrophthalmia-associated Transcription Factor (MITF) is a basic helix-loop-helix leucine zipper (bHLH-Zip) factor that plays an essential role in the differentiation, survival, and proliferation of normal melanocytes, and in controlling the properties of melanoma cells (Goding, 2000; Hoek, 2011; Steingrimsson et al., 2004; Widlund and Fisher, 2003). Murine melanocyte stem cells (MSCs) residing in the bulge region of the hair follicle do not express MITF, but its expression is induced when these cells are induced to proliferate during anagen to generate the transit amplifying cells (TACs) (Lin and Fisher, 2007; Nishimura, 2011; Osawa et al., 2005). MITF expression is further increased as these TACs migrate towards the bulb to form terminally differentiated melanin producing melanocytes (Robinson and Fisher, 2009; White and Zon, 2008).

Following malignant transformation, MITF expression is characteristic of proliferative melanoma cells, while cells expressing low or no MITF are slow cycling and invasive and display enhanced tumour initiating properties (Hoek and Goding, 2010). MITF silencing in proliferative melanoma cells or immortalised melanocytes leads to leads to cell cycle arrest and entry into senescence (Giuliano et al., 2011; Strub et al., 2011). These observations gave rise to the proposed 'rheostat' model where the level of functional MITF expression determines many biological properties of melanocytes and melanoma cells (Carreira et al., 2006; Goding and Meyskens, 2006); low or no MITF gives rise to MSCs or slow cycling melanoma cells, higher levels to proliferative TACs and proliferative melanoma cells and high levels terminally differentiated melanocytes. This property has been exploited to derive drugs that induce terminal differentiation of melanoma cells as a therapy for melanoma (Saez-Ayala et al., 2013).

MITF is both an activator and a repressor of transcription, and does not function by itself, but rather in conjunction with a host of cofactors (Laurette, 2014). We have previously reported a comprehensive analysis of the MITF 'interactome' by tandem affinity purification and mass-spectrometry in 501Mel melanoma cells (Laurette, 2014). This analysis identified two

chromatin-remodelling complexes, a complex comprising BRG1-CHD7 and NURF (Nucleosome Remodelling Factor), interacting with MITF. We showed the MITF recruits BRG1 to >6000 sites the 501Mel genome to regulate gene expression and that BRG1 is essential for proliferation of melanoma cells and melanocytes in vitro. Moreover, selective inactivation of BRG1 in the melanocyte lineage in vivo gives rise to white mice. BRG1 is therefore essential in the melanocyte lineage in vitro and in vivo.

The NURF chromatin-remodelling complex was first identified in Drosophila Melanogaster (Tsukiyama et al., 1995; Tsukiyama and Wu, 1995) and shown to comprise the IWSI-related SNF2L (SMARCA1) ATPase subunit as well as NURF301 (BPTF, Bromodomain, PHD-finger Transcription Factor), NURF55 (RbAp46, RBBP7) and NURF38 (Alkhatib and Landry, 2011; Mizuguchi et al., 1997; Mizuguchi and Wu, 1999; Wysocka et al., 2006). NURF promotes ATP dependent nucleosome sliding and transcription from chromatin templates in vitro (Hamiche et al., 2001; Kang et al., 2002; Xiao et al., 2001). An analogous complex comprising BPTF and SNF2L has also been characterised in human cells and may further comprise the SNF2H (SMARCA5) ATPase subunit as well as RbAp48 (RBBP4), BAP18 and HMG2L1 (Barak et al., 2003; Vermeulen et al., 2010). The 450 kDa BPTF is the defining subunit of NURF. It has been shown to bind to active promoters via the interaction of its PHD domain with trimethylated H3K4 and of its bromodomain with acetylated H4K16 (Li et al., 2006; Ruthenburg et al., 2011; Wysocka et al., 2006).

Despite extensive characterisation of the biochemical properties of NURF and BPTF (Badenhorst et al., 2002), much less is known about their biological functions in mammals. Inactivation of Bptf in mouse leads to embryonic lethality shortly after implantation where it is required for establishment of functional distal visceral endoderm and the ectoplacental cone (Landry et al., 2008). Gastrulation is initiated, but no complete anteroposterior axis of the epiblast appears (Goller et al., 2008). Consequently, it is possible to isolate Bptf-/- ES cells that are viable, but are unable to differentiate into mesoderm, endoderm, and ectoderm tissue lineages (Landry et al., 2008). Somatic inactivation has shown that Bptf is required for thymocyte maturation (Landry et al., 2011). Furthermore, BPTF may also be involved in regulating differentiation of human epidermal keratinocyte stem cells in vitro (Mulder et al., 2012). BPTF therefore acts in multiple tissues and pathway to regulate a variety of differentiation programmes.

The observation that NURF interacts with MITF prompted us to investigate its role in melanoma cells and in the melanocyte lineage. We show that BPTF is essential for the

proliferation of melanoma cells and melanocytes in vitro. Selective inactivation of Bptf in developing melanocytes (Bptfmel-/-) in vivo results in a unique phenotype, where mice are born with close to normal pigmentation, but are unable to pigment the hair produced by the first post-natal anagen resulting in rapid loss of pigmentation and a lasting white pelage. Contrary to previous models where premature post-natal greying results from loss of the MSCs, in Bptfmel-/- mice the stem cell population persists throughout the life of the animal, but is unable to respond to the proliferative signals in anagen. These data show a selective role of Bptf in the generation of functional MSCs.

Results

MITF associates with NURF.

We previously described the use of 501Mel cell lines stably expressing an N-terminal FLAG-HA epitope tagged MITF to perform tandem affinity purification of the soluble nuclear and chromatin associated fractions (Figure 1A). Amongst the proteins identified in this assay were the BPTF, SMARCA5, SMARCA1 and RBBP4 subunits of NURF. Multiple peptides for these proteins were detected in the chromatin associated fraction from the cells expressing tagged MITF, whereas no peptides for these factors were found in the immunoprecipitations from the control extract (Figure 1B). Interaction of these NURF components with MITF was confirmed in western blot experiments showing that BPTF, SMARCA1 and SMARCA5 all specifically precipitated with tagged, but not native MITF uniquely in the chromatin-associated fraction (Figure 1C). MITF therefore specifically associates with the NURF complex on chromatin from 501Mel cells. Interestingly, the genes encoding several of the subunits of NURF are associated with MITF occupied sites in 510Mel cells including BPTF where MITF is bound to an M-box in the proximal promoter (Supplemental Figure 1). This suggests that their expression is subject to a specific MITF-regulation in the melanocyte lineage.

BPTF is selectively required for proliferation of melanoma cells.

To address the function of BPTF in 501Mel cells, we performed both siRNA and shRNA knockdown experiments (Figure 2A). SiBPTF led to arrested proliferation and morphological changes in 501Mel cells similar to what is observed following siRNA silencing of MITF (Figure 2B). In both cases, cells showed an enlarged and flattened morphology with extensive cytoplasmic projections. Similar results were observed following infection with lentiviral

vectors expressing two different shRNAs directed against BPTF (Figure 2A). 5 days after infection and selection, cells showed slow growth (Figure 2C) and marked morphological changes analogous to those seen with the siBPTF silencing and shRNA-mediated MITF silencing (Figure 2D). These morphological changes are characteristic of those observed when 501Mel cells enter senescence and up to 90% of shBPTF or shMITF silenced cells showed staining for senescence-associated β-galactosidase (Figure 2E). BPTF is thus essential for 501Mel cell proliferation.

Analogous results were observed in several other MITF-expressing melanoma cell lines. ShRNA-mediated BPTF silencing in SK-Mel-28 cells led to slow growth and marked morphological changes (Supplemental Figure 2A-C). In MNT cells, shBPTF silencing led to proliferation arrest and a spindle-like bipolar morphology (Supplemental Figure 2B and C), while in 888-Mel cells, BPTF knockdown led to extensive cell death, with surviving cells again showing a spindle-like bipolar morphology (Supplemental Figure 2D). We also investigated BPTF function in MITF-negative 1205lu cells. In this line also, BPTF silencing arrested growth and induced an enlarged flattened and more rounded morphology suggestive of senescence (Supplemental Figure 3A and B). On the other hand, shMITF silencing had no effect on these cells consistent with the fact that they do not express MITF (Supplemental Figure 3B). In contrast to the above, shBPTF silencing in a variety of non-melanoma cells such as HeLa, HEK293T, as well as BJ and WI38 fibroblasts had no major effect on either proliferation or morphology (Supplemental Figure 2E-G). These observations show that BPTF plays a selective and essential role in the proliferation of melanoma cells that is not seen under the same conditions in non-melanoma cells. Moreover, as BPTF is essential in 1205Lu cells, it may play both MITF-dependent and independent functions in melanoma.

We also investigated the role of the SMARCA1 and SMARCA5 subunits of NURF in 501Mel cells. Lentiviral mediated knockdown of these subunits both led to a potent arrest of proliferation (Supplemental Figure 4). While the SMARCA1-knockdown cells did not show a strong change in their morphology, the SMARCA5-knockdown cells showed many of the changes seen upon loss of MITF and BPTF.

BPTF and MITF regulate overlapping gene expression programmes controlling 501mel cell proliferation.

To better understand the overlapping phenotypes of BPTF and MITF silencing in 501Mel cells, we performed RNA-seq following shRNA-mediated silencing to identify the de-

regulated genes and then compared the two data sets. Following BPTF knockdown, 494 genes were down-regulated (Figure 3A and B) that were enriched in ontology terms associated with regulation of transcription, response to stress and cell cycle (Figure 3C and Supplemental Dataset 1). 593 genes were down-regulated by MITF knockdown. These are strongly enriched in terms associated with cell cycle, in particular mitosis, consistent with our previous observations that MITF silencing leads to severe mitotic defects (Laurette, 2014; Strub et al., 2011). Comparison of the two data sets identified 191 common repressed genes that are enriched in those involved in transcription regulation, stress response and cell cycle (Figure 3B and C and Supplemental Dataset 1). Thus, 39% of genes down-regulated by BPTF silencing were also down-regulated by MITF silencing indicating a significant overlap between the programmes regulated by each factor.

Following BPTF knockdown, 669 genes were up-regulated (Figure 3A and B and Supplemental Dataset 1) and were enriched in ontology terms associated with cell adhesion, morphology and migration as well as a large set of secreted cytokines and growth factors that constitute the senescence associated secreted phenotype (SASP). 748 genes were up-regulated by MITF knockdown that are strongly enriched in terms analogous the those of BPTF including an extensive SASP (Laurette, 2014; Strub et al., 2011). Comparison of the two data sets identified 278 common induced genes, with 41 % of genes up-regulated by BPTF silencing also induced by MITF knockdown. Consistent with the very similar morphological changes, the common regulated genes included many involved in morphology, adhesion as well as the SASP.

These data show a large overlap between the gene expression programmes controlled by BPTF and MITF. Together these two factors positively regulate genes required for proliferation and negatively regulate genes involved in cell morphology. These data account for the cell cycle defects and entry into senescence with a highly overlapping SASP. Interestingly, none of the genes significantly repressed by MITF knockdown were activated by BPTF knockdown and only 8 of the genes repressed by BPTF knockdown, were activated by MITF knockdown.

To identify genes that are potentially directly regulated by MITF and BPTF, we first determined which up and down-regulated genes are associated with MITF-occupied sites. As described (Laurette, 2014; Strub et al., 2011), MITF occupies >16000 sites in 510Mel cells. Using a window of +/-10kb with respect to the TSS, 3467 potential target genes could be identified, while a larger +/-30kb window, identified up to 5694 potential targets (Figure 3D).

Depending on the window, between 114 and 176 genes appear to be directly activated by MITF. Amongst these genes are several critical regulators of the cell cycle such as CCND1 and CIT that account for the arrested proliferation and aberrant mitosis of the shMITF knockdown cells (Supplemental Dataset 2). Of these 34 and 56 are co-regulated by BPTF, including BIRC7 and BCL2A1 critical regulators of proliferation and apoptosis and survival and NPM1 an important cell cycle regulator involved in chromosome congression, spindle and kinetochore-microtubule formation required for normal centrosome function (Okuwaki, 2008; Vogler, 2012) (Supplemental Dataset 2). Similarly, between 117 and 187 genes appear to be repressed by MITF including several SASP components such as SERPINE1, IL24, and PDGFB. Of these 37 and 67 are co-regulated by BPTF. These subfamilies of genes therefore constitute the potential targets that are directly regulated by the cooperative action of MITF and BPTF.

BPTF and MITF regulate proliferation of Hermes 3A melanocytes.

The above results show that BPTF is required for proliferation of several melanoma cell lines and that in 501mel cells MITF and BPTF co-regulate genes involved in proliferation and cell morphology. To address the role of BPTF in untransformed melanocytes, we performed shBPTF silencing in Hermes 3A cells.

As previously shown, MITF silencing in these cells led to proliferation arrest, morphological changes and entry into senescence [(Laurette, 2014) and Figure 4A and B]. BPTF knockdown in these cells also arrested their proliferation, but the cells had less flattened morphology compared to MITF (Figure 4B and C). RNA-seq showed that BPTF silencing repressed 1356 genes and up-regulated 1139 genes (Figure 4D, Supplemental Dataset 3). The effects of BPTF loss on gene expression were therefore more extensive in these cells than in 501mel. The down-regulated genes are strongly enriched in those involved in cell cycle and pigmentation (Figure 4D). BPTF is therefore a major regulator of genes required for proliferation of Hermes 3A cells. The up-regulated genes on the other hand are involved in transcription regulation, cell adhesion and morphology, again consistent with the changed morphology of the knockdown cells.

A significant overlap between the gene expression programmes regulated by BPTF and MITF. 44% of genes down-regulated by MITF knockdown were also down-regulated by that of BPTF, while the same was observed for 37% of genes up-regulated by MITF silencing (Figure 4C). The common down-regulated genes are enriched in those involved in cell

cycle/mitosis, cell adhesion and apoptosis (Figure 4E and F). For example several critical regulators of cell cycle and mitosis such as AURKB, CDCA2 and CCND1 are repressed under both conditions accounting for the arrest of proliferation. On the other hand a plethora of signalling molecules and transcriptional regulators are up-regulated. It is noteworthy that silencing of BPTF and MITF in Hermes-3A cells does not give rise to an extensive SASP as found in 501Mel cells.

We also compared genes that are regulated by MITF and BPTF in both 501Mel and Hermes 3A cells. The transcriptional programmes regulated by MITF in 501Mel and Hermes3A cells are somewhat different as only 172 genes (22%) are down-regulated in both lines (Supplemental Figure 5 and Supplemental Dataset 4). Similarly, only 130 genes (19%) are up-regulated in both lines. Nevertheless, the common down-regulated genes comprise regulators of cell cycle and mitosis defining a critical set of MITF-regulated cell cycle genes and up-regulated genes are principally involved in signalling and cell motion/morphogenesis. An analogous comparison of BPTF regulated genes showed that 46% of genes down-regulated in 501Mel cells are also diminished in Hermes 3A, while the same is true for 34% of the genes up-regulated in 501Mel. As with MITF, the common down-regulated genes comprise critical regulators of cell cycle and up-regulated genes comprise genes involved in signalling and cell motion/morphogenesis (Supplemental Figure 5 and Supplemental Dataset 4).

Bptf is dispensable for establishment of the melanocyte lineage.

The above data define an essential role of BPTF in the regulation of genes required for the proliferation of melanoma and melanocytes cell in vitro. This prompted us to investigate the role that BPTF may play in the melanocyte lineage in vivo. We crossed mice with a floxed Bptf gene (Bptflox/lox) with those expressing Cre recombinase under the control of the Tyrosinase enhancer that allows selective inactivation in the developing melanocyte lineage (Delmas et al., 2003). The resulting Bptflox/lox::Tyr-Cre mice were further crossed with animals expressing the LacZ marker gene under the control of the Dct promoter that can be used as a tracer for the melanocyte lineage (Bptflox/lox::Tyr-Cre::Dct-LacZ).

In crosses of Bptflox/lox::Tyr-Cre and Bptflox/+::Tyr-Cre mice, animals lacking Bptf in the melanocyte lineage (Bptfmel-/-) were born at Mendelian frequency (Figure 5A) and by P10 displayed only a mild pigmentation phenotype characterised by a grey belly, and grey extremities of the paws, ears and tail compared to wild-type mice and the Bptflox/+::Tyr-Cre

littermates (Figure 5B, and Supplemental Figure 6A-B). This phenotype was confirmed upon growth of the first hair at P14 that was grey on the belly with a small and variable white belly spot (Figure 5C and Supplemental Figure 6C). Otherwise, the dorsal coat is almost indistinguishable from wild-type. Bptf therefore does not play an essential role in the establishment of the melanocyte lineage, but influences melanoblast proliferation and or migration.

To better characterise this phenotype, we used the Bptflox/lox::Tyr-Cre::Dct-LacZ mice to monitor melanoblast development. The number of Dct-LacZ positive melanoblasts was counted at E15.5 on the paws and the bellies of 4 mice of each genotype. While the front of migration on the belly and the paws was similar in the Bptflox/lox and Bptflox/+ genotypes and no major alterations of melanoblast morphology were observed (Supplemental Figure 7A and B), the number of melanoblasts was reduced by around 10% in the absence of Bptf (Supplemental Figure 7C). By E16.5, clear differences in the ventral and limb migration fronts were observed (Figure 6A). There also appears to be a defect in homing of the melanoblasts to the developing hair follicles. In wild-type, clusters of melanocytes are clearly visible on the trunk that correspond to melanocytes colonising the nascent hair follicles (Jordan and Jackson, 2000) (Figure 6B). Such clusters are less prominent in the Bptflox/lox animals suggesting that the melanoblasts are defective in homing to the hair follicle. Nevertheless, as the number of melanoblasts was now reduced by around 20% in the Bptfmel-/- foetuses (Figure 6C), the diminished prominence of clusters may also be due to the diminished cell numbers. These data show that loss of Bptf does not affect the establishment of the melanocyte lineage, but is required for normal melanoblast proliferation, migration and perhaps homing during embryogenesis. The progressive reduction in their numbers seen during the course of development accounts for the observed greyer phenotype of the first hair coat whose pigmentation is provided by the embryonic derived melanoblasts that colonise the hair follicle (Nishimura, 2011).

Bptf is essential for the normal function of melanocyte stem cells.

As the Bptflox/lox::Tyr-Cre animals grew older however, their coat showed progressive greying such that by 3-6 weeks both the ventral and dorsal coat became grey and then finally white (Figure 5D and Supplemental Figure 6D). The animals then maintained this completely

white coat throughout their lifespan (Figure 5E). This premature greying phenotype could be accelerated by depilation of 3-week animals, following which the newly grown hair was white (Figure 5F). These data show that in absence of Bptf, the mutant animals are unable to pigment the hair from second post-natal anagen that requires the generation of mature melanin producing melanocytes from the post-natal MSC population. This observation suggests that Bptf is required for establishment, maintenance and/or functionality of the MSC population.

To investigate this, we performed immunostaining of hair shafts from the Bptflox/lox and Bptflox/+ genotypes at different post-natal stages using antibodies against Dct that stains the MSC population, Sox10 that labels TACs and mature melanocytes and counterstaining with the cell cycle marker Ki67 that labels proliferating keratinocytes in the bulb (Nishikawa and Osawa, 2005; Nishimura, 2011). Control staining of a section from an adult wild-type mouse indeed showed that Dct stained the mature melanocytes in the bulb of the hair shaft along with the presumptive MSCs in the bulge and the TACs (Figure 7A, schematised in panel B). Staining of dorsal hair shafts from day 7 and 10 animals indicated that equivalent numbers of double Dct-Sox10 stained melanocytes were observed in the bulb region (Figure 7C and D). However at 3 weeks the number of Dct stained cells in the bulb strongly decreased in the Bptflox/lox animals and almost half the shafts were devoid of Dct-stained cells (Figure 7E-F). In 1-year animals, no Dct-stained cells were detected in the bulb (Figure 7G). These results are in accordance with the progressive loss of pigmentation in the mutant animals corresponding to a loss of mature bulb melanocytes.

In previous models, premature greying was associated with a loss of the MSC population (McGill et al., 2002; Schouwey et al., 2007; Schouwey et al., 2009). To determine the fate of the MSC population upon Bptf inactivation, we made sections from the epidermis of the Bptflox/lox::Tyr-Cre::Dct-LacZ and Bptflox/+::Tyr-Cre::Dct-LacZ animals at different ages and stained for the presence of LacZ to visualize the melanocytes. At P10, strong blue LacZ staining could be seen in both the bulge and bulb regions of the hair shafts of the Bptflox/lox and Bptflox/+ genotypes and the presence of melanin was clearly visible (Figure 8A). By six weeks, strong staining for melanin persisted in the Bptflox/+ animals along with the presence of LacZ-stained melanocytes in the both the bulge and bulb regions (Figure 8B). In the Bptflox/lox animals, many shafts devoid of melanin were visible and there was a loss of LacZ-stained melanocytes in the bulb. Strikingly however, even in shafts in which there is no melanin and no LacZ-stained melanocytes in the bulb, LacZ-positive cells were clearly visible in the bulge region. This was reinforced by the staining of 1 year-old animals that were white,

devoid of melanin and LacZ-stained bulb melanocytes, but where LacZ-positive cells remained visible in the bulge region. These results are consistent with the idea that MSCs persist in the Bptf-mutant mice, but are unable to give rise to differentiated pigment producing melanocytes. Bptf is thus required for the function of the MSC population.

Materials and Methods

Mice.

Mice were kept in accordance with the institutional guidelines regarding the care and use of laboratory animals and in accordance with National Animal Care Guidelines (European Commission directive 86/609/CEE; French decree no.87–848). All procedures were approved by the French national ethics committee. Mice with the following genotypes have been described elsewhere: conditional Bptflox/lox (Landry et al., 2008), Tyr::Cre (Delmas et al., 2003) and Dct::LacZ (Mackenzie et al., 1997) Genotyping of F1 offspring was carried out by PCR analysis of genomic tail DNA with primers detailed in the respective publications.

LacZ-staining of embryos and epidermis.

E15.5 and E16.5 embryos and were washed in PBS and fixed in 0.25% gluteraldehyde in PBS for 45 min at +4°C, after which they were washed with PBS for 15 min at +4°C. Next, embryos were incubated with permeabilization solution (0.1M phosphate buffer pH 7.4, 2mM MgCl2, 0.01% sodium deoxycholate, 0.02% NP40) for 30-45 min at room temperature (RT). Staining was performed overnight at 37°C with permeabilization buffer containing 5mM potassium ferricyanide (Sigma), 5mM potassium ferrocyanide (Sigma) and 0.04% X-gal solution (Euromedex). The samples were post-fixed for 3 h in 4% paraformaldehyde at RT and washed in PBS overnight at +4°C. To count embryonic melanoblasts, photos were taken with a Nikon AZ100 Multizoom microscope (Nikon, Tokyo, Japan) and defined regions were analyzed with Photoshop grid counter.

For epidermal samples, skin biopsies at the indicated stages (10 days, 3 weeks, 6 weeks, 1 year) were isolated and cut into small pieces, 4mm x 2mm and were treated with the same protocol as the embryos, with the exceptions of overnight staining at RT and an overnight post-fixation in 4% paraformaldehyde. For further immunohistochemical analysis, samples were dehydrated, embedded in paraffin and sectioned at 10 μm. Sections were

subsequently stained with nuclear fast red (Abcam) and pictures were taken with a brightfield microscope.

Immunostaining.

Biopsies of dorsal skin of mice were isolated and cut into small pieces, fixed overnight in 4% paraformaldehyde, washed with PBS, dehydrated, paraffin imbedded and sectioned at 5 μm. For antigen retrieval, the sections were incubated with 10mM sodium citrate buffer, within a closed plastic container placed in a boiling waterbath, for 20 min. Sections were permeabilised with 3x5 min 0.1% Triton in PBS, blocked for 1h in 5% skin milk in PBS, and incubated overnight in 5% skin milk with primary antibodies. The following antibodies were used: goat anti-Dct at dilution of 1/1000 (Santa Cruz Biotechnology, sc-10451), rabbit anti-Ki67, at 1/500 (Novocastra Laboratories, NCL-Ki67p), rabbit anti-Sox10, at 1/1000 (Abcam, ab155279). Sections were washed 3x5 min 0.1% Triton in PBS, and incubated with secondary antibodies, Alexa 488 donkey-anti-goat, and Alexa 555 donkey-anti-rabbit (Invitrogen) for 1 h. Sections were subsequently incubated with 1/2000 Hoechst nuclear stain for 10 min. Sections were washed 3x5 min in PBS, dried, mounted with Vectashild, coverslip immobilized with nail polish.

Cell culture, and shRNA silencing.

Melanoma cell lines SK-Mel-28, 501Mel and LU1205 were grown in RPMI 1640 medium (Sigma, St Louis, MO, USA) supplemented with 10% foetal calf serum (FCS). 293T, HeLa and fibroblast cells were grown in Dulbecco's modified Eagle's medium supplemented with 10% FCS and penicillin/streptomycin (7.5 μg/ml). Hermes-3A cells were grown in RPMI 1640 medium (Sigma) supplemented with 10% FCS, 200nM TPA, 200pM cholera toxin, 10ng/ml human stem cell factor (Invitrogen) 10 nM endothelin-1 (Bachem) and penicillin/streptomycin (7.5 μg/ml). Hermes 3A cells were obtained from the University of London St Georges repository. All lentiviral shRNA vectors were obtained from Sigma (Mission sh-RNA series) in the PLK0 vector.

All lentiviral shRNA vectors were obtained from Sigma (Mission sh-RNA series) in the PLK0 vector and virus was produced in 293T cells according to the manufacturers protocol. Full details are in Supplementary material. Cells were infected with the viral stocks and after 5 days (or as indicated in figure legend) of puromycin selection (3 g/ml), cells were photographed and collected for preparation of cell lysates or isolation of RNA. In each case between 5X105-1X106 cells were infected with the indicated shRNA lentivirus vectors and

all experiments were performed at least in triplicate. The siRNA knockdown of BPFT was performed with ON-TARGET-plus human SMARpool (L-010431-00) purchased from Dharmacon Inc. (Chicago, Il., USA). Control siRNA directed against luciferase was obtained from Eurogentec (Seraing, Belgium). siRNAs were transfected using Lipofectamine RNAiMax (Invitrogen, La Jolla, CA, USA).

Senescence-Associated β-Galactosidase Assay

The senescence-associated β -galactosidase staining kit from Cell signaling technology (Beverly, MA, USA) was used according to the manufacturer's instructions to histochemically detect β-galactosidase activity at pH 6.

mRNA preparation, quantitative PCR and RNA-seq.

mRNA isolation was performed according to standard procedure (Qiagen kit). qRT-PCR wascarried out with SYBR® Green I (Qiagen) and Multiscribe Reverse Transcriptase (Invitrogen) and monitored by a LightCycler® 480 (Roche). Detection of Actin gene was used to normalize the results. Primer sequences for each cDNA were designed using Primer3 Software and are available upon request. RNA-seq was performed essentially as previously described (Herquel et al., 2013). Gene ontology analyses were performed using the functional annotation clustering function of DAVID (http://david.abcc.ncifcrf.gov/).

Acknowledgements

We thank, S. Gygi and R. Tomaino for mass-spectrometry analysis, L. Larue for the Tyr::Cre mice and helpful discussions, C. Wu for the floxed Bptf mice, E. Sviderskaya and D. Bennet for the Hermes cells, B. Jost, and all the staff of the IGBMC high throughput sequencing facility, a member of "France Génomique" consortium (ANR10-INBS-09-08). This work was supported by grants from the CNRS, the INSERM, the Association pour la Recherche contre le Cancer, the Ligue Nationale et Départementale Région Alsace contre le Cancer and the Institut National du Cancer (INCa) the ANR-10-LABX-0030-INRT French state fund through the Agence Nationale de la Recherche under the frame programme Investissements d'Avenir labelled ANR-10-IDEX-0002-02.. ID is an 'équipe labellisée' of the Ligue Nationale contre le Cancer.

Author contributions.

D.K. performed and analysed the shBPTF knockdowns, performed and analysed the RNA-seq with C.K and P.L., generated and analysed the Tyr-Cre::Bptf recombinant mice with G.M.

T.S. generated the F-HA-MITF cell line, performed the tandem affinity purifications. I.D. D.K. conceived experiments, analysed data and wrote the paper.

References.

Alkhatib, S.G., and Landry, J.W. (2011). The nucleosome remodeling factor. FEBS Lett 585, 3197-3207.

Badenhorst, P., Voas, M., Rebay, I., and Wu, C. (2002). Biological functions of the ISWI chromatin remodeling complex NURF. Genes Dev 16, 3186-3198.

Barak, O., Lazzaro, M.A., Lane, W.S., Speicher, D.W., Picketts, D.J., and Shiekhattar, R. (2003). Isolation of human NURF: a regulator of Engrailed gene expression. EMBO J 22, 6089-6100.

Carreira, S., Goodall, J., Denat, L., Rodriguez, M., Nuciforo, P., Hoek, K.S., Testori, A., Larue, L., and Goding, C.R. (2006). Mitf regulation of Dia1 controls melanoma proliferation and invasiveness. Genes & development 20, 3426-3439.

Delmas, V., Martinozzi, S., Bourgeois, Y., Holzenberger, M., and Larue, L. (2003). Cre-mediated recombination in the skin melanocyte lineage. Genesis 36, 73-80.

Giuliano, S., Ohanna, M., Ballotti, R., and Bertolotto, C. (2011). Advances in melanoma senescence and potential clinical application. Pigment Cell Melanoma Res 24, 295-308.

Goding, C., and Meyskens, F.L., Jr. (2006). Microphthalmic-associated transcription factor integrates melanocyte biology and melanoma progression. Clin Cancer Res 12, 1069-1073.

Goding, C.R. (2000). Mitf from neural crest to melanoma: signal transduction and transcription in the melanocyte lineage. Genes Dev 14, 1712-1728.

Goller, T., Vauti, F., Ramasamy, S., and Arnold, H.H. (2008). Transcriptional regulator BPTF/FAC1 is essential for trophoblast differentiation during early mouse development. Mol Cell Biol 28, 6819-6827.

Hamiche, A., Kang, J.G., Dennis, C., Xiao, H., and Wu, C. (2001). Histone tails modulate nucleosome mobility and regulate ATP-dependent nucleosome sliding by NURF. Proceedings of the National Academy of Sciences of the United States of America 98, 14316-14321.

Herquel, B., Ouararhni, K., Martianov, I., Le Gras, S., Ye, T., Keime, C., Lerouge, T., Jost, B., Cammas, F., Losson, R., et al. (2013). Trim24-repressed VL30 retrotransposons regulate gene expression by producing noncoding RNA. Nature structural & molecular biology 20, 339-346.

Hoek, K.S. (2011). MITF: the power and the glory. Pigment cell & melanoma research 24, 262-263.

Hoek, K.S., and Goding, C.R. (2010). Cancer stem cells versus phenotype-switching in melanoma. Pigment Cell Melanoma Res 23, 746-759.

Jordan, S.A., and Jackson, I.J. (2000). MGF (KIT ligand) is a chemokinetic factor for melanoblast migration into hair follicles. Dev Biol 225, 424-436.

Kang, J.G., Hamiche, A., and Wu, C. (2002). GAL4 directs nucleosome sliding induced by NURF. Embo J 21, 1406-1413.

Landry, J., Sharov, A.A., Piao, Y., Sharova, L.V., Xiao, H., Southon, E., Matta, J., Tessarollo, L., Zhang, Y.E., Ko, M.S., et al. (2008). Essential role of chromatin remodeling protein Bptf in early mouse embryos and embryonic stem cells. PLoS Genet 4, e1000241.

Landry, J.W., Banerjee, S., Taylor, B., Aplan, P.D., Singer, A., and Wu, C. (2011). Chromatin remodeling complex NURF regulates thymocyte maturation. Genes Dev 25, 275-286.

Laurette, P., Strub., Koludrovic, D., Ennen, M., Keime, C., LeGras, S., Siddaway, R., Mengus, D., Kobi, D., and Davidson, I (2014). Microphthalmia-associated transcription factor (MITF) interacts with a novel BRG1-containing complex to regulate gene expression in melanoma cells. .

Li, H., Ilin, S., Wang, W., Duncan, E.M., Wysocka, J., Allis, C.D., and Patel, D.J. (2006). Molecular basis for site-specific read-out of histone H3K4me3 by the BPTF PHD finger of NURF. Nature 442, 91-95.

Lin, J.Y., and Fisher, D.E. (2007). Melanocyte biology and skin pigmentation. Nature 445, 843-850.

Mackenzie, M.A., Jordan, S.A., Budd, P.S., and Jackson, I.J. (1997). Activation of the receptor tyrosine kinase Kit is required for the proliferation of melanoblasts in the mouse embryo. Dev Biol 192, 99-107.

McGill, G.G., Horstmann, M., Widlund, H.R., Du, J., Motyckova, G., Nishimura, E.K., Lin, Y.L., Ramaswamy, S., Avery, W., Ding, H.F., et al. (2002). Bcl2 regulation by the melanocyte master regulator Mitf modulates lineage survival and melanoma cell viability. Cell 109, 707-718.

Mizuguchi, G., Tsukiyama, T., Wisniewski, J., and Wu, C. (1997). Role of nucleosome remodeling factor NURF in transcriptional activation of chromatin. Molecular Cell 1, 141-150.

Mizuguchi, G., and Wu, C. (1999). Nucleosome remodeling factor NURF and in vitro transcription of chromatin. Methods Mol Biol 119, 333-342.

Mulder, K.W., Wang, X., Escriu, C., Ito, Y., Schwarz, R.F., Gillis, J., Sirokmany, G., Donati, G., Uribe-Lewis, S., Pavlidis, P., et al. (2012). Diverse epigenetic strategies interact to control epidermal differentiation. Nat Cell Biol 14, 753-763.

Nishikawa, S.I., and Osawa, M. (2005). Melanocyte system for studying stem cell niche. Ernst Schering Research Foundation workshop, 1-13.

Nishimura, E.K. (2011). Melanocyte stem cells: a melanocyte reservoir in hair follicles for hair and skin pigmentation. Pigment Cell Melanoma Res 24, 401-410.

Okuwaki, M. (2008). The structure and functions of NPM1/Nucleophsmin/B23, a multifunctional nucleolar acidic protein. J Biochem 143, 441-448.

Osawa, M. (2008). Melanocyte stem cells. In StemBook (Cambridge (MA)).

Osawa, M., Egawa, G., Mak, S.S., Moriyama, M., Freter, R., Yonetani, S., Beermann, F., and Nishikawa, S. (2005). Molecular characterization of melanocyte stem cells in their niche. Development 132, 5589-5599.

Robinson, K.C., and Fisher, D.E. (2009). Specification and loss of melanocyte stem cells. Semin Cell Dev Biol 20, 111-116.

Ruthenburg, A.J., Li, H., Milne, T.A., Dewell, S., McGinty, R.K., Yuen, M., Ueberheide, B., Dou, Y., Muir, T.W., Patel, D.J., et al. (2011). Recognition of a mononucleosomal histone modification pattern by BPTF via multivalent interactions. Cell 145, 692-706.

Saez-Ayala, M., Montenegro, M.F., Sanchez-Del-Campo, L., Fernandez-Perez, M.P., Chazarra, S., Freter, R., Middleton, M., Pinero-Madrona, A., Cabezas-Herrera, J., Goding, C.R., et al. (2013). Directed phenotype switching as an effective antimelanoma strategy. Cancer Cell 24, 105-119.

Schouwey, K., Delmas, V., Larue, L., Zimber-Strobl, U., Strobl, L.J., Radtke, F., and Beermann, F. (2007). Notch1 and Notch2 receptors influence progressive hair graying in a dose-dependent manner. Dev Dyn 236, 282-289.

Schouwey, K., Larue, L., Radtke, F., Delmas, V., and Beermann, F. (2009). Transgenic expression of Notch in melanocytes demonstrates RBP-Jkappa-dependent signaling. Pigment Cell Melanoma Res.

Steingrimsson, E., Copeland, N.G., and Jenkins, N.A. (2004). Melanocytes and the microphthalmia transcription factor network. Annu Rev Genet 38, 365-411.

Strub, T., Giuliano, S., Ye, T., Bonet, C., Keime, C., Kobi, D., Le Gras, S., Cormont, M., Ballotti, R., Bertolotto, C., et al. (2011). Essential role of microphthalmia transcription factor for DNA replication, mitosis and genomic stability in melanoma. Oncogene 30, 2319-2332.

Tsukiyama, T., Daniel, C., Tamkun, J., and Wu, C. (1995). ISWI, a member of the SWI2/SNF2 ATPase family, encodes the 140 kDa subunit of the nucleosome remodeling factor. Cell 83, 1021-1026.

Tsukiyama, T., and Wu, C. (1995). Purification and properties of an ATP-dependent nucleosome remodeling factor. Cell 83, 1011-1020.

Vermeulen, M., Eberl, H.C., Matarese, F., Marks, H., Denissov, S., Butter, F., Lee, K.K., Olsen, J.V., Hyman, A.A., Stunnenberg, H.G., et al. (2010). Quantitative interaction proteomics and genome-wide profiling of epigenetic histone marks and their readers. Cell 142, 967-980.

Vogler, M. (2012). BCL2A1: the underdog in the BCL2 family. Cell Death Differ 19, 67-74.

White, R.M., and Zon, L.I. (2008). Melanocytes in development, regeneration, and cancer. Cell Stem Cell 3, 242-252.

Widlund, H.R., and Fisher, D.E. (2003). Microphthalamia-associated transcription factor: a critical regulator of pigment cell development and survival. Oncogene 22, 3035-3041.

Wysocka, J., Swigut, T., Xiao, H., Milne, T.A., Kwon, S.Y., Landry, J., Kauer, M., Tackett, A.J., Chait, B.T., Badenhorst, P., et al. (2006). A PHD finger of NURF couples histone H3 lysine 4 trimethylation with chromatin remodelling. Nature 442, 86-90.

Xiao, H., Sandaltzopoulos, R., Wang, H.M., Hamiche, A., Ranallo, R., Lee, K.M., Fu, D., and Wu, C. (2001). Dual functions of largest NURF subunit NURF301 in nucleosome sliding and transcription factor interactions. Mol Cell 8, 531-543.

Figure legends

Figure 1. NURF associates with MITF. A. The immunoprecipitated material from the indicated fractions (soluble nuclear extract, SNE; chromatin-associated extract, CAE) was separated by SDS PAGE and stained with silver nitrate. Several relevant proteins are indicated. Lane M corresponds to a molecular mass marker indicated in kDa. B. List of peptides identified for BPTF, SMARCA1 and SMARCA5 in the chromatin-associated fraction. C. Immunoblot detection of MITF, BPTF, SMARCA1 and SMARCA5 in the indicated extracts from cells expressing FLAG-HA tagged or native MITF.

Figure 2. BPTF is required for the proliferation of 501Mel cells. A. Western blot showing knockdown of BPTF and MITF in 501Mel cells. B. Phase contrast microscopy of 501Mel cells following siBPTF and siMITF knockdown. Magnification X20. C. Growth curves of 501Mel cells following shBPTF knockdown. D. Phase contrast microscopy of 501Mel cells following shBPTF and shMITF knockdown. Inlays show higher magnifications E. Staining of 501mel cells following shBPTF and shMITF knockdown for senescence-associated □-galactosidase. Quantification is shown on the right.

Figure 3. MITF and BPTF regulate distinct, but overlapping gene expression programmes in 501Mel cells. A. Venn diagrams illustrate the overlap between up and down-regulated genes following shBPTF and shMITF knockdown. B Several examples of commonly regulated up and down-regulated genes are indicated based on the results of RNA-seq. C Ontology of genes up and down-regulated by shBPTF and shMITF knockdown and of commonly regulated genes. The number of genes in each category is indicated along with the p value. D. Venn diagrams illustrate the overlap between up and down-regulated genes following shBPTF and shMITF knockdown and genes showing an associated MITF-occupied site in ChIP-seq experiments in either a +/-10 kb or +/-30 kb window with respect to the TSS.

Figure 4. BPTF and MITF are required for the proliferation of Hermes-3A cells. A. Western blot showing knockdown of BPTF and MITF in Hermes-3A cells. B. Phase contrast microscopy of Hermes-3A cells cells following shBPTF and shMITF knockdown. Magnification X20. C. Growth curves of Hermes-3A cells cells following shBPTF knockdown. D. Venn diagrams illustrate the overlap between up and down-regulated genes following shBPTF and shMITF knockdown. E Several examples of commonly regulated up and down-regulated genes are indicated based on the results of RNA-seq. F Ontology of genes up and down-regulated by shBPTF and shMITF knockdown and of commonly regulated genes.

Figure 5. Premature greying of mice lacking Bptf in the melanocyte lineage. A Statistics showing the genotypes and phenotypes of mice from crosses of Bptflox/+ and Bptflox/lox mice. B. Photographs of P10 mice of the indicated genotypes before onset of hair growth. C-D. Photographs of 14 day-old and 6 week-old mice of the indicated genotypes to illustrate the characteristics of the first coat and the premature greying phenotype. E. Photographs of 1 year old mice of the indicated genotypes. F. Photographs of 3 week-old mice following depilation. The depilated area of the Bptflox/lox mouse is illustrated.

Figure 6. Diminished melanoblast proliferation in Bptf-mutant mice. A-B. Photographs of representative Bptflox/+ and Bptflox/lox E16.5 foetuses in the Dct-LacZ background following LacZ staining to visualize melanoblasts. Panel A shows the ventral portion and panel B the trunk and a zoom of representative cells from the trunk region. C. Quantification of LacZ-labelled melanoblasts in the indicated regions. An example of the grid used is shown over the limb and paw.

Figure 7. Loss of differentiated melanocytes in the bulb region of post-natal Bptf-mutant mice. A. Staining of a dorsal hair follicle of a wild-type with antibody against Dct showing the presence of Dct-labelled cells in the bulge corresponding to MSCs, in the shaft corresponding to TACs and in the bulb corresponding to differentiated melanocytes. B. The distribution of melanocyte populations as visualised by LacZ staining of mice harbouring the Dct-LacZ reporter is schematised. Image adapted from (Osawa, 2008). C-D. Staining of a dorsal hair follicles from the indicated mice with antibodies against Dct and Sox10 to detect differentiated melanocytes in the bulb. Quantification is shown on the right. E-F. Staining of dorsal hair follicles from the indicated mice with antibodies against Dct and Ki67 to detect melanocytes in the bulb of 21 day-old animals. G. Staining of dorsal hair follicles from the one year-old mice with antibodies against Dct and Ki67 illustrating the absence of melanocytes in the bulb of Bptf-mutant animals.

Figure 8. Persistence of a MSC population in adult Bptf-mutant animals. A. Staining for LacZ-labelled melanocytes in dorsal hair follicles of P10 mice harbouring the Dct-LacZ reporter. Arrows indicate representative examples of MSCs in the bulge region and differentiated melanocytes in the bulb. B-C Staining for LacZ-labelled melanocytes in dorsal hair follicles of 6 week-old and one year-old mice. Arrows are as in panel A.

Supplementary data

Materials and Methods.

Tandem immunoaffinity purification and mass-spectrometry

Cells were lysed in hypotonic buffer (10 mM Tris-HCl at pH 7.65, 1.5 mM MgCl2, 10mM KCl) and disrupted by Dounce homogenizer. The cytosolic fraction was separated from the pellet by centrifugation at 4°C. The nuclear soluble fraction was obtained by incubation of the pellet in high salt buffer (final NaCl concentration of 300mM) and then separated by centrifugation at 4°C. To obtain the nuclear insoluble fraction (chromatin fraction), the remaining pellet was digested with micrococcal nuclease and sonicated. Tagged proteins were immunoprecipitated with anti-Flag M2-agarose (Sigma), eluted with Flag peptide (0.5

mg/mL), further affinity purified with anti-HA antibody-conjugated agarose (Sigma), and eluted with HA peptide (1 mg/mL). The HA and Flag peptides were first buffered with 50mM Tris-HCl (pH 8.5), then diluted to 4 mg/mL in TGEN 150 buffer (20 mM Tris at pH 7.65, 150 mM NaCl, 3 mM MgCl2, 0.1 mM EDTA, 10% glycerol, 0.01% NP40), and stored at -20°C until use. Between each step, beads were washed in TGEN 150 buffer. Complexes were resolved by SDS-PAGE and stained using the Silver Quest kit (Invitrogen). Mass-spectrometry was performed at the Taplin Biological Mass Spectrometry Facility (Harvard Medical School, Boston, MA).

Cell culture and lentiviral infections.

Melanoma cell lines SK-Mel-28 and 501Mel were grown in RPMI 1640 medium (Sigma, St Louis, MO, USA) supplemented with 10% foetal calf serum (FCS). 888Mel and MNT were grown RPMI 1640 medium, supplemented with 10% heat-inactivated foetal calf serum (FCSi). 1205LU were grown in medium W489 (MCDB 153 / LEIBOVITZ L-15 (3:1), Sigma, St Louis, MO, USA), supplemented with 4% heat-inactivated foetal calf serum (FCSi). 293T cells were grown in Dulbecco's modified Eagle's medium supplemented with 10% FCS and penicillin/streptomycin (7.5 □g/ml). Hermes-3A cells were grown in RPMI 1640 medium (Sigma) supplemented with 10% FCS, 200nM TPA, 200pM cholera toxin, 10ng/ml human stem cell factor (Invitrogen) 10 nM endothelin-1 (Bachem) and penicillin/streptomycin (7.5 □g/mL). All lentiviral shRNA vectors were obtained from Sigma (Mission sh-RNA series) in the PLK0 vector. The following constructs were used. shBPTF (TRCN0000319152, TRCN0000319153) , shMITF (TRCN0000019119), shSMARCA1 (TRCN0000303643, TRCN0000303644), shSMARCA5 (TRCN0000358474, TRCN0000358497). For lentivirus infection, virus was produced in 293T cells according to the manufacturers protocol described.

Transfections, extract preparation and antibodies.

Transient and stable transfections were performed with 5 µg of expression vectors and using FuGENE 6 reagent (Roche) following the manufacturers instructions. Medium was replaced 24 hours and cells were collected 48 hours after transfection. Cells lysis was performed using LSDB 500 buffer (500mM KCl, 25mM Tris at pH 7.9, 10% glycerol, 0;05 % NP-40, 1mM DTT and protease inhibitor cocktail). Up to 3 mg of whole cell extracts were diluted in LDSB without KCl to obtain a final concentration of 100mM KCl and incubated for 12h with 5 µg of specific antibody and 50µl Slurry of protein-G sepharose (GE Healthcare). Beads were washed three times in LSDB 300, twice in LSDB 150 and boiled in Laemmli buffer before

protein separation by SDS–PAGE. For flag immunoprecipitations, extracts were incubated with 50µl Slurry of Anti-Flag M2-agarose affinity gel (Sigma) and washed similarly prior to elution with Flag peptide (0,5 mg/mL). Immunoblots were performed with the following antibodies: MITF (Interchim, MS-771-P), actin (IGBMC, 2D7), BPTF antibody was a gift from Carl Wu and Joe Landry, SMARCA1 and SMARCA5 antibodies were a gift from Peter Becker.

Chromatin-immunoprecipitation

BRG1 ChIP experiments were performed on native Mnase-digested chromatin. 5x107 to 5x108 freshly harvested 501Mel cells were resuspended in 2mL ice-cold hypotinic buffer (0.3M Sucrose, 60mM KCl, 15mM NaCl, 5mM MgCl2, 0.1mM EDTA, 15mM Tris-HCl (pH 7.5), 0.5mM DTT, 0.1mM PMSF, protease inhibitor cocktail) and cytoplasmic fraction was released by incubation with 2mL of lysis-buffer (0.3M sucrose, 60 mM KCl, 15mM NaCl, 5mM MgCl2, 0.1mM EDTA, 15mM Tris-HCl (pH 7.5), 0.5mM DTT, 0.1mM PMSF, PIC, 0.5% (v/v) IGEPAL CA-630) for 10 minutes on ice. The suspension was layered onto a sucrose cushion (1.2M sucrose, 60 mM KCl, 15mM NaCl, 5mM MgCl2, 0.1mM EDTA, 15 mM Tris-HCl (pH 7.5), 0.5mM DTT, 0.1mM PMSF, PIC) and centrifuged for 25 minutes at 4700 rpm in a swing rotor. The nuclear pellet was resuspended in digestion buffer (0.32M sucrose,50mM Tris-HCl (pH 7.5), 4mM MgCl2,1mM CaCl2, 0.1mM PMSF) and subjected to Micrococcal Nuclease digestion for 5 minutes at 37°C. The reaction was stopped by addition of EDTA and suspension chilled on ice for 10 minutes. The suspension was cleared by centrifugation at 10,000 rpm (4°C) for 10 minutes and supernatant (chromatin) was used for further purposes. ChIP was performed on up to 60 µg of native chromatin essentially as previously described.

Legends to Supplemental Figures.

Supplemental Figure 1. Genes encoding subunit of NURF are associated with MITF-occupied sites. UCSC screenshot of the indicated loci showing MITF occupied sites indicated by arrows.

Supplemental Figure 2. Selective requirement for BPTF for the proliferation and survival of melanoma cells. A. Western blot showing knockdown of BPTF and MITF in SK-Mel-28 cells. B. Growth curves of SK-Mel-28 and Mnt cells following BPTF knockdown. C. Phase contrast microscopy of SK-Mel-28 and Mnt cells following BPTF knockdown. Magnification X20. D. Phase contrast microscopy of 888Mel cells following BPTF knockdown. E. Growth

non-melanoma cells following BPTF knockdown. F. Phase contrast microscopy of the indicated cell lines following BPTF knockdown.

Supplemental Figure 3. An MITF-independent role for BPTF in 1205Lu cells. A. Western blot showing knockdown of BPTF and absence of MITF in 1205Lu cells. B. Growth curves of 1205Lu cells following BPTF knockdown. C. Phase contrast microscopy of 1205Lu cells following BPTF knockdown. Magnification X20.

Supplemental Figure 4. Essential role of the NURF catalytic subunits SMARCA1 and SMARCA5 in 501mel cells. A. Western blot showing knockdown of SMARCA1 and SMARCA5 in 501Mel cells. B. Phase contrast microscopy of 501Mel cells following SMARCA1 and SMARCA5 knockdown. Magnification X20.

Supplemental Figure 5. MITF and BPTF regulate distinct, but overlapping gene expression programmes in 501Mel and Hermes-3A cells. Venn diagrams illustrate the overlap between up and down-regulated genes in the two cell types. Several examples of commonly regulated up and down-regulated genes are indicated.

Supplemental Figure 6. Premature greying of mice lacking Bptf in the melanocytes lineage. A-B. Photographs of mice of the indicated genotypes and post-natal days before onset of hair growth. C-D. Photographs of 14 and 21 day-old mice of the indicated genotypes illustrating the characteristics of the first coat.

Supplemental Figure 7. Diminished melanoblast proliferation in Bptf-mutant mice. A-B. Photographs of representative Bptflox/+ and Bptflox/lox E15.5 foetuses in the Dct-LacZ background following LacZ staining to visualize melanoblasts. Panel A shows the ventral portion and panel B the trunk and a zoom of representative cells from the trunk region. C. Quantification of LacZ-labelled melanoblasts in the indicated regions. An example of the grid used is shown over the limb and paw.

Supplementary Dataset 1. Excel spreadsheet of genes specifically and commonly regulated by BPTF and MITF knockdown in 501Mel cells along with the appropriate gene ontology as described in Figure 3A, B and C.

Supplementary Dataset 2. Excel spreadsheet of genes with associated MITF occupancy and regulated in shBPTF along with the appropriate gene ontology as described in Figure 3D.

Supplementary Dataset 3. Excel spreadsheet of genes regulated by shBPTF and shMITF in Hermes 3A cells along with common and specific genes and their ontology as described in Fig 4D.

Supplementary Dataset 4. Excel spreadsheet of genes regulated by shBPTF and shMITF common in 501Mel and Hermes 3A cells along with common and specific genes and their ontology as described in Supplemental Figure 5.

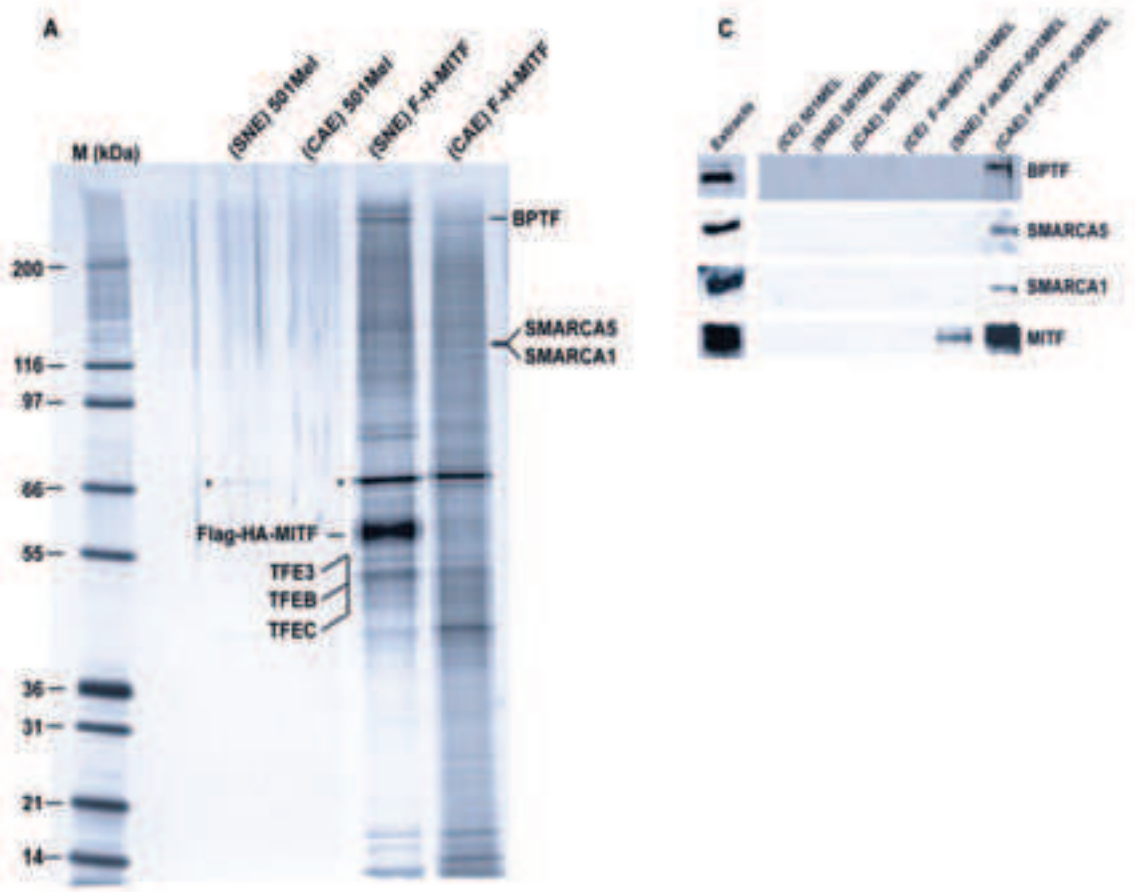

B

BPTF

Position	MH+	Sequence
1060-1066	815.9449	[redacted]
1786-1792	859.0581	[redacted]
774-781	903.1099	[redacted]
1066-1173	917.0801	[redacted]
1251-1259	926.0605	[redacted]
1431-1439	929.0612	[redacted]
708-715	970.0726	[redacted]
1776-1785	1047.3012	[redacted]
1101-1110	1088.2462	[redacted]
51-61	1142.3000	[redacted]
923-932	1148.2638	[redacted]
980-990	1208.2854	[redacted]
902-913	1341.5089	[redacted]
1970-1982	1377.5401	[redacted]
1949-1963	1448.7181	[redacted]
593-604	1524.5841	[redacted]
1635-1650	1561.7726	[redacted]

SMARCA1

Position	MH+	Sequence
915-921	861.0471	[redacted]
945-951	869.0140	[redacted]
505-513	1095.5491	[redacted]
307-315	1116.2621	[redacted]
642-651	1129.3016	[redacted]
754-764	1318.4748	[redacted]
640-651	1398.6485	[redacted]

SMARCA5

Position	MH+	Sequence
92-97	812.9842	[redacted]
993-999	848.9928	[redacted]
837-844	944.0756	[redacted]
553-560	1001.2318	[redacted]
431-440	1046.1654	[redacted]
607-616	1224.3129	[redacted]
837-847	1322.5083	[redacted]
212-223	1368.6745	[redacted]
72-83	1478.5525	[redacted]
729-736	1487.7417	[redacted]
666-680	1794.8113	[redacted]

Mass spectrometry allignement	BPTF	SMARCA1	SMARCA5
Protein coverage by amino acid count	176/2920 = 6%	59/1070 = 5.1%	111/1052 = 10.6%
Protein coverage by mass	18604/324124 = 5.8%	6563/124327 = 5.3%	13079/121906 = 10.7%

Koludrovic et al., Fig. 1

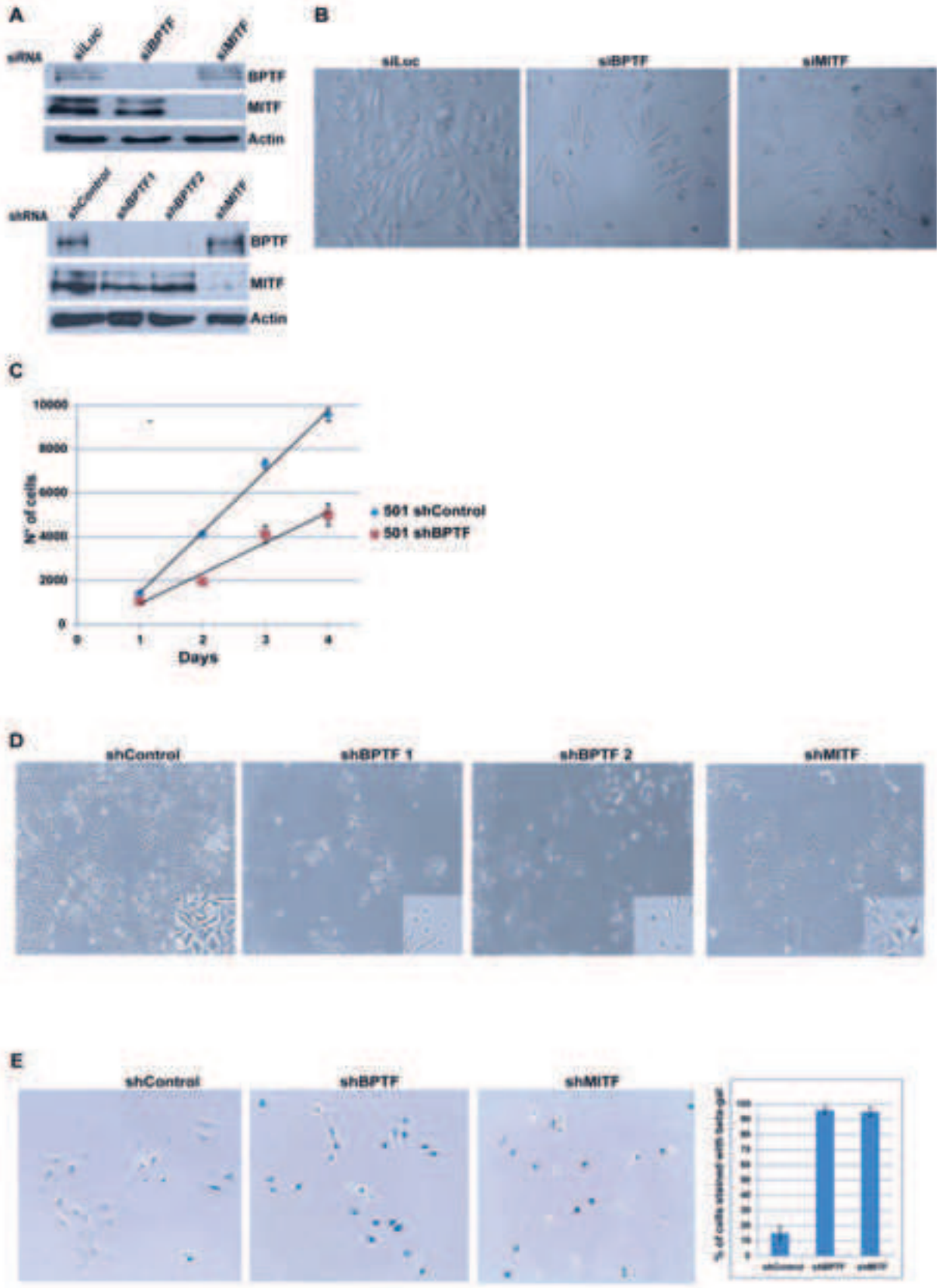

Koludrovic et al., Fig. 2.

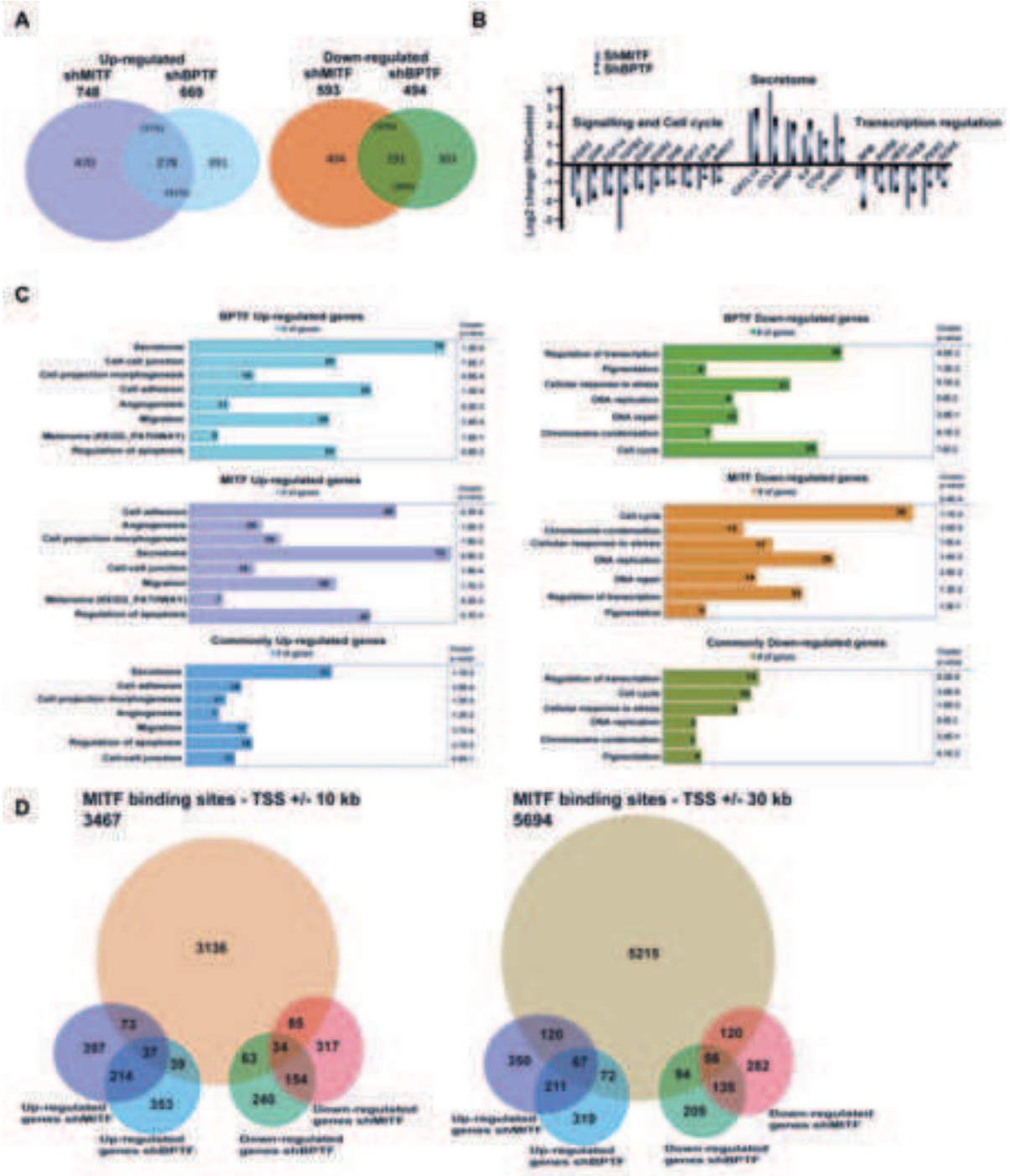

Koludrovic et al., Fig. 3

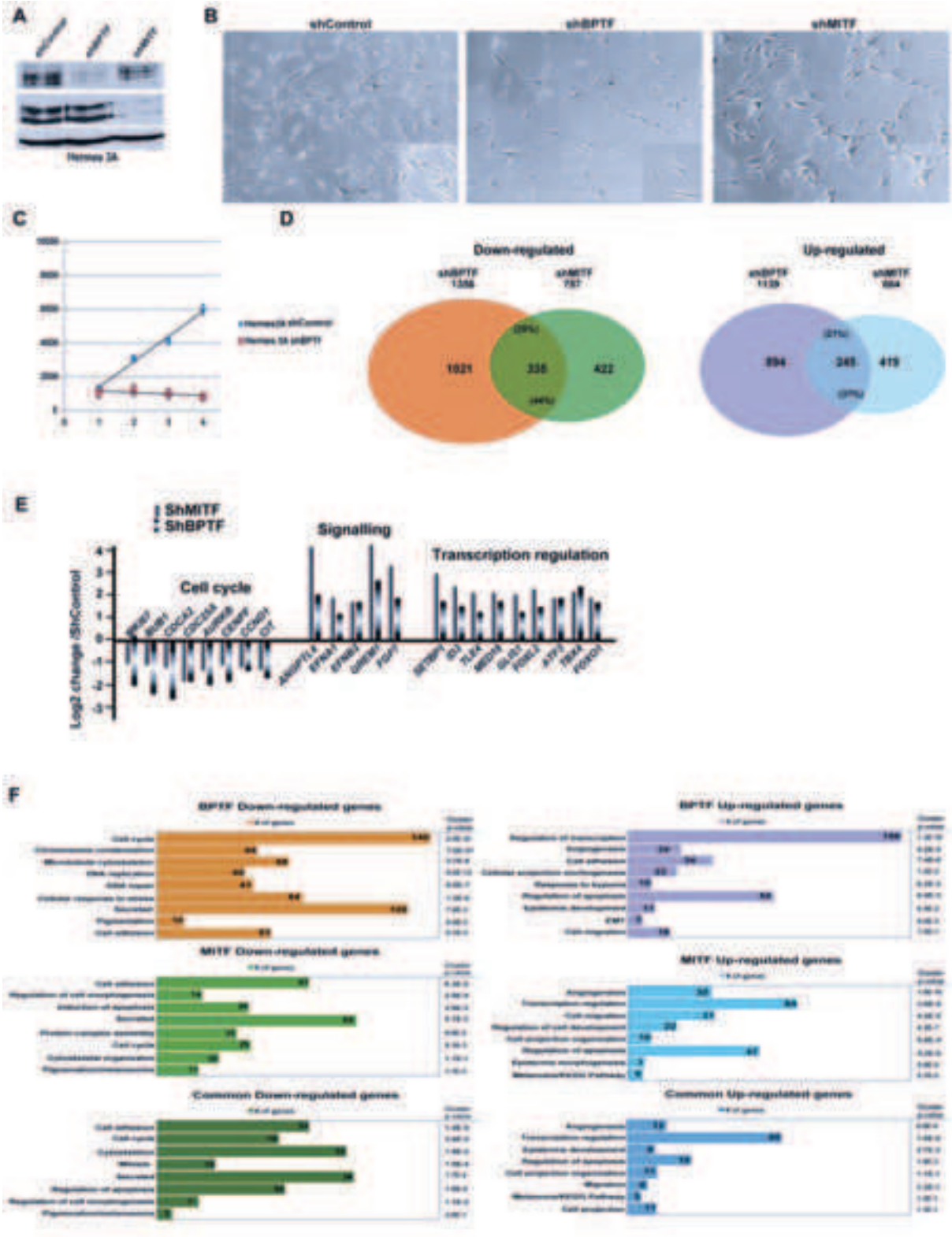

Koludrovic et al., Fig. 4

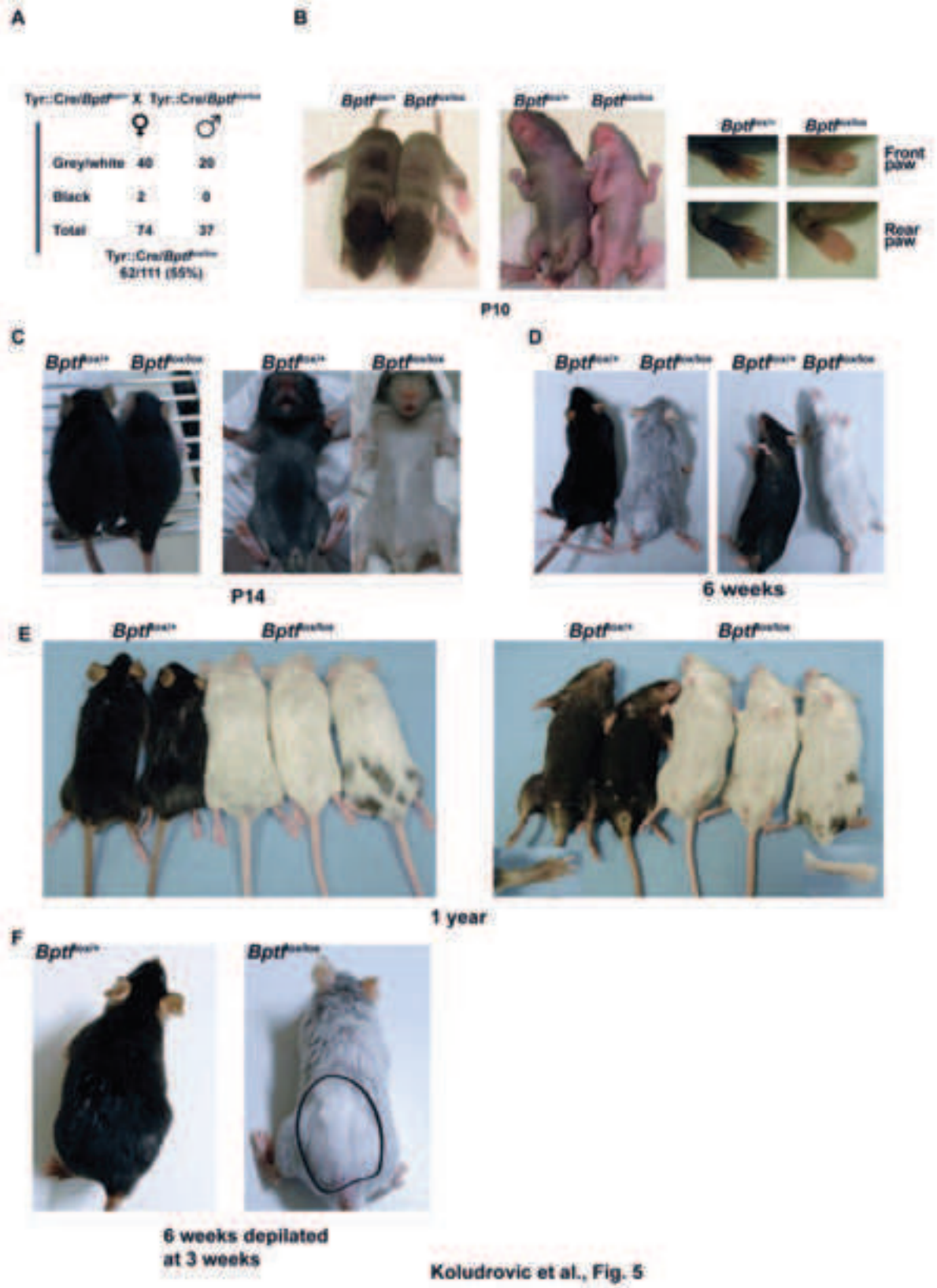

Koludrovic et al., Fig. 5

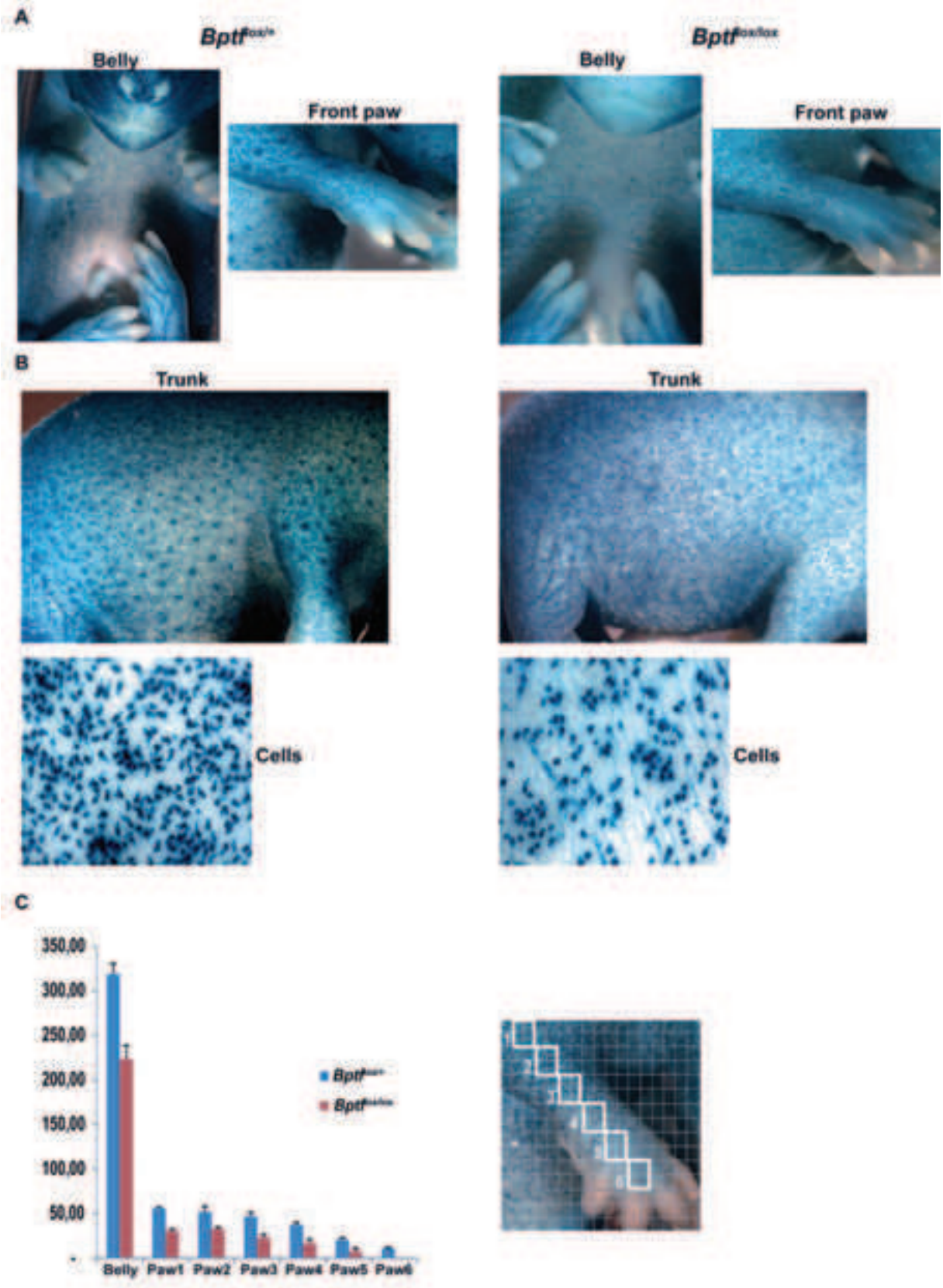

Koludrovic et al., Fig. 6

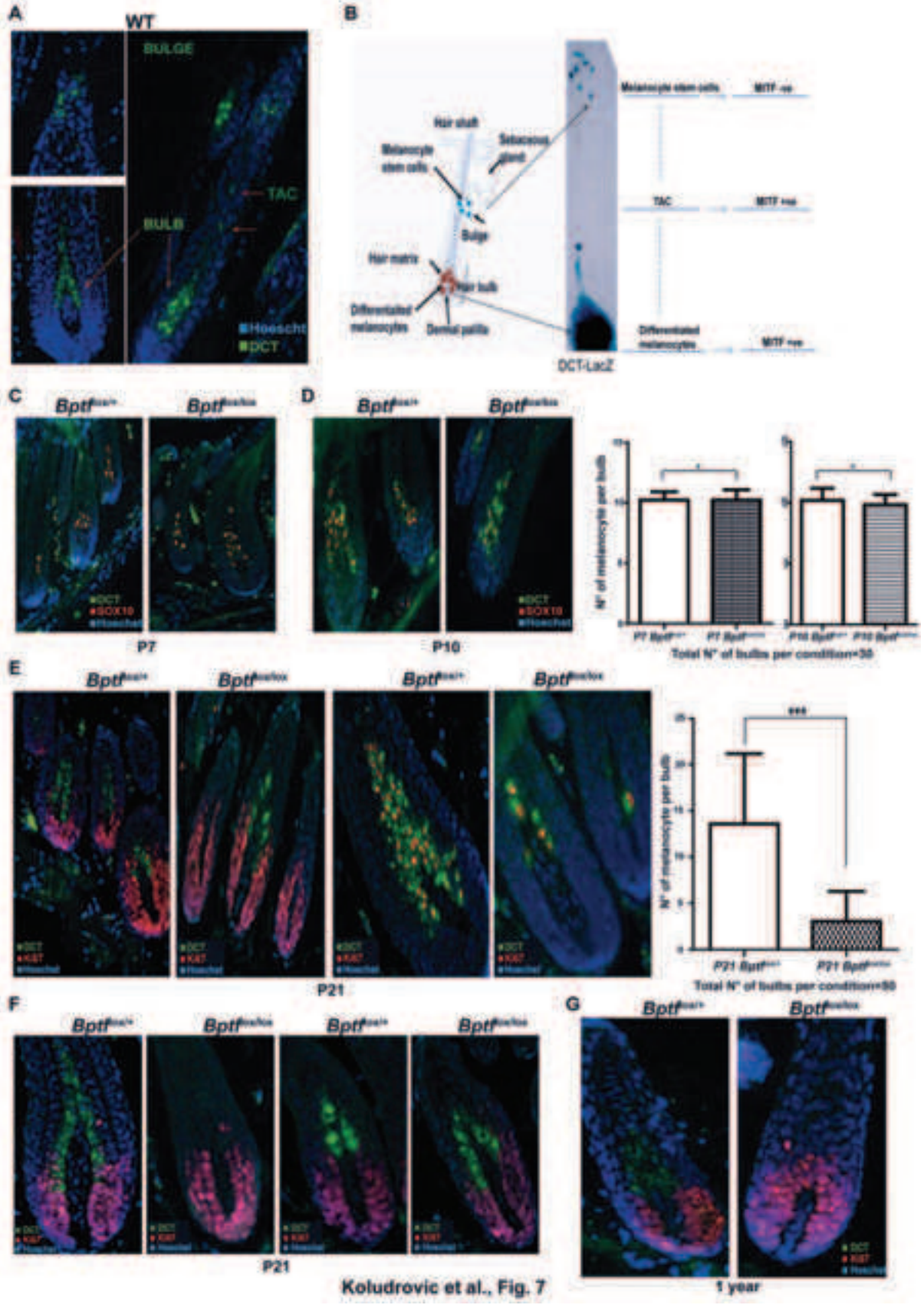
A
WT
BULGE
TAC
BULB
Hoescht
DCT
B
Melanocyte stem cells
MITF +ve
Hair shaft
Sebaceous gland
Melanocyte stem cells
Bulge
TAC
MITF +ve
Hair matrix
Hair bulb
Differentiated melanocytes
Dermal papilla
Differentiated melanocytes
MITF +ve
DCT-LacZ
C
D
DCT
SOX10
Hoechst
P7
P10
N° of melanocyte per bulb
Total N° of bulbs per condition=30
E
DCT
KI67
Hoechst
P21
***
N° of melanocyte per bulb
P21
Total N° of bulbs per condition=50
F
P21
G
DCT
KI67
Hoechst
1 year
Koludrovic et al., Fig. 7

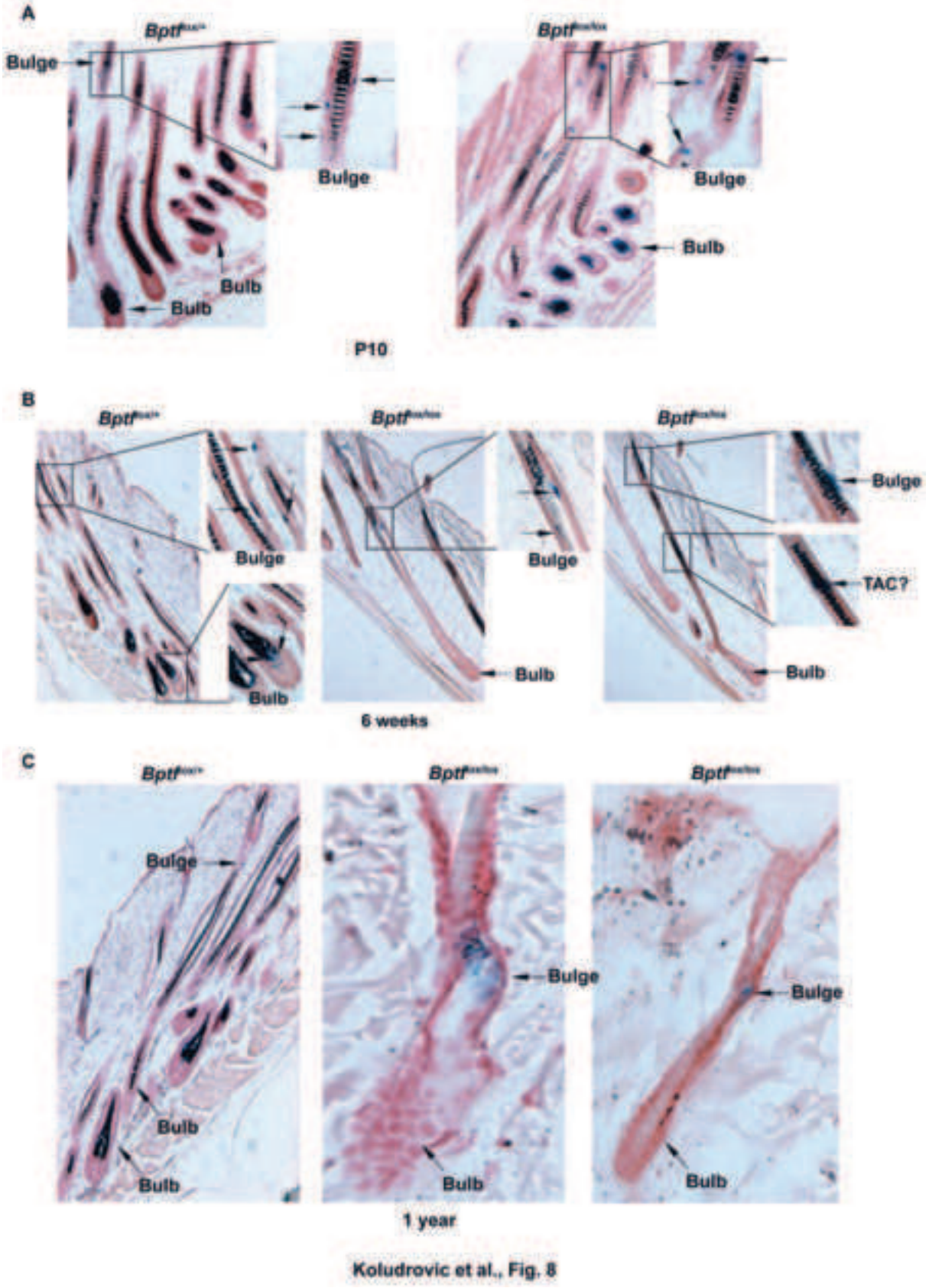

Koludrovic et al., Fig. 8

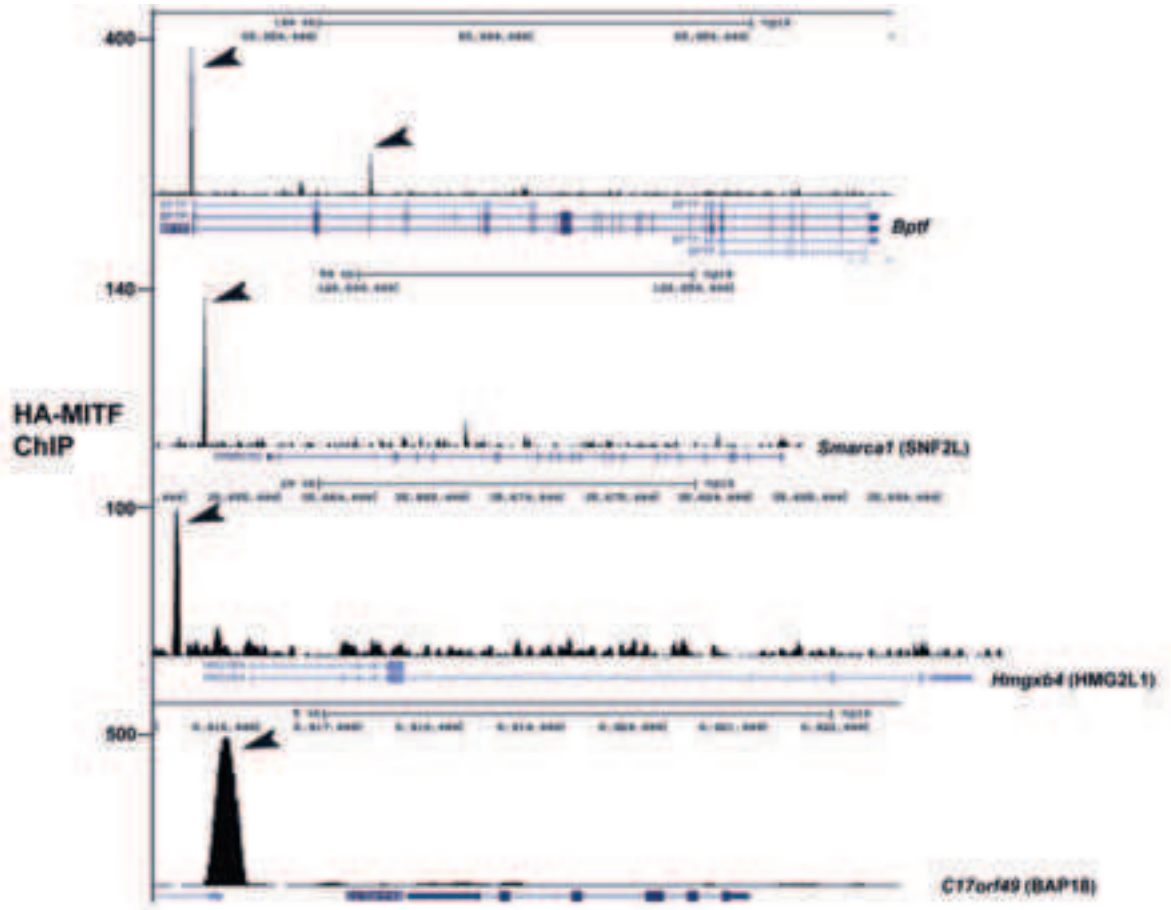

Koludrovic et al., Supplemental Fig. 1

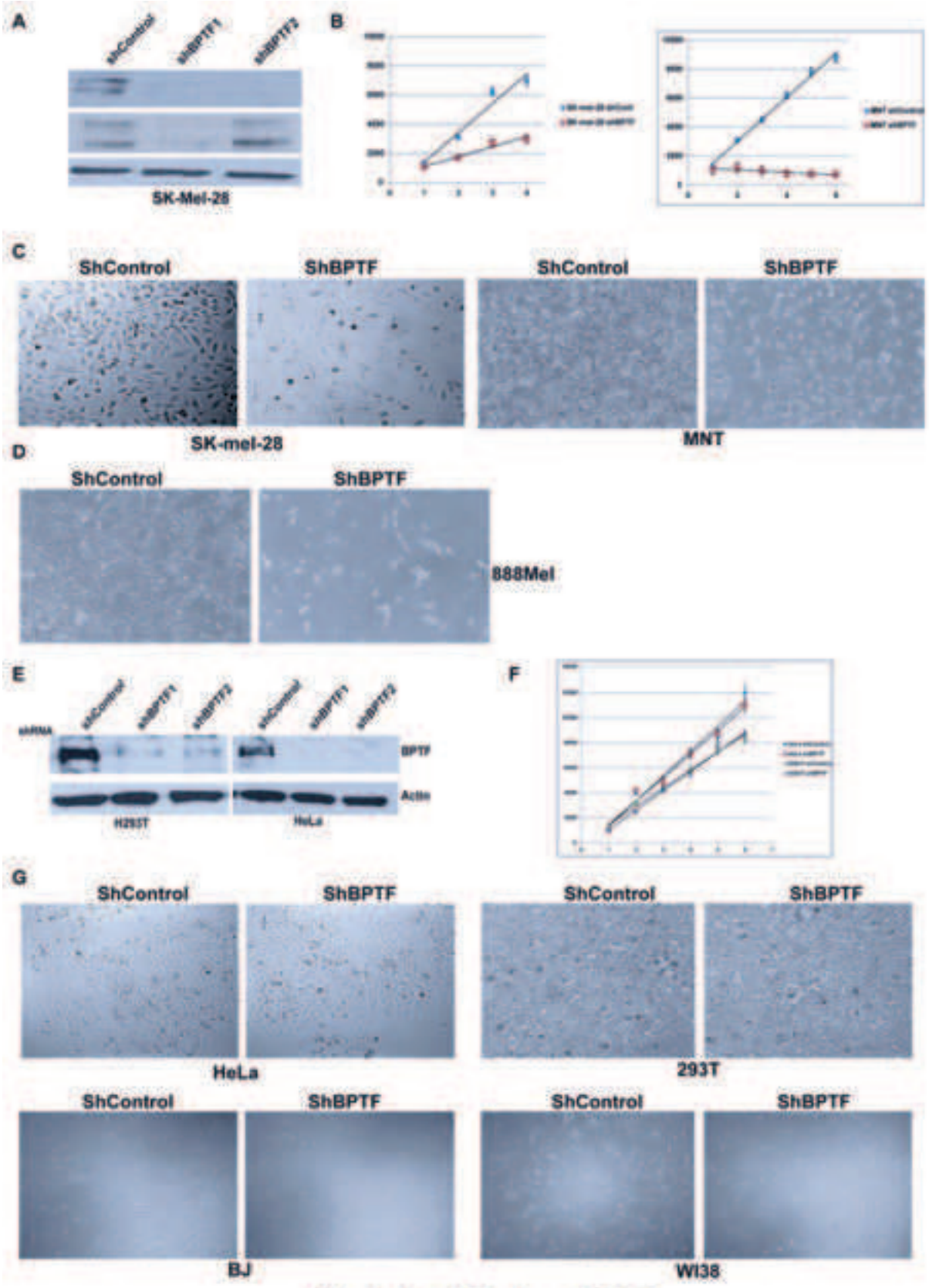

Koludrovic et al., Supplemental Fig. 2

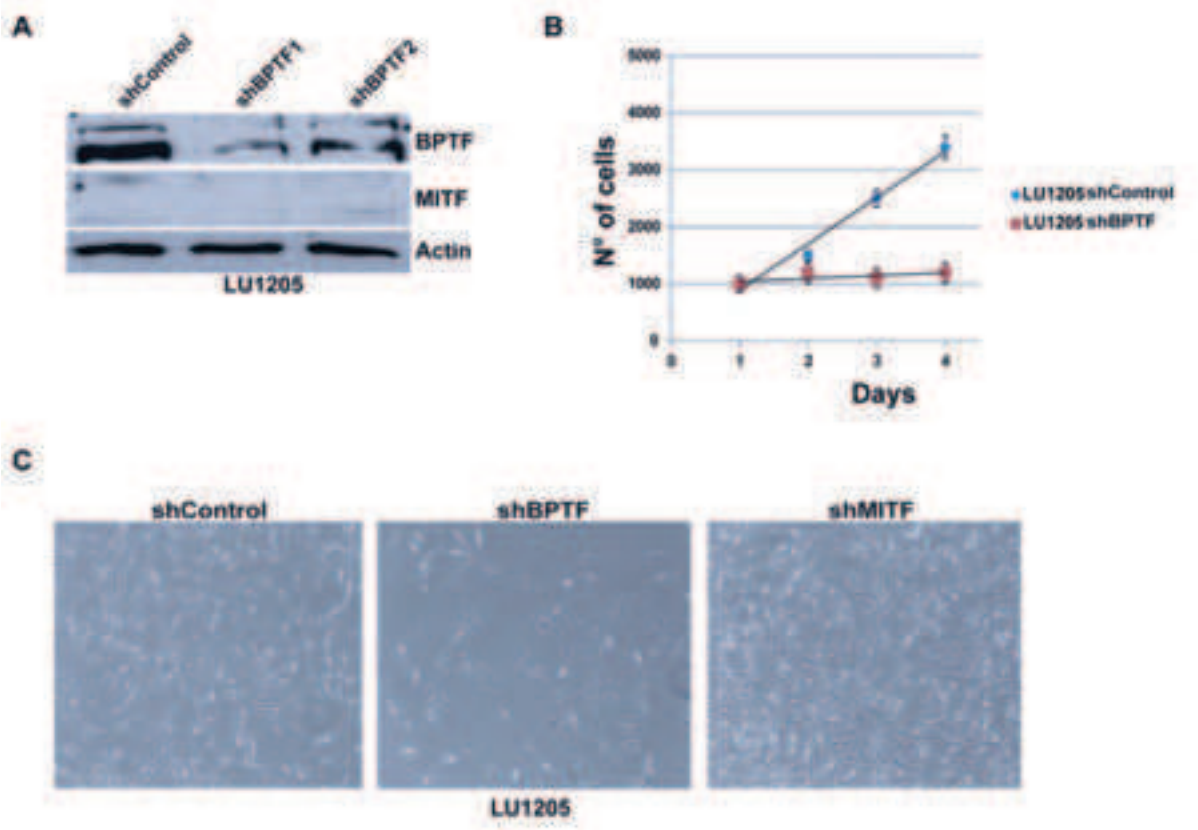

Koludrovic et al., Supplemental Fig. 3

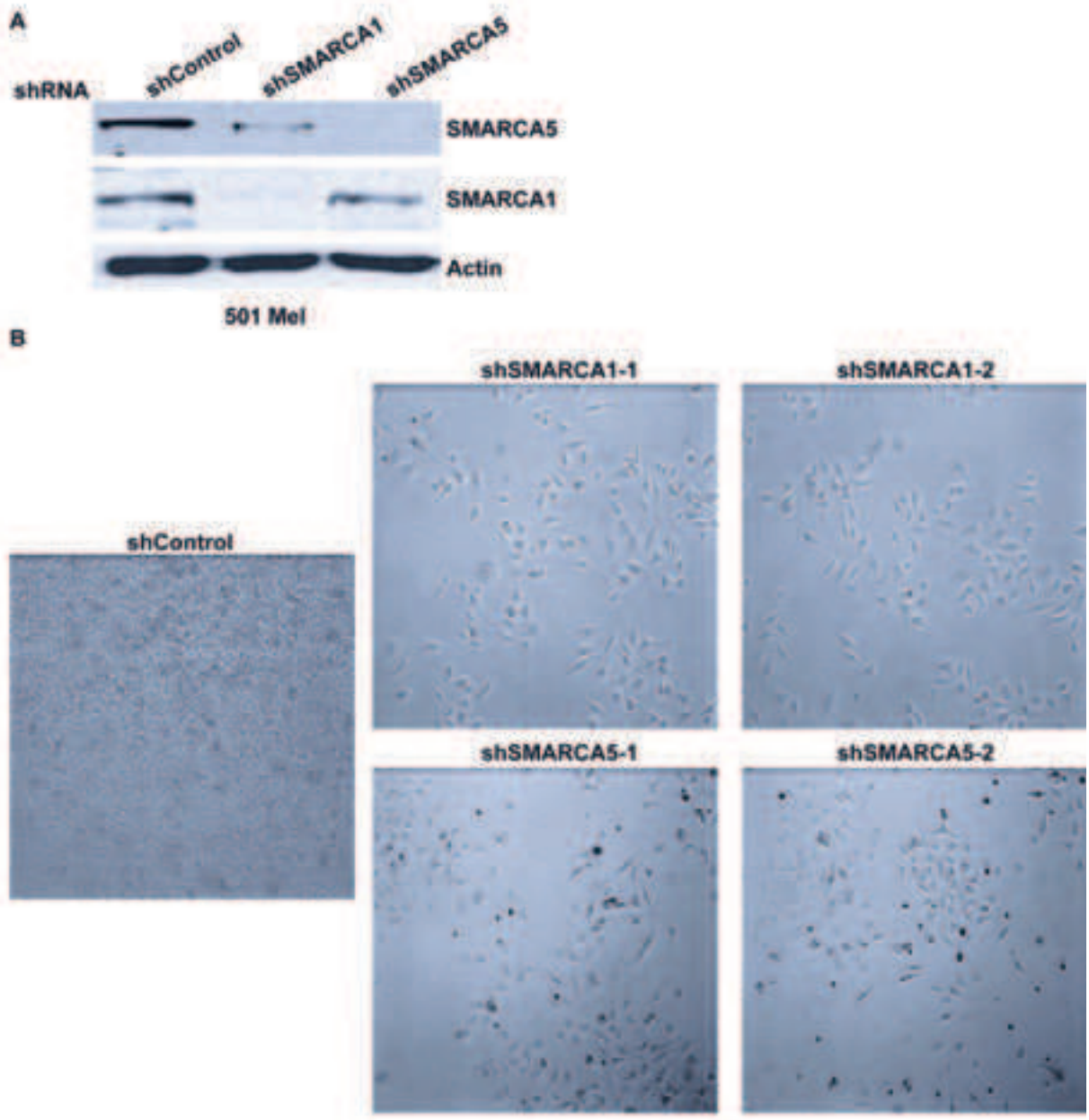

Koludrovic et al., Supplemental Fig. 4

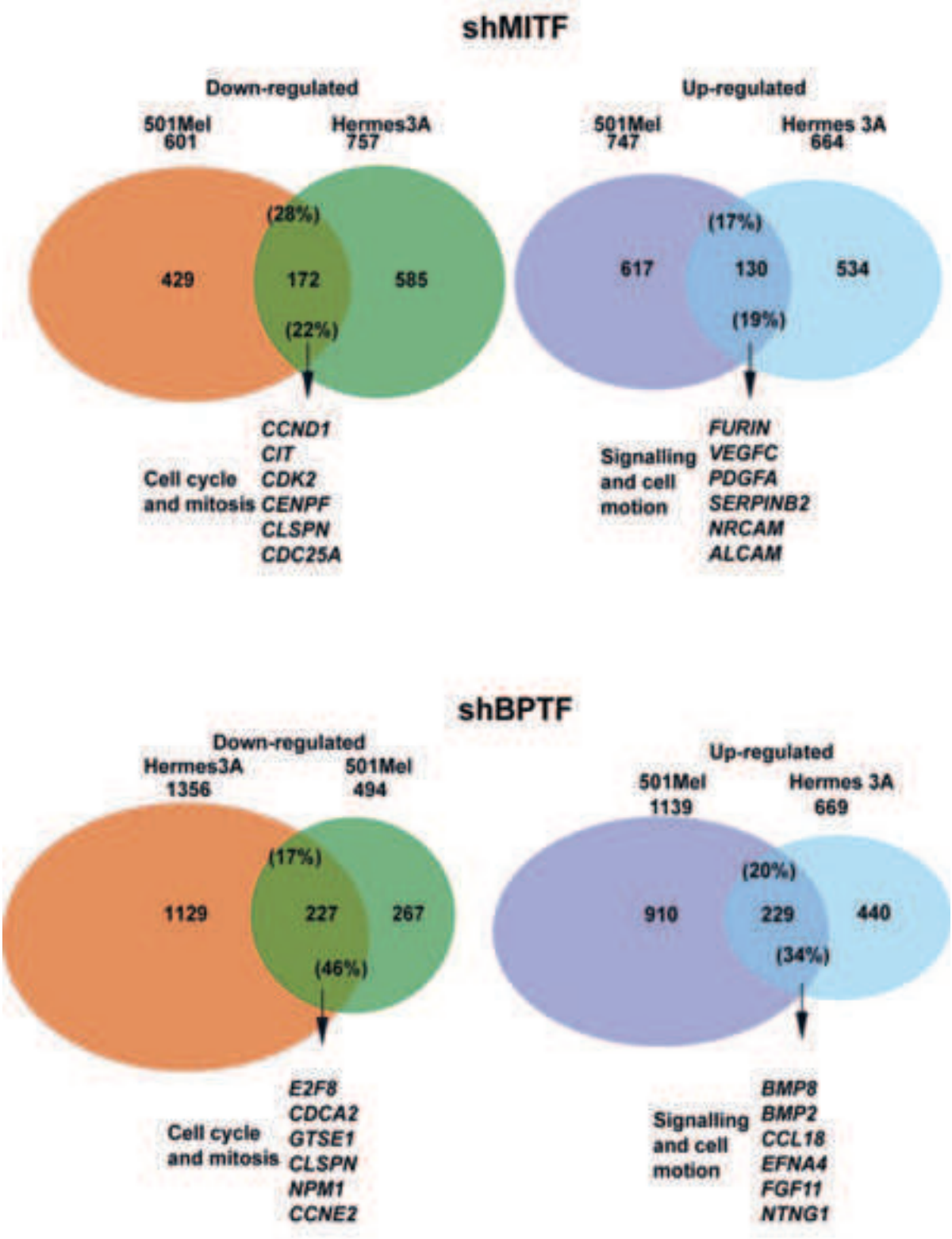

Koludrovic et al., Supplemental Fig. 5

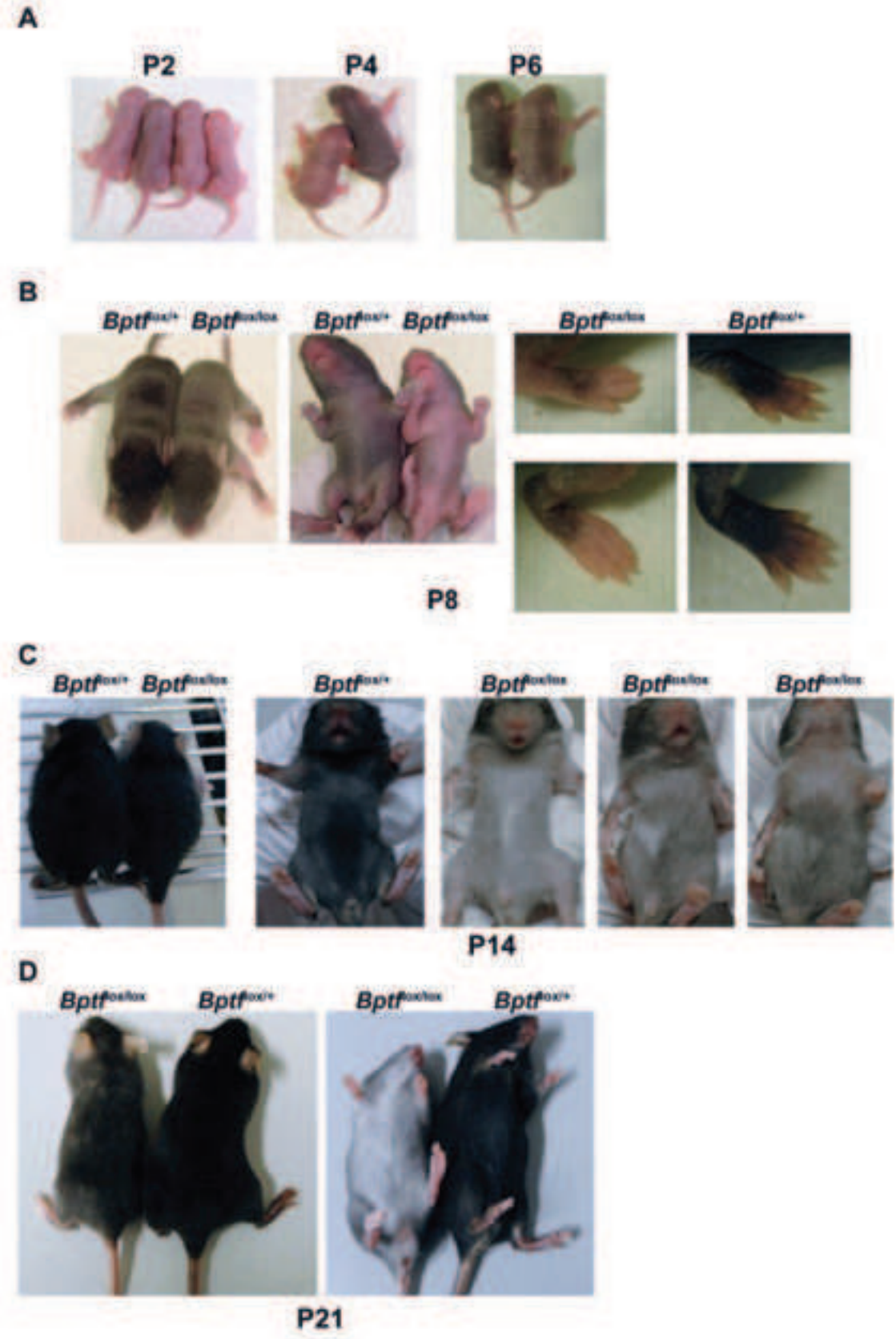

Koludrovic et al., Suppplemental Fig. 6

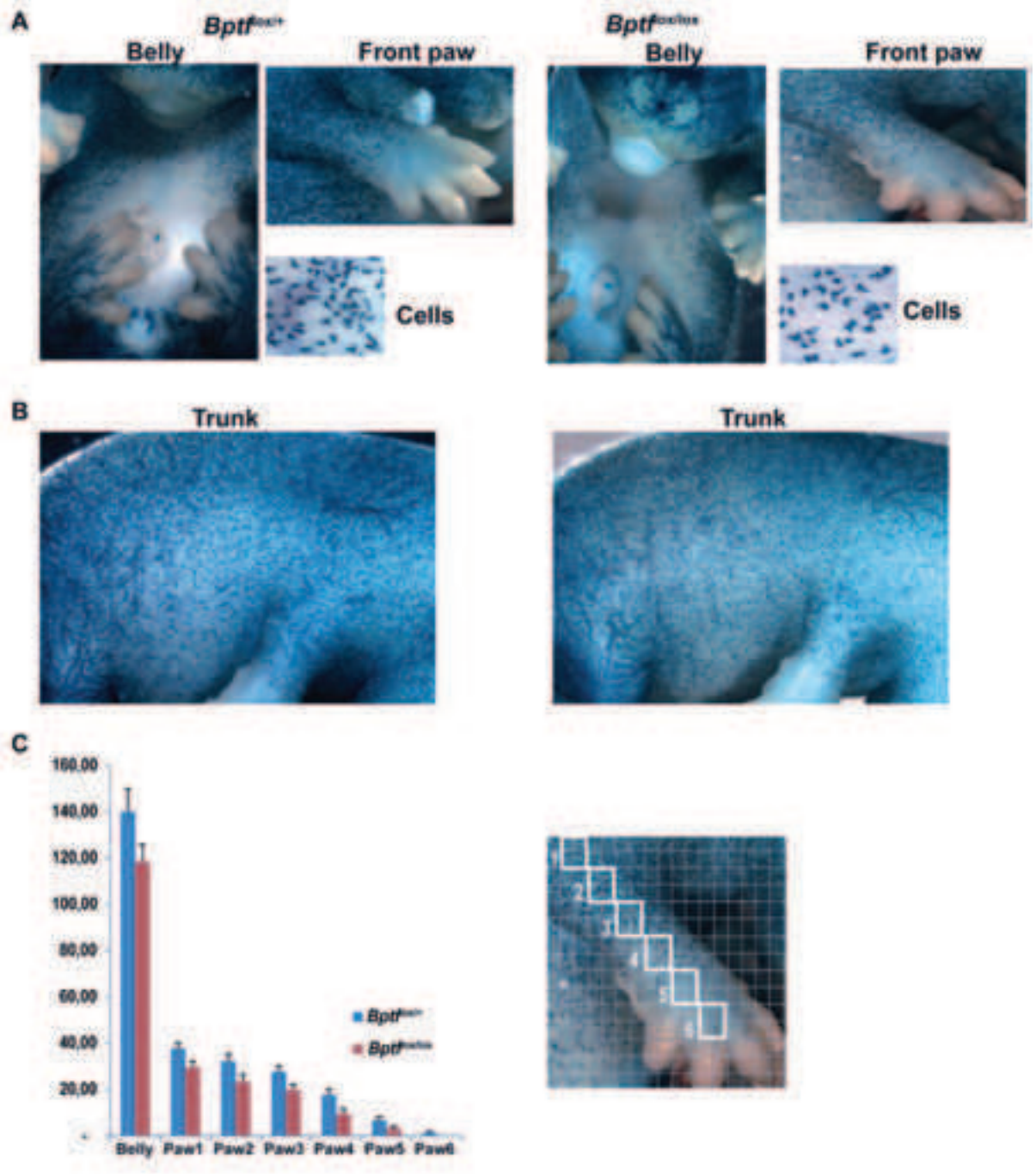

Koludrovic et al., Supplemental Fig. 7

DISCUSSION and PERSPECTIVES

BPTF/NURF has an essential and specific role in melanoma cells *in vitro*.

MITF regulates a comprehensive set of genes controlling multiple aspects of melanocyte and melanoma biology. In order understand how MITF regulates transcription, we used tandem affinity purification and mass-spectrometry to identify MITF interacting partners. Amongst these potential cofactors, we focused our attention on two chromatin-remodeling complexes that are BRG1 and NURF of which multiple subunits were present in the MITF interactome. We show that MITF interacts with a novel variant of the BRG1-containing complexes that includes CDH7, but lacks ARID1 and ARID2. MITF recruits BRG1 to the 501Mel genome to regulate a set of genes involved in lysosome formation, cell cycle and pigmentation. For NURF, we detected abundant peptides for BPTF, SNF2H and SNF2L along with RBBP4, although RBBP4 is present in several other chromatin-associated complexes (Loyola and Almouzni 2004). We did not detect the BAP18 and HMG2L1 subunits. Whether this is because the small number of peptides from these proteins was missed in the mass-spectrometry or whether they are not part of the complex in 501Mel cells remains to be determined. Also while we detect NURF subunits in the MITF interactome those that interact directly with MITF remain to be determined.

While subunits of BRG1 were detected in both the nuclear soluble and chromatin-associated fraction, NURF subunits were detected only in the chromatin-associated fraction. This was confirmed by immunoblot experiments where BPTF, SNF2H and SNF2L were observed only in the MITF immunoprecipitation from the chromatin-associated fraction. MITF and NURF therefore interact only on chromatin. So far we have been unable to generate a ChIP-grade BPTF antibody that would allow us to identify sites on the genome where MITF and BPTF co-localize. In the case of BRG1 we found that MITF and BRG1 co-localized to many region over the genome both at the TSS and more distal enhancer elements. However, it has previously been shown that BPTF localizes almost uniquely to the TSS by virtue of the interactions between its PHD and Bromodomains with the histone modification at the TSS

(Ruthenburg et al. 2011). Indeed, we have identified a collection of promoters where MITF binds close to the TSS and where it could interact with the nearby BPTF. However, the above BPTF ChIP-seq experiments were performed with a truncated protein containing only the PHD and Bromodomains and thus it remains possible that BPTF may be recruited to other regions of the genome not by interaction with chromatin marks but via interactions with transcriptional activators such as MITF.

The interaction between MITF and BPTF suggested that BPTF/NURF acts as a cofactor for MITF in melanoma cells. Here we provide evidence that BPTF plays an important role in cells of the melanocyte lineage *in vitro* and *in vivo* in mice. As BPTF is so far believed to be exclusive to the NURF complex (Alkhatib and Landry 2011), the effects seen upon its silencing are likely to reflect the loss of the chromatin remodeling activity of NURF, an idea supported by the fact that silencing of SNF2H and SNF2L, the catalytic subunits of NURF have similar phenotypes to that of BPTF. Nevertheless, as these subunits are present in other remodelers (Voss and Hager 2014, Swygert and Peterson 2014), their loss of function reflects more than that of NURF alone.

ShRNA-mediated silencing of BPTF in 501mel cells showed that it is essential for normal proliferation. To further validate the importance of BPTF in melanoma lines, we silenced its expression in a variety of melanoma cell lines including MNT, SKMel28, and 888Mel. The silencing of both MITF and BPTF in all these cell lines invariably resulted in irreversible proliferation arrest and onset of senescence, and in case of 888Mel drastic increase in cell death. The silencing of BPTF in the MITF-negative 1205LU line also resulted in arrested proliferation and changed cell morphology resembling senescence, whereas MITF silencing had no detectable effect. As these cells do not express MITF, BPTF must therefore act independently of MITF in this invasive cell line. Perhaps BPTF interacts with other transcription factors that replace MITF and are required for proliferation of these cells. Interestingly, BRG1 has also been reported to regulate melanoma progression in MITF-independent manner (Ondrusova et al. 2013) although its knockdown in 1205LU cells did not

have a notable phenotype (data not shown). This indicates a specific role of NURF complex in regulation of both proliferative and invasive-type melanoma lines.

In contrast to the above, BPTF (and MITF) silencing in a series of non-melanoma cell lines such as HeLa (cervical cancer) and H293T (immortalized human embryonic kidney) cells as well as primary BJ (foreskin) and WI38 (lung) fibroblasts had no detectable effect on their proliferation, with the exception of a mild slowing of BJ cell proliferation. BPTF is therefore not generally required for cell proliferation, in accordance with previous observations showing *Bptf*$^{-/-}$ ES and MEFs proliferate almost normally *in vitro*, and that thymocytes do not exhibit any proliferation or survival defects *in vivo* (Landry et al. 2011b, Landry et al. 2008). There is therefore no general requirement for BPTF for proliferation, but rather a specific requirement in melanoma cells.

Upon BPTF silencing, 501Mel cells adopted a morphology similar to that seen upon MITF knockdown and stained positively for senescence-associated □-galactosidase. Loss of BPTF therefore pheno-copied the silencing of MITF suggesting that they regulate an overlapping gene expression program required to maintain 501mel cell proliferation. To test this possibility, we performed RNA-sequencing of the shBPTF and shMITF cells and analyzed the overlap between the two datasets. Around 39% of shBPTF down-regulated and 41% of up-regulated genes were regulated in an analogous manner co-regulated by shMITF. Commonly down-regulated genes are involved in cell cycle and proliferation showing that BPTF and MITF cooperate to activate genes required for proliferation, In contrast, commonly up-regulated genes were involved in cell motility and cell morphology in agreement with the striking alterations in cell morphology that are observed. In order to verify if the co-regulated genes are direct MITF targets, we overlapped the commonly regulated genes with MITF ChIP-seq data to identify which of these genes are associated MITF binding sites. This analysis identified genes such as BIRC7, BCL2A1, and NPM1 that have critical roles in survival and/or in cell cycle regulation as potential direct targets whose expression is co-activated by MITF and BPTF. Similarly, The up-regulated genes with MITF binding sites

included SERPINE1, IL24, PDGFB, and CYR61 that are a part of SASP and also have roles in regulation of cell motility, along with ZEB1 that has been shown to have a crucial role in EMT (Denecker et al. 2014b). The above observations support the idea that MITF and BPTF cooperate to regulate expression of genes involved in proliferation and cell motility and development of invasive properties and that NURF is involved in the regulation of the phenotype switching process.

In order to determine if BPTF has a role in non-transformed melanocytes, we performed silencing of both BPTF and MITF in immortalized Hermes-3A cells. Silencing of either factor resulted in a strong decrease in cell proliferation and changes in cell morphology. In contrast to 501mel cells however, the phenotypic features shBPTF and shMITF cells were different. ShMITF cells show a senescence-like phenotype with rounded and flattened morphology yet <50% of these cells stain positively for senescence-associated □-galactosidase. ShBPTF cells on the other hand adopted a spindle-like bipolar morphology with reduced size. Despite this, comparison of the RNA-seq again showed a rather significant overlap between the two gene expression programs as 44% of genes repressed by shMITF are also repressed by shBPTF amongst which are several critical regulators of cell cycle. It is however noteworthy that BPTF regulates many more genes in Hermes-3A cells than in 501mel with in particular a prominent role in regulation of cell cycle genes. Nevertheless, BPTF regulates several genes critical for cell cycle in both cell types such as E2F8, CLSPN and NPM1. Similarly 37% of genes up-regulated by shMITF are also up-regulated by shBPTF and are predominantly involved in cell adhesion and morphology. Thus, similar to 501mel cells, MITF and BPTF regulate a common set of genes in Hermes-3A cells that are essential for control of proliferation and cell morphology. As we have at present no MITF ChIP-seq data for these cells, we cannot identify the potential direct MITF targets in these cells.

Together, the above data show that BPTF plays a specific and essential role in cells of the melanocyte lineage *in vitro* and that MITF and BPTF cooperate to both positively and

negatively regulate a set of target genes that controls the critical switch between the proliferative and invasive states. In the future it will be interesting to investigate the expression of BPTF in human tumour samples to confirm this idea, an experiment that is not possible with currently available antibodies.

Bptf is essential for normal function of murine melanocyte stem cells.

The above data from in vitro experiments prompted us to investigate the role of Bptf using somatic inactivation in the melanocyte lineage *in vivo*. While, BPTF was essential for proliferation of Hermes melanocytes *in vitro*, *in vivo* loss of Bptf had a more subtle effect on developing melanoblasts. At E15.5 a mild decrease in the ventral melanoblast count is seen, but there is no difference in the migration front of the melanoblasts when compared to the control. At E16.5, approximately the time when the lateral migration fronts meet on the belly center and migration is considered to be complete, we observed an around 20% reduction in the number of melanocytes and a less advanced migration front. Additionally, at E16.5, clusters of melanoblasts are observed in developing hair follicles of $Bptf^{lox/+}$ mice. The KIT/KITL signaling pathway guides melanoblast migration to the hair follicles (Jordan and Jackson 2000). These clusters are much less pronounced in the $Bptf^{mel-/-}$ mice. This may result from the diminished proliferation and/or migration of the melanoblasts or a more specific defect in their ability to respond to the KIT signaling pathway, or a combination of these factors. As a result of these embryonic defects, newborn $Bptf^{mel-/-}$ animals display mild greying on the back and a substantially lighter belly, with an occasional belly spot. In the mutant, the pigmentation pattern of the paws of the P10 animals suggests that migration arrested around E16.5.

The first cycle of hair growth pigmented by embryonic melanoblasts that colonize the developing hair follicles reflects these changes with an almost normal dorsal black coat, but a grayer ventral coat. However, by 3-4 weeks at the stage of the second anagen phase, the

mutant animals show progressive greying. The greying is accentuated by 5-6 weeks when almost all the first coat has been exchanged. Depilation of 3 week-old animal results in the growth of completely white hair indicating that mutant animals are unable to generate pigmentation for the hair of the second anagen. Immunostaining with antibodies against Dct and Sox10 as well as LacZ staining indicated a progressive loss of differentiated melanocytes in the bulb that was already evident by 3 weeks.

In contrast to the first anagen where pigmentation comes embryonic melanoblasts (Nishimura 2011), the melanocytes that provide pigmentation at the second anagen are derived from post-natal MSCs. The inability of the mutant mice to pigment the hair from the second anagen phase suggests that in the absence of Bptf, either the MSC population is missing or that MSCs are unable to respond to signals that induce their proliferation and/or differentiation at anagen. Examination of the Bptf mutant animals with the Dct-LacZ reporter revealed the presence of LacZ-positive cells in the bulge region of the hair follicle at P10 and at all subsequent stages including as late as 1 year when the mice have been completely white for 4-5 months. This observation suggests that the defect in the Bptf animals is not a result of the loss of the MSC population, but rather reflects a defect in their ability to give rise to differentiated progeny. The possible defects that would account for this phenotype are i) the MSCs are refractory to the activation signals in anagen, ii) MSCs respond to activation signals, but give rise to TACs that are unable to continue proliferation and/or are not able to differentiate. Immunostaining of hair follicles with differentiation markers such as Sox10 and Mitf, as well as LacZ staining, suggests that if such TACs arise they do not express these markers and thus it is impossible to determine whether such defective cells indeed exist. To better address this question, we are currently examining the LacZ staining at various times following depilation to determine whether we can observe a transient increase in the number of LacZ positive cells in the bulge region and/or the transient existence of TACs that initiate their migration towards the bulb. We are also performing BrdU-labeling at this stage in order

to investigate whether the LacZ-positive cells seen in the mutant bulge region are really label retaining stem cells.

At anagen, MSCs are induced to proliferate and differentiate by several signaling pathways. The KIT/KITL pathway serves as an activation signal from the niche to initiate their proliferation (Nishimura et al. 2002, Osawa et al. 2005). As the embryonic melanoblasts showed diminished colonization of the developing hair follicles that also requires response to this pathway, it is possible that Bptf is required to act downstream of KIT signaling by regulating target gene expression.

MSCs are also activated by Wnt signaling. At anagen, Ctnnb1 becomes nuclear in both epidermal stem cells (EpSCs) and MSCs indicating activation of the Wnt signaling pathway in both of these cell populations (Rabbani et al. 2011). Constitutive nuclear expression of Ctnnb1 in MSCs leads to a premature differentiation of the MSCs resulting in loss of the MSC population. On the other hand, deletion of Ctnnb1 in melanocytes results in a loss of differentiated progeny and hair greying, but the MSC population is maintained. This phenotype is very similar to what is observed here, although we note that the greying is much faster and more complete upon inactivation of Bptf, that upon Ctnnb1 inactivation. These observations suggest that Bptf may act downstream of the Wnt signaling pathway as observation reminiscent of the situation in Drosophila where NURF is required for Wnt signaling (Song, Spichiger-Haeusermann and Basler 2009). We are currently testing this possibility by immunostaining to determine whether Ctnnb1 localizes to the nucleus of mutant MSCs at anagen phase. If nuclear localization were observed this would indicate that Wnt signaling is activated but Bptf is again required downstream to active target genes. We also cannot exclude that Bptf plays a role in both of these pathways giving rise to a strong phenotype.

Another possibility is that Bptf is required to establish a functional MSC population, but is not required at later stages. This interesting possibility is suggested by our preliminary results using Cre-ER^{T2} transgenics to inactivate Bptf both immediately after birth and in adult

animals. The Cre-ER^{T2} transgene drives inactivation in TACs and differentiated melanocytes, but does not appear to be active in adult MSCs, although it may be active in neonatal MSCs (Yajima et al. 2006). Tamoxifen injection of 10 week-old animals from day 1 to day 8 following depilation has no effect on pigmentation either on the newborn hair or at subsequent cycles (our unpublished data). This is an important observation showing that Bptf is not required for the differentiation of TACs into mature melanocytes or for the function of mature melanocytes. This is a surprising observation in view of the *in vitro* results where BPTF was required for the proliferation of both human melanoma cells and melanocytes and it does not support the idea that BPTF acts as a cofactor for MITF in melanocytes *in vivo*. More intriguingly, application of hydroxy-tamoxifen to the backs of animals from P1 to P5 to inactivate Bptf in neonatal MSCs and the resident melanoblasts had no appreciable effect on pigmentation as these animals grew and maintained a black coat (our unpublished data). The fact that these animals grew a first black coat confirms the idea that Bptf is not required for function of mature melanocytes. More intriguingly, as these animals maintained a black coat into adulthood, the MSC population is not affected. If indeed the Tyr::Cre-ER^{T2} transgene is active in neonatal MSCs, these observations suggest that Bptf may be required during embryogenesis to program the MSCs such that they function normally in post-natal animals, but that loss of Bptf in MSCs just after birth does not affect their function. Verification of this hypothesis is however complicated by the lack of a Bptf antibody good enough to perform immunostaining on the epidermal sections. We are therefore currently unable to verify if indeed Bptf has been inactivated in the MSCs in these animals.

In previous models, premature greying was ascribed to a progressive loss of the stem cell population (Nishimura et al. 2005). For example, targeted ablation of Bcl2 in the melanocyte lineage results in loss of the MSC population showing that it is required for their survival (McGill et al. 2002). Similarly, melanocyte-specific knockout of Notch pathway components also shows the requirement of this pathway to maintain the MSC population (Osawa and Fisher 2008, Schouwey et al. 2009, Kumano et al. 2008). Bptf knockout on the

other hand results in a MSC population that persists throughout life, but is unable to give rise to differentiated progeny. Thus, irrespective of the underlying molecular mechanism, the phenotype observed here is unique and distinct from of previous mutants.

En Français: DISCUSION ET PERSPECTIVES

BPTF / NURF a un rôle essentiel et spécifique dans les cellules de mélanome in vitro.

MITF régule un ensemble de gènes contrôlant les multiples aspects de la biologie des mélanocytes et des mélanomes. Pour comprendre comment MITF régule la transcription, nous avons utilisé la méthode TAP et la spectrométrie de masse pour identifier les partenaires d'interaction de MITF. Parmi ces co-facteurs potentiels, nous avons concentré notre attention sur deux complexes de remodelage de la chromatine qui sont BRG1 et NURF dont plusieurs sous-unités étaient présentes dans l'interactome de MITF. Nous montrons que MITF interagit avec des complexes contenant BRG1 qui comprend CDH7, et remarquons l'absence de ARID1 et ARID2. MITF recrute BRG1 dans le génome des cellules 501Mel pour réguler un ensemble de gènes impliqués dans la formation de lysosomes, dans le cycle cellulaire et dans la pigmentation. Pour NURF, nous avons détecté des peptides pour BPTF, SNF2H et SNF2L avec RBBP4, bien que RBBP4 soit présent dans plusieurs autres complexes associés à la chromatine (Loyola et Almouzni 2004). Nous n'avons pas détecté les sous-unités BAP18 et HMG2L1. Il se peut qu'un petit nombre de peptides de ces protéines ai été manqué dans la spectrométrie de masse ou ils ne font pas partie du complexe dans les cellules 501Mel. Ceci reste à déterminer. Aussi lorsque nous détectons les sous-unités de NURF dans l'interactome de MITF, ceux qui interagissent directement avec MITF restent à déterminer.

Bien que les sous-unités de BRG1 ont été détectés à la fois dans la fraction soluble et la chromatine nucléaire associée, les sous-unités de NURF ont été détectés seulement dans la fraction associée à la chromatine. Cela a été confirmé par des expériences d'immunoblot. MITF et NURF interagissent uniquement sur la chromatine. Jusqu'ici, nous avons été incapables de générer un anticorps BPTF utilisable en ChIP, ce qui nous permettrait d'identifier les sites sur le génome où MITF et BPTF co-localisent. Dans le cas de BRG1, nous avons constaté que MITF et BRG1 sont co-localisés au niveau du TSS et dans des régions plus distales. Cependant, il a été montré précédemment que BPTF localise presque uniquement à au niveau du TSS en vertu des interactions entre son PHD et bromo-domaines avec la modification des histones au TSS (Ruthenburg et al., 2011). En effet, nous avons identifié un ensemble de promoteurs où MITF se lie à proximité du TSS et où il pourrait interagir avec BPTF. Cependant, les expériences de ChIP-seq BPTF ci-dessus ont été effectuées avec une protéine tronquée ne contenant que le PHD et bromo-domaines et donc

il reste possible que BPTF peut être recruté à d'autres régions du génome, non par interaction avec les marques de la chromatine, mais par des interactions avec des activateurs de la transcription.

L'interaction entre MITF et BPTF suggère que BPTF / NURF agit comme un cofacteur pour MITF dans les cellules de mélanome. Ici, nous apportons la preuve que BPTF joue un rôle important dans les cellules de la lignée de mélanocytes in vitro et in vivo chez la souris. Comme BPTF est jusqu'à présent considéré comme exclusif au complexe NURF (Alkhatib et Landry 2011), les effets observés lors de son extinction sont susceptibles de refléter la perte de l'activité de NURF dans le remodelage de la chromatine, une idée soutenue par le fait que l'inhibition de SNF2H et SNF2L, les sous-unités catalytiques de NURF, ont des phénotypes similaires à celui de BPTF. Néanmoins, comme ces sous-unités sont présentes dans d'autres complexes de remodelage de la chromatine (Voss et Hager 2014, Swygert et Peterson 2014), la perte de leur fonction reflète plus que celle de NURF seul.

L'extinction de BPTF par ShRNA dans les cellules 501mel a montré qu'il est essentiel pour la prolifération normale. Pour valider en outre l'importance de BPTF dans des lignées de mélanome, nous avons inhibé son expression dans une variété de lignées cellulaires de mélanome, y compris MNT, SKMel28, et 888Mel. L'inactivation à la fois de MITF et de BPTF dans toutes ces lignées cellulaires a entraîné un arrêt de la prolifération et de façon irréversible un début de sénescence, et dans le cas des cellules 888Mel, nous observons une augmentation drastique de la mort cellulaire. L'inhibition de BPTF dans la lignée de 1205Lu, MITF-négatives, a également entraîné un arrêt de la prolifération ainsi qu'un changement de la morphologie des cellules, semblable à de la sénescence, alors que l'inhibition de MITF n'a eu aucun effet détectable. Comme ces cellules n'expriment pas MITF, BPTF doit donc agir indépendamment de MITF dans cette lignée cellulaire invasive. Peut-être que BPTF interagit avec d'autres facteurs de transcription qui remplacent MITF et qui sont nécessaires pour la prolifération de ces cellules. De manière intéressante, BRG1 a également été rapporté pour réguler la progression du mélanome d'une manière indépendante de MITF (Ondrušová et al. 2013), bien que son effet drastique dans les cellules 1205Lu n'entraine pas un phénotype notable (données non présentées). Cela indique un rôle spécifique du complexe NURF dans la régulation de la prolifération dans ces deux lignes de mélanome de type invasif.

Contrairement à ce qui précède, l'inhibition de BPTF (et MITF) dans une série de lignées cellulaires non-mélanome telles que les cellules HeLa (cancer du col utérin) et H293T (immortalisée de rein embryonnaire humain), les cellules ainsi que BJ primaire (prépuce) et les cellules de fibroblastes WI38 (poumon) n'ont eu aucun effet détectable sur la

prolifération, à l'exception d'un léger ralentissement de la prolifération des cellules BJ. BPTF ne serait donc pas nécessaire à la prolifération cellulaire, ce qui confirme les observations antérieures montrant que Bptf - / - dans les cellules ES et les MEF prolifèrent presque normalement in vitro, et que les thymocytes ne présentent pas de défauts de prolifération ou de survie in vivo (Landry et al 2011b, Landry. et al., 2008). Il n'y a donc pas d'effet général de BPTF dans la prolifération, mais plutôt une action spécifique dans les cellules de mélanome.

Les cellules 501Mel inhibées pour BPTF adoptent une morphologie similaire à celle observée lors du knockdown de MITF. Ces cellules sont colorées positivement à la b-galactosidase ce qui détermine la sénescence. La perte de BPTF mime donc l'inhibition de MITF suggérant ainsi qu'ils règlent un programme d'expression génique nécessaire au maintien de la prolifération des cellules 501mel. Pour tester cette possibilité, nous avons réalisé le séquençage d'ARN des cellules shBPTF et shMITF et avons analysé les deux ensembles de données. 39% des gènes down-régulés dans les cellules shBPTF sont co-régulées dans le cas des shMITF et 41% des gènes up-régulés le sont également. Les gènes communs down-régulés sont impliqués dans le cycle cellulaire et la prolifération, indiquant que BPTF et MITF coopèrent pour activer des gènes nécessaires à la prolifération, à l'inverse, les gènes up-régulés sont impliqués dans la motilité cellulaire et la morphologie des cellules. Afin de vérifier si les gènes co-régulés sont des cibles directes de MITF, nous avons analysé les gènes communs avec des données de ChIP-seq MITF afin d'identifier les cibles directes de MITF. Cette analyse a identifié des gènes down-régulés tels que BIRC7, BCL2A1, et NPM1 qui ont des rôles majeures dans la survie et / ou dans la régulation du cycle cellulaire comme cibles potentiels directs dont l'expression est activée à la fois par MITF et BPTF. De même, les gènes up-régulés présentant des sites de liaison pour MITF comprennent les gènes suivants : SERPINE1, IL24, PDGFB et CYR61. Ces derniers font partie de la SASP et ont également un rôle dans la régulation de la motilité cellulaire, avec notamment ZEB1 qui a été montré pour son rôle crucial dans la TEM (2014b Denecker et al.). Les observations ci-dessus soutiennent l'idée que MITF et BPTF coopèrent pour réguler l'expression de gènes impliqués dans la prolifération et la motilité cellulaire et le développement de propriétés invasives et que NURF est impliqué dans la régulation du processus de switch phénotypique.

Afin de déterminer si BPTF a un rôle dans les mélanocytes non transformées, nous avons effectué deux inhibitions pour BPTF et MITF dans les cellules immortalisées Hermes-3A. Ces inhibitions se traduisent par une forte diminution de la prolifération cellulaire et des changements dans la morphologie des cellules. Toutefois, les caractéristiques

phénotypiques des cellules shBPTF et shMITF étaient différents. Les cellules ShMITF présentent un phénotype de sénescence avec une morphologie arrondie et encore <50% de ces cellules sont colorées positivement à la b-galactosidase (sénescence). D'autre part, les cellules ShBPTF ont adopté une morphologie bipolaire avec une taille réduite. Malgré cela, la comparaison avec le RNA-seq montre que 44% des gènes réprimés par le shMITF sont également réprimée par le shBPTF. Parmi ces gènes, plusieurs sont des régulateurs critiques du cycle cellulaire. Il faut cependant noter que BPTF régule beaucoup plus de gènes dans les cellules Hermes-3A que dans les cellules 501mel avec en particulier un rôle important dans la régulation des gènes du cycle cellulaire. Néanmoins, BPTF régule plusieurs gènes critiques pour le cycle cellulaire dans les deux types cellulaires tels que E2F8, CLSPN et NPM1. De même 37% des gènes up-régulés par le shMITF le sont également par shBPTF. Ces gènes sont principalement impliqués dans l'adhésion cellulaire et dans la morphologie. Ainsi, de façon similaire aux cellules 501mel, MITF et BPTF régulent un ensemble de gènes dans les cellules Hermes-3A. Ces gènes sont essentiels pour le contrôle de la prolifération et de la morphologie cellulaire. Comme nous n'avons pas à l'heure actuelle de données de ChIP-seq MITF pour ces cellules, nous ne pouvons pas identifier les cibles MITF directs potentiels dans ces cellules.

L'ensemble de ces données ci-dessus, montre que BPTF joue un rôle précis et essentiel dans les cellules de la lignée de mélanocytes in vitro et que MITF et BPTF coopèrent à la fois positivement et négativement pour la régulation d'un ensemble de gènes cibles qui contrôlent le switch entre les processus de prolifération et d'invasion. Dans l'avenir, il sera intéressant d'étudier l'expression de BPTF dans des échantillons de tumeurs humaines pour confirmer cette idée ; une expérience qui n' est pas possible avec les anticorps actuellement disponibles.

Bptf est essentiel pour la fonction normale des cellules souches des mélanocytes murins.

Les données ci-dessus à partir des expériences in vitro nous ont incitées à étudier le rôle de Bptf dans la lignée de mélanocytes in vivo. Bien que BPTF soit essentiel pour la prolifération des mélanocytes dans les cellules Hermes in vitro, in vivo, Bptf a un effet plus subtil sur dans le développement des mélanoblastes. A E15.5 une légère diminution dans le nombre de mélanoblastes ventral est vue, mais il n'y a pas de différence dans le front de migration des mélanoblastes par rapport au contrôle. A E16,5, environ le temps où les fronts migratoires latéraux se rencontrent sur le centre du ventre ; la migration est considérée comme complète, nous avons observé une réduction d'environ 20% dans le nombre de mélanocytes et un front de migration moins avancé. En outre, à E16,5, des groupes de mélanoblastes sont observés dans le développement de follicules pileux de souris Bptflox /

+. La voie de signalisation KIT / KITL guide la migration des mélanoblastes depuis les follicules pileux (la Jordanie et Jackson, 2000). Ces groupes sont beaucoup moins prononcés dans les souris Bptfmel - / -. Cela peut résulter de la prolifération et / ou d'une diminution de la migration des mélanoblastes ou d'un défaut quant à leur capacité à répondre à la voie de signalisation de KIT, ou une combinaison de ces facteurs. En raison de ces défauts embryonnaires, les nouveau-nés Bptfmel - / - affichent un léger grisonnement sur le dos et un ventre nettement plus claire, avec une tache sur le ventre occasionnelle. Chez le mutant, le motif de la pigmentation des pattes des animaux P10 suggère que la migration s'arrête autour de E16,5.

Le premier cycle de croissance des poils pigmentés par les mélanoblastes embryonnaires qui colonisent les follicules pileux en développement, reflète ces changements avec un manteau dorsal noir presque normale, mais une couche ventrale grise. Cependant, en 3-4 semaines à l'étape de la deuxième phase anagène, les animaux mutants montrent un grisonnement progressif. Le grisonnement est accentuée après 5-6 semaines, lorsque la quasi-totalité de la première couche a été échangée.' L'épilation des animaux âgés de 3 semaines montre que le pelage des souris est complètement blancs indiquant que les animaux mutants sont incapables de générer la pigmentation des poils dans la seconde phase anagène. Les Immunomarquages avec des anticorps contre Dct et Sox10 ainsi que la coloration LacZ indiquent une perte progressive des mélanocytes différenciés dans le bulbe qui était déjà évident en trois semaines.

Contrairement à la première phase anagène où la pigmentation est issue des mélanoblastes embryonnaires (Nishimura 2011), les mélanocytes qui fournissent la pigmentation à la seconde phase anagène sont dérivés de cellules souches mésenchymateuses post-natales. L'incapacité des souris mutantes pour pigmenter les poils de la seconde phase anagène suggère qu'en l'absence de Bptf, soit la population de MSC est manquante ou que les MSC sont incapables de répondre à des signaux qui induisent la prolifération et / ou différenciation à la phase anagène. L'examen des animaux mutants Bptf avec le reporter Dct-LacZ révéle la présence de cellules LacZ-positives dans la région de renflement du follicule pileux au P10 et à toutes les étapes ultérieures, y compris 1 année plus tard lorsque les souris sont complètement blanches à partir de 4-5 mois. Cette observation suggère que l'anomalie chez les animaux Bptf n'est pas un résultat de la perte de la population MSC, mais reflète plutôt un défaut dans leur capacité de donner lieu à une descendance différenciée. Les hypothèses susceptibles d'expliquer ce phénotype sont: i) les cellules souches mésenchymateuses sont réfractaires aux signaux d'activation en phase anagène, ii) les cellules souches mésenchymateuses réagissent aux signaux d'activation, mais donnent lieu à des TAC qui

sont incapables de poursuivre la prolifération et / ou ne sont pas capables de se différencier. L'immunomarquage des follicules pileux avec des marqueurs de différenciation tels que Sox10 et Mitf, ainsi que la coloration LacZ, suggère que si ces TAC surviennent, ils n'expriment pas ces marqueurs et il est donc impossible de déterminer si ces cellules défectueuses existent bel et bien. Pour mieux répondre à cette question, nous examinons actuellement la coloration LacZ à divers moments suivants l'épilation pour déterminer si nous pouvons observer une augmentation transitoire du nombre de cellules positives LacZ dans la région de renflement et / ou l'existence transitoire des cellules TAC qui initient leur migration vers le bulbe. Nous allons effectuer des marquages au BrdU à ce stade afin de vérifier si les cellules LacZ-positives observées dans la région de renflement des mutants sont vraiment des cellules souches.

A la phase anagène, les MSC sont induites à proliférer et à se différencier par plusieurs voies de signalisation. La voie KIT / KITL sert de signal d'activation pour initier leur prolifération (Nishimura et al. 2002, Osawa et al., 2005). Comme les mélanoblastes embryonnaires ont montré une diminution de la colonisation des follicules pileux en développement qui nécessite également la réponse à cette voie, il est possible que Bptf est nécessaire pour agir en aval de la signalisation de KIT en régulant l'expression du gène cible.

Les cellules MSC sont également activées par la signalisation Wnt. A la phase anagène, CTNNB1 devient nucléaire dans les cellules souches épidermiques (les EPSCs MSC) ce qui indique l'activation de la voie de signalisation Wnt dans ces deux populations cellulaires (Rabbani et al., 2011). L'expression constitutive de CTNNB1 nucléaire dans les MSC conduit à une différenciation précoce des cellules souches mésenchymateuses qui entraîne la perte de la population des MSC. D'autre part, la suppression de CTNNB1 dans les mélanocytes se traduit par une perte de la progéniture différenciée et le grisonnement des poils, mais la population des MSC est maintenue. Ce phénotype est très similaire à ce qui est observé ici, même si nous notons que le grisonnement est beaucoup plus rapide et plus complet sur l'inactivation de Bptf, que lors de l'inactivation de CTNNB1. Ces observations suggèrent que Bptf peut agir en aval de la voie de signalisation Wnt, ce qui rappelle ainsi la situation observée chez la drosophile où NURF est nécessaire pour la signalisation Wnt (Song, Spichiger-Haeusermann et Basler 2009). Nous testons actuellement cette possibilité par immunomarquage pour déterminer si CTNNB1 se localise dans le noyau des cellules souches mésenchymateuses mutantes à la phase anagène. Si une localisation nucléaire est observée, cela indiquerait que la signalisation Wnt est activée mais que Bptf est encore

nécessaire en aval des gènes cibles. Nous ne pouvons pas exclure que Bptf joue un rôle dans ces deux voies donnant lieu à un fort phénotype.

Une autre possibilité est que Bptf est nécessaire pour établir une population de MSC fonctionnelle, mais n'est pas nécessaire à un stade ultérieur. Cette possibilité intéressante est suggérée par nos résultats préliminaires utilisant les souris transgéniques Cre-ERT2 pour inactiver Bptf immédiatement après la naissance et chez les animaux adultes. Le transgène Cre-ERT2 entraîne l'inactivation des TAC et des mélanocytes différenciés, mais ne semble pas être actif dans les MSC adultes, bien qu'il puisse être actif dans les MSC néonatales (Yajima et al., 2006). L'injection de Tamoxifène dans des animaux âgés de 10 semaines du jour 1 au jour 8 après épilation n'a pas d'effet sur la pigmentation soit sur les poils des nouveau-nés ou à des cycles ultérieurs (données non publiées). Ceci est une observation importante montrant que Bptf n'est pas nécessaire pour la différenciation des TAC dans les mélanocytes matures ou pour la fonction de mélanocytes matures. Cette observation est surprenante compte tenu des résultats in vitro où BPTF est nécessaire pour la prolifération des cellules et des mélanocytes de mélanome humain et elle ne supporte pas l'idée que BPTF agit comme cofacteur pour MITF dans les mélanocytes in vivo. Plus curieusement, l'application de hydroxy-tamoxifène sur le dos des animaux de P1 à P5 pour inactiver Bptf dans les MSC néonatales et les mélanoblastes résidents n'a eu aucun effet notable sur la pigmentation et ces animaux ont grandi et ont maintenu un manteau noir (données non publiées). Le fait que ces animaux présentent un premier manteau noir confirme l'idée que Bptf n'est pas nécessaire pour la fonction des mélanocytes matures. Plus curieusement, car ces animaux ont maintenu un manteau noir à l'âge adulte, la population des MSC n'est pas affectée. En effet, si le transgène Tyr :: Cre-ERT2 est active dans les MSC néonatales, ces observations suggèrent que Bptf peut être nécessaire lors de l'embryogenèse pour programmer les cellules souches mésenchymateuses telles qu'elles fonctionnent normalement chez les animaux postnataux, mais que la perte de Bptf dans les MSC juste après la naissance n'affecte pas leur fonction. La vérification de cette hypothèse est toutefois compliquée par l'absence d'un anticorps Bptf pour réaliser des immunomarquages sur les sections de l'épiderme. Nous ne sommes donc actuellement pas en mesure de vérifier si effectivement Bptf a été inactivé dans les cellules souches mésenchymateuses dans ces animaux.

Dans les modèles précédents, le vieillissement prématuré a été attribuée à une perte progressive de la population de cellules souches (Nishimura et al., 2005). Par exemple, l'ablation de Bcl2 dans des mélanocytes de la population MSC montre qu'il est nécessaire pour leur survie (McGill et al., 2002). De même, un KO spécifique dans les mélanocytes de

de la voie Notch montre également l'importance de cette voie pour maintenir la population de MSC (Osawa et Fisher 2008, Schouwey et al. 2009, Kumano et al., 2008). Le KO de Bptf d'autre part résulte dans une population de MSC qui persiste toute la vie, mais est incapable de donner lieu à une descendance différenciée. Ainsi, quel que soit le mécanisme moléculaire sous-jacent, le phénotype observé ici est unique et distinct des mutants.

REFERENCES

Abdel-Malek, Z. A., A. L. Kadekaro & V. B. Swope (2010) Stepping up melanocytes to the challenge of UV exposure. *Pigment Cell Melanoma Res,* 23**,** 171-86.

Ables, E. T. & D. Drummond-Barbosa (2010) The steroid hormone ecdysone functions with intrinsic chromatin remodeling factors to control female germline stem cells in Drosophila. *Cell Stem Cell,* 7**,** 581-92.

Ackermann, J., M. Frutschi, K. Kaloulis, T. McKee, A. Trumpp & F. Beermann (2005) Metastasizing melanoma formation caused by expression of activated N-RasQ61K on an INK4a-deficient background. *Cancer Res,* 65**,** 4005-11.

Adameyko, I., F. Lallemend, J. B. Aquino, J. A. Pereira, P. Topilko, T. Muller, N. Fritz, A. Beljajeva, M. Mochii, I. Liste, D. Usoskin, U. Suter, C. Birchmeier & P. Ernfors (2009) Schwann cell precursors from nerve innervation are a cellular origin of melanocytes in skin. *Cell,* 139**,** 366-79.

Adameyko, I., F. Lallemend, A. Furlan, N. Zinin, S. Aranda, S. S. Kitambi, A. Blanchart, R. Favaro, S. Nicolis, M. Lubke, T. Muller, C. Birchmeier, U. Suter, I. Zaitoun, Y. Takahashi & P. Ernfors (2012) Sox2 and Mitf cross-regulatory interactions consolidate progenitor and melanocyte lineages in the cranial neural crest. *Development,* 139**,** 397-410.

Aksan, I. & C. R. Goding (1998) Targeting the microphthalmia basic helix-loop-helix-leucine zipper transcription factor to a subset of E-box elements in vitro and in vivo. *Mol Cell Biol,* 18**,** 6930-8.

Alexaki, V. I., D. Javelaud, L. C. Van Kempen, K. S. Mohammad, S. Dennler, F. Luciani, K. S. Hoek, P. Juarez, J. S. Goydos, P. J. Fournier, C. Sibon, C. Bertolotto, F. Verrecchia, S. Saule, V. Delmas, R. Ballotti, L. Larue, P. Saiag, T. A. Guise & A. Mauviel (2010) GLI2-mediated melanoma invasion and metastasis. *J Natl Cancer Inst,* 102**,** 1148-59.

Alkhatib, S. G. & J. W. Landry (2011) The nucleosome remodeling factor. *FEBS Lett,* 585**,** 3197-207.

Alonso, L. & E. Fuchs (2006) The hair cycle. *J Cell Sci,* 119**,** 391-3.

Aoki, H. & O. Moro (2002) Involvement of microphthalmia-associated transcription factor (MITF) in expression of human melanocortin-1 receptor (MC1R). *Life Sci,* 71**,** 2171-9.

Arents, G., R. W. Burlingame, B. C. Wang, W. E. Love & E. N. Moudrianakis (1991) The nucleosomal core histone octamer at 3.1 A resolution: a tripartite protein assembly and a left-handed superhelix. *Proc Natl Acad Sci U S A,* 88**,** 10148-52.

Arozarena, I., H. Bischof, D. Gilby, B. Belloni, R. Dummer & C. Wellbrock (2011) In melanoma, beta-catenin is a suppressor of invasion. *Oncogene,* 30**,** 4531-43.

Artandi, S. E. & R. A. DePinho (2000) Mice without telomerase: what can they teach us about human cancer? *Nat Med,* 6**,** 852-5.

Artandi, S. E. & R. A. DePinho (2010) Telomeres and telomerase in cancer. *Carcinogenesis,* 31**,** 9-18.

Aubin-Houzelstein, G., J. Djian-Zaouche, F. Bernex, S. Gadin, V. Delmas, L. Larue & J. J. Panthier (2008) Melanoblasts' proper location and timed differentiation depend on Notch/RBP-J signaling in postnatal hair follicles. *J Invest Dermatol,* 128**,** 2686-95.

Badenhorst, P., M. Voas, I. Rebay & C. Wu (2002) Biological functions of the ISWI chromatin remodeling complex NURF. *Genes Dev,* 16**,** 3186-98.

Badenhorst, P., H. Xiao, L. Cherbas, S. Y. Kwon, M. Voas, I. Rebay, P. Cherbas & C. Wu (2005) The Drosophila nucleosome remodeling factor NURF is required for Ecdysteroid signaling and metamorphosis. *Genes Dev,* 19**,** 2540-5.

Bai, X., E. Larschan, S. Y. Kwon, P. Badenhorst & M. I. Kuroda (2007) Regional control of chromatin organization by noncoding roX RNAs and the NURF remodeling complex in Drosophila melanogaster. *Genetics,* 176**,** 1491-9.

Balaji, S., L. M. Iyer & L. Aravind (2009) HPC2 and ubinuclein define a novel family of histone chaperones conserved throughout eukaryotes. *Mol Biosyst,* 5**,** 269-75.

Balbas-Martinez, C., A. Sagrera, E. Carrillo-de-Santa-Pau, J. Earl, M. Marquez, M. Vazquez, E. Lapi, F. Castro-Giner, S. Beltran, M. Bayes, A. Carrato, J. C. Cigudosa, O. Dominguez, M. Gut, J. Herranz, N. Juanpere, M. Kogevinas, X. Langa, E. Lopez-Knowles, J. A. Lorente, J. Lloreta, D. G. Pisano, L. Richart, D. Rico, R. N. Salgado, A. Tardon, S. Chanock, S. Heath, A. Valencia, A. Losada, I. Gut, N. Malats & F. X. Real (2013) Recurrent inactivation of STAG2 in bladder cancer is not associated with aneuploidy. *Nat Genet,* 45**,** 1464-9.

Bannister, A. J. & T. Kouzarides (2011) Regulation of chromatin by histone modifications. *Cell Res,* 21**,** 381-95.

Bao, Y. & X. Shen (2007) INO80 subfamily of chromatin remodeling complexes. *Mutat Res,* 618**,** 18-29.

Bao, Y. & X. Shen (2011) SnapShot: Chromatin remodeling: INO80 and SWR1. *Cell,* 144**,** 158-158 e2.

Barak, O., M. A. Lazzaro, W. S. Lane, D. W. Speicher, D. J. Picketts & R. Shiekhattar (2003) Isolation of human NURF: a regulator of Engrailed gene expression. *EMBO J,* 22**,** 6089-100.

Bastian, B. C. (2003) Understanding the progression of melanocytic neoplasia using genomic analysis: from fields to cancer. *Oncogene,* 22**,** 3081-6.

Baynash, A. G., K. Hosoda, A. Giaid, J. A. Richardson, N. Emoto, R. E. Hammer & M. Yanagisawa (1994) Interaction of endothelin-3 with endothelin-B receptor is essential for development of epidermal melanocytes and enteric neurons. *Cell,* 79**,** 1277-85.

Becker, T. M., S. Haferkamp, M. K. Dijkstra, L. L. Scurr, M. Frausto, E. Diefenbach, R. A. Scolyer, D. N. Reisman, G. J. Mann, R. F. Kefford & H. Rizos (2009) The chromatin remodelling factor BRG1 is a novel binding partner of the tumor suppressor p16INK4a. *Mol Cancer,* 8**,** 4.

Beckmann, H. & T. Kadesch (1991) The leucine zipper of TFE3 dictates helix-loop-helix dimerization specificity. *Genes Dev,* 5**,** 1057-66.

Bedford, M. T. & S. G. Clarke (2009) Protein arginine methylation in mammals: who, what, and why. *Mol Cell,* 33**,** 1-13.

Behrens, J., J. P. von Kries, M. Kuhl, L. Bruhn, D. Wedlich, R. Grosschedl & W. Birchmeier (1996) Functional interaction of beta-catenin with the transcription factor LEF-1. *Nature,* 382**,** 638-42.

Bennett, D. C. (2008) How to make a melanoma: what do we know of the primary clonal events? *Pigment Cell Melanoma Res,* 21**,** 27-38.

Bentley, D. J., C. Harrison, A. M. Ketchen, N. J. Redhead, K. Samuel, M. Waterfall, J. D. Ansell & D. W. Melton (2002) DNA ligase I null mouse cells show normal DNA repair activity but altered DNA replication and reduced genome stability. *J Cell Sci,* 115**,** 1551-61.

Berger, M. F., E. Hodis, T. P. Heffernan, Y. L. Deribe, M. S. Lawrence, A. Protopopov, E. Ivanova, I. R. Watson, E. Nickerson, P. Ghosh, H. Zhang, R. Zeid, X. Ren, K. Cibulskis, A. Y. Sivachenko, N. Wagle, A. Sucker, C. Sougnez, R. Onofrio, L. Ambrogio, D. Auclair, T. Fennell, S. L. Carter, Y. Drier, P. Stojanov, M. A. Singer, D. Voet, R. Jing, G. Saksena, J. Barretina, A. H. Ramos, T. J. Pugh, N. Stransky, M. Parkin, W. Winckler, S. Mahan, K. Ardlie, J. Baldwin, J. Wargo, D. Schadendorf, M. Meyerson, S. B. Gabriel, T. R. Golub, S. N. Wagner, E. S. Lander, G. Getz, L. Chin &

L. A. Garraway (2012) Melanoma genome sequencing reveals frequent PREX2 mutations. *Nature,* 485**,** 502-6.

Bertolotto, C., P. Abbe, T. J. Hemesath, K. Bille, D. E. Fisher, J. P. Ortonne & R. Ballotti (1998a) Microphthalmia gene product as a signal transducer in cAMP-induced differentiation of melanocytes. *J Cell Biol,* 142**,** 827-35.

Bertolotto, C., K. Bille, J. P. Ortonne & R. Ballotti (1996) Regulation of tyrosinase gene expression by cAMP in B16 melanoma cells involves two CATGTG motifs surrounding the TATA box: implication of the microphthalmia gene product. *J Cell Biol,* 134**,** 747-55.

Bertolotto, C., R. Busca, P. Abbe, K. Bille, E. Aberdam, J. P. Ortonne & R. Ballotti (1998b) Different cis-acting elements are involved in the regulation of TRP1 and TRP2 promoter activities by cyclic AMP: pivotal role of M boxes (GTCATGTGCT) and of microphthalmia. *Mol Cell Biol,* 18**,** 694-702.

Bertolotto, C., F. Lesueur, S. Giuliano, T. Strub, M. de Lichy, K. Bille, P. Dessen, B. d'Hayer, H. Mohamdi, A. Remenieras, E. Maubec, A. de la Fouchardiere, V. Molinie, P. Vabres, S. Dalle, N. Poulalhon, T. Martin-Denavit, L. Thomas, P. Andry-Benzaquen, N. Dupin, F. Boitier, A. Rossi, J. L. Perrot, B. Labeille, C. Robert, B. Escudier, O. Caron, L. Brugieres, S. Saule, B. Gardie, S. Gad, S. Richard, J. Couturier, B. T. Teh, P. Ghiorzo, L. Pastorino, S. Puig, C. Badenas, H. Olsson, C. Ingvar, E. Rouleau, R. Lidereau, P. Bahadoran, P. Vielh, E. Corda, H. Blanche, D. Zelenika, P. Galan, F. Aubin, B. Bachollet, C. Becuwe, P. Berthet, Y. J. Bignon, V. Bonadona, J. L. Bonafe, M. N. Bonnet-Dupeyron, F. Cambazard, J. Chevrant-Breton, I. Coupier, S. Dalac, L. Demange, M. d'Incan, C. Dugast, L. Faivre, L. Vincent-Fetita, M. Gauthier-Villars, B. Gilbert, F. Grange, J. J. Grob, P. Humbert, N. Janin, P. Joly, D. Kerob, C. Lasset, D. Leroux, J. Levang, J. M. Limacher, C. Livideanu, M. Longy, A. Lortholary, D. Stoppa-Lyonnet, S. Mansard, L. Mansuy, K. Marrou, C. Mateus, C. Maugard, N. Meyer, C. Nogues, P. Souteyrand, L. Venat-Bouvet, H. Zattara, V. Chaudru, G. M. Lenoir, M. Lathrop, I. Davidson, M. F. Avril, F. Demenais, R. Ballotti & B. Bressac-de Paillerets (2011) A SUMOylation-defective MITF germline mutation predisposes to melanoma and renal carcinoma. *Nature,* 480**,** 94-8.

Beser, A. R., S. Tuzlali, D. Guzey, S. Dolek Guler, S. Hacihanefioglu & N. Dalay (2007) HER-2, TOP2A and chromosome 17 alterations in breast cancer. *Pathol Oncol Res,* 13**,** 180-5.

Bismuth, K., D. Maric & H. Arnheiter (2005) MITF and cell proliferation: the role of alternative splice forms. *Pigment Cell Res,* 18**,** 349-59.

Blanpain, C., W. E. Lowry, A. Geoghegan, L. Polak & E. Fuchs (2004) Self-renewal, multipotency, and the existence of two cell populations within an epithelial stem cell niche. *Cell,* 118**,** 635-48.

Blosser, T. R., J. G. Yang, M. D. Stone, G. J. Narlikar & X. Zhuang (2009) Dynamics of nucleosome remodelling by individual ACF complexes. *Nature,* 462**,** 1022-7.

Boeger, H., J. Griesenbeck, J. S. Strattan & R. D. Kornberg (2003) Nucleosomes unfold completely at a transcriptionally active promoter. *Mol Cell,* 11**,** 1587-98.

Bogenrieder, T. & M. Herlyn (2002) Cell-surface proteolysis, growth factor activation and intercellular communication in the progression of melanoma. *Crit Rev Oncol Hematol,* 44**,** 1-15.

Bohm, M., G. Moellmann, E. Cheng, M. Alvarez-Franco, S. Wagner, P. Sassone-Corsi & R. Halaban (1995) Identification of p90RSK as the probable CREB-Ser133 kinase in human melanocytes. *Cell Growth Differ,* 6**,** 291-302.

Boissy, R. E. & J. J. Nordlund (1997) Molecular basis of congenital hypopigmentary disorders in humans: a review. *Pigment Cell Res,* 10**,** 12-24.

Bosenberg, M., V. Muthusamy, D. P. Curley, Z. Wang, C. Hobbs, B. Nelson, C. Nogueira, J. W. Horner, 2nd, R. Depinho & L. Chin (2006) Characterization of melanocyte-specific inducible Cre recombinase transgenic mice. *Genesis,* 44**,** 262-7.

Botchkareva, N. V., M. Khlgatian, B. J. Longley, V. A. Botchkarev & B. A. Gilchrest (2001) SCF/c-kit signaling is required for cyclic regeneration of the hair pigmentation unit. *FASEB J,* 15**,** 645-58.

Bowles, J., G. Schepers & P. Koopman (2000) Phylogeny of the SOX family of developmental transcription factors based on sequence and structural indicators. *Dev Biol,* 227**,** 239-55.

Bown, N., S. Cotterill, M. Lastowska, S. O'Neill, A. D. Pearson, D. Plantaz, M. Meddeb, G. Danglot, C. Brinkschmidt, H. Christiansen, G. Laureys, F. Speleman, J. Nicholson, A. Bernheim, D. R. Betts, J. Vandesompele & N. Van Roy (1999) Gain of chromosome arm 17q and adverse outcome in patients with neuroblastoma. *N Engl J Med,* 340**,** 1954-61.

Bowser, R., A. Giambrone & P. Davies (1995) FAC1, a novel gene identified with the monoclonal antibody Alz50, is developmentally regulated in human brain. *Dev Neurosci,* 17**,** 20-37.

Boye, K., J. M. Nesland, B. Sandstad, G. M. Maelandsmo & K. Flatmark (2010) Nuclear S100A4 is a novel prognostic marker in colorectal cancer. *Eur J Cancer,* 46**,** 2919-25.

Boyer, L. A., M. R. Langer, K. A. Crowley, S. Tan, J. M. Denu & C. L. Peterson (2002) Essential role for the SANT domain in the functioning of multiple chromatin remodeling enzymes. *Mol Cell,* 10**,** 935-42.

Boyer, L. A., R. R. Latek & C. L. Peterson (2004) The SANT domain: a unique histone-tail-binding module? *Nat Rev Mol Cell Biol,* 5**,** 158-63.

Bray, F., J. S. Ren, E. Masuyer & J. Ferlay (2013) Global estimates of cancer prevalence for 27 sites in the adult population in 2008. *Int J Cancer,* 132**,** 1133-45.

Breitkreutz, D., N. Mirancea & R. Nischt (2009) Basement membranes in skin: unique matrix structures with diverse functions? *Histochem Cell Biol,* 132**,** 1-10.

Britsch, S., D. E. Goerich, D. Riethmacher, R. I. Peirano, M. Rossner, K. A. Nave, C. Birchmeier & M. Wegner (2001) The transcription factor Sox10 is a key regulator of peripheral glial development. *Genes Dev,* 15**,** 66-78.

Brownell, J. E., J. Zhou, T. Ranalli, R. Kobayashi, D. G. Edmondson, S. Y. Roth & C. D. Allis (1996) Tetrahymena histone acetyltransferase A: a homolog to yeast Gcn5p linking histone acetylation to gene activation. *Cell,* 84**,** 843-51.

Budi, E. H., L. B. Patterson & D. M. Parichy (2011) Post-embryonic nerve-associated precursors to adult pigment cells: genetic requirements and dynamics of morphogenesis and differentiation. *PLoS Genet,* 7**,** e1002044.

Buganim, Y., I. Goldstein, D. Lipson, M. Milyavsky, S. Polak-Charcon, C. Mardoukh, H. Solomon, E. Kalo, S. Madar, R. Brosh, M. Perelman, R. Navon, N. Goldfinger, I. Barshack, Z. Yakhini & V. Rotter (2010) A novel translocation breakpoint within the BPTF gene is associated with a pre-malignant phenotype. *PLoS One,* 5**,** e9657.

Burgess, R. J. & Z. Zhang (2013) Histone chaperones in nucleosome assembly and human disease. *Nat Struct Mol Biol,* 20**,** 14-22.

Burridge, K. & K. Wennerberg (2004) Rho and Rac take center stage. *Cell,* 116**,** 167-79.

Busca, R. & R. Ballotti (2000) Cyclic AMP a key messenger in the regulation of skin pigmentation. *Pigment Cell Res,* 13**,** 60-9.

Bush, W. D. & J. D. Simon (2007) Quantification of Ca(2+) binding to melanin supports the hypothesis that melanosomes serve a functional role in regulating calcium homeostasis. *Pigment Cell Res,* 20**,** 134-9.

Cable, J., I. J. Jackson & K. P. Steel (1995) Mutations at the W locus affect survival of neural crest-derived melanocytes in the mouse. *Mech Dev,* 50**,** 139-50.

Caramel, J., E. Papadogeorgakis, L. Hill, G. J. Browne, G. Richard, A. Wierinckx, G. Saldanha, J. Osborne, P. Hutchinson, G. Tse, J. Lachuer, A. Puisieux, J. H. Pringle, S. Ansieau & E. Tulchinsky (2013) A switch in the expression of embryonic EMT-inducers drives the development of malignant melanoma. *Cancer Cell,* 24**,** 466-80.

Carre, C., A. Ciurciu, O. Komonyi, C. Jacquier, D. Fagegaltier, J. Pidoux, H. Tricoire, L. Tora, I. M. Boros & C. Antoniewski (2008) The Drosophila NURF remodelling and the ATAC histone acetylase complexes functionally interact and are required for global chromosome organization. *EMBO Rep,* 9**,** 187-92.

Carreira, S., J. Goodall, L. Denat, M. Rodriguez, P. Nuciforo, K. S. Hoek, A. Testori, L. Larue & C. R. Goding (2006) Mitf regulation of Dia1 controls melanoma proliferation and invasiveness. *Genes Dev,* 20**,** 3426-39.

Carvajal, R. D., C. R. Antonescu, J. D. Wolchok, P. B. Chapman, R. A. Roman, J. Teitcher, K. S. Panageas, K. J. Busam, B. Chmielowski, J. Lutzky, A. C. Pavlick, A. Fusco, L. Cane, N. Takebe, S. Vemula, N. Bouvier, B. C. Bastian & G. K. Schwartz (2011) KIT as a therapeutic target in metastatic melanoma. *JAMA,* 305**,** 2327-34.

Ceha, H. M., I. Nasser, R. H. Medema & R. J. Slebos (1998) Several noncontiguous domains of CDK4 are involved in binding to the P16 tumor suppressor protein. *Biochem Biophys Res Commun,* 249**,** 550-5.

Chabot, B., D. A. Stephenson, V. M. Chapman, P. Besmer & A. Bernstein (1988) The proto-oncogene c-kit encoding a transmembrane tyrosine kinase receptor maps to the mouse W locus. *Nature,* 335**,** 88-9.

Changolkar, L. N., C. Costanzi, N. A. Leu, D. Chen, K. J. McLaughlin & J. R. Pehrson (2007) Developmental changes in histone macroH2A1-mediated gene regulation. *Mol Cell Biol,* 27**,** 2758-64.

Chapman, P. B., A. Hauschild, C. Robert, J. B. Haanen, P. Ascierto, J. Larkin, R. Dummer, C. Garbe, A. Testori, M. Maio, D. Hogg, P. Lorigan, C. Lebbe, T. Jouary, D. Schadendorf, A. Ribas, S. J. O'Day, J. A. Sosman, J. M. Kirkwood, A. M. Eggermont, B. Dreno, K. Nolop, J. Li, B. Nelson, J. Hou, R. J. Lee, K. T. Flaherty & G. A. McArthur (2011) Improved survival with vemurafenib in melanoma with BRAF V600E mutation. *N Engl J Med,* 364**,** 2507-16.

Cherry, C. M. & E. L. Matunis (2010) Epigenetic regulation of stem cell maintenance in the Drosophila testis via the nucleosome-remodeling factor NURF. *Cell Stem Cell,* 6**,** 557-67.

Chiaverini, C., L. Beuret, E. Flori, R. Busca, P. Abbe, K. Bille, P. Bahadoran, J. P. Ortonne, C. Bertolotto & R. Ballotti (2008) Microphthalmia-associated transcription factor regulates RAB27A gene expression and controls melanosome transport. *J Biol Chem,* 283**,** 12635-42.

Chien, A. J., E. C. Moore, A. S. Lonsdorf, R. M. Kulikauskas, B. G. Rothberg, A. J. Berger, M. B. Major, S. T. Hwang, D. L. Rimm & R. T. Moon (2009) Activated Wnt/beta-catenin signaling in melanoma is associated with decreased proliferation in patient tumors and a murine melanoma model. *Proc Natl Acad Sci U S A,* 106**,** 1193-8.

Chin, L., J. Pomerantz & R. A. DePinho (1998) The INK4a/ARF tumor suppressor: one gene--two products--two pathways. *Trends Biochem Sci,* 23**,** 291-6.

Choi, J. S., L. T. Zheng, E. Ha, Y. J. Lim, Y. H. Kim, Y. P. Wang & Y. Lim (2006) Comparative genomic hybridization array analysis and real-time PCR reveals genomic copy number alteration for lung adenocarcinomas. *Lung,* 184**,** 355-62.

Clapier, C. R. & B. R. Cairns (2009) The biology of chromatin remodeling complexes. *Annu Rev Biochem,* 78**,** 273-304.

Clapier, C. R., G. Langst, D. F. Corona, P. B. Becker & K. P. Nightingale (2001) Critical role for the histone H4 N terminus in nucleosome remodeling by ISWI. *Mol Cell Biol,* 21**,** 875-83.

Clapier, C. R., K. P. Nightingale & P. B. Becker (2002) A critical epitope for substrate recognition by the nucleosome remodeling ATPase ISWI. *Nucleic Acids Res,* 30**,** 649-55.

Clark, W. H., Jr., L. From, E. A. Bernardino & M. C. Mihm (1969) The histogenesis and biologic behavior of primary human malignant melanomas of the skin. *Cancer Res,* 29**,** 705-27.

Clevers, H. & R. Nusse (2012) Wnt/beta-catenin signaling and disease. *Cell,* 149**,** 1192-205.

Collins, N., R. A. Poot, I. Kukimoto, C. Garcia-Jimenez, G. Dellaire & P. D. Varga-Weisz (2002) An ACF1-ISWI chromatin-remodeling complex is required for DNA replication through heterochromatin. *Nat Genet,* 32**,** 627-32.

Copeland, N. G., D. J. Gilbert, B. C. Cho, P. J. Donovan, N. A. Jenkins, D. Cosman, D. Anderson, S. D. Lyman & D. E. Williams (1990) Mast cell growth factor maps near the steel locus on mouse chromosome 10 and is deleted in a number of steel alleles. *Cell,* 63**,** 175-83.

Corona, D. F., G. Langst, C. R. Clapier, E. J. Bonte, S. Ferrari, J. W. Tamkun & P. B. Becker (1999) ISWI is an ATP-dependent nucleosome remodeling factor. *Mol Cell,* 3**,** 239-45.

Corre, S., A. Primot, E. Sviderskaya, D. C. Bennett, S. Vaulont, C. R. Goding & M. D. Galibert (2004) UV-induced expression of key component of the tanning process, the POMC and MC1R genes, is dependent on the p-38-activated upstream stimulating factor-1 (USF-1). *J Biol Chem,* 279**,** 51226-33.

Corry, G. N. & D. A. Underhill (2005) Pax3 target gene recognition occurs through distinct modes that are differentially affected by disease-associated mutations. *Pigment Cell Res,* 18**,** 427-38.

Cosgrove, M. S., J. D. Boeke & C. Wolberger (2004) Regulated nucleosome mobility and the histone code. *Nat Struct Mol Biol,* 11**,** 1037-43.

Cosgrove, M. S. & C. Wolberger (2005) How does the histone code work? *Biochem Cell Biol,* 83**,** 468-76.

Costanzi, C. & J. R. Pehrson (1998) Histone macroH2A1 is concentrated in the inactive X chromosome of female mammals. *Nature,* 393**,** 599-601.

Costin, G. E. & V. J. Hearing (2007) Human skin pigmentation: melanocytes modulate skin color in response to stress. *FASEB J,* 21**,** 976-94.

Cotsarelis, G., T. T. Sun & R. M. Lavker (1990) Label-retaining cells reside in the bulge area of pilosebaceous unit: implications for follicular stem cells, hair cycle, and skin carcinogenesis. *Cell,* 61**,** 1329-37.

Cui, R., H. R. Widlund, E. Feige, J. Y. Lin, D. L. Wilensky, V. E. Igras, J. D'Orazio, C. Y. Fung, C. F. Schanbacher, S. R. Granter & D. E. Fisher (2007) Central role of p53 in the suntan response and pathologic hyperpigmentation. *Cell,* 128**,** 853-64.

Dai, D. L., M. Martinka & G. Li (2005) Prognostic significance of activated Akt expression in melanoma: a clinicopathologic study of 292 cases. *J Clin Oncol,* 23**,** 1473-82.

Dang, W. & B. Bartholomew (2007) Domain architecture of the catalytic subunit in the ISW2-nucleosome complex. *Mol Cell Biol,* 27**,** 8306-17.

Dankort, D., D. P. Curley, R. A. Cartlidge, B. Nelson, A. N. Karnezis, W. E. Damsky, Jr., M. J. You, R. A. DePinho, M. McMahon & M. Bosenberg (2009) Braf(V600E) cooperates with Pten loss to induce metastatic melanoma. *Nat Genet,* 41**,** 544-52.

Davies, H., G. R. Bignell, C. Cox, P. Stephens, S. Edkins, S. Clegg, J. Teague, H. Woffendin, M. J. Garnett, W. Bottomley, N. Davis, E. Dicks, R. Ewing, Y. Floyd, K. Gray, S.

Hall, R. Hawes, J. Hughes, V. Kosmidou, A. Menzies, C. Mould, A. Parker, C. Stevens, S. Watt, S. Hooper, R. Wilson, H. Jayatilake, B. A. Gusterson, C. Cooper, J. Shipley, D. Hargrave, K. Pritchard-Jones, N. Maitland, G. Chenevix-Trench, G. J. Riggins, D. D. Bigner, G. Palmieri, A. Cossu, A. Flanagan, A. Nicholson, J. W. Ho, S. Y. Leung, S. T. Yuen, B. L. Weber, H. F. Seigler, T. L. Darrow, H. Paterson, R. Marais, C. J. Marshall, R. Wooster, M. R. Stratton & P. A. Futreal (2002) Mutations of the BRAF gene in human cancer. *Nature,* 417**,** 949-54.

Davis, M. J., B. H. Ha, E. C. Holman, R. Halaban, J. Schlessinger & T. J. Boggon (2013) RAC1P29S is a spontaneously activating cancer-associated GTPase. *Proc Natl Acad Sci U S A,* 110**,** 912-7.

Deindl, S., W. L. Hwang, S. K. Hota, T. R. Blosser, P. Prasad, B. Bartholomew & X. Zhuang (2013) ISWI remodelers slide nucleosomes with coordinated multi-base-pair entry steps and single-base-pair exit steps. *Cell,* 152**,** 442-52.

Delmas, V., F. Beermann, S. Martinozzi, S. Carreira, J. Ackermann, M. Kumasaka, L. Denat, J. Goodall, F. Luciani, A. Viros, N. Demirkan, B. C. Bastian, C. R. Goding & L. Larue (2007) Beta-catenin induces immortalization of melanocytes by suppressing p16INK4a expression and cooperates with N-Ras in melanoma development. *Genes Dev,* 21**,** 2923-35.

Delmas, V., S. Martinozzi, Y. Bourgeois, M. Holzenberger & L. Larue (2003) Cre-mediated recombination in the skin melanocyte lineage. *Genesis,* 36**,** 73-80.

Denecker, G., N. Vandamme, O. Akay, D. Koludrovic, J. Taminau, K. Lemeire, A. Gheldof, B. De Craene, M. Van Gele, L. Brochez, G. M. Udupi, M. Rafferty, B. Balint, W. M. Gallagher, G. Ghanem, D. Huylebroeck, J. Haigh, J. van den Oord, L. Larue, I. Davidson, J. C. Marine & G. Berx (2014a) Identification of a ZEB2-MITF-ZEB1 transcriptional network that controls melanogenesis and melanoma progression. *Cell Death Differ,* 21**,** 1250-61.

Denecker, G., N. Vandamme, O. Akay, D. Koludrovic, J. Taminau, K. Lemeire, A. Gheldof, B. De Craene, M. Van Gele, L. Brochez, G. M. Udupi, M. Rafferty, B. Balint, W. M. Gallagher, G. Ghanem, D. Huylebroeck, J. Haigh, J. van den Oord, L. Larue, I. Davidson, J. C. Marine & G. Berx (2014b) Identification of a ZEB2-MITF-ZEB1 transcriptional network that controls melanogenesis and melanoma progression. *Cell Death Differ*.

Dennler, S., J. Andre, F. Verrecchia & A. Mauviel (2009) Cloning of the human GLI2 Promoter: transcriptional activation by transforming growth factor-beta via SMAD3/beta-catenin cooperation. *J Biol Chem,* 284**,** 31523-31.

Deuring, R., L. Fanti, J. A. Armstrong, M. Sarte, O. Papoulas, M. Prestel, G. Daubresse, M. Verardo, S. L. Moseley, M. Berloco, T. Tsukiyama, C. Wu, S. Pimpinelli & J. W. Tamkun (2000) The ISWI chromatin-remodeling protein is required for gene expression and the maintenance of higher order chromatin structure in vivo. *Mol Cell,* 5**,** 355-65.

Dhomen, N., J. S. Reis-Filho, S. da Rocha Dias, R. Hayward, K. Savage, V. Delmas, L. Larue, C. Pritchard & R. Marais (2009) Oncogenic Braf induces melanocyte senescence and melanoma in mice. *Cancer Cell,* 15**,** 294-303.

Dillon, R. L. & W. J. Muller (2010) Distinct biological roles for the akt family in mammary tumor progression. *Cancer Res,* 70**,** 4260-4.

Dissanayake, S. K., M. Wade, C. E. Johnson, M. P. O'Connell, P. D. Leotlela, A. D. French, K. V. Shah, K. J. Hewitt, D. T. Rosenthal, F. E. Indig, Y. Jiang, B. J. Nickoloff, D. D. Taub, J. M. Trent, R. T. Moon, M. Bittner & A. T. Weeraratna (2007) The Wnt5A/protein kinase C pathway mediates motility in melanoma cells via the

inhibition of metastasis suppressors and initiation of an epithelial to mesenchymal transition. *J Biol Chem,* 282**,** 17259-71.
Dong, L., Y. Li, J. Cao, F. Liu, E. Pier, J. Chen, Z. Xu, C. Chen, R. A. Wang & R. Cui (2012) FGF2 regulates melanocytes viability through the STAT3-transactivated PAX3 transcription. *Cell Death Differ,* 19**,** 616-22.
Dorsky, R. I., R. T. Moon & D. W. Raible (1998) Control of neural crest cell fate by the Wnt signalling pathway. *Nature,* 396**,** 370-3.
Dorsky, R. I., D. W. Raible & R. T. Moon (2000) Direct regulation of nacre, a zebrafish MITF homolog required for pigment cell formation, by the Wnt pathway. *Genes Dev,* 14**,** 158-62.
Drane, P., K. Ouararhni, A. Depaux, M. Shuaib & A. Hamiche (2010) The death-associated protein DAXX is a novel histone chaperone involved in the replication-independent deposition of H3.3. *Genes Dev,* 24**,** 1253-65.
Du, J. & D. E. Fisher (2002) Identification of Aim-1 as the underwhite mouse mutant and its transcriptional regulation by MITF. *J Biol Chem,* 277**,** 402-6.
Du, J., A. J. Miller, H. R. Widlund, M. A. Horstmann, S. Ramaswamy & D. E. Fisher (2003) MLANA/MART1 and SILV/PMEL17/GP100 are transcriptionally regulated by MITF in melanocytes and melanoma. *Am J Pathol,* 163**,** 333-43.
Dunleavy, E. M., D. Roche, H. Tagami, N. Lacoste, D. Ray-Gallet, Y. Nakamura, Y. Daigo, Y. Nakatani & G. Almouzni-Pettinotti (2009) HJURP is a cell-cycle-dependent maintenance and deposition factor of CENP-A at centromeres. *Cell,* 137**,** 485-97.
Dunn, K. J., B. O. Williams, Y. Li & W. J. Pavan (2000) Neural crest-directed gene transfer demonstrates Wnt1 role in melanocyte expansion and differentiation during mouse development. *Proc Natl Acad Sci U S A,* 97**,** 10050-5.
Dupin, E., S. Creuzet & N. M. Le Douarin (2006) The contribution of the neural crest to the vertebrate body. *Adv Exp Med Biol,* 589**,** 96-119.
Dykhuizen, E. C., D. C. Hargreaves, E. L. Miller, K. Cui, A. Korshunov, M. Kool, S. Pfister, Y. J. Cho, K. Zhao & G. R. Crabtree (2013) BAF complexes facilitate decatenation of DNA by topoisomerase IIalpha. *Nature,* 497**,** 624-7.
Eckey, M., S. Kuphal, T. Straub, P. Rummele, E. Kremmer, A. K. Bosserhoff & P. B. Becker (2012) Nucleosome remodeler SNF2L suppresses cell proliferation and migration and attenuates Wnt signaling. *Mol Cell Biol,* 32**,** 2359-71.
Eggermont, A. M. & C. Robert (2011) New drugs in melanoma: it's a whole new world. *Eur J Cancer,* 47**,** 2150-7.
Ellerhorst, J. A., V. R. Greene, S. Ekmekcioglu, C. L. Warneke, M. M. Johnson, C. P. Cooke, L. E. Wang, V. G. Prieto, J. E. Gershenwald, Q. Wei & E. A. Grimm (2011) Clinical correlates of NRAS and BRAF mutations in primary human melanoma. *Clin Cancer Res,* 17**,** 229-35.
Eltsov, M., K. M. Maclellan, K. Maeshima, A. S. Frangakis & J. Dubochet (2008) Analysis of cryo-electron microscopy images does not support the existence of 30-nm chromatin fibers in mitotic chromosomes in situ. *Proc Natl Acad Sci U S A,* 105**,** 19732-7.
English, C. M., M. W. Adkins, J. J. Carson, M. E. Churchill & J. K. Tyler (2006) Structural basis for the histone chaperone activity of Asf1. *Cell,* 127**,** 495-508.
Erdel, F. & K. Rippe (2011) Chromatin remodelling in mammalian cells by ISWI-type complexes--where, when and why? *FEBS J,* 278**,** 3608-18.
Fagiani, E., G. Giardina, L. Luzi, M. Cesaroni, M. Quarto, M. Capra, G. Germano, M. Bono, M. Capillo, P. Pelicci & L. Lanfrancone (2007) RaLP, a new member of the Src homology and collagen family, regulates cell migration and tumor growth of metastatic melanomas. *Cancer Res,* 67**,** 3064-73.

Feil, R. (2007) Conditional somatic mutagenesis in the mouse using site-specific recombinases. *Handb Exp Pharmacol*, 3-28.

Ferlay, J., E. Steliarova-Foucher, J. Lortet-Tieulent, S. Rosso, J. W. Coebergh, H. Comber, D. Forman & F. Bray (2013) Cancer incidence and mortality patterns in Europe: estimates for 40 countries in 2012. *Eur J Cancer,* 49, 1374-403.

Ferreira, H., A. Flaus & T. Owen-Hughes (2007) Histone modifications influence the action of Snf2 family remodelling enzymes by different mechanisms. *J Mol Biol,* 374, 563-79.

Finch, J. T. & A. Klug (1976) Solenoidal model for superstructure in chromatin. *Proc Natl Acad Sci U S A,* 73, 1897-901.

Fitzpatrick, T. B. (1988) The validity and practicality of sun-reactive skin types I through VI. *Arch Dermatol,* 124, 869-71.

Flaherty, K. T., J. R. Infante, A. Daud, R. Gonzalez, R. F. Kefford, J. Sosman, O. Hamid, L. Schuchter, J. Cebon, N. Ibrahim, R. Kudchadkar, H. A. Burris, 3rd, G. Falchook, A. Algazi, K. Lewis, G. V. Long, I. Puzanov, P. Lebowitz, A. Singh, S. Little, P. Sun, A. Allred, D. Ouellet, K. B. Kim, K. Patel & J. Weber (2012a) Combined BRAF and MEK inhibition in melanoma with BRAF V600 mutations. *N Engl J Med,* 367, 1694-703.

Flaherty, K. T., C. Robert, P. Hersey, P. Nathan, C. Garbe, M. Milhem, L. V. Demidov, J. C. Hassel, P. Rutkowski, P. Mohr, R. Dummer, U. Trefzer, J. M. Larkin, J. Utikal, B. Dreno, M. Nyakas, M. R. Middleton, J. C. Becker, M. Casey, L. J. Sherman, F. S. Wu, D. Ouellet, A. M. Martin, K. Patel & D. Schadendorf (2012b) Improved survival with MEK inhibition in BRAF-mutated melanoma. *N Engl J Med,* 367, 107-14.

Foltz, D. R., L. E. Jansen, A. O. Bailey, J. R. Yates, 3rd, E. A. Bassett, S. Wood, B. E. Black & D. W. Cleveland (2009) Centromere-specific assembly of CENP-a nucleosomes is mediated by HJURP. *Cell,* 137, 472-84.

Fujimoto, A., Y. Totoki, T. Abe, K. A. Boroevich, F. Hosoda, H. H. Nguyen, M. Aoki, N. Hosono, M. Kubo, F. Miya, Y. Arai, H. Takahashi, T. Shirakihara, M. Nagasaki, T. Shibuya, K. Nakano, K. Watanabe-Makino, H. Tanaka, H. Nakamura, J. Kusuda, H. Ojima, K. Shimada, T. Okusaka, M. Ueno, Y. Shigekawa, Y. Kawakami, K. Arihiro, H. Ohdan, K. Gotoh, O. Ishikawa, S. Ariizumi, M. Yamamoto, T. Yamada, K. Chayama, T. Kosuge, H. Yamaue, N. Kamatani, S. Miyano, H. Nakagama, Y. Nakamura, T. Tsunoda, T. Shibata & H. Nakagawa (2012) Whole-genome sequencing of liver cancers identifies etiological influences on mutation patterns and recurrent mutations in chromatin regulators. *Nat Genet,* 44, 760-4.

Fuse, N., K. Yasumoto, K. Takeda, S. Amae, M. Yoshizawa, T. Udono, K. Takahashi, M. Tamai, Y. Tomita, M. Tachibana & S. Shibahara (1999) Molecular cloning of cDNA encoding a novel microphthalmia-associated transcription factor isoform with a distinct amino-terminus. *J Biochem,* 126, 1043-51.

Fussner, E., M. Strauss, U. Djuric, R. Li, K. Ahmed, M. Hart, J. Ellis & D. P. Bazett-Jones (2012) Open and closed domains in the mouse genome are configured as 10-nm chromatin fibres. *EMBO Rep,* 13, 992-6.

Galibert, M. D., S. Carreira & C. R. Goding (2001) The Usf-1 transcription factor is a novel target for the stress-responsive p38 kinase and mediates UV-induced Tyrosinase expression. *EMBO J,* 20, 5022-31.

Galibert, M. D., U. Yavuzer, T. J. Dexter & C. R. Goding (1999) Pax3 and regulation of the melanocyte-specific tyrosinase-related protein-1 promoter. *J Biol Chem,* 274, 26894-900.

Gallagher, S. J., F. Rambow, M. Kumasaka, D. Champeval, A. Bellacosa, V. Delmas & L. Larue (2012) Beta-catenin inhibits melanocyte migration but induces melanoma metastasis. *Oncogene*.

Gamble, M. J. & W. L. Kraus (2010) Multiple facets of the unique histone variant macroH2A: from genomics to cell biology. *Cell Cycle,* 9**,** 2568-74.

Gammill, L. S. & M. Bronner-Fraser (2003) Neural crest specification: migrating into genomics. *Nat Rev Neurosci,* 4**,** 795-805.

Ghiorzo, P., L. Pastorino, P. Queirolo, W. Bruno, M. G. Tibiletti, S. Nasti, V. Andreotti, B. B. Paillerets & G. Bianchi Scarra (2013) Prevalence of the E318K MITF germline mutation in Italian melanoma patients: associations with histological subtypes and family cancer history. *Pigment Cell Melanoma Res,* 26**,** 259-62.

Goding, C. R. (2000) Mitf from neural crest to melanoma: signal transduction and transcription in the melanocyte lineage. *Genes Dev,* 14**,** 1712-28.

Goel, V. K., A. J. Lazar, C. L. Warneke, M. S. Redston & F. G. Haluska (2006) Examination of mutations in BRAF, NRAS, and PTEN in primary cutaneous melanoma. *J Invest Dermatol,* 126**,** 154-60.

Goldberg, A. D., L. A. Banaszynski, K. M. Noh, P. W. Lewis, S. J. Elsaesser, S. Stadler, S. Dewell, M. Law, X. Guo, X. Li, D. Wen, A. Chapgier, R. C. DeKelver, J. C. Miller, Y. L. Lee, E. A. Boydston, M. C. Holmes, P. D. Gregory, J. M. Greally, S. Rafii, C. Yang, P. J. Scambler, D. Garrick, R. J. Gibbons, D. R. Higgs, I. M. Cristea, F. D. Urnov, D. Zheng & C. D. Allis (2010) Distinct factors control histone variant H3.3 localization at specific genomic regions. *Cell,* 140**,** 678-91.

Goldman, J. A., J. D. Garlick & R. E. Kingston (2010) Chromatin remodeling by imitation switch (ISWI) class ATP-dependent remodelers is stimulated by histone variant H2A.Z. *J Biol Chem,* 285**,** 4645-51.

Goodall, J., S. Martinozzi, T. J. Dexter, D. Champeval, S. Carreira, L. Larue & C. R. Goding (2004) Brn-2 expression controls melanoma proliferation and is directly regulated by beta-catenin. *Mol Cell Biol,* 24**,** 2915-22.

Gordon, M. D. & R. Nusse (2006) Wnt signaling: multiple pathways, multiple receptors, and multiple transcription factors. *J Biol Chem,* 281**,** 22429-33.

Goto, H., Y. Yasui, E. A. Nigg & M. Inagaki (2002) Aurora-B phosphorylates Histone H3 at serine28 with regard to the mitotic chromosome condensation. *Genes Cells,* 7**,** 11-7.

Grant, P. A., L. Duggan, J. Cote, S. M. Roberts, J. E. Brownell, R. Candau, R. Ohba, T. Owen-Hughes, C. D. Allis, F. Winston, S. L. Berger & J. L. Workman (1997) Yeast Gcn5 functions in two multisubunit complexes to acetylate nucleosomal histones: characterization of an Ada complex and the SAGA (Spt/Ada) complex. *Genes Dev,* 11**,** 1640-50.

Greer, E. L. & Y. Shi (2012) Histone methylation: a dynamic mark in health, disease and inheritance. *Nat Rev Genet,* 13**,** 343-57.

Grune, T., J. Brzeski, A. Eberharter, C. R. Clapier, D. F. Corona, P. B. Becker & C. W. Muller (2003) Crystal structure and functional analysis of a nucleosome recognition module of the remodeling factor ISWI. *Mol Cell,* 12**,** 449-60.

Guillemette, B., A. R. Bataille, N. Gevry, M. Adam, M. Blanchette, F. Robert & L. Gaudreau (2005) Variant histone H2A.Z is globally localized to the promoters of inactive yeast genes and regulates nucleosome positioning. *PLoS Biol,* 3**,** e384.

Gupta, P. B., C. Kuperwasser, J. P. Brunet, S. Ramaswamy, W. L. Kuo, J. W. Gray, S. P. Naber & R. A. Weinberg (2005) The melanocyte differentiation program predisposes to metastasis after neoplastic transformation. *Nat Genet,* 37**,** 1047-54.

Haass, N. K., K. S. Smalley, L. Li & M. Herlyn (2005) Adhesion, migration and communication in melanocytes and melanoma. *Pigment Cell Res,* 18**,** 150-9.

Hallsson, J. H., J. Favor, C. Hodgkinson, T. Glaser, M. L. Lamoreux, R. Magnusdottir, G. J. Gunnarsson, H. O. Sweet, N. G. Copeland, N. A. Jenkins & E. Steingrimsson (2000) Genomic, transcriptional and mutational analysis of the mouse microphthalmia locus. *Genetics,* 155**,** 291-300.

Hallsson, J. H., B. S. Haflidadottir, A. Schepsky, H. Arnheiter & E. Steingrimsson (2007) Evolutionary sequence comparison of the Mitf gene reveals novel conserved domains. *Pigment Cell Res,* 20**,** 185-200.

Hamiche, A., J. G. Kang, C. Dennis, H. Xiao & C. Wu (2001) Histone tails modulate nucleosome mobility and regulate ATP-dependent nucleosome sliding by NURF. *Proc Natl Acad Sci U S A,* 98**,** 14316-21.

Hamiche, A., R. Sandaltzopoulos, D. A. Gdula & C. Wu (1999) ATP-dependent histone octamer sliding mediated by the chromatin remodeling complex NURF. *Cell,* 97**,** 833-42.

Happel, N. & D. Doenecke (2009) Histone H1 and its isoforms: contribution to chromatin structure and function. *Gene,* 431**,** 1-12.

Hari, L., I. Miescher, O. Shakhova, U. Suter, L. Chin, M. Taketo, W. D. Richardson, N. Kessaris & L. Sommer (2012) Temporal control of neural crest lineage generation by Wnt/beta-catenin signaling. *Development,* 139**,** 2107-17.

Harris, M. L., K. Buac, O. Shakhova, R. M. Hakami, M. Wegner, L. Sommer & W. J. Pavan (2013) A dual role for SOX10 in the maintenance of the postnatal melanocyte lineage and the differentiation of melanocyte stem cell progenitors. *PLoS Genet,* 9**,** e1003644.

Havas, K., A. Flaus, M. Phelan, R. Kingston, P. A. Wade, D. M. Lilley & T. Owen-Hughes (2000) Generation of superhelical torsion by ATP-dependent chromatin remodeling activities. *Cell,* 103**,** 1133-42.

Hearing, V. J. (2011) Determination of melanin synthetic pathways. *J Invest Dermatol,* 131**,** E8-E11.

Hemesath, T. J., E. R. Price, C. Takemoto, T. Badalian & D. E. Fisher (1998) MAP kinase links the transcription factor Microphthalmia to c-Kit signalling in melanocytes. *Nature,* 391**,** 298-301.

Hemesath, T. J., E. Steingrimsson, G. McGill, M. J. Hansen, J. Vaught, C. A. Hodgkinson, H. Arnheiter, N. G. Copeland, N. A. Jenkins & D. E. Fisher (1994) microphthalmia, a critical factor in melanocyte development, defines a discrete transcription factor family. *Genes Dev,* 8**,** 2770-80.

Henikoff, S. & K. Ahmad (2005) Assembly of variant histones into chromatin. *Annu Rev Cell Dev Biol,* 21**,** 133-53.

Herlyn, M., J. Thurin, G. Balaban, J. L. Bennicelli, D. Herlyn, D. E. Elder, E. Bondi, D. Guerry, P. Nowell, W. H. Clark & et al. (1985) Characteristics of cultured human melanocytes isolated from different stages of tumor progression. *Cancer Res,* 45**,** 5670-6.

Hershey, C. L. & D. E. Fisher (2005) Genomic analysis of the Microphthalmia locus and identification of the MITF-J/Mitf-J isoform. *Gene,* 347**,** 73-82.

Hershko, A. & A. Ciechanover (1998) The ubiquitin system. *Annu Rev Biochem,* 67**,** 425-79.

Hochheimer, A., S. Zhou, S. Zheng, M. C. Holmes & R. Tjian (2002) TRF2 associates with DREF and directs promoter-selective gene expression in Drosophila. *Nature,* 420**,** 439-45.

Hodawadekar, S. C. & R. Marmorstein (2007) Chemistry of acetyl transfer by histone modifying enzymes: structure, mechanism and implications for effector design. *Oncogene,* 26**,** 5528-40.

Hodgkinson, C. A., K. J. Moore, A. Nakayama, E. Steingrimsson, N. G. Copeland, N. A. Jenkins & H. Arnheiter (1993) Mutations at the mouse microphthalmia locus are

associated with defects in a gene encoding a novel basic-helix-loop-helix-zipper protein. *Cell,* 74**,** 395-404.

Hodi, F. S., S. J. O'Day, D. F. McDermott, R. W. Weber, J. A. Sosman, J. B. Haanen, R. Gonzalez, C. Robert, D. Schadendorf, J. C. Hassel, W. Akerley, A. J. van den Eertwegh, J. Lutzky, P. Lorigan, J. M. Vaubel, G. P. Linette, D. Hogg, C. H. Ottensmeier, C. Lebbe, C. Peschel, I. Quirt, J. I. Clark, J. D. Wolchok, J. S. Weber, J. Tian, M. J. Yellin, G. M. Nichol, A. Hoos & W. J. Urba (2010) Improved survival with ipilimumab in patients with metastatic melanoma. *N Engl J Med,* 363**,** 711-23.

Hodis, E., I. R. Watson, G. V. Kryukov, S. T. Arold, M. Imielinski, J. P. Theurillat, E. Nickerson, D. Auclair, L. Li, C. Place, D. Dicara, A. H. Ramos, M. S. Lawrence, K. Cibulskis, A. Sivachenko, D. Voet, G. Saksena, N. Stransky, R. C. Onofrio, W. Winckler, K. Ardlie, N. Wagle, J. Wargo, K. Chong, D. L. Morton, K. Stemke-Hale, G. Chen, M. Noble, M. Meyerson, J. E. Ladbury, M. A. Davies, J. E. Gershenwald, S. N. Wagner, D. S. Hoon, D. Schadendorf, E. S. Lander, S. B. Gabriel, G. Getz, L. A. Garraway & L. Chin (2012) A landscape of driver mutations in melanoma. *Cell,* 150**,** 251-63.

Hoek, K. S., O. M. Eichhoff, N. C. Schlegel, U. Dobbeling, N. Kobert, L. Schaerer, S. Hemmi & R. Dummer (2008) In vivo switching of human melanoma cells between proliferative and invasive states. *Cancer Res,* 68**,** 650-6.

Hoek, K. S., N. C. Schlegel, P. Brafford, A. Sucker, S. Ugurel, R. Kumar, B. L. Weber, K. L. Nathanson, D. J. Phillips, M. Herlyn, D. Schadendorf & R. Dummer (2006) Metastatic potential of melanomas defined by specific gene expression profiles with no BRAF signature. *Pigment Cell Res,* 19**,** 290-302.

Hosoda, K., R. E. Hammer, J. A. Richardson, A. G. Baynash, J. C. Cheung, A. Giaid & M. Yanagisawa (1994) Targeted and natural (piebald-lethal) mutations of endothelin-B receptor gene produce megacolon associated with spotted coat color in mice. *Cell,* 79**,** 1267-76.

Hou, L. & W. J. Pavan (2008) Transcriptional and signaling regulation in neural crest stem cell-derived melanocyte development: do all roads lead to Mitf? *Cell Res,* 18**,** 1163-76.

Hsu, M. Y., M. J. Wheelock, K. R. Johnson & M. Herlyn (1996) Shifts in cadherin profiles between human normal melanocytes and melanomas. *J Investig Dermatol Symp Proc,* 1**,** 188-94.

Huber, W. E., E. R. Price, H. R. Widlund, J. Du, I. J. Davis, M. Wegner & D. E. Fisher (2003) A tissue-restricted cAMP transcriptional response: SOX10 modulates alpha-melanocyte-stimulating hormone-triggered expression of microphthalmia-associated transcription factor in melanocytes. *J Biol Chem,* 278**,** 45224-30.

Hughes, M. J., J. B. Lingrel, J. M. Krakowsky & K. P. Anderson (1993) A helix-loop-helix transcription factor-like gene is located at the mi locus. *J Biol Chem,* 268**,** 20687-90.

Ikeya, M., S. M. Lee, J. E. Johnson, A. P. McMahon & S. Takada (1997) Wnt signalling required for expansion of neural crest and CNS progenitors. *Nature,* 389**,** 966-70.

Ito, M., K. Kizawa, K. Hamada & G. Cotsarelis (2004) Hair follicle stem cells in the lower bulge form the secondary germ, a biochemically distinct but functionally equivalent progenitor cell population, at the termination of catagen. *Differentiation,* 72**,** 548-57.

Javelaud, D., V. I. Alexaki, M. J. Pierrat, K. S. Hoek, S. Dennler, L. Van Kempen, C. Bertolotto, R. Ballotti, S. Saule, V. Delmas & A. Mauviel (2011) GLI2 and M-MITF transcription factors control exclusive gene expression programs and inversely regulate invasion in human melanoma cells. *Pigment Cell Melanoma Res,* 24**,** 932-43.

Jin, E. J., C. A. Erickson, S. Takada & L. W. Burrus (2001) Wnt and BMP signaling govern lineage segregation of melanocytes in the avian embryo. *Dev Biol,* 233**,** 22-37.

Jones, M. H., N. Hamana & M. Shimane (2000) Identification and characterization of BPTF, a novel bromodomain transcription factor. *Genomics,* 63**,** 35-9.
Jordan-Sciutto, K. L., J. M. Dragich & R. Bowser (1999) DNA binding activity of the fetal Alz-50 clone 1 (FAC1) protein is enhanced by phosphorylation. *Biochem Biophys Res Commun,* 260**,** 785-9.
Jordan-Sciutto, K. L., J. M. Dragich, J. Caltagarone, D. J. Hall & R. Bowser (2000) Fetal Alz-50 clone 1 (FAC1) protein interacts with the Myc-associated zinc finger protein (ZF87/MAZ) and alters its transcriptional activity. *Biochemistry,* 39**,** 3206-15.
Jordan, S. A. & I. J. Jackson (2000) MGF (KIT ligand) is a chemokinetic factor for melanoblast migration into hair follicles. *Dev Biol,* 225**,** 424-36.
Joti, Y., T. Hikima, Y. Nishino, F. Kamada, S. Hihara, H. Takata, T. Ishikawa & K. Maeshima (2012) Chromosomes without a 30-nm chromatin fiber. *Nucleus,* 3**,** 404-10.
Kabbarah, O. & L. Chin (2005) Revealing the genomic heterogeneity of melanoma. *Cancer Cell,* 8**,** 439-41.
Kadoch, C., D. C. Hargreaves, C. Hodges, L. Elias, L. Ho, J. Ranish & G. R. Crabtree (2013) Proteomic and bioinformatic analysis of mammalian SWI/SNF complexes identifies extensive roles in human malignancy. *Nat Genet,* 45**,** 592-601.
Kagalwala, M. N., B. J. Glaus, W. Dang, M. Zofall & B. Bartholomew (2004) Topography of the ISW2-nucleosome complex: insights into nucleosome spacing and chromatin remodeling. *EMBO J,* 23**,** 2092-104.
Kamijo, T., J. D. Weber, G. Zambetti, F. Zindy, M. F. Roussel & C. J. Sherr (1998) Functional and physical interactions of the ARF tumor suppressor with p53 and Mdm2. *Proc Natl Acad Sci U S A,* 95**,** 8292-7.
Kasten, M. M., C. R. Clapier & B. R. Cairns (2011) SnapShot: Chromatin remodeling: SWI/SNF. *Cell,* 144**,** 310 e1.
Kawakami, T., Y. Soma, Y. Kawa, M. Ito, E. Yamasaki, H. Watabe, E. Hosaka, K. Yajima, K. Ohsumi & M. Mizoguchi (2002) Transforming growth factor beta1 regulates melanocyte proliferation and differentiation in mouse neural crest cells via stem cell factor/KIT signaling. *J Invest Dermatol,* 118**,** 471-8.
Keenen, B., H. Qi, S. V. Saladi, M. Yeung & I. L. de la Serna (2010) Heterogeneous SWI/SNF chromatin remodeling complexes promote expression of microphthalmia-associated transcription factor target genes in melanoma. *Oncogene,* 29**,** 81-92.
Khorasanizadeh, S. (2004) The nucleosome: from genomic organization to genomic regulation. *Cell,* 116**,** 259-72.
Kim, J., M. Guermah, R. K. McGinty, J. S. Lee, Z. Tang, T. A. Milne, A. Shilatifard, T. W. Muir & R. G. Roeder (2009) RAD6-Mediated transcription-coupled H2B ubiquitylation directly stimulates H3K4 methylation in human cells. *Cell,* 137**,** 459-71.
Kim, K., V. Punj, J. Choi, K. Heo, J. M. Kim, P. W. Laird & W. An (2013) Gene dysregulation by histone variant H2A.Z in bladder cancer. *Epigenetics Chromatin,* 6**,** 34.
Kim, N. W., M. A. Piatyszek, K. R. Prowse, C. B. Harley, M. D. West, P. L. Ho, G. M. Coviello, W. E. Wright, S. L. Weinrich & J. W. Shay (1994) Specific association of human telomerase activity with immortal cells and cancer. *Science,* 266**,** 2011-5.
Kippenberger, S., A. Bernd, J. Bereiter-Hahn, A. Ramirez-Bosca, R. Kaufmann & H. Holzmann (1996) Transcription of melanogenesis enzymes in melanocytes: dependence upon culture conditions and co-cultivation with keratinocytes. *Pigment Cell Res,* 9**,** 179-84.
Klose, R. J. & A. P. Bird (2006) Genomic DNA methylation: the mark and its mediators. *Trends Biochem Sci,* 31**,** 89-97.

Klose, R. J. & Y. Zhang (2007) Regulation of histone methylation by demethylimination and demethylation. *Nat Rev Mol Cell Biol,* 8**,** 307-18.

Kobayashi, T., K. Urabe, S. J. Orlow, K. Higashi, G. Imokawa, B. S. Kwon, B. Potterf & V. J. Hearing (1994) The Pmel 17/silver locus protein. Characterization and investigation of its melanogenic function. *J Biol Chem,* 269**,** 29198-205.

Kobor, M. S., S. Venkatasubrahmanyam, M. D. Meneghini, J. W. Gin, J. L. Jennings, A. J. Link, H. D. Madhani & J. Rine (2004) A protein complex containing the conserved Swi2/Snf2-related ATPase Swr1p deposits histone variant H2A.Z into euchromatin. *PLoS Biol,* 2**,** E131.

Kohli, R. M. & Y. Zhang (2013) TET enzymes, TDG and the dynamics of DNA demethylation. *Nature,* 502**,** 472-9.

Koludrovic, D. & I. Davidson (2013) MITF, the Janus transcription factor of melanoma. *Future Oncol,* 9**,** 235-44.

Komiya, Y. & R. Habas (2008) Wnt signal transduction pathways. *Organogenesis,* 4**,** 68-75.

Kouzarides, T. (2007) Chromatin modifications and their function. *Cell,* 128**,** 693-705.

Krauthammer, M., Y. Kong, B. H. Ha, P. Evans, A. Bacchiocchi, J. P. McCusker, E. Cheng, M. J. Davis, G. Goh, M. Choi, S. Ariyan, D. Narayan, K. Dutton-Regester, A. Capatana, E. C. Holman, M. Bosenberg, M. Sznol, H. M. Kluger, D. E. Brash, D. F. Stern, M. A. Materin, R. S. Lo, S. Mane, S. Ma, K. K. Kidd, N. K. Hayward, R. P. Lifton, J. Schlessinger, T. J. Boggon & R. Halaban (2012) Exome sequencing identifies recurrent somatic RAC1 mutations in melanoma. *Nat Genet,* 44**,** 1006-14.

Krispin, S., E. Nitzan, Y. Kassem & C. Kalcheim (2010) Evidence for a dynamic spatiotemporal fate map and early fate restrictions of premigratory avian neural crest. *Development,* 137**,** 585-95.

Kugler, S. J., E. M. Gehring, V. Wallkamm, V. Kruger & A. C. Nagel (2011) The Putzig-NURF nucleosome remodeling complex is required for ecdysone receptor signaling and innate immunity in Drosophila melanogaster. *Genetics,* 188**,** 127-39.

Kugler, S. J. & A. C. Nagel (2010) A novel Pzg-NURF complex regulates Notch target gene activity. *Mol Biol Cell,* 21**,** 3443-8.

Kumano, K., S. Masuda, M. Sata, T. Saito, S. Y. Lee, M. Sakata-Yanagimoto, T. Tomita, T. Iwatsubo, H. Natsugari, M. Kurokawa, S. Ogawa & S. Chiba (2008) Both Notch1 and Notch2 contribute to the regulation of melanocyte homeostasis. *Pigment Cell Melanoma Res,* 21**,** 70-8.

Kunisada, T., H. Yoshida, H. Yamazaki, A. Miyamoto, H. Hemmi, E. Nishimura, L. D. Shultz, S. Nishikawa & S. Hayashi (1998) Transgene expression of steel factor in the basal layer of epidermis promotes survival, proliferation, differentiation and migration of melanocyte precursors. *Development,* 125**,** 2915-23.

Kwon, S. Y., H. Xiao, B. P. Glover, R. Tjian, C. Wu & P. Badenhorst (2008) The nucleosome remodeling factor (NURF) regulates genes involved in Drosophila innate immunity. *Dev Biol,* 316**,** 538-47.

Kwon, S. Y., H. Xiao, C. Wu & P. Badenhorst (2009) Alternative splicing of NURF301 generates distinct NURF chromatin remodeling complexes with altered modified histone binding specificities. *PLoS Genet,* 5**,** e1000574.

Lan, F., R. E. Collins, R. De Cegli, R. Alpatov, J. R. Horton, X. Shi, O. Gozani, X. Cheng & Y. Shi (2007) Recognition of unmethylated histone H3 lysine 4 links BHC80 to LSD1-mediated gene repression. *Nature,* 448**,** 718-22.

Lan, F. & Y. Shi (2009) Epigenetic regulation: methylation of histone and non-histone proteins. *Sci China C Life Sci,* 52**,** 311-22.

Lan, L., A. Ui, S. Nakajima, K. Hatakeyama, M. Hoshi, R. Watanabe, S. M. Janicki, H. Ogiwara, T. Kohno, S. Kanno & A. Yasui (2010) The ACF1 complex is required for DNA double-strand break repair in human cells. *Mol Cell,* 40**,** 976-87.

Landry, J., A. A. Sharov, Y. Piao, L. V. Sharova, H. Xiao, E. Southon, J. Matta, L. Tessarollo, Y. E. Zhang, M. S. Ko, M. R. Kuehn, T. P. Yamaguchi & C. Wu (2008) Essential role of chromatin remodeling protein Bptf in early mouse embryos and embryonic stem cells. *PLoS Genet,* 4**,** e1000241.

Landry, J. W., S. Banerjee, B. Taylor, P. D. Aplan, A. Singer & C. Wu (2011a) Chromatin remodeling complex NURF regulates thymocyte maturation. *Genes Dev,* 25**,** 275-86.

Landry, J. W., S. Banerjee, B. Taylor, P. D. Aplan, A. Singer & C. Wu (2011b) Chromatin remodeling complex NURF regulates thymocyte maturation. *Genes & development,* 25**,** 275-86.

Lang, D. & J. A. Epstein (2003) Sox10 and Pax3 physically interact to mediate activation of a conserved c-RET enhancer. *Hum Mol Genet,* 12**,** 937-45.

Lang, D., M. M. Lu, L. Huang, K. A. Engleka, M. Zhang, E. Y. Chu, S. Lipner, A. Skoultchi, S. E. Millar & J. A. Epstein (2005) Pax3 functions at a nodal point in melanocyte stem cell differentiation. *Nature,* 433**,** 884-7.

Lang, D., J. B. Mascarenhas & C. R. Shea (2013) Melanocytes, melanocyte stem cells, and melanoma stem cells. *Clin Dermatol,* 31**,** 166-78.

Larue, L., M. Kumasaka & C. R. Goding (2003) Beta-catenin in the melanocyte lineage. *Pigment Cell Res,* 16**,** 312-7.

Lazar, I., R. Perlman, M. Lotem, T. Peretz, D. Ben-Yehuda & L. Kadouri (2012) The clinical effect of the inhibitor of apopotosis protein livin in melanoma. *Oncology,* 82**,** 197-204.

Le Douarin, N. & C. Kalcheim. 1999. *The neural crest*. Cambridge: Cambridge University Press.

Lee, A. Y. (2012) Role of keratinocytes in the development of vitiligo. *Ann Dermatol,* 24**,** 115-25.

Lee, H. O., J. M. Levorse & M. K. Shin (2003) The endothelin receptor-B is required for the migration of neural crest-derived melanocyte and enteric neuron precursors. *Dev Biol,* 259**,** 162-75.

Lee, H. Y., M. Kleber, L. Hari, V. Brault, U. Suter, M. M. Taketo, R. Kemler & L. Sommer (2004) Instructive role of Wnt/beta-catenin in sensory fate specification in neural crest stem cells. *Science,* 303**,** 1020-3.

Lee, J. S., A. Shukla, J. Schneider, S. K. Swanson, M. P. Washburn, L. Florens, S. R. Bhaumik & A. Shilatifard (2007) Histone crosstalk between H2B monoubiquitination and H3 methylation mediated by COMPASS. *Cell,* 131**,** 1084-96.

Lewis, P. W., S. J. Elsaesser, K. M. Noh, S. C. Stadler & C. D. Allis (2010) Daxx is an H3.3-specific histone chaperone and cooperates with ATRX in replication-independent chromatin assembly at telomeres. *Proc Natl Acad Sci U S A,* 107**,** 14075-80.

Li, A., Y. Ma, M. Jin, S. Mason, R. L. Mort, K. Blyth, L. Larue, O. J. Sansom & L. M. Machesky (2012a) Activated mutant NRas(Q61K) drives aberrant melanocyte signaling, survival, and invasiveness via a Rac1-dependent mechanism. *J Invest Dermatol,* 132**,** 2610-21.

Li, A., Y. Ma, X. Yu, R. L. Mort, C. R. Lindsay, D. Stevenson, D. Strathdee, R. H. Insall, J. Chernoff, S. B. Snapper, I. J. Jackson, L. Larue, O. J. Sansom & L. M. Machesky (2011a) Rac1 drives melanoblast organization during mouse development by orchestrating pseudopod- driven motility and cell-cycle progression. *Dev Cell,* 21**,** 722-34.

Li, G., K. Satyamoorthy, F. Meier, C. Berking, T. Bogenrieder & M. Herlyn (2003) Function and regulation of melanoma-stromal fibroblast interactions: when seeds meet soil. *Oncogene,* 22**,** 3162-71.

Li, H., S. Ilin, W. Wang, E. M. Duncan, J. Wysocka, C. D. Allis & D. J. Patel (2006) Molecular basis for site-specific read-out of histone H3K4me3 by the BPTF PHD finger of NURF. *Nature,* 442**,** 91-5.

Li, J., J. S. Song, R. J. Bell, T. N. Tran, R. Haq, H. Liu, K. T. Love, R. Langer, D. G. Anderson, L. Larue & D. E. Fisher (2012b) YY1 regulates melanocyte development and function by cooperating with MITF. *PLoS Genet,* 8**,** e1002688.

Li, Q., H. Zhou, H. Wurtele, B. Davies, B. Horazdovsky, A. Verreault & Z. Zhang (2008) Acetylation of histone H3 lysine 56 regulates replication-coupled nucleosome assembly. *Cell,* 134**,** 244-55.

Li, X., S. Wang, Y. Li, C. Deng, L. A. Steiner, H. Xiao, C. Wu, J. Bungert, P. G. Gallagher, G. Felsenfeld, Y. Qiu & S. Huang (2011b) Chromatin boundaries require functional collaboration between the hSET1 and NURF complexes. *Blood,* 118**,** 1386-94.

Lieberman-Aiden, E., N. L. van Berkum, L. Williams, M. Imakaev, T. Ragoczy, A. Telling, I. Amit, B. R. Lajoie, P. J. Sabo, M. O. Dorschner, R. Sandstrom, B. Bernstein, M. A. Bender, M. Groudine, A. Gnirke, J. Stamatoyannopoulos, L. A. Mirny, E. S. Lander & J. Dekker (2009) Comprehensive mapping of long-range interactions reveals folding principles of the human genome. *Science,* 326**,** 289-93.

Lin, H., R. P. Wong, M. Martinka & G. Li (2010) BRG1 expression is increased in human cutaneous melanoma. *Br J Dermatol,* 163**,** 502-10.

Lindsay, C. R., S. Lawn, A. D. Campbell, W. J. Faller, F. Rambow, R. L. Mort, P. Timpson, A. Li, P. Cammareri, R. A. Ridgway, J. P. Morton, B. Doyle, S. Hegarty, M. Rafferty, I. G. Murphy, E. W. McDermott, K. Sheahan, K. Pedone, A. J. Finn, P. A. Groben, N. E. Thomas, H. Hao, C. Carson, J. C. Norman, L. M. Machesky, W. M. Gallagher, I. J. Jackson, L. Van Kempen, F. Beermann, C. Der, L. Larue, H. C. Welch, B. W. Ozanne & O. J. Sansom (2011) P-Rex1 is required for efficient melanoblast migration and melanoma metastasis. *Nat Commun,* 2**,** 555.

Liu, L., X. D. Zhu, W. Q. Wang, Y. Shen, Y. Qin, Z. G. Ren, H. C. Sun & Z. Y. Tang (2010) Activation of beta-catenin by hypoxia in hepatocellular carcinoma contributes to enhanced metastatic potential and poor prognosis. *Clin Cancer Res,* 16**,** 2740-50.

Long, J., G. Wang, D. He & F. Liu (2004) Repression of Smad4 transcriptional activity by SUMO modification. *Biochem J,* 379**,** 23-9.

Lorch, Y., B. Maier-Davis & R. D. Kornberg (2006) Chromatin remodeling by nucleosome disassembly in vitro. *Proc Natl Acad Sci U S A,* 103**,** 3090-3.

Loyola, A. & G. Almouzni (2004) Histone chaperones, a supporting role in the limelight. *Biochim Biophys Acta,* 1677**,** 3-11.

Ludwig, A., S. Rehberg & M. Wegner (2004) Melanocyte-specific expression of dopachrome tautomerase is dependent on synergistic gene activation by the Sox10 and Mitf transcription factors. *FEBS Lett,* 556**,** 236-44.

Luger, K., A. W. Mader, R. K. Richmond, D. F. Sargent & T. J. Richmond (1997) Crystal structure of the nucleosome core particle at 2.8 A resolution. *Nature,* 389**,** 251-60.

Mackenzie, M. A., S. A. Jordan, P. S. Budd & I. J. Jackson (1997) Activation of the receptor tyrosine kinase Kit is required for the proliferation of melanoblasts in the mouse embryo. *Dev Biol,* 192**,** 99-107.

MacKie, R. M., A. Hauschild & A. M. Eggermont (2009) Epidemiology of invasive cutaneous melanoma. *Ann Oncol,* 20 Suppl 6**,** vi1-7.

Mansky, K. C., U. Sankar, J. Han & M. C. Ostrowski (2002) Microphthalmia transcription factor is a target of the p38 MAPK pathway in response to receptor activator of NF-kappa B ligand signaling. *J Biol Chem,* 277**,** 11077-83.

Marmigere, F. & P. Ernfors (2007) Specification and connectivity of neuronal subtypes in the sensory lineage. *Nat Rev Neurosci,* 8**,** 114-27.

Marquardt, T., R. Ashery-Padan, N. Andrejewski, R. Scardigli, F. Guillemot & P. Gruss (2001) Pax6 is required for the multipotent state of retinal progenitor cells. *Cell,* 105**,** 43-55.

Marques, M., L. Laflamme, A. L. Gervais & L. Gaudreau (2010) Reconciling the positive and negative roles of histone H2A.Z in gene transcription. *Epigenetics,* 5**,** 267-72.

Mayer, T. C. (1973) The migratory pathway of neural crest cells into the skin of mouse embryos. *Dev Biol,* 34**,** 39-46.

McGill, G. G., M. Horstmann, H. R. Widlund, J. Du, G. Motyckova, E. K. Nishimura, Y. L. Lin, S. Ramaswamy, W. Avery, H. F. Ding, S. A. Jordan, I. J. Jackson, S. J. Korsmeyer, T. R. Golub & D. E. Fisher (2002) Bcl2 regulation by the melanocyte master regulator Mitf modulates lineage survival and melanoma cell viability. *Cell,* 109**,** 707-18.

Metzger, D., J. Clifford, H. Chiba & P. Chambon (1995) Conditional site-specific recombination in mammalian cells using a ligand-dependent chimeric Cre recombinase. *Proc Natl Acad Sci U S A,* 92**,** 6991-5.

Meulemans, D. & M. Bronner-Fraser (2004) Gene-regulatory interactions in neural crest evolution and development. *Dev Cell,* 7**,** 291-9.

Michaloglou, C., L. C. Vredeveld, M. S. Soengas, C. Denoyelle, T. Kuilman, C. M. van der Horst, D. M. Majoor, J. W. Shay, W. J. Mooi & D. S. Peeper (2005) BRAFE600-associated senescence-like cell cycle arrest of human naevi. *Nature,* 436**,** 720-4.

Miller, A. J., C. Levy, I. J. Davis, E. Razin & D. E. Fisher (2005) Sumoylation of MITF and its related family members TFE3 and TFEB. *J Biol Chem,* 280**,** 146-55.

Miller, A. J. & M. C. Mihm, Jr. (2006) Melanoma. *N Engl J Med,* 355**,** 51-65.

Milner, Y., J. Sudnik, M. Filippi, M. Kizoulis, M. Kashgarian & K. Stenn (2002) Exogen, shedding phase of the hair growth cycle: characterization of a mouse model. *J Invest Dermatol,* 119**,** 639-44.

Mizuguchi, G., T. Tsukiyama, J. Wisniewski & C. Wu (1997) Role of nucleosome remodeling factor NURF in transcriptional activation of chromatin. *Mol Cell,* 1**,** 141-50.

Moll, I., M. Roessler, J. M. Brandner, A. C. Eispert, P. Houdek & R. Moll (2005) Human Merkel cells--aspects of cell biology, distribution and functions. *Eur J Cell Biol,* 84**,** 259-71.

Monni, O., M. Barlund, S. Mousses, J. Kononen, G. Sauter, M. Heiskanen, P. Paavola, K. Avela, Y. Chen, M. L. Bittner & A. Kallioniemi (2001) Comprehensive copy number and gene expression profiling of the 17q23 amplicon in human breast cancer. *Proc Natl Acad Sci U S A,* 98**,** 5711-6.

Monsoro-Burq, A. H., E. Wang & R. Harland (2005) Msx1 and Pax3 cooperate to mediate FGF8 and WNT signals during Xenopus neural crest induction. *Dev Cell,* 8**,** 167-78.

Moore, K. J. (1995) Insight into the microphthalmia gene. *Trends Genet,* 11**,** 442-8.

Moriyama, M., M. Osawa, S. S. Mak, T. Ohtsuka, N. Yamamoto, H. Han, V. Delmas, R. Kageyama, F. Beermann, L. Larue & S. Nishikawa (2006) Notch signaling via Hes1 transcription factor maintains survival of melanoblasts and melanocyte stem cells. *J Cell Biol,* 173**,** 333-9.

Mosammaparast, N. & Y. Shi (2010) Reversal of histone methylation: biochemical and molecular mechanisms of histone demethylases. *Annu Rev Biochem,* 79**,** 155-79.

Mu, X., J. E. Springer & R. Bowser (1997) FAC1 expression and localization in motor neurons of developing, adult, and amyotrophic lateral sclerosis spinal cord. *Exp Neurol,* 146**,** 17-24.

Mulder, K. W., X. Wang, C. Escriu, Y. Ito, R. F. Schwarz, J. Gillis, G. Sirokmany, G. Donati, S. Uribe-Lewis, P. Pavlidis, A. Murrell, F. Markowetz & F. M. Watt (2012) Diverse epigenetic strategies interact to control epidermal differentiation. *Nat Cell Biol,* 14**,** 753-63.

Muller-Rover, S., B. Handjiski, C. van der Veen, S. Eichmuller, K. Foitzik, I. A. McKay, K. S. Stenn & R. Paus (2001) A comprehensive guide for the accurate classification of murine hair follicles in distinct hair cycle stages. *J Invest Dermatol,* 117**,** 3-15.

Murakami, H. & H. Arnheiter (2005) Sumoylation modulates transcriptional activity of MITF in a promoter-specific manner. *Pigment Cell Res,* 18**,** 265-77.

Murawska, M. & A. Brehm (2011) CHD chromatin remodelers and the transcription cycle. *Transcription,* 2**,** 244-53.

Murukesh, N., C. Dive & G. C. Jayson (2010) Biomarkers of angiogenesis and their role in the development of VEGF inhibitors. *Br J Cancer,* 102**,** 8-18.

Nathan, D., K. Ingvarsdottir, D. E. Sterner, G. R. Bylebyl, M. Dokmanovic, J. A. Dorsey, K. A. Whelan, M. Krsmanovic, W. S. Lane, P. B. Meluh, E. S. Johnson & S. L. Berger (2006) Histone sumoylation is a negative regulator in Saccharomyces cerevisiae and shows dynamic interplay with positive-acting histone modifications. *Genes Dev,* 20**,** 966-76.

Nelson, A. A. & H. Tsao (2009) Melanoma and genetics. *Clin Dermatol,* 27**,** 46-52.

Nelson, W. J. & R. Nusse (2004) Convergence of Wnt, beta-catenin, and cadherin pathways. *Science,* 303**,** 1483-7.

Ng, S. S., W. W. Yue, U. Oppermann & R. J. Klose (2009) Dynamic protein methylation in chromatin biology. *Cell Mol Life Sci,* 66**,** 407-22.

Nishikawa, S., M. Kusakabe, K. Yoshinaga, M. Ogawa, S. Hayashi, T. Kunisada, T. Era & T. Sakakura (1991) In utero manipulation of coat color formation by a monoclonal anti-c-kit antibody: two distinct waves of c-kit-dependency during melanocyte development. *EMBO J,* 10**,** 2111-8.

Nishimura, E. K. (2011) Melanocyte stem cells: a melanocyte reservoir in hair follicles for hair and skin pigmentation. *Pigment Cell Melanoma Res,* 24**,** 401-10.

Nishimura, E. K., S. R. Granter & D. E. Fisher (2005) Mechanisms of hair graying: incomplete melanocyte stem cell maintenance in the niche. *Science,* 307**,** 720-4.

Nishimura, E. K., S. A. Jordan, H. Oshima, H. Yoshida, M. Osawa, M. Moriyama, I. J. Jackson, Y. Barrandon, Y. Miyachi & S. Nishikawa (2002) Dominant role of the niche in melanocyte stem-cell fate determination. *Nature,* 416**,** 854-60.

Nishimura, E. K., M. Suzuki, V. Igras, J. Du, S. Lonning, Y. Miyachi, J. Roes, F. Beermann & D. E. Fisher (2010) Key roles for transforming growth factor beta in melanocyte stem cell maintenance. *Cell Stem Cell,* 6**,** 130-40.

Noll, M. & R. D. Kornberg (1977) Action of micrococcal nuclease on chromatin and the location of histone H1. *J Mol Biol,* 109**,** 393-404.

O'Reilly-Pol, T. & S. L. Johnson (2013) Kit signaling is involved in melanocyte stem cell fate decisions in zebrafish embryos. *Development,* 140**,** 996-1002.

Oboki, K., E. Morii, T. R. Kataoka, T. Jippo & Y. Kitamura (2002) Isoforms of mi transcription factor preferentially expressed in cultured mast cells of mice. *Biochem Biophys Res Commun,* 290**,** 1250-4.

Okabe, I., L. C. Bailey, O. Attree, S. Srinivasan, J. M. Perkel, B. C. Laurent, M. Carlson, D. L. Nelson & R. L. Nussbaum (1992) Cloning of human and bovine homologs of

SNF2/SWI2: a global activator of transcription in yeast S. cerevisiae. *Nucleic Acids Res,* 20**,** 4649-55.
Oki, M., H. Aihara & T. Ito (2007) Role of histone phosphorylation in chromatin dynamics and its implications in diseases. *Subcell Biochem,* 41**,** 319-36.
Okura, M., H. Maeda, S. Nishikawa & M. Mizoguchi (1995) Effects of monoclonal anti-c-kit antibody (ACK2) on melanocytes in newborn mice. *J Invest Dermatol,* 105**,** 322-8.
Olins, D. E. & A. L. Olins (2003) Chromatin history: our view from the bridge. *Nat Rev Mol Cell Biol,* 4**,** 809-14.
Olmeda, D., M. Jorda, H. Peinado, A. Fabra & A. Cano (2007) Snail silencing effectively suppresses tumour growth and invasiveness. *Oncogene,* 26**,** 1862-74.
Ondrusova, L., J. Vachtenheim, J. Reda, P. Zakova & K. Benkova (2013) MITF-independent pro-survival role of BRG1-containing SWI/SNF complex in melanoma cells. *PLoS One,* 8**,** e54110.
Osawa, M. (2008) Melanocyte stem cells.
Osawa, M., G. Egawa, S. S. Mak, M. Moriyama, R. Freter, S. Yonetani, F. Beermann & S. Nishikawa (2005) Molecular characterization of melanocyte stem cells in their niche. *Development,* 132**,** 5589-99.
Osawa, M. & D. E. Fisher (2008) Notch and melanocytes: diverse outcomes from a single signal. *J Invest Dermatol,* 128**,** 2571-4.
Oshima, H., A. Rochat, C. Kedzia, K. Kobayashi & Y. Barrandon (2001) Morphogenesis and renewal of hair follicles from adult multipotent stem cells. *Cell,* 104**,** 233-45.
Oudet, P., M. Gross-Bellard & P. Chambon (1975) Electron microscopic and biochemical evidence that chromatin structure is a repeating unit. *Cell,* 4**,** 281-300.
Ouhtit, A., R. L. Gaur, Z. Y. Abd Elmageed, A. Fernando, R. Thouta, A. K. Trappey, M. E. Abdraboh, H. I. El-Sayyad, P. Rao & M. G. Raj (2009) Towards understanding the mode of action of the multifaceted cell adhesion receptor CD146. *Biochim Biophys Acta,* 1795**,** 130-6.
Panteleyev, A. A., C. A. Jahoda & A. M. Christiano (2001) Hair follicle predetermination. *J Cell Sci,* 114**,** 3419-31.
Papamichos-Chronakis, M., S. Watanabe, O. J. Rando & C. L. Peterson (2011) Global regulation of H2A.Z localization by the INO80 chromatin-remodeling enzyme is essential for genome integrity. *Cell,* 144**,** 200-13.
Parthun, M. R. (2007) Hat1: the emerging cellular roles of a type B histone acetyltransferase. *Oncogene,* 26**,** 5319-28.
Peinado, H., D. Olmeda & A. Cano (2007) Snail, Zeb and bHLH factors in tumour progression: an alliance against the epithelial phenotype? *Nat Rev Cancer,* 7**,** 415-28.
Perrot, C. Y., C. Gilbert, V. Marsaud, A. Postigo, D. Javelaud & A. Mauviel (2013) GLI2 cooperates with ZEB1 for transcriptional repression of CDH1 expression in human melanoma cells. *Pigment Cell Melanoma Res,* 26**,** 861-73.
Phung, B., J. Sun, A. Schepsky, E. Steingrimsson & L. Ronnstrand (2011) C-KIT signaling depends on microphthalmia-associated transcription factor for effects on cell proliferation. *PLoS One,* 6**,** e24064.
Pierrat, M. J., V. Marsaud, A. Mauviel & D. Javelaud (2012) Expression of Microphthalmia-associated Transcription Factor (MITF), Which Is Critical for Melanoma Progression, Is Inhibited by Both Transcription Factor GLI2 and Transforming Growth Factor-beta. *J Biol Chem,* 287**,** 17996-8004.
Pingault, V., D. Ente, F. Dastot-Le Moal, M. Goossens, S. Marlin & N. Bondurand (2010) Review and update of mutations causing Waardenburg syndrome. *Hum Mutat,* 31**,** 391-406.

Pogenberg, V., M. H. Ogmundsdottir, K. Bergsteinsdottir, A. Schepsky, B. Phung, V. Deineko, M. Milewski, E. Steingrimsson & M. Wilmanns (2012) Restricted leucine zipper dimerization and specificity of DNA recognition of the melanocyte master regulator MITF. *Genes Dev,* 26**,** 2647-58.

Pollock, P. M., U. L. Harper, K. S. Hansen, L. M. Yudt, M. Stark, C. M. Robbins, T. Y. Moses, G. Hostetter, U. Wagner, J. Kakareka, G. Salem, T. Pohida, P. Heenan, P. Duray, O. Kallioniemi, N. K. Hayward, J. M. Trent & P. S. Meltzer (2003) High frequency of BRAF mutations in nevi. *Nat Genet,* 33**,** 19-20.

Pollock, P. M., G. J. Walker, J. M. Glendening, T. Que Noy, N. C. Bloch, J. W. Fountain & N. K. Hayward (2002) PTEN inactivation is rare in melanoma tumours but occurs frequently in melanoma cell lines. *Melanoma Res,* 12**,** 565-75.

Poot, R. A., L. Bozhenok, D. L. van den Berg, S. Steffensen, F. Ferreira, M. Grimaldi, N. Gilbert, J. Ferreira & P. D. Varga-Weisz (2004) The Williams syndrome transcription factor interacts with PCNA to target chromatin remodelling by ISWI to replication foci. *Nat Cell Biol,* 6**,** 1236-44.

Poser, I., D. Dominguez, A. G. de Herreros, A. Varnai, R. Buettner & A. K. Bosserhoff (2001) Loss of E-cadherin expression in melanoma cells involves up-regulation of the transcriptional repressor Snail. *J Biol Chem,* 276**,** 24661-6.

Potterf, S. B., M. Furumura, K. J. Dunn, H. Arnheiter & W. J. Pavan (2000) Transcription factor hierarchy in Waardenburg syndrome: regulation of MITF expression by SOX10 and PAX3. *Hum Genet,* 107**,** 1-6.

Potterf, S. B., R. Mollaaghababa, L. Hou, E. M. Southard-Smith, T. J. Hornyak, H. Arnheiter & W. J. Pavan (2001) Analysis of SOX10 function in neural crest-derived melanocyte development: SOX10-dependent transcriptional control of dopachrome tautomerase. *Dev Biol,* 237**,** 245-57.

Primot, A., A. Mogha, S. Corre, K. Roberts, J. Debbache, H. Adamski, B. Dreno, A. Khammari, T. Lesimple, A. Mereau, C. R. Goding & M. D. Galibert (2010) ERK-regulated differential expression of the Mitf 6a/b splicing isoforms in melanoma. *Pigment Cell Melanoma Res,* 23**,** 93-102.

Rabbani, P., M. Takeo, W. Chou, P. Myung, M. Bosenberg, L. Chin, M. M. Taketo & M. Ito (2011) Coordinated activation of Wnt in epithelial and melanocyte stem cells initiates pigmented hair regeneration. *Cell,* 145**,** 941-55.

Radtke, F., F. Schweisguth & W. Pear (2005) The Notch 'gospel'. *EMBO Rep,* 6**,** 1120-5.

Rai, T. S., A. Puri, T. McBryan, J. Hoffman, Y. Tang, N. A. Pchelintsev, J. van Tuyn, R. Marmorstein, D. C. Schultz & P. D. Adams (2011) Human CABIN1 is a functional member of the human HIRA/UBN1/ASF1a histone H3.3 chaperone complex. *Mol Cell Biol,* 31**,** 4107-18.

Raidl, M., C. Pirker, R. Schulte-Hermann, M. Aubele, D. Kandioler-Eckersberger, F. Wrba, M. Micksche, W. Berger & B. Grasl-Kraupp (2004) Multiple chromosomal abnormalities in human liver (pre)neoplasia. *J Hepatol,* 40**,** 660-8.

Raviv, S., K. Bharti, S. Rencus-Lazar, Y. Cohen-Tayar, R. Schyr, N. Evantal, E. Meshorer, A. Zilberberg, M. Idelson, B. Reubinoff, R. Grebe, R. Rosin-Arbesfeld, J. Lauderdale, G. Lutty, H. Arnheiter & R. Ashery-Padan (2014) PAX6 Regulates Melanogenesis in the Retinal Pigmented Epithelium through Feed-Forward Regulatory Interactions with MITF. *PLoS Genet,* 10**,** e1004360.

Ray-Gallet, D., J. P. Quivy, C. Scamps, E. M. Martini, M. Lipinski & G. Almouzni (2002) HIRA is critical for a nucleosome assembly pathway independent of DNA synthesis. *Mol Cell,* 9**,** 1091-100.

Rea, S., F. Eisenhaber, D. O'Carroll, B. D. Strahl, Z. W. Sun, M. Schmid, S. Opravil, K. Mechtler, C. P. Ponting, C. D. Allis & T. Jenuwein (2000) Regulation of chromatin structure by site-specific histone H3 methyltransferases. *Nature,* 406**,** 593-9.

Reid, K., A. M. Turnley, G. D. Maxwell, Y. Kurihara, H. Kurihara, P. F. Bartlett & M. Murphy (1996) Multiple roles for endothelin in melanocyte development: regulation of progenitor number and stimulation of differentiation. *Development,* 122**,** 3911-9.

Rigel, D. S. (2010) Epidemiology of melanoma. *Semin Cutan Med Surg,* 29**,** 204-9.

Riley, P. A. (1997) Melanin. *Int J Biochem Cell Biol,* 29**,** 1235-9.

Rimm, D. L., K. Caca, G. Hu, F. B. Harrison & E. R. Fearon (1999) Frequent nuclear/cytoplasmic localization of beta-catenin without exon 3 mutations in malignant melanoma. *Am J Pathol,* 154**,** 325-9.

Rodriguez, M., E. Aladowicz, L. Lanfrancone & C. R. Goding (2008) Tbx3 represses E-cadherin expression and enhances melanoma invasiveness. *Cancer Res,* 68**,** 7872-81.

Rodriguez, M. S., C. Dargemont & R. T. Hay (2001) SUMO-1 conjugation in vivo requires both a consensus modification motif and nuclear targeting. *J Biol Chem,* 276**,** 12654-9.

Rosa, A. & R. Everaers (2008) Structure and dynamics of interphase chromosomes. *PLoS Comput Biol,* 4**,** e1000153.

Rothbart, S. B. & B. D. Strahl (2014) Interpreting the language of histone and DNA modifications. *Biochim Biophys Acta,* 1839**,** 627-643.

Ruan, H. B., N. Zhang & X. Gao (2005) Identification of a novel point mutation of mouse proto-oncogene c-kit through N-ethyl-N-nitrosourea mutagenesis. *Genetics,* 169**,** 819-31.

Rudolph, K. L., S. Chang, H. W. Lee, M. Blasco, G. J. Gottlieb, C. Greider & R. A. DePinho (1999) Longevity, stress response, and cancer in aging telomerase-deficient mice. *Cell,* 96**,** 701-12.

Ruthenburg, A. J., H. Li, T. A. Milne, S. Dewell, R. K. McGinty, M. Yuen, B. Ueberheide, Y. Dou, T. W. Muir, D. J. Patel & C. D. Allis (2011) Recognition of a mononucleosomal histone modification pattern by BPTF via multivalent interactions. *Cell,* 145**,** 692-706.

Ruthenburg, A. J., H. Li, D. J. Patel & C. D. Allis (2007) Multivalent engagement of chromatin modifications by linked binding modules. *Nat Rev Mol Cell Biol,* 8**,** 983-94.

Saha, B., S. K. Singh, C. Sarkar, R. Bera, J. Ratha, D. J. Tobin & R. Bhadra (2006) Activation of the Mitf promoter by lipid-stimulated activation of p38-stress signalling to CREB. *Pigment Cell Res,* 19**,** 595-605.

Saito, H., K. Yasumoto, K. Takeda, K. Takahashi, A. Fukuzaki, S. Orikasa & S. Shibahara (2002) Melanocyte-specific microphthalmia-associated transcription factor isoform activates its own gene promoter through physical interaction with lymphoid-enhancing factor 1. *J Biol Chem,* 277**,** 28787-94.

Saladi, S. V., B. Keenen, H. G. Marathe, H. Qi, K. V. Chin & I. L. de la Serna (2010) Modulation of extracellular matrix/adhesion molecule expression by BRG1 is associated with increased melanoma invasiveness. *Mol Cancer,* 9**,** 280.

Saladi, S. V., P. G. Wong, A. R. Trivedi, H. G. Marathe, B. Keenen, S. Aras, Z. Q. Liew, V. Setaluri & I. L. de la Serna (2013) BRG1 promotes survival of UV-irradiated melanoma cells by cooperating with MITF to activate the melanoma inhibitor of apoptosis gene. *Pigment Cell Melanoma Res,* 26**,** 377-91.

Saldana-Caboverde, A. & L. Kos (2010) Roles of endothelin signaling in melanocyte development and melanoma. *Pigment Cell Melanoma Res,* 23**,** 160-70.

Sanchez-Martin, M., J. Perez-Losada, A. Rodriguez-Garcia, B. Gonzalez-Sanchez, B. R. Korf, W. Kuster, C. Moss, R. A. Spritz & I. Sanchez-Garcia (2003) Deletion of the SLUG (SNAI2) gene results in human piebaldism. *Am J Med Genet A,* 122A**,** 125-32.

Sanchez, R. & M. M. Zhou (2009) The role of human bromodomains in chromatin biology and gene transcription. *Curr Opin Drug Discov Devel,* 12**,** 659-65.

Santos-Rosa, H., R. Schneider, A. J. Bannister, J. Sherriff, B. E. Bernstein, N. C. Emre, S. L. Schreiber, J. Mellor & T. Kouzarides (2002) Active genes are tri-methylated at K4 of histone H3. *Nature,* 419**,** 407-11.

Sato-Jin, K., E. K. Nishimura, E. Akasaka, W. Huber, H. Nakano, A. Miller, J. Du, M. Wu, K. Hanada, D. Sawamura, D. E. Fisher & G. Imokawa (2008) Epistatic connections between microphthalmia-associated transcription factor and endothelin signaling in Waardenburg syndrome and other pigmentary disorders. *FASEB J,* 22**,** 1155-68.

Sato, S., K. Roberts, G. Gambino, A. Cook, T. Kouzarides & C. R. Goding (1997) CBP/p300 as a co-factor for the Microphthalmia transcription factor. *Oncogene,* 14**,** 3083-92.

Sauer, B. (1998) Inducible gene targeting in mice using the Cre/lox system. *Methods,* 14**,** 381-92.

Sauter, E. R., U. C. Yeo, A. von Stemm, W. Zhu, S. Litwin, D. S. Tichansky, G. Pistritto, M. Nesbit, D. Pinkel, M. Herlyn & B. C. Bastian (2002) Cyclin D1 is a candidate oncogene in cutaneous melanoma. *Cancer Res,* 62**,** 3200-6.

Schauer, E., F. Trautinger, A. Kock, A. Schwarz, R. Bhardwaj, M. Simon, J. C. Ansel, T. Schwarz & T. A. Luger (1994) Proopiomelanocortin-derived peptides are synthesized and released by human keratinocytes. *J Clin Invest,* 93**,** 2258-62.

Schenk, R., A. Jenke, M. Zilbauer, S. Wirth & J. Postberg (2011) H3.5 is a novel hominid-specific histone H3 variant that is specifically expressed in the seminiferous tubules of human testes. *Chromosoma,* 120**,** 275-85.

Schepsky, A., K. Bruser, G. J. Gunnarsson, J. Goodall, J. H. Hallsson, C. R. Goding, E. Steingrimsson & A. Hecht (2006) The microphthalmia-associated transcription factor Mitf interacts with beta-catenin to determine target gene expression. *Mol Cell Biol,* 26**,** 8914-27.

Schmelz, M. (2011) Neuronal sensitivity of the skin. *Eur J Dermatol,* 21 Suppl 2**,** 43-7.

Schmidt, D. & S. Muller (2003) PIAS/SUMO: new partners in transcriptional regulation. *Cell Mol Life Sci,* 60**,** 2561-74.

Schouwey, K., V. Delmas, L. Larue, U. Zimber-Strobl, L. J. Strobl, F. Radtke & F. Beermann (2007) Notch1 and Notch2 receptors influence progressive hair graying in a dose-dependent manner. *Dev Dyn,* 236**,** 282-9.

Schouwey, K., L. Larue, F. Radtke, V. Delmas & F. Beermann (2009) Transgenic expression of Notch in melanocytes demonstrates RBP-Jkappa-dependent signaling. *Pigment Cell Melanoma Res*.

Schreiber, R. D., L. J. Old & M. J. Smyth (2011) Cancer immunoediting: integrating immunity's roles in cancer suppression and promotion. *Science,* 331**,** 1565-70.

Schwanbeck, R., H. Xiao & C. Wu (2004) Spatial contacts and nucleosome step movements induced by the NURF chromatin remodeling complex. *J Biol Chem,* 279**,** 39933-41.

Scortegagna, M., C. Ruller, Y. Feng, R. Lazova, H. Kluger, J. L. Li, S. K. De, R. Rickert, M. Pellecchia, M. Bosenberg & Z. A. Ronai (2014) Genetic inactivation or pharmacological inhibition of Pdk1 delays development and inhibits metastasis of Braf(V600E)::Pten(-/-) melanoma. *Oncogene,* 33**,** 4330-9.

Seeler, J. S. & A. Dejean (2003) Nuclear and unclear functions of SUMO. *Nat Rev Mol Cell Biol,* 4**,** 690-9.

Seneschal, J., R. A. Clark, A. Gehad, C. M. Baecher-Allan & T. S. Kupper (2012) Human epidermal Langerhans cells maintain immune homeostasis in skin by activating skin resident regulatory T cells. *Immunity,* 36**,** 873-84.

Serrano, M., G. J. Hannon & D. Beach (1993) A new regulatory motif in cell-cycle control causing specific inhibition of cyclin D/CDK4. *Nature,* 366**,** 704-7.

Settembre, C., C. Di Malta, V. A. Polito, M. Garcia Arencibia, F. Vetrini, S. Erdin, S. U. Erdin, T. Huynh, D. Medina, P. Colella, M. Sardiello, D. C. Rubinsztein & A. Ballabio (2011) TFEB links autophagy to lysosomal biogenesis. *Science,* 332**,** 1429-33.

Shah, D. J. & R. S. Dronca (2014) Latest advances in chemotherapeutic, targeted, and immune approaches in the treatment of metastatic melanoma. *Mayo Clin Proc,* 89**,** 504-19.

Sharpless, E. & L. Chin (2003) The INK4a/ARF locus and melanoma. *Oncogene,* 22**,** 3092-8.

Shi, Y., F. Lan, C. Matson, P. Mulligan, J. R. Whetstine, P. A. Cole & R. A. Casero (2004) Histone demethylation mediated by the nuclear amine oxidase homolog LSD1. *Cell,* 119**,** 941-53.

Shiio, Y. & R. N. Eisenman (2003) Histone sumoylation is associated with transcriptional repression. *Proc Natl Acad Sci U S A,* 100**,** 13225-30.

Shin, M. K., J. M. Levorse, R. S. Ingram & S. M. Tilghman (1999) The temporal requirement for endothelin receptor-B signalling during neural crest development. *Nature,* 402**,** 496-501.

Simon, J. D., D. Peles, K. Wakamatsu & S. Ito (2009) Current challenges in understanding melanogenesis: bridging chemistry, biological control, morphology, and function. *Pigment Cell Melanoma Res,* 22**,** 563-79.

Simpson, R. T. (1978) Structure of the chromatosome, a chromatin particle containing 160 base pairs of DNA and all the histones. *Biochemistry,* 17**,** 5524-31.

Sims, J. K. & P. A. Wade (2011) SnapShot: Chromatin remodeling: CHD. *Cell,* 144**,** 626-626 e1.

Slominski, A., D. J. Tobin, S. Shibahara & J. Wortsman (2004) Melanin pigmentation in mammalian skin and its hormonal regulation. *Physiol Rev,* 84**,** 1155-228.

Slominski, A., J. Wortsman, P. M. Plonka, K. U. Schallreuter, R. Paus & D. J. Tobin (2005) Hair follicle pigmentation. *J Invest Dermatol,* 124**,** 13-21.

Smalley, K. S., R. Contractor, T. K. Nguyen, M. Xiao, R. Edwards, V. Muthusamy, A. J. King, K. T. Flaherty, M. Bosenberg, M. Herlyn & K. L. Nathanson (2008) Identification of a novel subgroup of melanomas with KIT/cyclin-dependent kinase-4 overexpression. *Cancer Res,* 68**,** 5743-52.

Smoller, B. R. (2006) Histologic criteria for diagnosing primary cutaneous malignant melanoma. *Mod Pathol,* 19 Suppl 2**,** S34-40.

Soengas, M. S. & S. W. Lowe (2003) Apoptosis and melanoma chemoresistance. *Oncogene,* 22**,** 3138-51.

Sommer, L. (2005) Checkpoints of melanocyte stem cell development. *Sci STKE,* 2005**,** pe42.

Song, H., C. Spichiger-Haeusermann & K. Basler (2009) The ISWI-containing NURF complex regulates the output of the canonical Wingless pathway. *EMBO Rep,* 10**,** 1140-6.

Stahl, J. M., A. Sharma, M. Cheung, M. Zimmerman, J. Q. Cheng, M. W. Bosenberg, M. Kester, L. Sandirasegarane & G. P. Robertson (2004) Deregulated Akt3 activity promotes development of malignant melanoma. *Cancer Res,* 64**,** 7002-10.

Stanchina, L., V. Baral, F. Robert, V. Pingault, N. Lemort, V. Pachnis, M. Goossens & N. Bondurand (2006) Interactions between Sox10, Edn3 and Ednrb during enteric nervous system and melanocyte development. *Dev Biol,* 295**,** 232-49.

Steingrimsson, E. (2010) Interpretation of complex phenotypes: lessons from the Mitf gene. *Pigment Cell Melanoma Res,* 23**,** 736-40.

Steingrimsson, E., N. G. Copeland & N. A. Jenkins (2004) Melanocytes and the microphthalmia transcription factor network. *Annu Rev Genet,* 38**,** 365-411.

Steingrimsson, E., L. Tessarollo, B. Pathak, L. Hou, H. Arnheiter, N. G. Copeland & N. A. Jenkins (2002) Mitf and Tfe3, two members of the Mitf-Tfe family of bHLH-Zip transcription factors, have important but functionally redundant roles in osteoclast development. *Proc Natl Acad Sci U S A,* 99**,** 4477-82.

Stenn, K. S. & R. Paus (2001) Controls of hair follicle cycling. *Physiol Rev,* 81**,** 449-494.

Stillman, B. (1986) Chromatin assembly during SV40 DNA replication in vitro. *Cell,* 45**,** 555-65.

Stirnimann, C. U., E. Petsalaki, R. B. Russell & C. W. Muller (2010) WD40 proteins propel cellular networks. *Trends Biochem Sci,* 35**,** 565-74.

Strahl, B. D. & C. D. Allis (2000) The language of covalent histone modifications. *Nature,* 403**,** 41-5.

Strub, T., S. Giuliano, T. Ye, C. Bonet, C. Keime, D. Kobi, S. Le Gras, M. Cormont, R. Ballotti, C. Bertolotto & I. Davidson (2011) Essential role of microphthalmia transcription factor for DNA replication, mitosis and genomic stability in melanoma. *Oncogene,* 30**,** 2319-32.

Stucker, M., A. Struk, P. Altmeyer, M. Herde, H. Baumgartl & D. W. Lubbers (2002) The cutaneous uptake of atmospheric oxygen contributes significantly to the oxygen supply of human dermis and epidermis. *J Physiol,* 538**,** 985-94.

Sturm, R. A., C. Fox, P. McClenahan, K. Jagirdar, M. Ibarrola-Villava, P. Banan, N. C. Abbott, G. Ribas, B. Gabrielli, D. L. Duffy & H. P. Soyer (2014) Phenotypic characterization of nevus and tumor patterns in MITF E318K mutation carrier melanoma patients. *J Invest Dermatol,* 134**,** 141-9.

Sugiyama, K., K. Sugiura, T. Hara, K. Sugimoto, H. Shima, K. Honda, K. Furukawa, S. Yamashita & T. Urano (2002) Aurora-B associated protein phosphatases as negative regulators of kinase activation. *Oncogene,* 21**,** 3103-11.

Sullivan, R. J. & K. T. Flaherty (2013) Resistance to BRAF-targeted therapy in melanoma. *Eur J Cancer,* 49**,** 1297-304.

Sun, J., L. Purcell, Z. Gao, S. D. Isaacs, K. E. Wiley, F. C. Hsu, W. Liu, D. Duggan, J. D. Carpten, H. Gronberg, J. Xu, B. L. Chang, A. W. Partin, P. C. Walsh, W. B. Isaacs & S. L. Zheng (2008) Association between sequence variants at 17q12 and 17q24.3 and prostate cancer risk in European and African Americans. *Prostate,* 68**,** 691-7.

Suto, R. K., M. J. Clarkson, D. J. Tremethick & K. Luger (2000) Crystal structure of a nucleosome core particle containing the variant histone H2A.Z. *Nat Struct Biol,* 7**,** 1121-4.

Sviderskaya, E. V., V. C. Gray-Schopfer, S. P. Hill, N. P. Smit, T. J. Evans-Whipp, J. Bond, L. Hill, V. Bataille, G. Peters, D. Kipling, D. Wynford-Thomas & D. C. Bennett (2003) p16/cyclin-dependent kinase inhibitor 2A deficiency in human melanocyte senescence, apoptosis, and immortalization: possible implications for melanoma progression. *J Natl Cancer Inst,* 95**,** 723-32.

Swygert, S. G. & C. L. Peterson (2014) Chromatin dynamics: Interplay between remodeling enzymes and histone modifications. *Biochim Biophys Acta,* 1839**,** 728-736.

Tachibana, M., L. A. Perez-Jurado, A. Nakayama, C. A. Hodgkinson, X. Li, M. Schneider, T. Miki, J. Fex, U. Francke & H. Arnheiter (1994) Cloning of MITF, the human homolog of the mouse microphthalmia gene and assignment to chromosome 3p14.1-p12.3. *Hum Mol Genet,* 3**,** 553-7.

Tagami, H., D. Ray-Gallet, G. Almouzni & Y. Nakatani (2004) Histone H3.1 and H3.3 complexes mediate nucleosome assembly pathways dependent or independent of DNA synthesis. *Cell,* 116**,** 51-61.

Takeda, K., C. Takemoto, I. Kobayashi, A. Watanabe, Y. Nobukuni, D. E. Fisher & M. Tachibana (2000a) Ser298 of MITF, a mutation site in Waardenburg syndrome type 2, is a phosphorylation site with functional significance. *Hum Mol Genet,* 9**,** 125-32.

Takeda, K., K. Yasumoto, N. Kawaguchi, T. Udono, K. Watanabe, H. Saito, K. Takahashi, M. Noda & S. Shibahara (2002) Mitf-D, a newly identified isoform, expressed in the retinal pigment epithelium and monocyte-lineage cells affected by Mitf mutations. *Biochimica et biophysica acta,* 1574**,** 15-23.

Takeda, K., K. Yasumoto, R. Takada, S. Takada, K. Watanabe, T. Udono, H. Saito, K. Takahashi & S. Shibahara (2000b) Induction of melanocyte-specific microphthalmia-associated transcription factor by Wnt-3a. *J Biol Chem,* 275**,** 14013-6.

Takemoto, C. M., Y. J. Yoon & D. E. Fisher (2002) The identification and functional characterization of a novel mast cell isoform of the microphthalmia-associated transcription factor. *The Journal of biological chemistry,* 277**,** 30244-52.

Talbert, P. B. & S. Henikoff (2010) Histone variants--ancient wrap artists of the epigenome. *Nat Rev Mol Cell Biol,* 11**,** 264-75.

Taneja, S. S. (2012) Re: Safety and activity of anti-PD-L1 antibody in patients with advanced cancer. *J Urol,* 188**,** 2148-9.

Tarhini, A. A. & S. S. Agarwala (2006) Cutaneous melanoma: available therapy for metastatic disease. *Dermatol Ther,* 19**,** 19-25.

Tassabehji, M., V. E. Newton & A. P. Read (1994) Waardenburg syndrome type 2 caused by mutations in the human microphthalmia (MITF) gene. *Nat Genet,* 8**,** 251-5.

Taunton, J., C. A. Hassig & S. L. Schreiber (1996) A mammalian histone deacetylase related to the yeast transcriptional regulator Rpd3p. *Science,* 272**,** 408-11.

Taverna, S. D., H. Li, A. J. Ruthenburg, C. D. Allis & D. J. Patel (2007) How chromatin-binding modules interpret histone modifications: lessons from professional pocket pickers. *Nat Struct Mol Biol,* 14**,** 1025-40.

Taylor, G., M. S. Lehrer, P. J. Jensen, T. T. Sun & R. M. Lavker (2000) Involvement of follicular stem cells in forming not only the follicle but also the epidermis. *Cell,* 102**,** 451-61.

Thiery, J. P., H. Acloque, R. Y. Huang & M. A. Nieto (2009) Epithelial-mesenchymal transitions in development and disease. *Cell,* 139**,** 871-90.

Thomas, A. J. & C. A. Erickson (2009) FOXD3 regulates the lineage switch between neural crest-derived glial cells and pigment cells by repressing MITF through a non-canonical mechanism. *Development,* 136**,** 1849-58.

Thompson, J. F., R. A. Scolyer & R. F. Kefford (2005) Cutaneous melanoma. *Lancet,* 365**,** 687-701.

Tjeertes, J. V., K. M. Miller & S. P. Jackson (2009) Screen for DNA-damage-responsive histone modifications identifies H3K9Ac and H3K56Ac in human cells. *EMBO J,* 28**,** 1878-89.

Tobin, D. J. (2011) The cell biology of human hair follicle pigmentation. *Pigment Cell Melanoma Res,* 24**,** 75-88.

Tokuda, N., T. P. Terada & M. Sasai (2012) Dynamical modeling of three-dimensional genome organization in interphase budding yeast. *Biophys J,* 102**,** 296-304.

Tolstorukov, M. Y., J. A. Goldman, C. Gilbert, V. Ogryzko, R. E. Kingston & P. J. Park (2012) Histone variant H2A.Bbd is associated with active transcription and mRNA processing in human cells. *Mol Cell,* 47**,** 596-607.

Tomkinson, A. E. & Z. B. Mackey (1998) Structure and function of mammalian DNA ligases. *Mutat Res,* 407**,** 1-9.

Trievel, R. C., B. M. Beach, L. M. Dirk, R. L. Houtz & J. H. Hurley (2002) Structure and catalytic mechanism of a SET domain protein methyltransferase. *Cell,* 111**,** 91-103.

Tsao, H., M. B. Atkins & A. J. Sober (2004a) Management of cutaneous melanoma. *N Engl J Med,* 351**,** 998-1012.

Tsao, H., V. Goel, H. Wu, G. Yang & F. G. Haluska (2004b) Genetic interaction between NRAS and BRAF mutations and PTEN/MMAC1 inactivation in melanoma. *J Invest Dermatol,* 122**,** 337-41.

Tsukada, Y., J. Fang, H. Erdjument-Bromage, M. E. Warren, C. H. Borchers, P. Tempst & Y. Zhang (2006) Histone demethylation by a family of JmjC domain-containing proteins. *Nature,* 439**,** 811-6.

Tsukiyama, T., P. B. Becker & C. Wu (1994) ATP-dependent nucleosome disruption at a heat-shock promoter mediated by binding of GAGA transcription factor. *Nature,* 367**,** 525-32.

Tsukiyama, T., C. Daniel, J. Tamkun & C. Wu (1995) ISWI, a member of the SWI2/SNF2 ATPase family, encodes the 140 kDa subunit of the nucleosome remodeling factor. *Cell,* 83**,** 1021-6.

Tsukiyama, T. & C. Wu (1995) Purification and properties of an ATP-dependent nucleosome remodeling factor. *Cell,* 83**,** 1011-20.

Tumbar, T., G. Guasch, V. Greco, C. Blanpain, W. E. Lowry, M. Rendl & E. Fuchs (2004) Defining the epithelial stem cell niche in skin. *Science,* 303**,** 359-63.

Turner, B. M. (2000) Histone acetylation and an epigenetic code. *Bioessays,* 22**,** 836-45.

Tyler, J. K., C. R. Adams, S. R. Chen, R. Kobayashi, R. T. Kamakaka & J. T. Kadonaga (1999) The RCAF complex mediates chromatin assembly during DNA replication and repair. *Nature,* 402**,** 555-60.

Udono, T., K. Yasumoto, K. Takeda, S. Amae, K. Watanabe, H. Saito, N. Fuse, M. Tachibana, K. Takahashi, M. Tamai & S. Shibahara (2000) Structural organization of the human microphthalmia-associated transcription factor gene containing four alternative promoters. *Biochim Biophys Acta,* 1491**,** 205-19.

Vachtenheim, J., L. Ondrusova & J. Borovansky (2010) SWI/SNF chromatin remodeling complex is critical for the expression of microphthalmia-associated transcription factor in melanoma cells. *Biochem Biophys Res Commun,* 392**,** 454-9.

Valverde, P., E. Healy, I. Jackson, J. L. Rees & A. J. Thody (1995) Variants of the melanocyte-stimulating hormone receptor gene are associated with red hair and fair skin in humans. *Nat Genet,* 11**,** 328-30.

van Elsas, A., S. Zerp, S. van der Flier, M. Kruse-Wolters, A. Vacca, D. J. Ruiter & P. Schrier (1995) Analysis of N-ras mutations in human cutaneous melanoma: tumor heterogeneity detected by polymerase chain reaction/single-stranded conformation polymorphism analysis. *Recent Results Cancer Res,* 139**,** 57-67.

Vandesompele, J., E. Michels, K. De Preter, B. Menten, A. Schramm, A. Eggert, P. F. Ambros, V. Combaret, N. Francotte, F. Antonacci, A. De Paepe, G. Laureys, F. Speleman & N. Van Roy (2008) Identification of 2 putative critical segments of 17q gain in neuroblastoma through integrative genomics. *Int J Cancer,* 122**,** 1177-82.

Vermeulen, M., H. C. Eberl, F. Matarese, H. Marks, S. Denissov, F. Butter, K. K. Lee, J. V. Olsen, A. A. Hyman, H. G. Stunnenberg & M. Mann (2010) Quantitative interaction proteomics and genome-wide profiling of epigenetic histone marks and their readers. *Cell,* 142**,** 967-80.

Verreault, A., P. D. Kaufman, R. Kobayashi & B. Stillman (1996) Nucleosome assembly by a complex of CAF-1 and acetylated histones H3/H4. *Cell,* 87**,** 95-104.

Vicent, G. P., A. S. Nacht, J. Font-Mateu, G. Castellano, L. Gaveglia, C. Ballare & M. Beato (2011) Four enzymes cooperate to displace histone H1 during the first minute of hormonal gene activation. *Genes Dev,* 25**,** 845-62.

Voigt, P., G. LeRoy, W. J. Drury, 3rd, B. M. Zee, J. Son, D. B. Beck, N. L. Young, B. A. Garcia & D. Reinberg (2012) Asymmetrically modified nucleosomes. *Cell,* 151**,** 181-93.

Voigt, P., W. W. Tee & D. Reinberg (2013) A double take on bivalent promoters. *Genes Dev,* 27**,** 1318-38.

Voss, T. C. & G. L. Hager (2014) Dynamic regulation of transcriptional states by chromatin and transcription factors. *Nat Rev Genet,* 15**,** 69-81.

Wang, H., L. Wang, H. Erdjument-Bromage, M. Vidal, P. Tempst, R. S. Jones & Y. Zhang (2004) Role of histone H2A ubiquitination in Polycomb silencing. *Nature,* 431**,** 873-8.

Wang, L., Y. Du, J. M. Ward, T. Shimbo, B. Lackford, X. Zheng, Y. L. Miao, B. Zhou, L. Han, D. C. Fargo, R. Jothi, C. J. Williams, P. A. Wade & G. Hu (2014) INO80 facilitates pluripotency gene activation in embryonic stem cell self-renewal, reprogramming, and blastocyst development. *Cell Stem Cell,* 14**,** 575-91.

Wang, W. (2007) Emergence of a DNA-damage response network consisting of Fanconi anaemia and BRCA proteins. *Nat Rev Genet,* 8**,** 735-48.

Wang, Z. & D. J. Patel (2011) Combinatorial readout of dual histone modifications by paired chromatin-associated modules. *J Biol Chem,* 286**,** 18363-8.

Watanabe, A., K. Takeda, B. Ploplis & M. Tachibana (1998) Epistatic relationship between Waardenburg syndrome genes MITF and PAX3. *Nat Genet,* 18**,** 283-6.

Watanabe, K., K. Takeda, K. Yasumoto, T. Udono, H. Saito, K. Ikeda, T. Takasaka, K. Takahashi, T. Kobayashi, M. Tachibana & S. Shibahara (2002) Identification of a distal enhancer for the melanocyte-specific promoter of the MITF gene. *Pigment Cell Res,* 15**,** 201-11.

Weeraratna, A. T., Y. Jiang, G. Hostetter, K. Rosenblatt, P. Duray, M. Bittner & J. M. Trent (2002) Wnt5a signaling directly affects cell motility and invasion of metastatic melanoma. *Cancer Cell,* 1**,** 279-88.

Wehrle-Haller, B. & J. A. Weston (1995) Soluble and cell-bound forms of steel factor activity play distinct roles in melanocyte precursor dispersal and survival on the lateral neural crest migration pathway. *Development,* 121**,** 731-42.

Wellbrock, C., C. Weisser, E. Geissinger, J. Troppmair & M. Schartl (2002) Activation of p59(Fyn) leads to melanocyte dedifferentiation by influencing MKP-1-regulated mitogen-activated protein kinase signaling. *J Biol Chem,* 277**,** 6443-54.

Whetstine, J. R., A. Nottke, F. Lan, M. Huarte, S. Smolikov, Z. Chen, E. Spooner, E. Li, G. Zhang, M. Colaiacovo & Y. Shi (2006) Reversal of histone lysine trimethylation by the JMJD2 family of histone demethylases. *Cell,* 125**,** 467-81.

Widlund, H. R., M. A. Horstmann, E. R. Price, J. Cui, S. L. Lessnick, M. Wu, X. He & D. E. Fisher (2002) Beta-catenin-induced melanoma growth requires the downstream target Microphthalmia-associated transcription factor. *J Cell Biol,* 158**,** 1079-87.

Widmer, D. S., P. F. Cheng, O. M. Eichhoff, B. C. Belloni, M. C. Zipser, N. C. Schlegel, D. Javelaud, A. Mauviel, R. Dummer & K. S. Hoek (2012) Systematic classification of melanoma cells by phenotype-specific gene expression mapping. *Pigment Cell Melanoma Res,* 25**,** 343-53.

Wiedemann, S. M., S. N. Mildner, C. Bonisch, L. Israel, A. Maiser, S. Matheisl, T. Straub, R. Merkl, H. Leonhardt, E. Kremmer, L. Schermelleh & S. B. Hake (2010) Identification and characterization of two novel primate-specific histone H3 variants, H3.X and H3.Y. *J Cell Biol,* 190**,** 777-91.

Willmore-Payne, C., J. A. Holden, S. Tripp & L. J. Layfield (2005) Human malignant melanoma: detection of BRAF- and c-kit-activating mutations by high-resolution amplicon melting analysis. *Hum Pathol,* 36**,** 486-93.

Winkler, D. D., H. Zhou, M. A. Dar, Z. Zhang & K. Luger (2012) Yeast CAF-1 assembles histone (H3-H4)2 tetramers prior to DNA deposition. *Nucleic Acids Res,* 40**,** 10139-49.

Wolchok, J. D., H. Kluger, M. K. Callahan, M. A. Postow, N. A. Rizvi, A. M. Lesokhin, N. H. Segal, C. E. Ariyan, R. A. Gordon, K. Reed, M. M. Burke, A. Caldwell, S. A. Kronenberg, B. U. Agunwamba, X. Zhang, I. Lowy, H. D. Inzunza, W. Feely, C. E. Horak, Q. Hong, A. J. Korman, J. M. Wigginton, A. Gupta & M. Sznol (2013) Nivolumab plus ipilimumab in advanced melanoma. *N Engl J Med,* 369**,** 122-33.

Wolf, S. S. (2009) The protein arginine methyltransferase family: an update about function, new perspectives and the physiological role in humans. *Cell Mol Life Sci,* 66**,** 2109-21.

Wood, A. & A. Shilatifard (2004) Posttranslational modifications of histones by methylation. *Adv Protein Chem,* 67**,** 201-22.

Woodcock, C. L. & R. P. Ghosh (2010) Chromatin higher-order structure and dynamics. *Cold Spring Harb Perspect Biol,* 2**,** a000596.

Wrana, J. L. (2013) Signaling by the TGFbeta superfamily. *Cold Spring Harb Perspect Biol,* 5**,** a011197.

Wu, G. J., C. S. Sinclair, J. Paape, J. N. Ingle, P. C. Roche, C. D. James & F. J. Couch (2000a) 17q23 amplifications in breast cancer involve the PAT1, RAD51C, PS6K, and SIGma1B genes. *Cancer Res,* 60**,** 5371-5.

Wu, H., V. Goel & F. G. Haluska (2003) PTEN signaling pathways in melanoma. *Oncogene,* 22**,** 3113-22.

Wu, M., T. J. Hemesath, C. M. Takemoto, M. A. Horstmann, A. G. Wells, E. R. Price, D. Z. Fisher & D. E. Fisher (2000b) c-Kit triggers dual phosphorylations, which couple activation and degradation of the essential melanocyte factor Mi. *Genes Dev,* 14**,** 301-12.

Wysocka, J., T. Swigut, H. Xiao, T. A. Milne, S. Y. Kwon, J. Landry, M. Kauer, A. J. Tackett, B. T. Chait, P. Badenhorst, C. Wu & C. D. Allis (2006) A PHD finger of NURF couples histone H3 lysine 4 trimethylation with chromatin remodelling. *Nature,* 442**,** 86-90.

Xiao, A., H. Li, D. Shechter, S. H. Ahn, L. A. Fabrizio, H. Erdjument-Bromage, S. Ishibe-Murakami, B. Wang, P. Tempst, K. Hofmann, D. J. Patel, S. J. Elledge & C. D. Allis (2009) WSTF regulates the H2A.X DNA damage response via a novel tyrosine kinase activity. *Nature,* 457**,** 57-62.

Xiao, F., Y. C. Kim, C. Snyder, H. Wen, P. X. Chen, J. Luo, D. Becirovic, B. Downs, K. H. Cowan, H. Lynch & S. M. Wang (2014) Genome instability in blood cells of a BRCA1+ breast cancer family. *BMC Cancer,* 14**,** 342.

Xiao, H., R. Sandaltzopoulos, H. M. Wang, A. Hamiche, R. Ranallo, K. M. Lee, D. Fu & C. Wu (2001) Dual functions of largest NURF subunit NURF301 in nucleosome sliding and transcription factor interactions. *Mol Cell,* 8**,** 531-43.

Xue, Y., R. Gibbons, Z. Yan, D. Yang, T. L. McDowell, S. Sechi, J. Qin, S. Zhou, D. Higgs & W. Wang (2003) The ATRX syndrome protein forms a chromatin-remodeling complex with Daxx and localizes in promyelocytic leukemia nuclear bodies. *Proc Natl Acad Sci U S A,* 100**,** 10635-40.

Yadon, A. N. & T. Tsukiyama (2011) SnapShot: Chromatin remodeling: ISWI. *Cell,* 144**,** 453-453 e1.

Yajima, I., E. Belloir, Y. Bourgeois, M. Kumasaka, V. Delmas & L. Larue (2006) Spatiotemporal gene control by the Cre-ERT2 system in melanocytes. *Genesis,* 44**,** 34-43.

Yamaguchi, Y., M. Brenner & V. J. Hearing (2007) The regulation of skin pigmentation. *J Biol Chem,* 282**,** 27557-61.

Yang, G., Y. Li, E. K. Nishimura, H. Xin, A. Zhou, Y. Guo, L. Dong, M. F. Denning, B. J. Nickoloff & R. Cui (2008) Inhibition of PAX3 by TGF-beta modulates melanocyte viability. *Mol Cell,* 32**,** 554-63.

Yang, J. G., T. S. Madrid, E. Sevastopoulos & G. J. Narlikar (2006) The chromatin-remodeling enzyme ACF is an ATP-dependent DNA length sensor that regulates nucleosome spacing. *Nat Struct Mol Biol,* 13**,** 1078-83.

Yang, X. J. & E. Seto (2007) HATs and HDACs: from structure, function and regulation to novel strategies for therapy and prevention. *Oncogene,* 26**,** 5310-8.

Yang, X. J. & E. Seto (2008) The Rpd3/Hda1 family of lysine deacetylases: from bacteria and yeast to mice and men. *Nat Rev Mol Cell Biol,* 9**,** 206-18.

Yasumoto, K., K. Takeda, H. Saito, K. Watanabe, K. Takahashi & S. Shibahara (2002) Microphthalmia-associated transcription factor interacts with LEF-1, a mediator of Wnt signaling. *EMBO J,* 21**,** 2703-14.

Yokoyama, S., S. L. Woods, G. M. Boyle, L. G. Aoude, S. MacGregor, V. Zismann, M. Gartside, A. E. Cust, R. Haq, M. Harland, J. C. Taylor, D. L. Duffy, K. Holohan, K. Dutton-Regester, J. M. Palmer, V. Bonazzi, M. S. Stark, J. Symmons, M. H. Law, C. Schmidt, C. Lanagan, L. O'Connor, E. A. Holland, H. Schmid, J. A. Maskiell, J. Jetann, M. Ferguson, M. A. Jenkins, R. F. Kefford, G. G. Giles, B. K. Armstrong, J. F. Aitken, J. L. Hopper, D. C. Whiteman, P. D. Pharoah, D. F. Easton, A. M. Dunning, J. A. Newton-Bishop, G. W. Montgomery, N. G. Martin, G. J. Mann, D. T. Bishop, H. Tsao, J. M. Trent, D. E. Fisher, N. K. Hayward & K. M. Brown (2011) A novel recurrent mutation in MITF predisposes to familial and sporadic melanoma. *Nature,* 480**,** 99-103.

You, M. J., D. H. Castrillon, B. C. Bastian, R. C. O'Hagan, M. W. Bosenberg, R. Parsons, L. Chin & R. A. DePinho (2002) Genetic analysis of Pten and Ink4a/Arf interactions in the suppression of tumorigenesis in mice. *Proc Natl Acad Sci U S A,* 99**,** 1455-60.

Yuan, G. & B. Zhu (2013) Histone variants and epigenetic inheritance. *Biochim Biophys Acta,* 1819**,** 222-9.

Zeng, L., Q. Zhang, S. Li, A. N. Plotnikov, M. J. Walsh & M. M. Zhou (2010) Mechanism and regulation of acetylated histone binding by the tandem PHD finger of DPF3b. *Nature,* 466**,** 258-62.

Zhang, R., M. V. Poustovoitov, X. Ye, H. A. Santos, W. Chen, S. M. Daganzo, J. P. Erzberger, I. G. Serebriiskii, A. A. Canutescu, R. L. Dunbrack, J. R. Pehrson, J. M. Berger, P. D. Kaufman & P. D. Adams (2005) Formation of MacroH2A-containing senescence-associated heterochromatin foci and senescence driven by ASF1a and HIRA. *Dev Cell,* 8**,** 19-30.

Zhang, Y., C. L. Smith, A. Saha, S. W. Grill, S. Mihardja, S. B. Smith, B. R. Cairns, C. L. Peterson & C. Bustamante (2006) DNA translocation and loop formation mechanism of chromatin remodeling by SWI/SNF and RSC. *Mol Cell,* 24**,** 559-68.

Zhang, Y., Y. Xiong & W. G. Yarbrough (1998) ARF promotes MDM2 degradation and stabilizes p53: ARF-INK4a locus deletion impairs both the Rb and p53 tumor suppression pathways. *Cell,* 92**,** 725-34.

Zhou, Y. B., S. E. Gerchman, V. Ramakrishnan, A. Travers & S. Muyldermans (1998) Position and orientation of the globular domain of linker histone H5 on the nucleosome. *Nature,* 395**,** 402-5.

Zhuang, L., C. S. Lee, R. A. Scolyer, S. W. McCarthy, A. A. Palmer, X. D. Zhang, J. F. Thompson, L. P. Bron & P. Hersey (2005) Activation of the extracellular signal regulated kinase (ERK) pathway in human melanoma. *J Clin Pathol,* 58**,** 1163-9.

Zuo, L., J. Weger, Q. Yang, A. M. Goldstein, M. A. Tucker, G. J. Walker, N. Hayward & N. C. Dracopoli (1996) Germline mutations in the p16INK4a binding domain of CDK4 in familial melanoma. *Nat Genet,* 12**,** 97-9.

ANNEX

Cell Death and Differentiation (2014), 1–12

www.nature.com/cdd

Identification of a ZEB2-MITF-ZEB1 transcriptional network that controls melanogenesis and melanoma progression

G Denecker[1,2], N Vandamme[1,2], Ö Akay[1,2], D Koludrovic[3], J Taminau[1,2], K Lemeire[2], A Gheldof[1,2], B De Craene[1,2], M Van Gele[4], L Brochez[4], GM Udupi[5,6], M Rafferty[6], B Balint[6], WM Gallagher[5,6], G Ghanem[7], D Huylebroeck[8,9], J Haigh[2,10], J van den Oord[11], L Larue[12], I Davidson[3], J-C Marine[13,14] and G Berx*[,1,2]

Deregulation of signaling pathways that control differentiation, expansion and migration of neural crest-derived melanoblasts during normal development contributes also to melanoma progression and metastasis. Although several epithelial-to-mesenchymal (EMT) transcription factors, such as zinc finger E-box binding protein 1 (ZEB1) and ZEB2, have been implicated in neural crest cell biology, little is known about their role in melanocyte homeostasis and melanoma. Here we show that mice lacking *Zeb2* in the melanocyte lineage exhibit a melanoblast migration defect and, unexpectedly, a severe melanocyte differentiation defect. Loss of *Zeb2* in the melanocyte lineage results in a downregulation of the Microphthalmia-associated transcription factor *(Mitf)* and melanocyte differentiation markers concomitant with an upregulation of *Zeb1*. We identify a transcriptional signaling network in which the EMT transcription factor ZEB2 regulates MITF levels to control melanocyte differentiation. Moreover, our data are also relevant for human melanomagenesis as loss of ZEB2 expression is associated with reduced patient survival.
Cell Death and Differentiation advance online publication, 25 April 2014; doi:10.1038/cdd.2014.44

Melanocytes are specialized cells in the skin that produce melanin, a pigment that is responsible for skin and hair color and that provides protection against ultraviolet (UV) radiation. During mouse embryogenesis, melanoblasts originate from the neural crest and migrate along a dorsolateral pathway from the neural tube to the developing dermis.[1] Around embryonic day (E) E11 they move into the epidermis and eventually populate the developing hair follicle.[2] Here they separate into two distinct populations: the differentiated pigmented melanocytes, which reside in the hair matrix, and the non-pigmented melanocyte stem cells (MSC) in the bulge. The latter cells are responsible for replenishing the hair follicle with new melanocytes during each hair cycle. Genetic studies in mice demonstrated the importance of several key players (such as sex-determining region Y (SRY)-box 10 (*Sox10*), paired-box 3 (*Pax3*), microphthalmia-associated transcription factor (*Mitf*), endothelin 3/endothelin receptor B (*Edn3/Ednrb*), *Kitl/Kit*, *Slug*, cellular myelocytomatosis oncogene cellular homolog (*cMyc*) and *β-Catenin* (*β-Cat*)) for melanoblast cell fate specification, proliferation, migration and survival.[2–4] The master regulator of the melanocyte development is MITF, which is spatio-temporally controlled by several key transcription factors such as SOX10, PAX3 and β-catenin.[5–7] Fundamentally, MITF induces gene expression patterns that prompt a melanocyte to differentiate and initiate pigment production by activating genes important for melanin biosynthesis (such as Tyrosinase (*Tyr*), Dopachrome tautomerase (*Dct*), Tyrosinase-related protein 1 (*Tyrp1*) and

[1]Unit of Molecular and Cellular Oncology, Inflammation Research Center, VIB, 9052 Ghent, Belgium; [2]Department of Biomedical Molecular Biology, Ghent University, 9052 Ghent, Belgium; [3]Institut de Génétique et de Biologie Moléculaire et Cellulaire, CNRS, INSERM, Université de Strasbourg, Illkirch, France; [4]Department of Dermatology, Ghent University Hospital, 9000 Ghent, Belgium; [5]UCD School of Biomolecular and Biomedical Science, UCD Conway Institute, University College, Dublin 4, Ireland; [6]OncoMark Limited, Nova UCD, Belfield Innovation Park, University College Dublin, Belfield, Dublin 4, Ireland; [7]Institute Jules Bordet, Brussels, Belgium; [8]Laboratory of Molecular Biology (Celgen), Department of Development and Regeneration, KU Leuven, 3000 Leuven, Belgium; [9]Department of Cell Biology, Erasmus MC, 3015 GE Rotterdam, The Netherlands; [10]Vascular Cell Biology Unit, Department for Molecular Biomedical Research, VIB, Ghent, Belgium; [11]Department of Pathology, University Hospital Leuven, KU Leuven, Leuven, Belgium; [12]Curie Institute, Developmental Genetics of Melanocytes, Centre National de la Recherche Scientifique (CNRS) UMR3347, Institut National de la Santé et de la Recherche Médicale (INSERM) U1021, Orsay, France; [13]Center for the Biology of Disease, Laboratory for Molecular Cancer Biology, VIB, Leuven, Belgium and [14]Center for Human Genetics, KU Leuven, Leuven, Belgium
*Corresponding author: G Berx, Unit of Molecular and Cellular Oncology, Inflammation Research Center, VIB, Technologiepark 927, B-9052 Ghent (Zwijnaarde), Belgium. Tel: +32 9 331 36 60; Fax: +32 9 331 36 09; E-mail: Geert.Berx@irc.VIB-UGent.be

Abbreviations: β-Cat, β-Catenin; BCL-2, B-Cell CLL/Lymphoma 2; bHLH, basic Helix Loop Helix; BRAF, viral RAF murine sarcoma viral oncogene homolog B1; Cdkn2a, cyclin-dependent kinase inhibitor 2A; ChIP, chromatin immunoprecipitation; c-MYC, cellular myelocytomatosis oncogene cellular homolog; CRE, cyclisation recombination; CTRL, control; DCT, dopachrome tautomerase; E, embryonic day; EDN3/EDNRB, endothelin 3/endothelin receptor B; ERK, extracellular signal-regulated kinase; EMT, epithelial-to-mesenchymal transition; FL, floxed; HF, hair follicle; KD, knockdown; LacZ, β-D-galactosidase; MC1R, melanocortin 1 receptor; MCKO, melanocyte-specific knockout; MCWT, melanocyte-specific wild-type; MEK, MAPK/ERK kinase; MITF, microphthalmia-associated transcription factor; P, postnatal day; PAX3, paired-box 3; PGP, P-glycoprotein; PMEL, premelanosome protein; NHM, normal human primary melanocytes; NRAS, neuroblastoma RAS viral oncogene homolog; qRT-PCR, quantitative reverse transcription-polymerase chain reaction; S100b, S100 calcium-binding protein B; shRNA, short hairpin RNA; siRNA, short interfering RNA; SOX10, sex-determining region Y (SRY)-box 10; TG, transgenic; TGF-β, transforming growth factor β; TYRP1, tyrosinase-related protein 1; TYR, tyrosinase; UV, ultraviolet; X-gal, 5-bromo-4-chloro-3-indolyl-β-D-galactopyranoside; ZEB, zinc finger E-box binding protein

Received 18.9.13; revised 17.2.14; accepted 10.3.14; Edited by G Melino

melanocortin 1 receptor (*Mc1r*)) and melanosome formation (such as the premelanosome protein (*Pmel*)).[8,9] Maintenance of the melanocyte stem cell compartment is mainly determined by transforming growth factor β (TGF-β), NOTCH signaling and MITF-dependent BCL-2 activity.[10,11] Deficiency in melanoblast development and migration generally result in white spotting phenotypes, whereas defects in melanocyte stem cell maintenance result in progressive hair graying phenomena.[3]

Melanoma is a malignant tumor arising from the melanocyte lineage and is the most therapy-resistant and deadly form of skin cancer. Several pathways have been identified to have a major role in the development of malignant melanoma, among

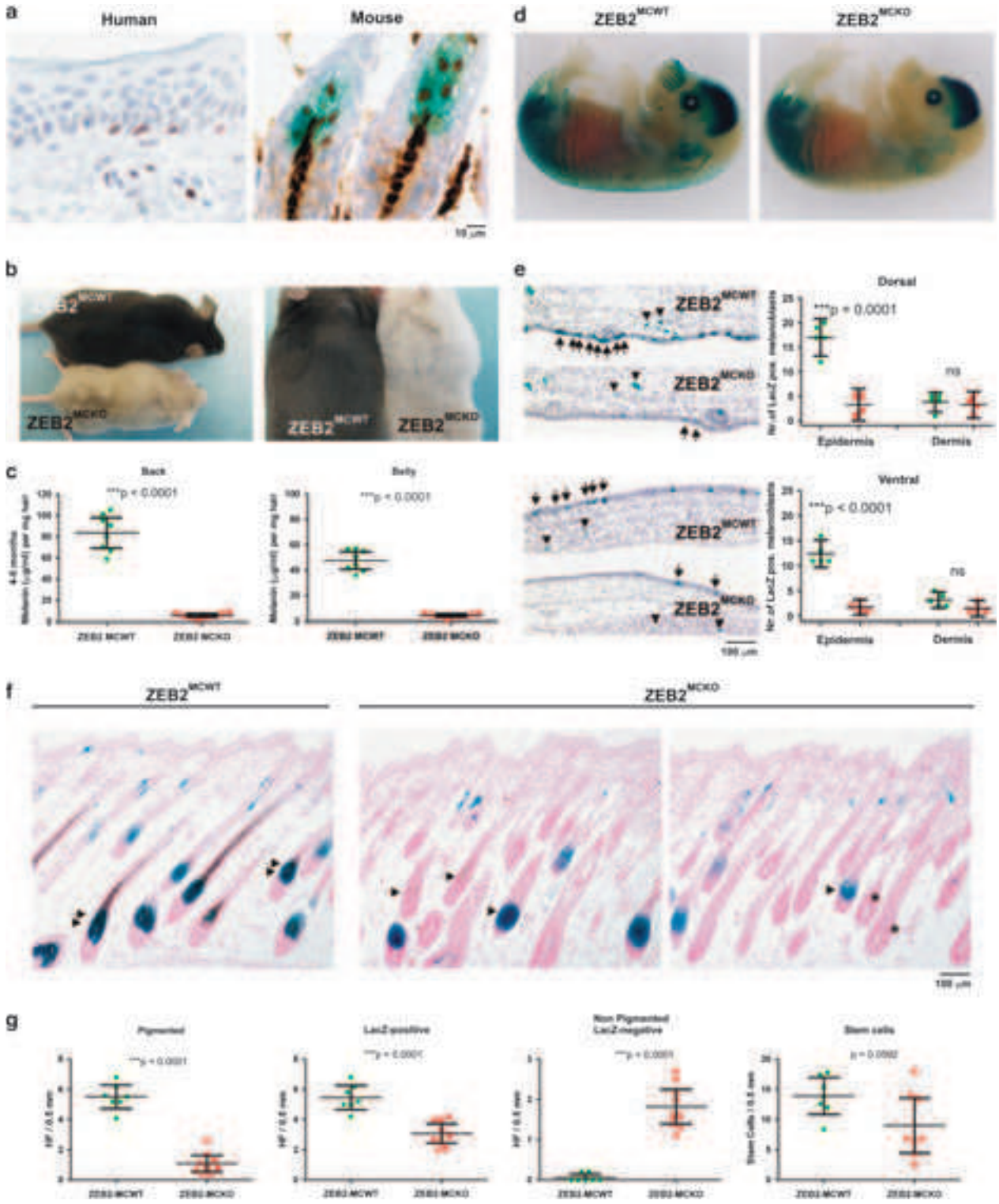

which the RAS/RAF/MEK/ERK pathway is probably the most studied and has recently become the target for anti-melanoma therapy.[12] Activating mutations in *RAS* (Q61K), with *NRAS* being the most frequent, occur in 15% of cases of human melanoma.[12] Melanocyte-specific expression of $NRAS^{Q61K}$ together with cyclin-dependent kinase inhibitor 2A (*Cdkn2a)* or *p53* deficiency leads to accelerated melanoma formation in mice.[13,14] *BRAF* activating mutations (V600E) occur at high frequencies (50–60%) in human melanoma. Specific inhibitors of $BRAF^{V600E}$ are being successfully used in melanoma therapy.[15] However, patients become rapidly resistant to this therapy, and combination therapies with MEK inhibitors are being investigated.[16,17] Drug resistance of malignant melanoma cells has been associated with the expression of the drug transporter P-glycoprotein (PGP) and increased migratory and invasive behavior.[18] EMT (Epithelial-to-mesenchymal transition) has a key role in the collective movement of normal cells during different stages of embryonic development, whereas in adults it has been associated with several pathologies, including fibrosis and cancer progression.[19,20] EMT is a process in which epithelial cells lose their epithelial characteristics, gain mesenchymal features and become migratory. Several pathways have been shown to induce EMT, all of which function through the induction of three families of transcription factors, the Snail (SNAIL, SLUG), Zeb (ZEB1, ZEB2) and basic Helix Loop Helix (bHLH) (E47, TWIST and others) families.[21] Melanoblasts undergo a migration process during embryogenesis and mature melanocytes are periodically replenished from the stem cells and undergo a constant cycling and migration process. The EMT transcription factor SLUG, has been shown to have an important role in the melanocyte lineage, as *Slug*-deficient mice have pigmentation abnormalities due to melanoblast migration defects and *SLUG* mutations have also been found in some cases of human piebaldism.[22–24] Furthermore, homozygous deletions of the *SLUG* gene were found in patients with type 2D of Waardenburg syndrome, an auditory-pigmentary syndrome caused by a migration deficiency of melanocytes and other neural crest-derived cells.[25,26] However, although it has been shown that siRNA-mediated inhibition of *Slug* leads to the suppression of metastasis in an orthotopic mouse model of melanoma, SLUG expression has not been correlated with melanoma metastasis.[27] Recently, it became clear that *in vitro* activation of the MEK-ERK signaling drives the reversion of the EMT transcription factor expression pattern in melanocytes with the downregulation of SLUG and ZEB2 and the induction of TWIST1 and ZEB1.[28]

ZEB2 is a transcription factor required for neural crest cell development. It belongs to the Zeb family of zinc-finger-homeodomain transcription factors and binds the E-box sequences CACCT(G).[29,30] We previously showed that conditional *Zeb2* expression in epithelial cells results in specific downregulation of E-cadherin and gain of malignant features characterized by a mesenchymal gene expression profile, such as N-cadherin and Vimentin.[29,31] Furthermore, it has recently become clear that during EMT not only epithelial characteristics are abolished, but that cells are reprogrammed to different extents.[32] Mouse embryos deficient in *Zeb2* exhibit defects from E8.5 onwards, with early arrest of cranial neural crest cell migration and absence of neural crest cells at the postotic vagal level.[33] Tissue specific disruption of *Zeb2* very early in neural crest cell development using a *Wnt1-Cre*-based approach, results in abnormalities in craniofacial and heart development, as well as defects in the peripheral nervous system.[34]

On the basis of these observations we hypothesized that ZEB2 may have a key role in the process of melanogenesis. To test this possibility we used a melanocyte-specific loss of function approach in mice. Unexpectedly we find that in addition to a role in proper melanoblast development, ZEB2 is required for the correct differentiation of melanocytes through its ability to act as an upstream regulator of *Mitf*. Our results propose a model whereby in melanocytes ZEB2 is necessary for *Mitf* expression and activity which in its turn is responsible for *Zeb1* repression. Measurement of nuclear ZEB2 levels shows a significantly shorter melanoma-specific survival in those patients with low ZEB2 expression.

Results

Melanocyte-specific ZEB2 deficiency causes congenital loss of hair pigmentation. We show for the first time that ZEB2 is expressed in the melanocytes of human skin epidermis, as well as in the differentiated melanocytes of mouse hair follicles (Figure 1a). ZEB2 is also expressed in migrating melanoblasts of the mouse embryo and their precursors, the neural crest cells.[33,35] As both complete knockout and *Wnt1-Cre*-mediated neural-crest-specific deletion of *Zeb2* are embryonic lethal (E9.5 and E12.5-postnatal (P) 0, respectively),[33,34] we conditionally deleted *Zeb2* in the melanocyte lineage by using the tyrosinase(*Tyr*)*::Cre* mouse line, which allows CRE-mediated *Zeb2* deletion under the control of the Tyrosinase promoter starting at E10.5 (Supplementary Figure S1a).[34,36] Homozygous melanocyte-specific deletion of *Zeb2* ($ZEB2^{MCKO}$) caused a severe loss of hair pigmentation compared with wild-type littermates

Figure 1 *Zeb2* loss in the melanocyte lineage causes congenital loss of pigmentation and impairs melanoblast development. (**a**) ZEB2 is expressed in differentiated melanocytes in the human epidermis, and in the hair follicles of mouse skin. (**b**) Melanocyte-specific deletion of *Zeb2* ($ZEB2^{MCKO}$) causes congenital loss of hair pigmentation in homozygous knockout mice (2 months old). This loss of pigmentation was more pronounced on the belly than on the back. (**c**) Determination of melanin pigment (μg/ml) in the dorsal and ventral hair of $ZEB2^{MCWT}$ and $ZEB2^{MCKO}$ mice ($n = 7$–8 for each group) at the age of 4–6 months. (**d**) ZEB2 is required for proper melanoblast development in homozygous embryos at E15.5. Whole-mount LacZ staining of E15.5 $ZEB2^{MCWT}$;Dct-LacZ and $ZEB2^{MCKO}$;Dct-LacZ embryos. (**e**) Comparison of melanoblast migration in the epidermis and dermis of dorsal and ventral areas of $ZEB2^{MCWT}$;Dct-LacZ and $ZEB2^{MCKO}$;Dct-LacZ embryos ($n = 4$ and 5, respectively). Results represent the number of melanoblasts per area analyzed. (**f**) Nuclear fast-red staining of LacZ-stained skin sections of $ZEB2^{MCWT}$;Dct-LacZ and $ZEB2^{MCKO}$;Dct-LacZ mice to visualize hair follicles (HF) (arrow: pigmented HF, arrowhead: LacZ-positive HF, *: LacZ-negative HF). (**g**) Quantitative analysis of the pigmented, LacZ-positive, non-pigmented LacZ-negative HF and LacZ-positive stem cells in the bulge area of $ZEB2^{MCWT}$ ($n = 7$) and $ZEB2^{MCKO}$ ($n = 8$) mice per 0.5 mm analyzed. Data of $ZEB2^{MCWT}$ and $ZEB2^{MCKO}$ mice were compared by using unpaired Student's *t*-test and are presented as means ± 95% CI. *P*-values are indicated with ($P < 0.001$). Micrograph images were taken with a × 60/0.8 objective (**a**) or a × 10/0.25 objective (**e** and **f**)

(ZEB2^{MCWT}). This hair pigmentation loss was present from the first hair cycle and continued through adulthood (Supplementary Figure S1b and Figure 1b). The melanin content of the dorsal and ventral hair were reduced by 93 and 91%, respectively (Figure 1c). Light microscopic analysis confirmed the disappearance of melanin pigment from the hair shafts (Supplementary Figure S1c), but hair with mixed pigmentation were also observed (data not shown).

The absence of ZEB2 impairs melanoblast development. Congenital loss of hair pigmentation indicates a disturbance of melanoblast migration or proliferation due to the absence of ZEB2. To further analyze this phenotype in-depth, we crossed conditional melanocyte-specific *Zeb2* knockout mice with *Dct::LacZ* melanoblast reporter mice[37] and analyzed the LacZ-positive melanoblast population in ZEB2^{MCWT} and ZEB2^{MCKO} embryos at E15.5. Absence of *Zeb2* severely impaired melanoblast development (Figure 1d) and quantification of the LacZ-positive melanoblasts on the back and belly of embryos further confirmed a significant reduction of melanoblast numbers in both areas (Supplementary Figure S1d). In agreement with an expected defect in migration, melanoblast numbers decreased more on the belly (95%) than on the back (70%) of the ZEB2-deficient embryos. To visualize the distribution of melanoblasts in the dermis and their subsequent migration to the epidermis, we made transversal sections of E15.5 LacZ embryos and quantified the melanoblasts in both areas. There was no difference in the number of melanoblasts present in the dermis between ZEB2^{MCKO} compared with control embryos (Figure 1e). However, in the epidermis of both the belly and back there was a significant reduction of melanoblasts in the ZEB2^{MCKO} embryos, suggesting an important role for ZEB2 in this process. In addition, melanoblast of ZEB2^{MCKO} embryos had fewer cell protrusions, compatible with their altered characteristics (Supplementary Figure S1e).

ZEB2 is necessary for proper melanocyte differentiation. Although melanoblast development was severely affected, 30% of them reached the dorsal area at E15.5. This raised the question whether the remaining melanoblasts could still populate the hair follicles of ZEB2^{MCKO} mice. Histological analysis of ZEB2^{MCWT};Dct-LacZ and ZEB2^{MCKO};Dct-LacZ skin from 5.5-day-old (P5) mice showed that some hair follicles in ZEB2^{MCKO} mice are still LacZ positive and/or (hypo-)pigmented, indicating that ZEB2-deficient melanoblasts can migrate and populate the bulb area of the hair follicles (Figure 1f). However, quantitative analysis of the hair follicles showed that there were significantly fewer pigmented or LacZ-positive hair follicles present in ZEB2^{MCKO} mice (Figure 1g). Furthermore, ZEB2^{MCKO} skin contained some completely undifferentiated hair follicles that were neither pigmented nor LacZ positive, which was not the case for ZEB2^{MCWT} skin (Figures 1f and g). Immunohistochemical analysis of depigmented ZEB2-stained sections confirmed nuclear ZEB2 presence in the differentiated melanocytes of the bulb area, the migrating melanocytes in the epidermis and importantly also in the melanocyte stem cells of ZEB2^{MCWT} mice, whereas ZEB2 was absent in all cells of the melanocyte lineage of ZEB2^{MCKO} skin (Supplementary Figure S2a). Quantitative analysis of the melanocyte stem cells revealed a reduction in LacZ-positive stem cells in ZEB2^{MCKO} mice compared with ZEB2^{MCWT} mice (Figure 1g), which agrees with the presence of fewer melanoblasts in the epidermis in ZEB2^{MCKO} embryos. To visualize melanocytes independently of Dct promoter reporter activity, we analyzed the expression of the general melanocyte marker S100 calcium-binding protein B (S100b), which does not depend on the differentiation status of the melanocytes. S100b staining showed that melanocytes were present in most of ZEB2^{MCKO} hair follicles (Figure 2a). Moreover, quantifying S100-positive melanocytes per hair follicle showed that the number of S100-positive ZEB2^{MCKO} melanocytes was reduced by 40% per hair follicle, which further points to a role of ZEB2 in migration and/or survival of melanocytes (Supplementary Figures S2b and c). Further immunohistochemical analysis and quantification of positive cells of the melanocyte-specific transcription factor MITF and one of its regulators (i.e., PAX3) showed that in the absence of ZEB2 the amount of MITF-positive melanocytes was strongly reduced, when compared with the total amount of melanocytes per hair follicle (S100-positive melanocytes), whereas the amount of PAX3-positive melanocytes was not affected (Figure 2a, Supplementary Figures S2b and c). The intensity of MITF staining was also lower, indicating a decrease in both the number of MITF-positive cells and in MITF protein levels in still MITF-positive cells. These observations indicate that ZEB2 is an important regulator of MITF-dependent melanocyte differentiation. We analyzed the presence of other terminal differentiation markers, such as TYRP1 and tyrosinase enzymatic activity. Most ZEB2^{MCKO} hair follicles were indeed negative for these markers (Figure 2a and data not shown). mRNA expression analysis of several melanocyte differentiation markers (*Tyrp1*, *Tyr*, *Dct*, *Pmel*, *Mc1R* and *Mitf*) on whole skin mRNA of ZEB2^{MCKO} and ZEB2^{MCWT} mice further showed that the differentiation status of ZEB2^{MCKO} melanocytes was affected, as all of these markers are significantly downregulated in ZEB2^{MCKO} skin (Supplementary Figure S2d). Close examination of the melanosomes in ZEB2-stained sections of ZEB2^{MCWT}

Figure 2 Melanocyte-specific *Zeb2* deficiency causes the formation of undifferentiated melanocytes in the bulge area of hair follicles. (**a**) Immunohistochemical staining of sections of ZEB2^{MCWT} and ZEB2^{MCKO};Dct-LacZ-positive skin sections with S100b, PAX3, MITF and TYRP1 antibodies. (**b**) Detailed microscopic analysis of melanosomes in the hair shafts and the bulb area of the hair follicles, combined with immunohistochemical staining of ZEB2 on LacZ-positive skin sections of ZEB2^{MCWT} and ZEB2^{MCKO}; Dct-LacZ-positive mice. Insets show the altered morphology of melanosomes in the ZEB2^{MCKO} sections compared with ZEB2^{MCWT}. (**c**) Electron microscopic analysis of melanosomes in the bulb area of ZEB2^{MCWT} and ZEB2^{MCKO} mice demonstrates the absence or irregular morphology of melanosomes in the ZEB2^{MCKO} hair follicles. (**d**) Genetic compensation of the loss of *Zeb2* in the ZEB2^{MCKO};Dct-LacZ mice with melanocyte-specific overexpression of ZEB2 (ZEB2^{MCTG}). Left panel: complete compensation of pigmentation in ZEB2^{MCKO} ZEB2^{MCTG};Dct-LacZ mice compared with ZEB2^{MCKO};Dct-LacZ mice. Right panels: reappearance of pigmented melanosomes and ZEB2 expression in the ZEB2^{MCKO} ZEB2^{MCTG};Dct-LacZ hair follicles. All microscopic analyses were done on skin sections of 5.5-day-old (**a**–**c**) or 13.5-day-old mice (**d**) and Immunohistochemical micrograph images were taken with a $\times$ 60/0.8 objective (**a** and **d**) or a $\times$ 100/1.25 objective (**b**)

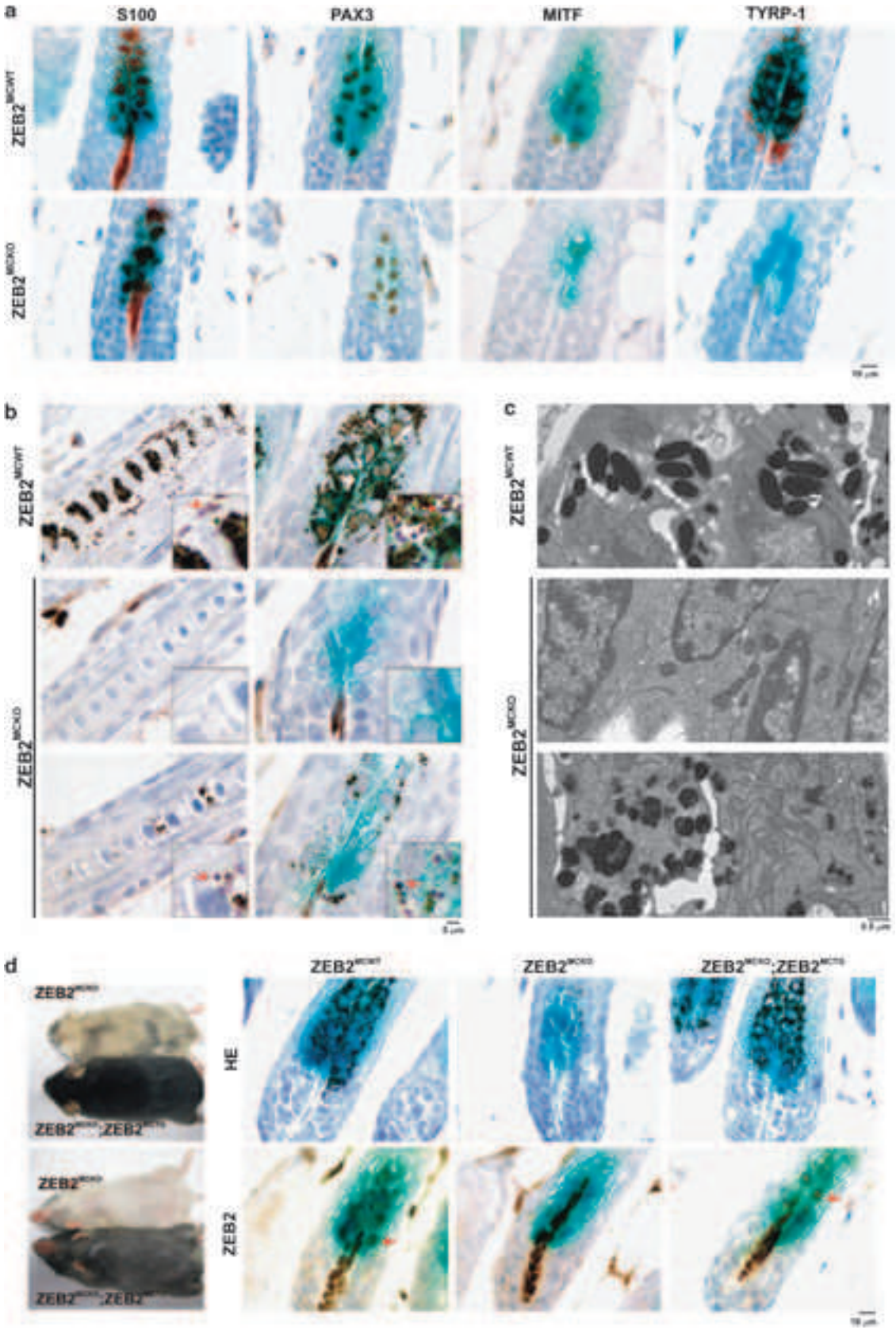
a
S100
PAX3
MITF
TYRP-1
ZEB2MCWT
ZEB2MCKO
b
c
d
HE
ZEB2

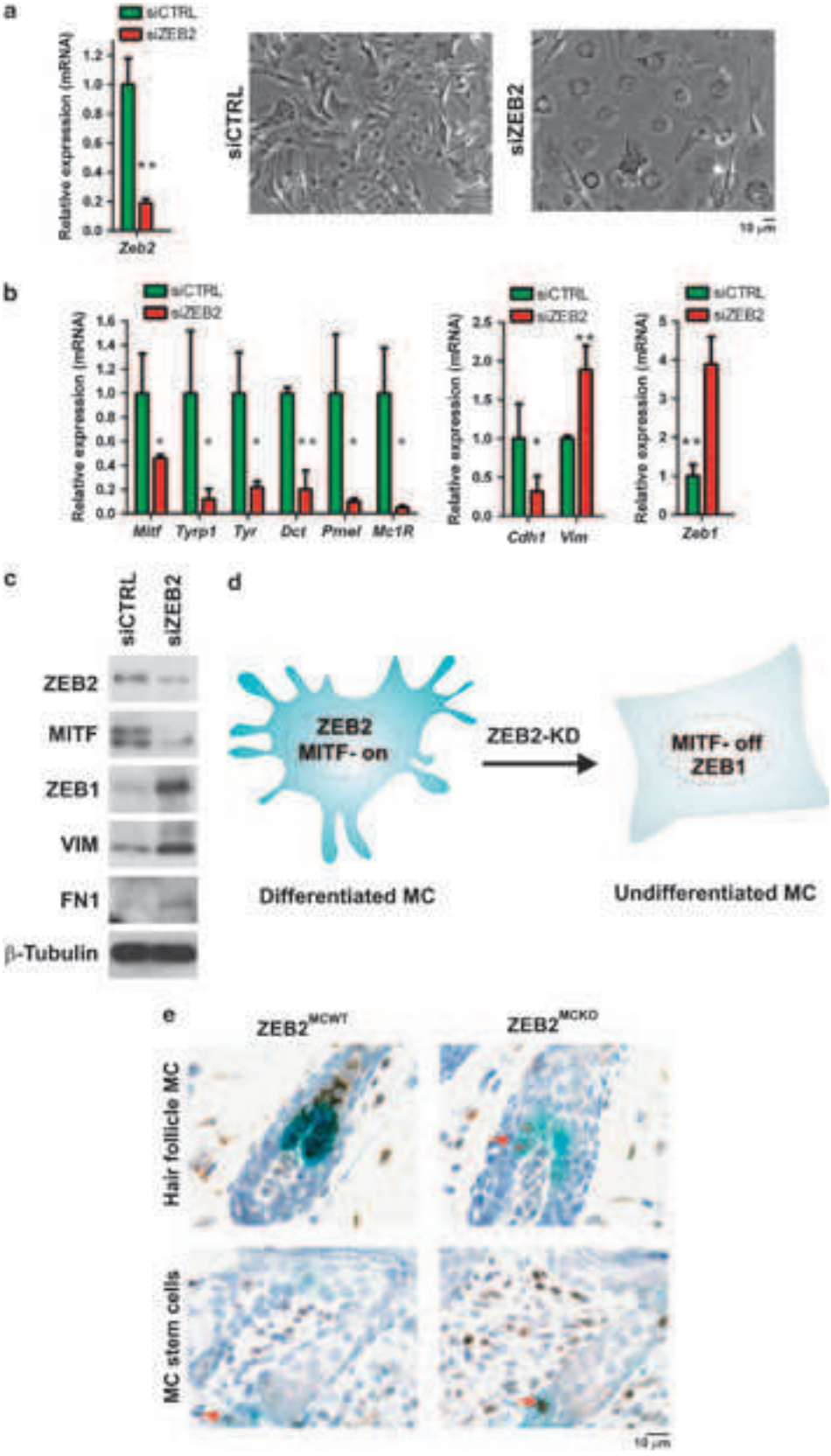
a
siCTRL
siZEB2
Relative expression (mRNA)
Zeb2
siCTRL
siZEB2
b
Mitf
Tyrp1
Tyr
Dct
Pmel
Mc1R
Cdh1
Vim
Zeb1
c
siCTRL
siZEB2
ZEB2
MITF
ZEB1
VIM
FN1
β-Tubulin
d
ZEB2
MITF- on
ZEB2-KD
MITF- off
ZEB1
Differentiated MC
Undifferentiated MC
e
ZEB2MCWT
ZEB2MCKO
Hair follicle MC
MC stem cells

and ZEB2^{MCKO} skin confirmed the absence of melanin in most melanocytes of the bulb area and in hair shafts of ZEB2^{MCKO} skin, although in some hair follicles a few remaining melanosomes were visible (Figure 2b). Electron microscopy analysis showed that these melanosomes were spherical with irregular borders, in contrast to the rod-shaped melanosomes of ZEB2^{MCWT} hair follicles (Figure 2c). These results collectively show that melanocytes form but do not differentiate properly, pointing to a crucial role for ZEB2 in melanocyte differentiation. These effects were strictly ZEB2-dependent, as in a complementation experiment in which we crossed the ZEB2^{MCKO} mice with a conditional *Zeb2* transgenic strain (*Rosa26-ZEB2$^{TG/TG-IRES-GFP}$*) activated by the same Tyr-Cre as for the deletion of *Zeb2*, melanogenesis was completely rescued (Supplementary Figure S3a and Figure 2d). Such *Zeb2* complemented mice (ZEB2^{MCKO}; ZEB2^{MCTG}) regained pigmentation, and histological sections demonstrated that ZEB2-positive melanocytes are pigmented (Figure 2d), confirming the cell autonomous action of ZEB2. Furthermore, *in vivo* mRNA expression analysis of the melanocyte differentiation markers (*Tyrp1*, *Tyr*, *Dct*, *PmeL*, *Mc1R* and *Mitf*) confirmed the full functional complementation of *Zeb2* deficiency with transgenic *Zeb2* (data not shown).

ZEB2 controls an MITF-ZEB1-dependent transcriptional network essential for melanocyte differentiation. The melanocyte differentiation block observed upon *Zeb2* ablation could also be due to a change in the functionality of the melanoblasts or melanocyte stem cells. We therefore investigated whether ZEB2 is required for the maintenance of the differentiation program in melanocytes. To this end, we transfected primary mouse melanocytes with an siRNA pool targeting *Zeb2* (siZEB2) or with a control siRNA pool (siCTRL). Significant knockdown of *Zeb2* caused nearly complete loss of differentiation of the melanocytes (Figure 3a) and a concomitant decrease in the steady-state mRNA levels of *Mitf* and several genes of the melanin synthesis pathway (Figure 3b). To examine whether EMT was also affected, we assessed the expression levels of two representative EMT target genes, *E-cadherin* (*Cdh1*; epithelial marker) and *Vimentin* (*Vim*; mesenchymal marker). Unexpectedly, *Cdh1* was downregulated, whereas *Vim* was upregulated (Figure 3b). Interestingly we found that *Zeb2* knockdown caused transcriptional upregulation of *Zeb1* (Figure 3b). The latter results were confirmed at the protein level in the immortalized melanocyte cell line Melan-a in which *Zeb2* knockdown caused a strong downregulation of MITF and concomitant upregulation of ZEB1, and the mesenchymal markers Vimentin (VIM) and Fibronectin (FN1) (Figure 3c). These observations support the hypothetical model of ZEB2 dictating MITF expression and activity. In the absence of *Zeb2*, MITF expression is lost, coinciding with ZEB1 upregulation (Figure 3d). This model is confirmed *in vivo* as ZEB1 staining intensity was clearly increased in a fraction of the undifferentiated ZEB2-deficient melanocytes (Figure 3e), whereas ZEB1 could not be detected in differentiated melanocytes of ZEB2^{MCWT} mice. ZEB1 protein was also undetectable in primary melanocytes of human origin (Supplementary Figure S3b and see below). On the other hand, ZEB1 was readily observed in the stem cells of both ZEB2^{MCWT} and ZEB2^{MCKO} mice (Figure 3e). Thus, an intricate balance between these two ZEB-family members appears to be important in the transcriptional regulation of melanocyte differentiation.

Strong nuclear ZEB2 expression in primary melanomas is associated with better survival. A role for ZEB2 in the regulation of MITF levels and/or activity, melanoblast development and melanocyte differentiation raises the possibility that deregulation of ZEB2 expression may contribute to melanoma progression/metastasis. Consistently, immunohistochemical analyses of ZEB2 in a cohort of human benign naevi, primary and metastatic melanoma samples revealed a very heterogeneous pattern of expression particularly in primary melanoma, with areas of high expression next to strong local downregulation (Supplementary Figure S3c and Figure 4a). This heterogeneous downregulation of ZEB2 expression is reminiscent to the profile of MITF expression in human melanoma.[38] Interestingly we found that human melanoma metastases express high nuclear ZEB2 levels suggesting reversible loss of expression during melanoma dissemination (Supplementary Figure S3c). We extended this study by analyzing 178 primary melanoma samples on a tissue array. This study showed that ZEB2 has significant prognostic relevance in melanoma, as strong nuclear ZEB2 expression is beneficial for the patients in terms of melanoma-specific survival and recurrence-free survival (Figure 4b). In contrast, weak nuclear ZEB2 expression was associated with a worse patient outcome (Figure 4b). Therefore, ZEB2 might serve as a gatekeeper controlling human melanoma progression and provide a novel prognostic marker for melanoma.

ZEB2 loss results in reduced MITF expression, and is associated with melanoma progression. We have provided genetic evidence that ZEB2 regulates *Mitf* expression levels in primary melanocytes *in vivo* (Figure 2a and Supplementary Figure S2d). This was confirmed in melanoma cells, as *Zeb2* knockdown in the B16 mouse melanoma cell line caused a transcriptional decrease in expression of *Mitf* and its well-established target genes and a concomitant increase in ZEB1 expression (Figure 5a).

Figure 3 ZEB2 is necessary for proper differentiation of primary melanocytes. (**a** and **b**) Morphology of primary melanocytes after knockdown of *Zeb2* by siRNA transfection and relative mRNA expression of *Zeb2*, melanocytes-specific differentiation genes *Tyrp1*, *Tyr*, *Dct*, *PmeL* and *Mc1R*, the epithelial/mesenchymal markers E-cadherin/Vimentin and *Zeb1*. Scrambled siRNA was used as a control (siCTRL). (**c**) Western blot analysis after siRNA knockdown of *Zeb2* in the primary Melan a cell line. (**d**) Hypothetical model of the ZEB2-MITF-ZEB1 balance in melanocytes (**e**) ZEB1 expression in dedifferentiated LacZ-positive melanocytes of the hair follicles of ZEB2^{MCKO} mice and in the melanocyte stem cells of both ZEB2^{MCWT} and ZEB2^{MCKO} mice. QPCR data were compared by using unpaired Student's *t*-test ($n=3$) and are presented as averages ± S.D. *P*-values are indicated with (**$P<0.005$ and *$P<0.05$). Micrograph images were taken with a $\times$20/0.2 objective (**a**) or a $\times$60/0.8 objective (**e**)

Importantly, transfection of the *Zeb2* KD cells with an *Mitf* expression vector rescued the differentiation defect indicating that this phenotype is MITF-dependent (Figure 5b). This expression switching of ZEBs was confirmed in short-term culture human melanoma cells, in which we observed this particular ZEB heterogeneity in NRAS- or BRAF-mutated samples: 67% (8 out of 12) express both ZEB1 and ZEB2 whereas the remaining express either ZEB1 (2 out of 12)

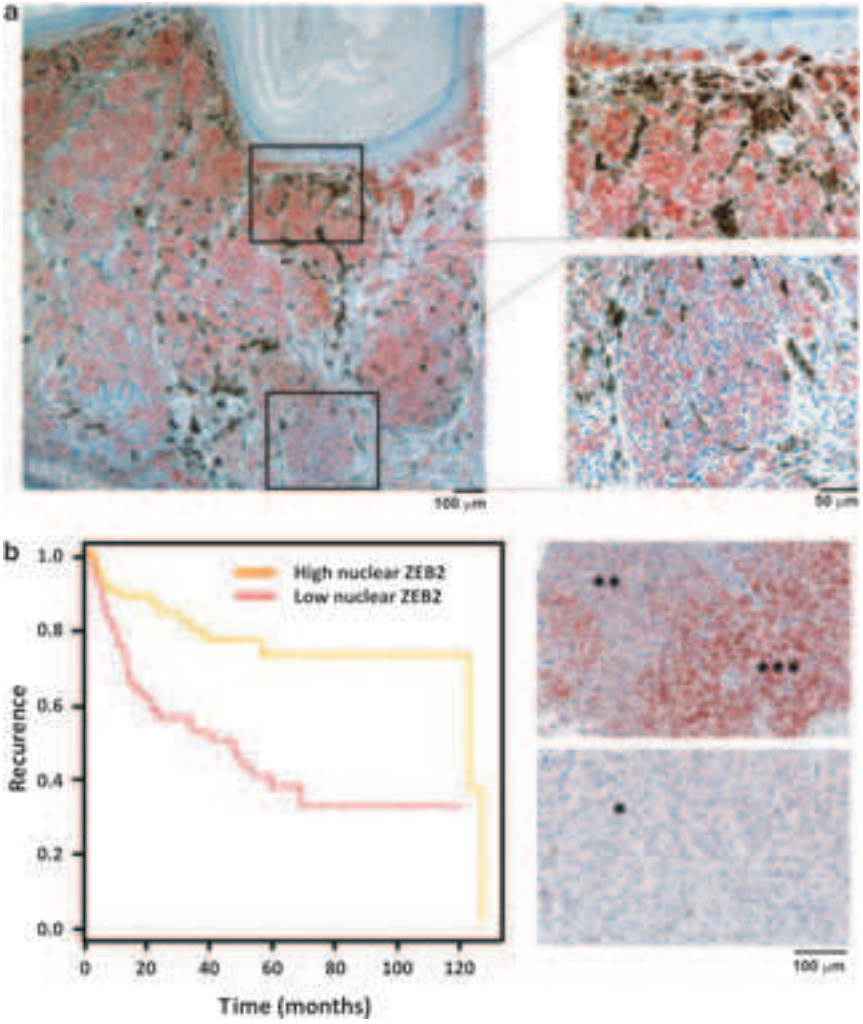

Figure 4 ZEB2 expression in melanoma. (**a**) Heterogeneous ZEB2 expression in primary human melanoma with vertical growth phase. (**b**) Kaplan–Meier curves for melanoma recurrence-free survival, comparing human melanoma samples with strong nuclear ZEB2 expression ($n = 83$) and weak nuclear ZEB2 expression ($n = 82$) from a melanoma tissue array. Data were compared using the log-rank test and $^{**}P = 0.0065$. A representative ZEB2 staining of both groups is shown in the right panel (*** very high nuclear ZEB2, ** high nuclear ZEB2, * low nuclear ZEB2). ZEB2 protein expression values were determined using an automated image analysis approach (IHC-MARK, Oncomark, Dublin, Ireland) designed to quantify immunohistochemically stained slides. Micrograph images were taken with a $\times$ 4/0.1 and $\times$ 20/0.4 objective (**a**) or a $\times$ 10/0.25 objective (**b**)

Figure 5 The ZEB2-MITF-ZEB1 transcriptional network. (**a**) Knockdown of *Zeb2* by siRNA transfection of the B16 melanoma cell line. Scrambled siRNA was used as a control (siCTRL). Relative mRNA expression of endogenous *Zeb2,* the melanocyte-specific differentiation genes *Mitf*, *Tyrp1*, *Tyr*, *Dct*, *Mc1R* and *Zeb1* after *Zeb2* knockdown are shown. (**b**) Relative mRNA expression of subset of MITF target genes after siRNA knockdown of *Zeb2* in the B16 melanoma cell line after compensation with *Mitf*. (**c**) Western blot analysis of ZEB2 and ZEB1 expression in short-term culture human melanoma cell lines with different NRAS (blue circles) or BRAF (red circles) mutated or WT (green circles) status. Primary human melanocytes were used as a reference. (→) specific ZEB1 band, (*) aspecific band. (**d**) Western blot analysis of ZEB2, MITF and ZEB1 in a panel of human melanoma cell lines. Primary human melanocytes were used as a reference. (**e**) 501Mel cells were infected with lentiviral vectors expressing control shRNA (shCTRL) or shRNA directed against *MITF* (shMITF). Left panel: western blot analysis shows strongly downregulated MITF expression after shMITF infection. Right panel: shMITF knockdown leads to increased *ZEB1* mRNA expression. Two independent primer pairs located in exons 1–2 and 4–5 for the *ZEB1* gene were used. (**f**) UCSC screenshot of a wig file of an HA-ChIP-seq from 501Mel cells expressing a 3HA-Control vector or 3HA-tagged MITF at the *ZEB1* locus. Several MITF binding sites are observed (shown by arrows) both upstream and downstream of the *ZEB1* gene. (**g**) Anti-HA-ChIP-qPCR from native 501Mel cells (CTRL) or 501MEL cells stably expressing 3HA-tagged MITF (HA-MITF). qPCR was performed with primers that amplify a region 1 kb upstream of the *TYR* transcription start site (TSS) as negative control, the *TYR* TSS as positive control and two sites from the *ZEB1* locus 5′ and 3′ of the gene as indicated in **f**. QPCR data were compared by using unpaired Student's *t*-test ($n = 3$, for **a**, **e** and **g**) or paired Student's *t*-test ($n = 5$, for **b**) and are presented as averages ± S.D. or are presented as log-transformed relative expression values with 95% CI. *P*-values are indicated with $^{***}P < 0.0005$, $^{**}P < 0.005$ and $^{*}P < 0.05$

or ZEB2 (2 out of 12) (Figure 5c and Supplementary Figure S3d). Melanoma cells that are wild type for NRAS or BRAF mainly express ZEB2 only (67%, 6 out of 9), resembling the expression pattern of normal melanocytes which also only express ZEB2. In addition, the analysis of a cohort of human melanoma cell lines supported the tendency of an inverse correlation between ZEB2 and MITF *versus* ZEB1 expression (Figure 5d). These results were further

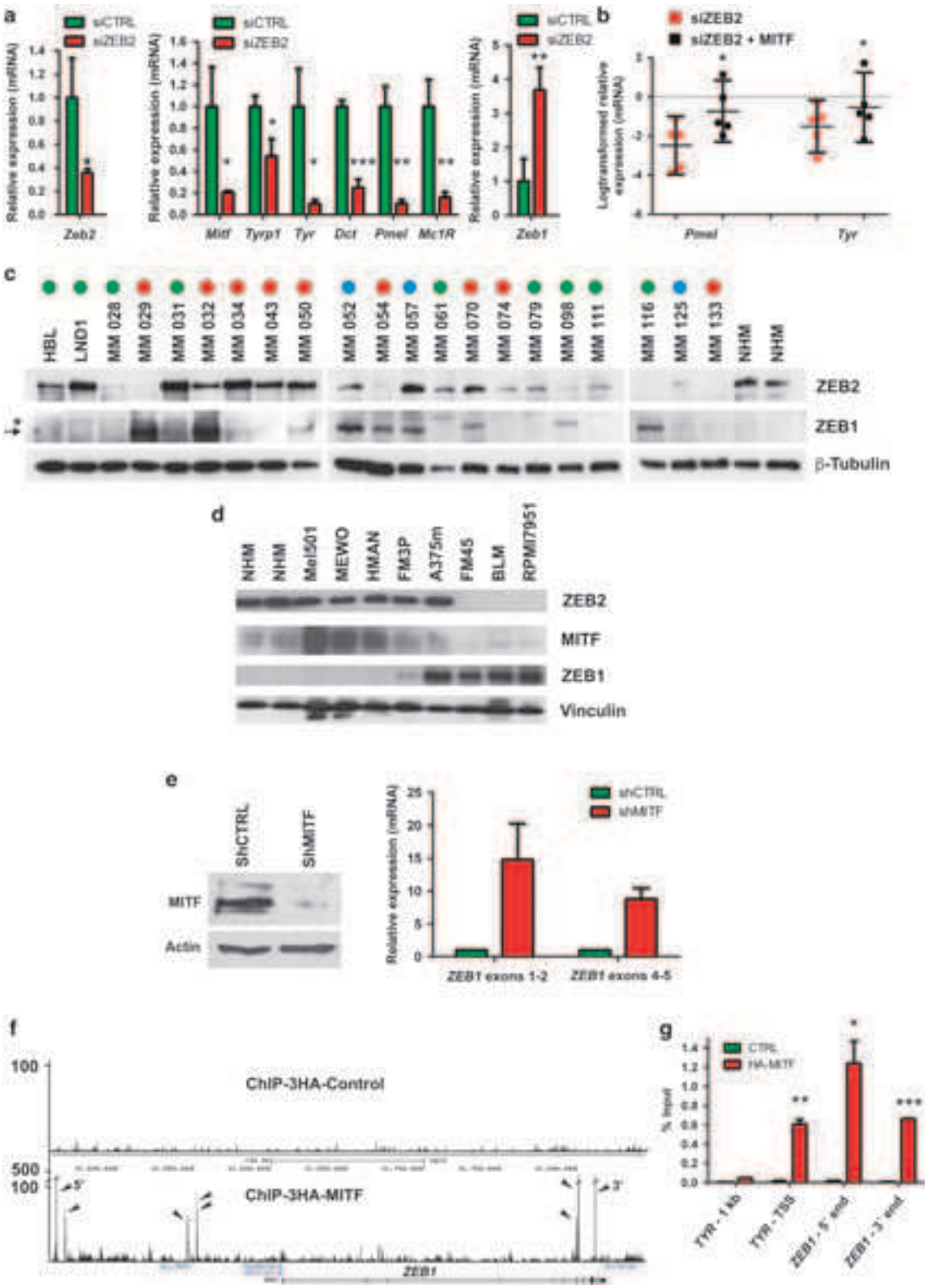

confirmed on the human SKMel28 melanoma cell line in which we performed siRNA-mediated KD of *ZEB2*, which caused a strong downregulation of MITF and concomitant upregulation of ZEB1 (Supplementary Figure S3e). Furthermore, knockdown of *MITF* in human melanoma 501Mel cells results in upregulation of *ZEB1* expression suggesting that MITF contributes to the direct repression of *ZEB1* (Figure 5e). Interestingly, MITF-ChIP-seq analysis recently identified the *ZEB1* locus as a potential MITF target in human melanoma 501Mel cells (Figure 5f).[39] The specificity of this binding to the *ZEB1* locus was confirmed by anti-HA-ChIP-qRT-PCR for both the 5′- and 3′-end of the gene (Figure 5g).

Discussion

In this work we have identified an important novel function for ZEB2 in melanocytes: ZEB2 regulates the expression of MITF and thereby coordinates the development and differentiation of the melanocyte lineage. Moreover we provide evidence that ZEB2 is expressed in a heterogeneous manner in human melanoma. These observations have important implications for our understanding of melanoma biology as well as for anti-melanoma therapy.

Emerging evidence indicates that the transcriptional pathways critical for melanogenesis, like those controlled by MITF, could be disturbed in pigmentation-associated diseases and melanoma progression and metastasis.[40] MITF is considered to be the master regulator of melanocytes as it is essential for melanoblast survival and melanocyte-specific lineage differentiation. On the basis of the proven role of *Zeb2* in neural crest cell delamination, we expected a major defect in melanoblast development.[34] However, although mice deficient for *Zeb2* in the melanocyte lineage have an impaired melanoblast development; a significant fraction of ZEB2-deficient melanoblasts was still able to migrate to the epidermis where they populate the hair follicles. Unexpectedly, the ZEB2-deficient melanocytes in the hair follicle bulb area remain undifferentiated, causing a congenital loss of pigmentation. These melanocytes have a very low MITF expression, supporting the role of ZEB2 as a driver for melanocyte differentiation. *In vitro* data further confirm the crucial role of ZEB2 as a regulator of MITF and melanocyte differentiation coinciding with an upregulation of ZEB1. In this context, it is noteworthy that the loss of *Zeb2* in non-transformed melanocytes *in vivo* can result in ZEB1 misexpression. Furthermore the strongly reduced expression of the melanocortin receptor upon *Zeb2* loss potentially contributes to the maintenance of the observed low *Mitf* transcriptional levels.

EMT has a key role during different stages of embryonic development including the formation and migration of the neural crest cells. Neural crest cells are a multipotent, migratory, transient cell population that migrate through the vertebrate embryo to infiltrate different organs and differentiate in various cell lineages including melanocytes.[41] During the progression to melanoma, melanocytes may acquire multiple traits of high grade malignancy in context of additional oncogenic changes by reactivating this silenced embryonic program.[25] In contrast to epithelial cells where EMT-inducing transcription factors favor dedifferentiation and dissemination, we shedded light on a more complex interaction between ZEB2 and MITF in the melanocyte lineage. As ZEB2 expression favors MITF expression and thus differentiation in melanocytes, the loss of *Zeb2* in the melanocyte lineage results in the formation of undifferentiated melanocytes with loss of *Mitf* and upregulation of *Zeb1*. Together with our finding that ZEB1 is expressed in melanocyte stem cells, it seems that ZEB switching is a naturally occurring transcription factor reprogramming that also can be facilitated by activated oncogenic RAS/RAF signaling.[28]

Examination of human melanoma samples and cell lines assessed the relevance of the identified effects upon *in vivo* loss of ZEB2 in a clinical context. It seems that ZEB2, particularly in the highly invasive vertical growth phase of human melanoma, gets downregulated in a very heterogeneous manner. Importantly, nuclear ZEB2 expression in melanomas is linked with good prognostic markers whereas loss of ZEB2 is associated with poor melanoma-specific survival. The partial or total clearance of ZEB2 in human melanoma could be caused by the well-known negative control of *ZEB2* expression by the miR200 family. However this reasoning is not supported by the observation that expression of the miR200 family is lost during melanoma progression ruling out their potential dominant action of *ZEB2* repression, at least during melanoma progression.[42,43]

As MITF depletion forces melanocytes to senescence,[39] ZEB1 may be a failsafe program for a melanoma cell to overcome the senescent state, exemplifying why ZEB1 expression in human melanoma is inversely correlated with MITF status. In this context, it is noteworthy that loss of ZEB2 in non-transformed melanocytes *in vivo* can result in ZEB1 misexpression, which potentially takes over in an alternative way the function of ZEB2 on the expense of differentiation. Our novel finding demonstrates that the switch from ZEB2 to ZEB1 is associated with a reduction of MITF, the master controller of differentiation, growth and migration in melanocytes. In melanoma, *MITF* has been described as a lineage addiction oncogene that is controlling melanoma progression following a rheostat model, in which high MITF expression is required for proliferation whereas its reduced level results in invasive behavior. We postulate that low MITF expression favors melanoma invasion and metastasis, which corresponds with the poor patient prognosis predicted by the loss of ZEB2, as shown in our study.

Materials and Methods

Mice. Mice were kept in accordance with the institutional guidelines regarding the care and use of laboratory animals and all procedures were approved by the institutional ethics committee. Mice with the following genotypes have been described elsewhere: conditional *Zeb2*$^{fl/fl}$,[44] *Tyr::Cre*[36] and *Dct::LacZ*.[37] Conditionally, *Rosa-Zeb2*$^{TG/TG\text{-}IRES\text{-}GFP}$ overexpressing mice were generated using G_4 hybrid ES cells and the Gateway-compatible *Rosa26* locus targeting vector, as previously described.[45,46]

Melanin content determination. Melanin was extracted with an alkaline solution as previously described.[47]

Whole-mount LacZ staining of embryos and skin. To obtain E15.5 embryos, timed matings were set up, and the day on which a vaginal plug was detected was set as E0.5. For skin samples, back skin of 5.5-day-old mice was isolated. Embryos and back skin were washed in PBS and fixed in 4% paraformaldehyde for 3 h at room temperature (RT), after which they were washed

with permeabilization solution (0.1 M phosphate buffer pH 7.4, 2 mM $MgCl_2$, 2.5 mM EGTA, 0.01% sodium deoxycholate, 0.02% NP40, 0.005% BSA) and stained overnight at RT with permeabilization buffer containing 5 mM potassium ferricyanide, 5 mM potassium ferrocyanide and 0.1% LacZ solution. The samples were washed in PBS and postfixed for 2 h in 4% paraformaldehyde at RT. To count embryonic melanoblasts externally, photos were taken with a Nikon AZ100 Multizoom microscope (Nikon, Tokyo, Japan) and defined regions were analyzed for LacZ-positive melanoblasts with Volocity software. For further immunohistochemical analysis of the back skin, samples were dehydrated, embedded in paraffin and sectioned at 6 μm.

Human tissues. Tissue samples were obtained from the Department of Dermatology, Universitair Ziekenhuis Gent, Ghent, Belgium, from the Department of Pathology, University Hospital Leuven, KU Leuven, Leuven, Belgium and from archival paraffin-embedded patient samples from St. Vincent's University Hospital, Dublin, Ireland. All patient specimens were used in accordance with institutional and national policies at the respective locations, with appropriate approval provided by the relevant Ethics committees at the respective institutions. All patient-related information was anonymized.

Immunohistochemistry. Tumors, organs and skin were isolated and fixed overnight in 4% paraformaldehyde solution, dehydrated, embedded in paraffin and cut into 5-μm sections. For histology, samples were stained with hematoxylin and eosin, or with nuclear fast red. For immunohistochemical staining, antigen retrieval was done in citrate buffer and endogenous peroxidases were blocked with 3% H_2O_2 in methanol. The sections were incubated with primary antibodies and stained with biotin-conjugated secondary antibodies followed by Streptavidin-HRP based development (substrate development with DAB or AEC). When necessary, the signal was amplified using the Tyramide Signal Amplification (TSA) kit (Perkin Elmer Applied Biosystems, Zaventem, Belgium), indicated with asterisk. The following antibodies were used: mouse anti-ZEB2 (1/300*) (in-house monoclonal antibody, clone 7F7) for normal mouse sections, rabbit anti-ZEB2 (1/500*) (HPA003456, Sigma, Diegem, Belgium) for human sections, goat anti-ZEB1 (1/50) (sc-10572, Santa Cruz, Heidelberg, Germany) for mouse sections, rabbit anti-ZEB1 (1/10 000*) (gift from Professor D Darling) for human sections; rabbit anti-S100b (1/1000*) (ZO311, Dakopatts, Leuven, Belgium), rabbit TYRP1 (1/1000*) (gift received kindly from Professor V Hearing); mouse anti-MITF (1/300) (Ab 12039, Abcam, Cambridge, UK), mouse anti-PAX3 (1/200) (DSHB, Iowa city, IA, USA).

Tyrosinase assay. The Tyrosinase assay was performed as described previously.[47]

Transmission electron microscopy. Back skin from 5.5-day-old $ZEB2^{MCWT}$ and $ZEB2^{MCKO}$ mice was immersed in a fixative solution of 2.5% glutaraldehyde, 3% formaldehyde and 0.02% $CaCl_2$ in 0.1 M Na-cacodylate buffer, and processed as previously described.[48] Ultrathin sections of a gold interference color were cut using an ultra microtome (Leica EM UC6, Diegem, Belgium), post-stained with uranyl acetate and lead citrate in a Leica EM AC20, and collected on Formvar-coated copper slot grids. They were viewed with a JEOL 1010 transmission electron microscope ($\times$ 10 000 images) (JEOL, Tokyo, Japan).

Primary melanocyte cultures. Primary melanocytes were isolated from 5.5-day-old pups as previously described.[47]

siRNA and plasmid transfections. To knock down *Zeb2* in primary *NRAS* transformed melanocytes, primary Melan a mouse melanocytes, B16-BL6 mouse melanoma and SKMel28 human melanoma, we used siRNA pools for mouse *Zeb2* (Dharmacon, St. Leon Rot, Germany) and a scrambled siRNA pool (Dharmacon) as a control. Transfections were performed with HiPerfect (Qiagen, Antwerpen, Belgium) according to the manufacturer's instructions. Five days after siRNA transfection, RNA and protein lysates were prepared. To overexpress mouse *Mitf* we used a mouse *Mitf* expression vector and an empty vector as a control. Transfections were performed with GenJet (Stratagene, Amsterdam, The Netherlands) according to the manufacturer's instructions. *Mitf* transfections were done 1 day after siRNA knockdown of *Zeb2*.

Lentiviral transfections. To knock down *MITF* in 501Mel cells we used an shRNA for human *MITF* and a scrambled shRNA (shCTRL) as a control. The shRNA vectors are pLKO based from Sigma, the Mission shRNA series. 501Mel cells were infected with shRNA directed against *MITF* or the Mission shRNA control sequence and selected for 4 days with 3.0 μg/ml of puromycin.

ChIP analysis. ChIP and ChIP-Seq experiments were performed on chromatin from native 501Mel and on 501Mel cells stably expressing 3HA-tagged MITF to standard protocols as previously described.[39]

Real-time qPCR analysis. RNA was extracted from cell cultures or ears of 15.5-day-old $ZEB2^{MCWT}$ and $ZEB2^{MCKO}$ mice by using RNeasy extraction columns (Qiagen). RNA was treated with 1 U of RNAse-free DNase RQ1 (Promega, Leiden, The Netherlands) per μg RNA for 30 min at 37 °C in appropriate buffer. DNAse was inactivated by incubation in Promega stop solution for 10 min at 65 °C. Bulk Mg^{2+} was removed by using Amicon ultra 0.5-ml centrifugal filters (Millipore, Brussels, Belgium) in two consecutive diluting washes. cDNA synthesis was performed with iScript (Bio-Rad, Hercules, CA, USA) following the manufacturer's instructions. Quantitative PCR was done using the Fast SYBR master mix kit (Applied Biosystems, Gent, Belgium) or SensiFastTM SYBR No-Rox kit (Bioline, Alpen aan de Rijn, The Netherlands) for the genes of interest and reference genes. Primers were designed using Primer Express 1.0 Software (Perkin Elmer Applied Biosystems) or obtained from the literature.[47,49] Plates were run on the LightCycler 480 (Roche, Vilvoorde, Belgium). The average threshold cycle of triplicate reactions was used for all subsequent calculations using the deltaCT method. Graphs represent the average normalized relative expression values of $ZEB2^{MCWT}$ and $ZEB2^{MCKO}$ mice, with the WT average normalized relative to the expression value at 4 days set to 1.

Western blot analysis. Cells were lysed in Laemli-lysis buffer (50 mM Tris-HCl pH 6.8, 10% glycerol, 2% SDS). After sonicating and centrifuging the samples, 20 μg of protein was separated on gel and transferred to a PVDF membrane. Membranes were incubated with primary antibodies and appropriate HRP-labeled secondary antibodies (GE Healthcare, Diegem, Belgium). Detection was performed with the Western LightningT chemiluminescence reagent plus kit (Perkin Elmer, Waltham, MA, USA) or the Immobilion western HRP substrate (Millipore). The following antibodies were used: rabbit anti-ZEB2 (1/1000) (HPA003456, Sigma); rabbit anti-ZEB1 (1/1000) (Gift from Professor Darling); mouse anti-β-Tubulin (1/1000) (T4026, Sigma); mouse anti-MITF (Ab 12039 Abcam); mouse anti-Vinculin (1/3000) (V9131, Sigma); mouse anti-Fibronectin (1/1000) (Abcam, ab23750).

Statistical analysis. Data were analyzed with GraphPad Prism 5 (GraphPad Software Inc., La Jolla, CA, USA) and R (The Comprehensive R Archive Network, http://www.cran.r-project.org).

Conflict of Interest

The authors declare no conflict of interest.

Acknowledgements. This research was funded by grants from the FWO, the Geconcerteerde Onderzoeksacties of Ghent University, the Stichting tegen Kanker, the Association for International Cancer Research (Scotland), the EU-FP6 framework program BRECOSM LSHC-CT-2004-503224, the EU-FP7 framework programs TuMIC 2008-201662 and Target-Melanoma (www.targetmelanoma.com). Work in the lab of ID was supported by grants from the Ligue National Contre le Cancer, the INCa, the Université de Strasbourg and the ANR. The IGBMC high throughput sequencing facility is a member of the 'France Génomique' consortium (ANR10-INBS-09-08). We acknowledge Riet DeRycke for expert electron microscopic analysis, Dr. Amin Bredan for critical reading of the manuscript and the members of our research group for valuable discussions. We thank Professor D Darling for providing the ZEB1 antibody, Professor K Hearing for providing the TYRP1 antibody.

Author contributions

GD, NV, ÖA, DK, JT, KL, AG, BDC, BB, ID, JCM and GB performed the experiments and analyzed the interpreted data. MVG, LB, GMU, MR, WMG, GG, DH, JvdO, LL and JH provided valuable reagents/material. GD and GB conceived-designed the project, analyzed the interpreted data and wrote the paper with inputs particularly from NV, DH, LL, JH, JCM and all other authors.

1. Ernfors P. Cellular origin and developmental mechanisms during the formation of skin melanocytes. *Exp Cell Res* 2010; **316**: 1397–1407.
2. Luciani F, Champeval D, Herbette A, Denat L, Aylaj B, Martinozzi S *et al.* Biological and mathematical modeling of melanocyte development. *Development* 2011; **138**: 3943–3954.
3. Osawa M. Melanocyte stem cells (June 30, 2009), StemBook, ed. The Stem Cell Research Community, StemBook, doi:10.3824/stembook.1.46.1.
4. Pshenichnaya I, Schouwey K, Armaro M, Larue L, Knoepfler PS, Eisenman RN *et al.* Constitutive gray hair in mice induced by melanocyte-specific deletion of c-Myc. *Pigment Cell Melanoma Res* 2012; **25**: 312–325.
5. Steingrimsson E, Copeland NG, Jenkins NA. Melanocyte stem cell maintenance and hair graying. *Cell* 2005; **121**: 9–12.
6. White RM, Zon LI. Melanocytes in development, regeneration, and cancer. *Cell Stem Cell* 2008; **3**: 242–252.
7. Kubic JD, Young KP, Plummer RS, Ludvik AE, Lang D. Pigmentation PAX-ways: the role of Pax3 in melanogenesis, melanocyte stem cell maintenance, and disease. *Pigment Cell Melanoma Res* 2008; **21**: 627–645.
8. Hearing VJ. Determination of melanin synthetic pathways. *J Invest Dermatol* 2011; **131**: E8–E11.
9. Schiaffino MV. Signaling pathways in melanosome biogenesis and pathology. *Int J Biochem Cell Biol* 2010; **42**: 1094–1104.
10. Nishimura EK, Granter SR, Fisher DE. Mechanisms of hair graying: incomplete melanocyte stem cell maintenance in the niche. *Science* 2005; **307**: 720–724.
11. Moriyama M, Osawa M, Mak SS, Ohtsuka T, Yamamoto N, Han H *et al.* Notch signaling via Hes1 transcription factor maintains survival of melanoblasts and melanocyte stem cells. *J Cell Biol* 2006; **173**: 333–339.
12. Tsao H, Chin L, Garraway LA, Fisher DE. Melanoma: from mutations to medicine. *Genes Dev* 2012; **26**: 1131–1155.
13. Gembarska A, Luciani F, Fedele C, Russell EA, Dewaele M, Villar S *et al.* MDM4 is a key therapeutic target in cutaneous melanoma. *Nat Med* 2012; **18**: 1239–1249.
14. Ackermann J, Frutschi M, Kaloulis K, McKee T, Trumpp A, Beermann F. Metastasizing melanoma formation caused by expression of activated N-RasQ61K on an INK4a-deficient background. *Cancer Res* 2005; **65**: 4005–4011.
15. Flaherty KT, Puzanov I, Kim KB, Ribas A, McArthur GA, Sosman JA *et al.* Inhibition of mutated, activated BRAF in metastatic melanoma. *N Engl J Med* 2010; **363**: 809–819.
16. Nazarian RM, Prieto VG, Elder DE, Duncan LM. Melanoma biomarker expression in melanocytic tumor progression: a tissue microarray study. *J Cutan Pathol* 2010; **37** (Suppl 1): 41–47.
17. Flaherty KT, Infante JR, Daud A, Gonzalez R, Kefford RF, Sosman J *et al.* Combined BRAF and MEK inhibition in melanoma with BRAF V600 mutations. *N Engl J Med* 2012; **367**: 1694–1703.
18. Colone M, Calcabrini A, Toccacieli L, Bozzuto G, Stringaro A, Gentile M *et al.* The multidrug transporter P-glycoprotein: a mediator of melanoma invasion? *J Invest Dermatol* 2008; **128**: 957–971.
19. Sanchez-Tillo E, Liu Y, de Barrios O, Siles L, Fanlo L, Cuatrecasas M *et al.* EMT-activating transcription factors in cancer: beyond EMT and tumor invasiveness. *Cell Mol Life Sci* 2012; **69**: 3429–3456.
20. Thiery JP, Acloque H, Huang RY, Nieto MA. Epithelial-mesenchymal transitions in development and disease. *Cell* 2009; **139**: 871–890.
21. Peinado H, Olmeda D, Cano A. Snail, Zeb and bHLH factors in tumour progression: an alliance against the epithelial phenotype? *Nat Rev Cancer* 2007; **7**: 415–428.
22. Sanchez-Martin M, Perez-Losada J, Rodriguez-Garcia A, Gonzalez-Sanchez B, Korf BR, Kuster W *et al.* Deletion of the SLUG (SNAI2) gene results in human piebaldism. *Am J Med Genet A* 2003; **122A**: 125–132.
23. Perez-Losada J, Sanchez-Martin M, Rodriguez-Garcia A, Sanchez ML, Orfao A, Flores T *et al.* Zinc-finger transcription factor Slug contributes to the function of the stem cell factor c-kit signaling pathway. *Blood* 2002; **100**: 1274–1286.
24. Jiang R, Lan Y, Norton CR, Sundberg JP, Gridley T. The Slug gene is not essential for mesoderm or neural crest development in mice. *Dev Biol* 1998; **198**: 277–285.
25. Gupta PB, Kuperwasser C, Brunet JP, Ramaswamy S, Kuo WL, Gray JW *et al.* The melanocyte differentiation program predisposes to metastasis after neoplastic transformation. *Nat Genet* 2005; **37**: 1047–1054.
26. Sanchez-Martin M, Rodriguez-Garcia A, Perez-Losada J, Sagrera A, Read AP, Sanchez-Garcia I. SLUG (SNAI2) deletions in patients with Waardenburg disease. *Hum Mol Genet* 2002; **11**: 3231–3236.
27. Shirley SH, Greene VR, Duncan LM, Torres Cabala CA, Grimm EA, Kusewitt DF. Slug expression during melanoma progression. *Am J Pathol* 2012; **180**: 2479–2489.
28. Caramel J, Papadogeorgakis E, Hill L, Browne GJ, Richard G, Wierinckx A *et al.* A switch in the expression of embryonic EMT-inducers drives the development of malignant melanoma. *Cancer Cell* 2013; **24**: 466–480.
29. Vandewalle C, Van Roy F, Berx G. The role of the ZEB family of transcription factors in development and disease. *Cell Mol Life Sci* 2009; **66**: 773–787.
30. Gheldof A, Hulpiau P, van Roy F, De Craene B, Berx G. Evolutionary functional analysis and molecular regulation of the ZEB transcription factors. *Cell Mol Life Sci* 2012; **69**: 2527–2541.
31. Comijn J, Berx G, Vermassen P, Verschueren K, van Grunsven L, Bruyneel E *et al.* The two-handed E box binding zinc finger protein SIP1 downregulates E-cadherin and induces invasion. *Mol Cell* 2001; **7**: 1267–1278.
32. De Craene BD, Berx G. Regulatory networks defining EMT during cancer initiation and progression. *Nat Rev Cancer* 2013; **13**: 97–110.
33. Van de Putte T, Maruhashi M, Francis A, Nelles L, Kondoh H, Huylebroeck D *et al.* Mice lacking ZFHX1B, the gene that codes for Smad-interacting protein-1, reveal a role for multiple neural crest cell defects in the etiology of Hirschsprung disease-mental retardation syndrome. *Am J Hum Genet* 2003; **72**: 465–470.
34. Van de Putte T, Francis A, Nelles L, van Grunsven LA, Huylebroeck D. Neural crest-specific removal of Zfhx1b in mouse leads to a wide range of neurocristopathies reminiscent of Mowat-Wilson syndrome. *Hum Mol Genet* 2007; **16**: 1423–1436.
35. Colombo S, Champeval D, Rambow F, Larue L. Transcriptomic analysis of mouse embryonic skin cells reveals previously unreported genes expressed in melanoblasts. *J Invest Dermatol* 2012; **132**: 170–178.
36. Delmas V, Martinozzi S, Bourgeois Y, Holzenberger M, Larue L. Cre-mediated recombination in the skin melanocyte lineage. *Genesis* 2003; **36**: 73–80.
37. Mackenzie MA, Jordan SA, Budd PS, Jackson IJ. Activation of the receptor tyrosine kinase Kit is required for the proliferation of melanoblasts in the mouse embryo. *Dev Biol* 1997; **192**: 99–107.
38. Thurber AE, Douglas G, Sturm EC, Zabierowski SE, Smit DJ, Ramakrishnan SN *et al.* Inverse expression states of the BRN2 and MITF transcription factors in melanoma spheres and tumour xenografts regulate the NOTCH pathway. *Oncogene* 2011; **30**: 3036–3048.
39. Strub T, Giuliano S, Ye T, Bonet C, Keime C, Kobi D *et al.* Essential role of microphthalmia transcription factor for DNA replication, mitosis and genomic stability in melanoma. *Oncogene* 2011; **30**: 2319–2332.
40. Chin L, Garraway LA, Fisher DE. Malignant melanoma: genetics and therapeutics in the genomic era. *Genes Dev* 2006; **20**: 2149–2182.
41. Southall TD, Brand AH. Neural stem cell transcriptional networks highlight genes essential for nervous system development. *EMBO J* 2009; **28**: 3799–3807.
42. Xu Y, Brenn T, Brown ER, Doherty V, Melton DW. Differential expression of microRNAs during melanoma progression: miR-200c, miR-205 and miR-211 are downregulated in melanoma and act as tumour suppressors. *Br J Cancer* 2012; **106**: 553–561.
43. van Kempen LC, van den Hurk K, Lazar V, Michiels S, Winnepenninckx V, Stas M *et al.* Loss of microRNA-200a and c, and microRNA-203 expression at the invasive front of primary cutaneous melanoma is associated with increased thickness and disease progression. *Virchows Arch* 2012; **461**: 441–448.
44. Higashi Y, Maruhashi M, Nelles L, Van de Putte T, Verschueren K, Miyoshi T *et al.* Generation of the floxed allele of the SIP1 (Smad-interacting protein 1) gene for Cre-mediated conditional knockout in the mouse. *Genesis* 2002; **32**: 82–84.
45. Nyabi O, Naessens M, Haigh K, Gembarska A, Goossens S, Maetens M *et al.* Efficient mouse transgenesis using Gateway-compatible ROSA26 locus targeting vectors and F1 hybrid ES cells. *Nucleic Acids Res* 2009; **37**: e55.
46. van den Berghe V, Stappers E, Vandesande B, Dimidschstein J, Kroes R, Francis A *et al.* Directed migration of cortical interneurons depends on the cell-autonomous action of Sip1. *Neuron* 2013; **77**: 70–82.
47. Berlin I, Luciani F, Gallagher SJ, Rambow F, Conde-Perez A, Colombo S *et al.* General strategy to analyse coat colour phenotypes in mice. *Pigment Cell Melanoma Res* 2012; **25**: 117–119.
48. Denecker G, Hoste E, Gilbert B, Hochepied T, Ovaere P, Lippens S *et al.* Caspase-14 protects against epidermal UVB photodamage and water loss. *Nat Cell Biol* 2007; **9**: 666–674.
49. Gallagher SJ, Luciani F, Berlin I, Rambow F, Gros G, Champeval D *et al.* General strategy to analyse melanoma in mice. *Pigment Cell Melanoma Res* 2012; **24**: 987–988.

Supplementary Information accompanies this paper on Cell Death and Differentiation website (http://www.nature.com/cdd)

Dana KOLUDROVIC

Le rôle du complexe de remodelage de la chromatine NURF dans les mélanocytes et les mélanomes

Résumé

Le rôle du complexe de remodelage de la chromatine NURF dans les mélanocytes et les mélanomes

Le mélanome est un cancer de la peau très agressif. Microphthalmia-associated transcription factor (MITF) est un facteur de transcription clé contrôlant le développement de la lignée mélanocytaire, ainsi que la prolifération et l'invasion des cellules de mélanome. Pour mieux comprendre les fonctions de MITF, nous avons identifié ses cofacteurs impliques dans la régulation de la transcription. Nous avons montré que le complexe de remodelage de la chromatine NURF interagit avec MITF. Ma thèse a consisté à élucider le rôle de NURF dans le mélanome et les melanocytes. La perte de BPTF, la principale sous-unité de ce complexe, induit un arrêt de la prolifération et une entrée en senescence des cellules de mélanome. Nous avons montré que BPTF et MITF coopèrent pour réguler l'expression de gènes impliqués dans la prolifération and invasion suggérant que BPTF et un cofacteur de MITF. De façon inattendue, l'inactivation de BPTF spécifiquement dans les melanocytes entraine la perte progressive et totale de la pigmentation du pelage en raison de l'incapacité des cellules souches mélanocytaire à produire une descendance fonctionnelle. C'est la première fois que l'interaction fonctionnelle entre NURF et MITF est démontrée in vitro, complétée par des observations phénotypique uniques in vivo, contribuant à la compréhension de la biologie des melanocytes et du mélanome.

Mots-clés : MITF, NURF, mélanome, remodelage de la chromatine, cellules souches mélanocytaire

Résumé en anglais

The role of the NURF chromatin remodeling complex in melanocytes and melanoma

Melanoma is a highly aggressive form of skin cancer. Microphthalmia-associated transcription factor (MITF) is a key regulator of development of the melanocyte lineage and proliferation and invasion of melanoma cells. To further elucidate the functions of MITF, we identified factors co-regulating transcription with MITF. We identified the NURF chromatin-remodeling complex as MITF interactor. My thesis aims to elucidate the role of NURF in melanoma and melanocytes. Loss of BPTF, the principal subunit of the complex, led to arrest of proliferation and entry into senescence of melanoma lines. We showed BPTF and MITF co-regulate genes involved in proliferation and invasion suggesting that BPTF acts as cofactor for MITF. Remarkably, the mouse model of melanocyte-specific BPTF ablation led to progressive and complete loss of coat pigmentation due to the inability of the melanocyte stem cells to produce functional progeny. This is the first report of NURF-MITF functional interaction in vitro, complemented with a unique in vivo phenotype, both adding to a general understanding of melanocyte and melanoma biology.

Key words: MITF, NURF, melanoma, chromatin remodeling, melanocyte stem cells